

Regulation of the biofilm development at the chromatin level in *Candida albicans*

A thesis submitted for the degree of

Doctor of Philosophy

by

Rima Singha



Molecular Biology and Genetics Unit

Jawaharlal Nehru Centre for Advanced Scientific Research

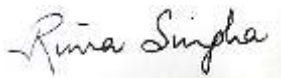
Jakkur, Bengaluru- 560064, India

July 2020

Dedicated to my parents

DECLARATION

I do hereby declare that this thesis entitled “**Regulation of biofilm development at the chromatin level in *Candida albicans***” is an authentic record of research work carried out by me towards my Doctor of Philosophy under the guidance and supervision of Prof. Kaustuv Sanyal at the Molecular Biology and Genetics Unit, Jawaharlal Nehru Centre for Advanced Scientific Research, Bangalore, India and that this work has not been submitted elsewhere for the award of any other degree. In keeping with the norm of reporting scientific observations, due acknowledgments have been made whenever the work described was based on the findings of other investigators. Any omission, which might have occurred by oversight or misjudgment, is regretted.



Rima Singha

Bangalore

Date:24/07/2020



Jawaharlal Nehru Centre for Advanced Scientific Research

Kaustuv Sanyal *PHD, FAAM (USA), FNA, FASc, FNASc*
Professor & Tata Innovation Fellow

Visiting Professor
Graduate School of Frontier Biosciences
Osaka University
Suita, Osaka 565 0871, Japan

To whom it may concern

This is to certify that the work described in the thesis titled 'Regulation of biofilm development at the chromatin level in *Candida albicans*' is the result of investigations carried out by **Ms. Rima Singha** towards her Doctor of Philosophy degree at the Molecular Biology and Genetics Unit, Jawaharlal Nehru Centre for Advanced Scientific Research, Bangalore, India under my supervision and guidance. The results presented here have not previously formed the basis for the award of any other diploma or degree.

Bangalore
24 July 2020

Kaustuv Sanyal, Ph.D.
Professor
Molecular Biology Laboratory
Molecular Biology and Genetics Unit
Jawaharlal Nehru Centre for
Advanced Scientific Research
Jakkur Post, Bangalore - 560064, India
Ph: +91-81-22082878, Email: ksanyal@jncasr.ac.in

Acknowledgements

This thesis is the culmination of the unconditional support and encouragement of several people during my formative years as well as my time in JNCASR. I would like to take this opportunity to express my sincere gratitude and acknowledge all of them for their contribution.

First, I would like to thank Prof. Kaustuv Sanyal, who has been a marvelous mentor and has helped me build the correct scientific temper. He has actively guided me in my research problems and tried to bring out the best in me. He had involved in multiple projects from the beginning of my PhD, which helped me understand and appreciate the beauty of chromatin plasticity in fungi. His unparalleled enthusiasm to discuss and formulate hypotheses and constructive criticism to results and interpretations had pushed me to work harder. I try to imbibe in myself his eye for minute details and excellent presentation skills. I hope that in future, I am worthy enough for the amount of effort he has put in mentoring me as a researcher. I thank him immensely for all his guidance and belief in me.

I am grateful to all the members of the MBGU faculty - Prof. MRS Rao, Prof. Uday Kumar Ranga, Prof. Anuranjan Anand, Prof. Maneesha Inamdar, Prof. Tapas Kumar Kundu, Prof. Hemalatha Balaram, Prof. Namita Surolia, Dr. James Chelliah and Dr. Kushagra Bansal for their active participation and discussions during the departmental work presentations. I appreciate all of them for maintaining the ideal scientific temperament in the department. I specially thank Prof. Hemalatha Balaram and Dr. Ravi Manjithaya for their exhaustive course work.

I thank University Grants Commission, Government of India for the financial assistance and JNCASR for intramural funding. I also thank JNCASR administration, academic section, Dhanvantari, Library and Complab for their support and facilities. I am also thankful to Genotypic Technologies for their services.

I would like to thank Prof. Karl Kuchler and his lab members where I had been a visiting student for two months. My visit to his lab was indeed a learning experience for me. I had the opportunity to handle immune cells and learn certain immunological assays which I hope to implement in future. I take this opportunity to thank Prof. Ganesh Nagaraju and Prof. Utpal Nath for their suggestions during my comprehensive exam presentation.

I feel lucky to be a part of Molecular Mycology Laboratory. I thank all the members of MML for their support and advice. My heartfelt thanks to the super seniors- Sreyoshi, Laxmi, and Gautam for their insightful discussions, hands-on training and tips. I especially thank Laxmi who laid the foundation of this project and taught me the basics of handling *Candida*. I would like to thank the past members of the lab - Asif, Tanmoy, Lakshmi, Vikas, Jigyasa, Parijat, Bornika, Promit, Bhagya and Aditi for the fond memories. I am equally thankful to the present members - Hashim, Shweta, Aswathy, Krishnendu, Shreyas, Priya Jaitly, Priya Brahma, Satyadev, Kuldeep, Rashi, Ankita, Padma, Srijana, Rohit for keeping the spirits of MML high. I

am extremely grateful to Mr. Nagaraj and Sahana for making lab equipments and reagents available on time.

I had the opportunity to work with Neha in one of the projects at the initial days of my PhD. The scientific collaboration helped us not only in bringing together the work but I also developed a special bond with her. Over these years, Neha and Sundar had constantly supported and encouraged me. I have very fond memories with both of them. I really cherish the time we spent together and hope each one of us succeeds in life.

Finally, this acknowledgement would be incomplete without mentioning my family. It is impossible to thank them as words won't do justice. I am grateful to my parents for the values they instilled in me. My father had been my backbone since my childhood who had taught me the importance of discipline and hard work. He believed in me when I didn't believe in myself. His optimism and perseverance push me till today to work harder. Losing him to death was the biggest setback in my life. But I believe his death won't be any excuse to not achieve anything in life which he wished for me. My mother's unconditional love and support especially after my father's demise has been my biggest pillar of strength. She had been very motivating through the toughest of times which has helped me sail through. Her enthusiasm and unending curiosity to know things still inspire me. She has been more of a friend than a mother to me. I also sincerely acknowledge my brother for his support and encouragement. I cherish all the memories of our childhood and with our busy schedules and geographical constraints, I wish to meet him in person at least once a year and spend some time together pulling each other's legs as before. I also thank my sister-in-law Pallavi for her support and our silly banter.

I am extremely thankful to my husband, Subhradeep for his constant support and encouragement in past few months. I also grateful to him for putting up with my antics and not letting me go into a panic mode at times. I take this opportunity to thank my in-laws for their faith in me.

Lastly once again I thank my father for giving me the wings to fly!

Rima Singha
Bangalore
Date-24.07.2020

Table of contents

Chapter 1 Introduction	1
Chromatin structure and organization	2
Primary structure of chromatin.....	2
Core histone structure	3
Secondary structure.....	3
Tertiary structure	4
Chromatin plasticity	6
Histone variants	7
Linker histone H1	8
Histone H2A	10
Histone H2B	13
Histone H3	14
Histone H4	19
Nucleosome occupancy and regulation of gene expression	19
Evolution of histones in eukaryotes	20
Chaperones and their role in the incorporation of histone variants	22
<i>Candida albicans</i>	27
CUG clade species.....	28
Pathogenic traits of <i>C. albicans</i>	31
Morphological plasticity of <i>C. albicans</i>	34
Switching between yeast and hypha.....	35
White opaque gray transition	36
White-GUT transition	38
Planktonic-biofilm transition.....	38
Types of biofilm formation in <i>C. albicans</i>	41
Steps in biofilm formation.....	43
Adhesion	43
Initiation	46
Maturation	47
Dispersal.....	47
Histone H3 variants in <i>C. albicans</i>	48
Rationale of the present study	51

Summary of the present study	52
Chapter 2 Results	55
Mechanism by which H3V^{CTG} regulates biofilm formation in <i>Candida albicans</i>	56
Introduction.....	57
Occupancy of H3V ^{CTG} is higher at the promoter of biofilm genes in planktonic as compared to biofilm growth conditions.....	59
Occupancy of H3V ^{CTG} at the promoter and gene body of biofilm genes decreases as the cell switches from planktonic to biofilm condition.....	61
Occupancy of canonical H3 is unaltered during the planktonic to biofilm growth transition.....	63
Occupancy of biofilm specific transcription factor Bcr1 is increased at the promoter of biofilm genes in H3V ^{CTG} null mutant in the planktonic condition of growth.....	63
Co-occurrence of amino acid residues at position 31 and 32 is essential for the function of variant histone H3.....	65
A copy of H3V ^{CTG} with mutations at position 31 and 32 could not complement H3V ^{CTG} function.....	67
Occupancy of a biofilm specific transcription factor, Bcr1 is increased at the promoters of biofilm relevant genes in the presence of a full-length protein with mutations at position 31 and 32 of H3V ^{CTG}	68
Occupancy of the double point mutant H3V ^{CTG} (Hht1 ^{V31S, S32T}) decreases at the promoter of biofilm genes.....	71
Conservation of variant-specific residues of H3V ^{CTG} across the CUG clade species in Ascomycota.....	72
<i>cac2</i> mutants mimic the hyperfilamentation phenotype of H3V ^{CTG} null mutant.....	77
H3V ^{CTG} levels at the promoter of biofilm genes are reduced in the absence of <i>Cac2</i>	78
Chapter 3	80
Temporal regulation of biofilm development by variant histone H3 in <i>C. albicans</i>	81
Introduction.....	82
Substrate adherence defects of <i>ace2</i> null cells of <i>C. albicans</i> is partially rescued in <i>ace2</i> and <i>hht1</i> double null mutant cells.....	83
Identification of genes involved in <i>Ace2</i> mediated adherence.....	85
Global gene expression array analysis of the double mutant of <i>ace2</i> and <i>hht1</i> reveals the up-regulation of adherence genes compared to <i>ace2</i> null mutant.....	88
Chapter 4 Discussion	94
Chapter 5 Materials and Methods	106
Strains and primers.....	107
Buffers and solutions used.....	107
Reagents for biofilm assay.....	108

Antibodies and affinity beads	108
Media, growth conditions and transformation.....	109
Strain construction.....	109
Construction of plasmids	115
<i>E. coli</i> competent cells preparation and transformation	116
Genomic DNA preparation	117
Cell lysate preparation and western blot analysis	117
Chromatin Immunoprecipitation (ChIP).....	118
ChIP-qPCR analysis	118
RNA extraction.....	119
cDNA preparation and Reverse transcription PCR.....	119
Quantitative PCR	120
Gene expression microarray design and data analysis	120
Biofilm assay on six-well polystyrene plates	121
Quantitative adherence assay using crystal violet staining and XTT assay.....	121
Quantitative adherence assay using colony-forming unit (CFU) counting.....	122
References	131
List of publications	154

List of tables

Table 1-1 List of linker histone H1 variants.....	9
Table 1-2 List of core histone H2A variants.....	13
Table 1-3 List of core histone H2B variants.....	14
Table 1-4 List of core histone H3 variants.....	18
Table 1-5 List of core histone H4 variants.....	19
Table 1-6 List of histone chaperones identified till date.....	25
Table 2-1 Table representing the conservation/divergence of amino acid residues at a particular position in H3 variants of the CUG-Ser1 clade species.....	75
Table 5-1 Strains used in the study.....	123
Table 5-2 Oligonucleotides used in this study.....	128

List of figures

Figure 1.1 Structural features of core histone proteins.	3
Figure 1.2 Higher-order structures of chromatin.	5
Figure 1.3 Factors regulating versatility in the chromatin landscape.	7
Figure 1.4 Core histone variants in humans.	17
Figure 1.5 Phylogenetic tree depicting the CUG clade species.	30
Figure 1.6 Outline of the pathogenic traits of <i>C. albicans</i>	33
Figure 1.7 Phenotypic transitions in <i>C. albicans</i>	35
Figure 1.8 Different types of biofilm in <i>C. albicans</i>	40
Figure 1.9 The core transcriptional biofilm circuit in <i>Candida albicans</i>	42
Figure 1.10 Schematic of transcriptional network of 30 adherence regulators in <i>C. albicans</i>	46
Figure 1.11 A nonessential histone H3 variant, H3V ^{CTG} , represses the biofilm gene circuit.	50
Figure 2.1 Variant histone H3 limits the access of transcription modulators to promoters of biofilm-related genes.	60
Figure 2.2 The binding of H3V ^{CTG} drops at the promoter and gene bodies of biofilm genes in biofilm conditions.	62
Figure 2.3 Total histone H3 levels at the promoter of biofilm genes decline as the cells transit from the planktonic to biofilm mode of growth in <i>C. albicans</i>	63
Figure 2.4 Variant histone H3 restricts the access of transcription factors to the biofilm gene promoters.	64
Figure 2.5 Co-occurrence of valine and serine at 31 and 32 position is critical for the biofilm repressive function of H3V ^{CTG} in <i>C. albicans</i>	66
Figure 2.6 Amino acid residues valine, and serine at 31 and 32 position are essential for the filamentation function of H3V ^{CTG} in <i>C. albicans</i>	67
Figure 2.7 The filamentation phenotype of H3V ^{CTG} mutants is observed at a single-cell level.	67
Figure 2.8 Mutation of H3V ^{CTG} at positions 31, 32 induces the biofilm gene circuitry during the planktonic mode.	68
Figure 2.9 Occupancy of Bcr1 is increased at the promoter of biofilm genes in double point mutants.	70
Figure 2.10 Occupancy of the double point mutants of H3V ^{CTG} decreases at the promoter of biofilm genes.	71
Figure 2.11 Phylogenetic tree depicting conservation of variant-specific residues of H3V ^{CTG} across CUG-Ser1 clade of ascomycetes.	74

Figure 2.12 <i>cac2</i> null mutants mimic the hyperfilamentation and enhanced biofilm formation phenotype of the H3V ^{CTG} null mutant.....	78
Figure 2.13 Reduction of H3V ^{CTG} levels in the absence of <i>Cac2</i>	79
Figure 3.1 The deletion of H3V ^{CTG} rescues the adherence defects associated with <i>ace2</i> null mutants in <i>C. albicans</i>	84
Figure 3.2 The deletion of variant histone H3V ^{CTG} rescues biofilm defects in <i>ace2</i> null mutants in <i>C. albicans</i>	85
Figure 3.3 Identification of <i>Ace2</i> mediated adherence specific genes (AcASGs).	87
Figure 3.4 Gene expression profile of <i>ace2</i> and <i>hht1</i> double mutant reveals a differential expression pattern compared to <i>ace2</i> null mutant.	90
Figure 3.5 Transcriptional circuit of adherence induced genes is rewired upon the deletion of H3V ^{CTG} in the <i>ace2</i> null mutant.	92
Figure 3.6 The transcriptome profile of down-regulated genes in <i>ace2</i> null mutants is rewired upon the deletion of H3V ^{CTG}	93
Figure 4.1 The CUG Ser1 clade-specific histone H3 variant evolved as the molecular switch of morphological growth transitions in <i>C. albicans</i>	98
Figure 4.2 Co-occurrence of amino acid residues at 31 and 32 positions of H3V ^{CTG} is essential for its function.	101
Figure 4.3 Variant specific amino acid residues in H3V ^{CTG} might determine its interaction with chaperones.	102
Figure 4.4 A proposed mechanism depicting H3V ^{CTG} acting as a molecular switch of morphological growth transitions (planktonic-biofilm) in <i>C. albicans</i>	105
Figure 5.1 Western blot confirmation for V5 epitope tagging of <i>HHT1</i> and <i>HHT21</i> in LR143 and LR144.	110
Figure 5.2 Confirmation of <i>HHT1</i> deletion in LR133.	110
Figure 5.3 Confirmation of integration of mutated <i>HHT1</i> ORF at position 31, 32 and 80 in RS103, RS105, RS108, RS109 and RS110.	111
Figure 5.4 Confirmation of integration of mutated <i>HHT1</i> ORF at positions 31, 32, and 80 in RS111, and RS112.	112
Figure 5.5 Western blot confirmation for V5 epitope tagging of point mutants of <i>HHT1</i> at 31 and 32 positions in RS113, RS114, RS115.	112
Figure 5.6 Western blot confirmation for V5 epitope tagging of <i>HHT1</i> and <i>HHT21</i> in <i>cac2</i> null mutant background.	113
Figure 5.7 Confirmation of <i>ACE2</i> deletion in RS404, RS405.	114
Figure 5.8 Confirmation of <i>ACE2</i> deletion in RS408, RS409 by PCR.	115
Figure 5.9 Confirmation of <i>HHT1</i> reintegration in RS411, RS412 by PCR.	115

Abbreviations

ALS-Agglutinin-like sequence
ANOVA - Analysis of variance
ASG-Adherence specific genes
bp - base pair
BRG-Biofilm relevant genes
BSA-Bovine serum albumin
CATD- Centromere targeting domain
CGD-Candida Genome Database
ChIP - Chromatin immunoprecipitation
DMSO - Dimethyl sulfoxide
DNA - Deoxyribonucleic acid
DTT-Dithiothreitol
EDTA-Ethylenediaminetetraacetic acid
EGTA- Ethylene glycol-bis (β -aminoethyl ether)-N, N, N',N'-tetraacetic acid
EtBr- Ethidium bromide
g - gram
GUT- Gastrointestinally induced transition
h - hour
kb - kilobase
L - litre
M - molar
min - minute
Mb - megabase
mg - milligram
mL - millilitre
mM - millimolar
MTL - Mating type locus
MYA - Million years ago
N - normal
NAT - Nourseothricin
ORF - Open reading frame
PAGE - Polyacrylamide gel electrophoresis
PBS - Phosphate buffer saline
PTMs-Post-translational modifications
RNA - Ribonucleic acid
RPM - Revolutions per minute
PCR - Polymerase chain reaction
qPCR - Quantitative PCR
RC-Replication coupled
RI-Replication independent

RT- Room temperature

s - second

SD - Standard deviation

SDS-Sodium Dodecyl sulphate

SEM - Standard error of mean

TE-Tris-EDTA

$^{\circ}\text{C}$ - Degree Celsius

μg - microgram

μL - microlitre

μM - micromolar

μm - micrometer

Chapter 1 Introduction

Chromatin structure and organization

The eukaryotic genome is packaged into the specialized organelle, the nucleus. The enormous size of DNA poses a major challenge to be accommodated inside the nuclear space. Within the nucleus, the DNA is packaged with basic proteins called histones to form chromatin. The wrapping of DNA around the histones contributes to the efficient condensation of the genetic material. However, compaction of DNA makes it inaccessible to DNA regulatory elements. Thus, chromatin has been evolved as a dynamic structure with different degrees of condensation. The structural plasticity of chromatin plays a key role in regulating global gene expression. Specific chromatin structure regulates the accessibility of binding of transcription factors and regulatory elements thereby controlling the DNA dependent basic processes such as transcription, DNA replication, DNA recombination and repair. Besides, the genetic information within the DNA is laden with various chemical modifications of DNA bases and histone tails at specific genomic locations conferring to the dynamic nature of chromatin.

Primary structure of chromatin

The recurring unit of chromatin is the nucleosome, consisting of a histone octamer core wrapped around tightly by two superhelical turns of 147 bp of DNA (Luger, Mader et al. 1997, Davey, Sargent et al. 2002). A histone octamer comprises of two copies each of histones H2A, H2B, H3, and H4 (Kornberg 1974, Kornberg and Thomas 1974). An octamer after being wrapped with DNA associates with linker histone H1 to complete the assembly process. Histones are the most abundant proteins associated with DNA and are highly conserved across eukaryotes (Harvey Lodish, Arnold Berk et al. 2000). The nucleosomes are stabilized by protein-protein interactions within the histone octamer and by electrostatic DNA-protein interactions (Bruce Alberts, Alexander Johnson et al. 2002). The core histones are separated by linker DNA of variable length to form the nucleosomal arrays (Ramakrishnan 1997, Vignali and Workman 1998, Widom 1998, Woodcock, Skoultschi et al. 2006). This arrangement of nucleosomes with bound DNA of about 10 nm in diameter, observed under electron microscope as “beads on a string organization” is known as the “primary” structure of chromatin and represents the first state of chromatin

compaction (Bruce Alberts, Alexander Johnson et al. 2002). The primary structure in turn decides and defines the higher order configurations (secondary and tertiary structures) that form an entire chromosome (Felsenfeld and McGhee 1986, Zlatanova, Leuba et al. 1998, Woodcock and Dimitrov 2001). This open and simple state of chromatin is rarely observed in physiological conditions.

Core histone structure

Each of the four core histones consists of an unstructured N-terminal tail, a globular histone fold domain (HFD), and a short C-terminus. HFD consists of three alpha-helices (α) connected by two short loops (L1, L2), which regulate the heterodimeric interactions between the core histones (Arents and Moudrianakis 1995) (**Figure 1.1**). The dimerization of core histones (H2A-H2B or H3-H4) is mediated by the formation of a handshake motif, where loop L1 of one histone interacts with loop L2 of the other histone (Arents, Burlingame et al. 1991). The flexible N-terminal tails are sites of post-translational modifications (PTMs) and thus are critical players in regulating the chromatin structure and gene expression.

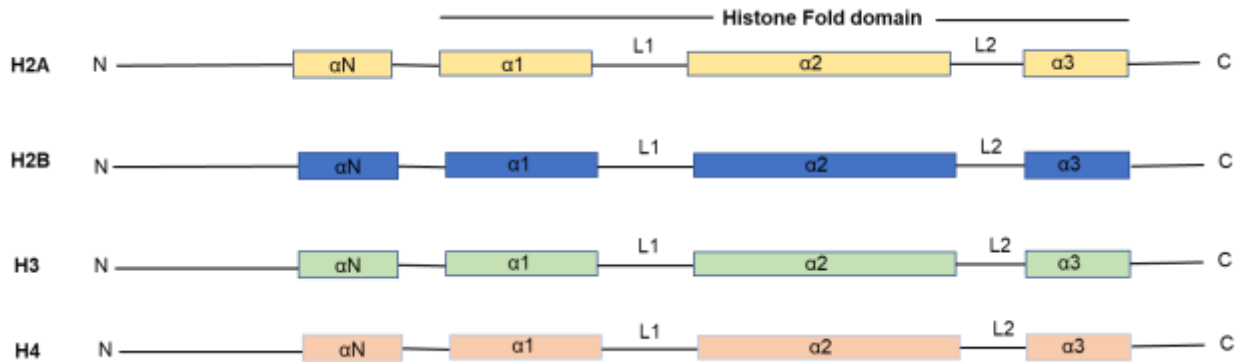


Figure 1.1 Structural features of core histone proteins.

The core histones consist of an unstructured N-terminal tail, a globular histone fold domain (HFD), and a short C-terminus. The histone fold domain is comprised of three helices- α 1, α 2, α 3, and two loops - L1 and L2.

Secondary structure

The second level of compaction is achieved by linear nucleosomal arrays that fold to produce secondary chromatin structures. The secondary structure is stabilized by histone

H1 and non-histone chromatin proteins like HP1. The secondary structures are about 30 nm in diameter *in vitro* and there are two competing models explaining the secondary chromatin structure: solenoid (Robinson, Fairall et al. 2006) and zigzag (Bednar, Horowitz et al. 1998, Zlatanova, Leuba et al. 1998) (**Figure 1.2**). In the “one-start” solenoid model, successive nucleosomes interact with each other in a helical pattern with bent linker DNA (Kruithof, Chien et al. 2009). Whereas, in “two-start” zigzag model, two rows of nucleosomes wound together forming a helix where alternate nucleosomes interact with the straight linker DNA (Dorigo, Schalch et al. 2004). However, none of the models is exclusive because both these models have their own limitations in terms of the linker length, physiological conditions, and thus lacks biological relevance (Robinson and Rhodes 2006, Routh, Sandin et al. 2008). Electron microscopy assisted nucleosome capture and modeling approaches by formaldehyde fixation and imaging of the dispersed nucleosome arrays suggests of a non-uniform heterogeneous model (Grigoryev, Arya et al. 2009). The model states that predominantly the arrays have a two-start zigzag type of organization but in between are interspersed with one-start solenoid model. This heteromorphic model is energetically more favorable than solenoid or zigzag models under conditions that promote compaction. However, all the studies mentioned above are done in homogenous nucleosome arrays with constant linker length, but *in vivo*, chromatin is comprised of heterogenous histones with diverse PTMs and variable linker length (Luger, Dechassa et al. 2012). Both genetic and epigenetic changes influence the folding of chromatin into higher order structures and the transcriptional status. Thus, there is no universal model for chromatin organization rather multiple conformations exist depending on the physiological conditions.

Tertiary structure

The final mode of compaction is observed in the metaphase chromosome. The most probable arrangement of the metaphase chromosome is the ‘molten globule’ or ‘polymer melt’ state (**Figure 1.2**) (Eltsov, Maclellan et al. 2008). This state is achieved by interdigitation of irregularly folded nucleosome arrays facilitated by nucleosome remodeling factors and histone-modifying enzymes. In addition, chromatin-organizing and compacting proteins, such as topoisomerases, cohesins, and condensins also have a crucial

role in achieving this ultimate organizational level. The cohesin complex is required for maintenance of topologically associated domains (TADs) where genes are partitioned and segregated in megabase size of compartments (Hadjur, Williams et al. 2009, Seitan, Faure et al. 2013, Flyamer, Gassler et al. 2017). Another level of chromosome organization is in the form of compartments where the nucleus is categorized into zones of active (euchromatin) and inactive (heterochromatin) chromatin. The interactions between the boundaries of compartments appear to be mediated by condensins (Yuen, Slaughter et al. 2017).

This structure of chromatin ensures dynamicity in the accessibility of the chromatin. Therefore, a much less ordered arrangement of the nucleosome is plausible and favorable than the textbook concepts of chromatin as an ordered hierarchical assembly. An essential feature of the higher-order chromatin structure is its 3-D organization in which interacting nucleosomes might be at distant locations in the primary structure. Thus, to understand the chromatin structure and function, it is vital to correlate the linear epigenetic maps with the 3D organization.

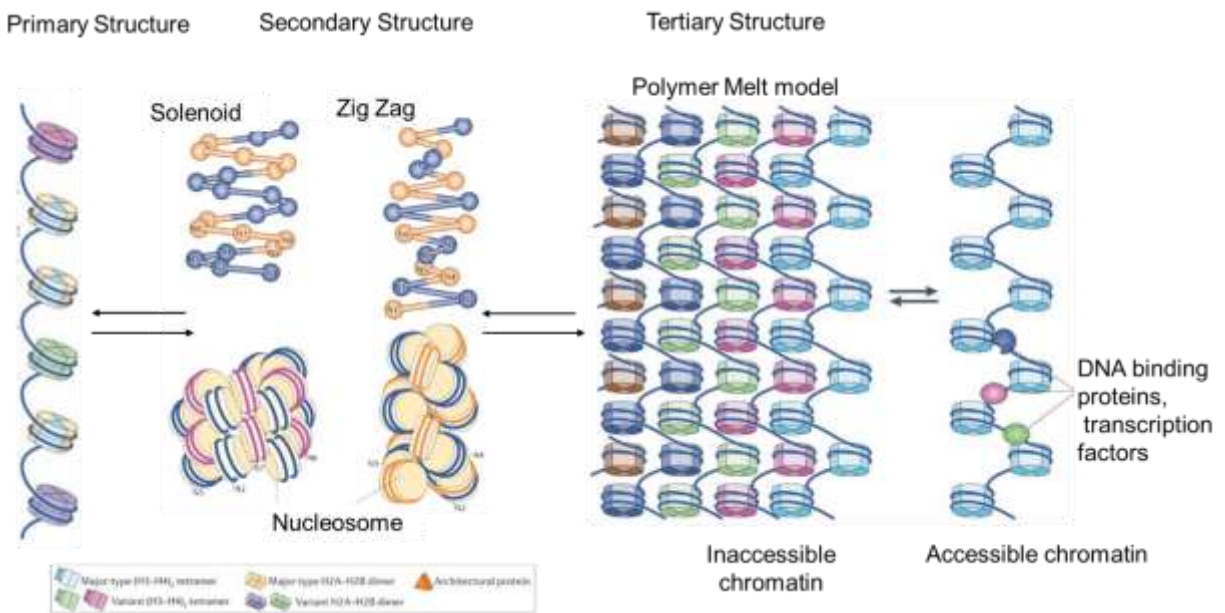


Figure 1.2 Higher-order structures of chromatin.

A cartoon depicting the plasticity of the primary, secondary, and tertiary structure of chromatin. The dynamic nature of the higher-order chromatin, with the help of nucleosome remodeling factors and histone-modifying enzymes allows partial decompaction of

nucleosome arrays from the chromatin fibers. Thus, the 'beads on the string' (shown on the right) is released from the compact array and become accessible to transcription factors. This flexible nature of the compact chromatin fibre enables access to DNA sequences buried deep inside the chromatin. Modified from (Luger, Dechassa et al. 2012).

Chromatin plasticity

Despite of the efficient condensation of DNA in higher order structures the packaging ensures DNA template-based processes like replication, repair and transcription to occur in response to cellular requirements and external stimuli. Nucleosomes are modulated at different levels to perform these cellular processes in addition to playing fundamental roles in the packaging of DNA. These modifications include histone variants, variant-specific chaperones, post-translational modifications, DNA modifications, chromatin remodelers and PTM readers.

Histones can occur as distinct variants that might undergo specific post-translational modifications (PTMs) to provide variation within core particles (Henikoff and Smith 2015). Histones can also have specific chaperones [reviewed in (Campos and Reinberg 2009, Gurard-Levin, Quivy et al. 2014, Hammond, Stromme et al. 2017, Grover, Asa et al. 2018)], chromatin remodelers, histone- and DNA-modifying enzymes associated, PTM readers, or transcription factors, which can generate specialized domains within the genome (Gelato and Fischle 2008, Probst, Dunleavy et al. 2009, Tost 2009, Wu, Lessard et al. 2009). ATP-dependent chromatin remodelers and histone chaperones play a pivotal role in the deposition of histones during nucleosome formation and also regulate their stability and degradation (Gurard-Levin, Quivy et al. 2014, Mattioli, D'Arcy et al. 2015). Histones also carry single or several PTMs consecutively to establish a histone code (Hake and Allis 2006) that either alters the structure of chromatin (*cis* mechanisms) or creates a binding platform for effector proteins (*trans* mechanisms). The effectors can in turn recognize specific PTM(s) and lead to gene activation or silencing over a short period of time till the stimuli remain. One of the well-studied examples of chromatin modulations includes centromeric regions. In most eukaryotes the centromeric regions possess unique nucleosome composition (presence of a centromere-specific histone H3 variant) (Sullivan,

Hechenberger et al. 1994) and structure (Black, Jansen et al. 2010, Black and Cleveland 2011). The centromere-associated nucleosomes also carry specific PTM marks (Zeitlin, Barber et al. 2001, Boeckmann, Takahashi et al. 2013, Hoffmann, Samel-Pommerencke et al. 2018). Thus, modulations at any of these levels in response to different environmental signals or cellular needs generate versatility in the chromatin landscape (**Figure 1.3**).

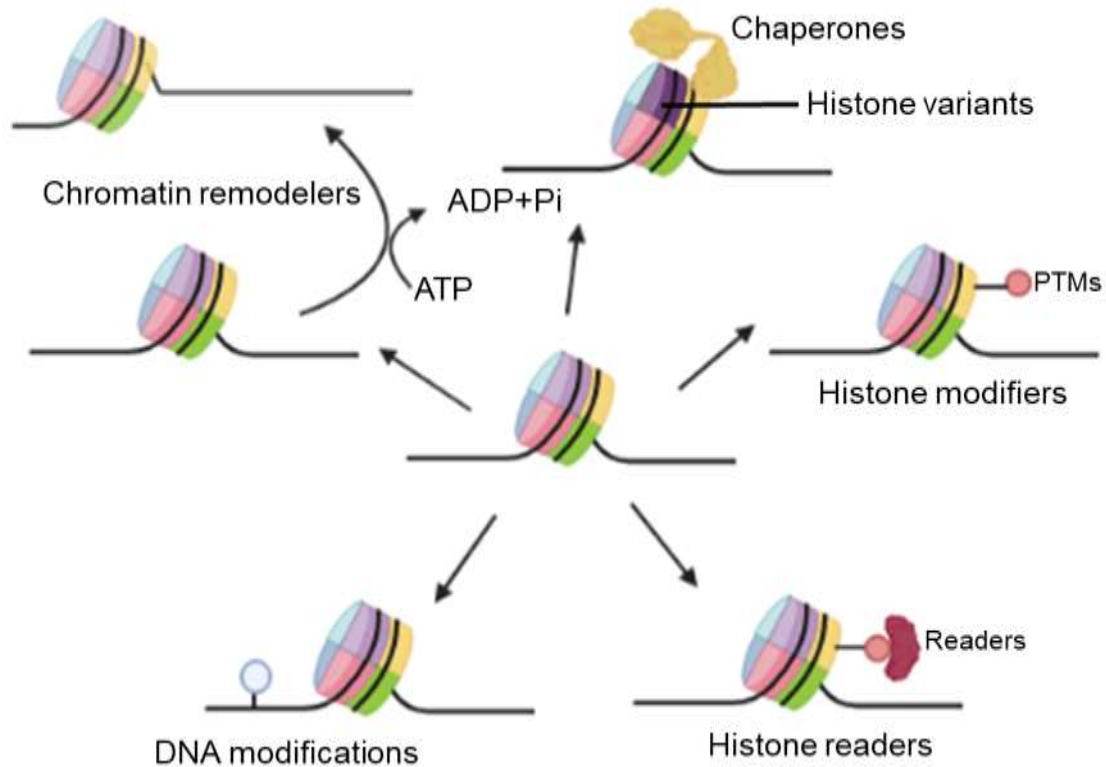


Figure 1.3 Factors regulating versatility in the chromatin landscape.

Nucleosomes are modified at the level of histone variants, modifications of DNA bases, reversible post-translational modifications (PTM) of histone tails, incorporation of histone variants by specific chaperones, and ATP dependent chromatin remodelers.

Histone variants

Histone variants are non-allelic isoforms of canonical histones that endow unique properties to chromatin and occupy specific loci in the genome [reviewed in (Pina and Suau 1987, Lennox and Cohen 1988, Fretzin, Allan et al. 1991, Ahmad and Henikoff 2002, Malik and Henikoff 2003, Hake and Allis 2006, Hake, Garcia et al. 2006, Talbert and Henikoff 2010, Henikoff and Smith 2015)]. All core histones (H2A, H2B, H3 and H4) have variant

isoforms (Henikoff and Smith 2015). Multiple gene clusters that encode the canonical histones are intronless, expressed in S-phase, and deposited on DNA during replication (replication coupled loading, RC). The translation is tightly regulated by a stem-loop structure forming sequence, 40 bp downstream of the stop codon and responsible for processing and degradation of the histone mRNAs (Marzluff, Gongidi et al. 2002). In contrast, the gene coding for histone variants are located outside the gene clusters and contains introns in most cases that give rise to multiple alternative spliced forms (Krimer, Cheng et al. 1993). The mRNAs are polyadenylated (Krimer, Cheng et al. 1993, Akhmanova, Bindels et al. 1995), and they differ in protein sequence from canonical histones ranging from a few amino acids to domains and are expressed throughout the cell cycle (replication independent loading, RI) (Wu, Tsai et al. 1982, Frank, Doenecke et al. 2003). They occupy distinct regions in the genome, thus playing specific functions.

Specific deposition and eviction machinery control the spatio-temporal distribution of canonical and variant histones. Histone variants can influence chromatin functions directly by altering the nucleosome stability making chromatin more labile, thereby facilitating or inhibiting the recruitment of transcriptional regulators. They can also indirectly affect chromatin functions by recruiting specific readers of PTMs or variant-specific complexes (Hammond, Stromme et al. 2017). Histone variants, along with PTMs can also provide binding specificity to other histones in the same nucleosome (Jin and Felsenfeld 2007). Since the focus of this thesis work is on histone variants, I will discuss the same in detail in the following sections.

Linker histone H1

Histone H1 is the linker histones involved in nucleosome compaction and maintenance of higher-order chromatin structures (Schlissel and Brown 1984, Brown 2003, Bustin, Catez et al. 2005, Weber and Henikoff 2014). Histone H1 is more dynamic than core histones while bound to DNA (Phair, Scaffidi et al. 2004). In humans, histone H1 has seven somatic variants (H1.0-H1.5 and H1X), three testis-specific variants (H1t, H1T2m, and H1LS1), and one oocyte-specific variant (H1oo) (Izzo, Kamieniarz et al. 2008, Happel and Doenecke 2009) (**Table 1-1**). Histone H1 is majorly observed to be involved in

structural compaction by making chromatin inaccessible to transcription factors and RNA polymerase (Terme, Sese et al. 2011). Histone H1 also plays a role in silencing of transposable elements by physically interacting with the histone methyltransferase Su(var)39 and tethering it to heterochromatin. However, histone H1 variants have also been linked to gene activation. For example binding of histone H1 opens the chromatin at the mouse mammary tumor virus (MMTV) promoter for increased accessibility of hormone receptors and transcription factors (Koop, Di Croce et al. 2003). Histone H1 variants can also serve as a recruitment platform for transcriptional activators or repressors. They are modified during DNA repair and are actively turned over during early stages of embryogenesis (Hergeth and Schneider 2015).

Table 1-1 List of linker histone H1 variants.

All known linker histone variants and their cell cycle stage-specific expression, functions and knockout phenotype are summarized. ND- Not determined, RC- Replication coupled, RI- Replication independent. Adapted from (Maze, Noh et al. 2014).

Histone	Stage specific expression	Location	Function	Knockout phenotype
H1	RC	Throughout the nucleus	Linker histone	Non-essential for viability in <i>S. cerevisiae</i> , <i>A. nidulans</i>
H1.1- H1.5	RC	Throughout the nucleus. H1.3 and H1.4 display a punctuate staining pattern. H1.5 concentrated at the nuclear periphery. H1.1 specific to certain tissues.	transcriptional silencing (H1.1), DSB induced apoptosis (H1.1)	severe defects in germline proliferation in <i>C. elegans</i> (H1.1)
H1.0	RI	Terminally differentiated cells	Role in dendritic cell differentiation, MMTV promoter activation	Defective immune system in mice

H1.X	RI	Throughout the nucleus	Regulation of correct mitotic progression	Defects in chromosome alignment, chromosome segregation and spindle morphology. Uncoordinated and egg laying defective <i>C. elegans</i>
H1.t	Possibly RI	Testis specific	ND	No phenotype in spermatogenesis, expression of H1.1, H1.2 and H1.4 increased
H1T2m	Possibly RI	Testis specific	Linker histone	Reduced male fertility
H1oo	Possibly RI	Oocyte specific	regulation of gene expression during oogenesis and early embryogenesis.	ND

Histone H2A

Histone H2A is one of the most diverse groups of histones found across eukaryotes. The diversification of H2A variants is mostly restricted to the C-termini in terms of amino acid sequence and length. Histone H2A has a plethora of variants, including the universal ones such as H2AX and H2A.Z, the vertebrate-specific one such as macroH2A and the mammal-specific H2A.B (formerly known as H2ABbd) (Pehrson and Fried 1992, Chadwick and Willard 2001) (**Table 1-2, Figure 1.4**). H2A.X is present in most of the eukaryotes from *Giardia lamblia* to humans. H2AX variant is characterized by the presence of an amino acid sequence motif, SQ (E or D) ϕ in which ϕ indicates hydrophobic amino acids at the C-terminal (Mannironi, Bonner et al. 1989, Nagata, Kato et al. 1991). The serine in the sequence motif is the site of phosphorylation during the DNA double-stranded breaks producing γ H2AX (Rogakou, Pilch et al. 1998). The γ H2AX forms domains around the break by recruiting and retaining repair proteins during DNA repair. H2AX is also involved in the

phosphorylation of XY bodies for silencing of sex-linked genes (Redon, Pilch et al. 2002, Fernandez-Capetillo, Mahadevaiah et al. 2003).

Another universal histone H2A variant is H2A.Z, which has non-overlapping functions with canonical H2A (Thatcher and Gorovsky 1994). It is essential from ciliated protozoan to mammals. It presents an extended acidic patch domain on the surface of the nucleosome, which is responsible for its interaction with H3 (Fan, Rangasamy et al. 2004). The presence of H2A.Z in a nucleosome affects the physical property and the stability of the nucleosome. H2A.Z is involved in a wide array of functions, including cell cycle regulation (Rangasamy, Greaves et al. 2004), acting as an anti-silencing factor near telomeres in budding yeast (Meneghini, Wu et al. 2003) and preventing antisense transcription in fission yeast (Zofall, Fischer et al. 2009). In budding yeast, nematodes (Updike and Mango 2006), and plants (Deal, Topp et al. 2007), the occupancy of H2A.Z is prevalent at the promoter of non-transcribed genes, whereas in flies (Leach, Mazzeo et al. 2000) and animals (Barski, Cuddapah et al. 2007, Ku, Jaffe et al. 2012), it mostly occurs at active gene promoters. H2A.Z is preferentially enriched at the +1 nucleosome bordering the transcription start sites (TSS)(Barski, Cuddapah et al. 2007). H2A.Z undergoes a myriad of post-translational modifications like acetylation, ubiquitinylation, sumoylation (Sevilla and Binda 2014), thereby affecting its localization and function.

MacroH2A (mH2A) is another class of unique H2A histone variants characterized by the presence of a large (30-kDa) non-histone C-terminal domain (macro domain) (Pehrson and Fried 1992). This domain acts as the binding platform for various chromatin-dependent transcription regulators (Chakravarthy, Gundimella et al. 2005, Ouararhni, Hadj-Slimane et al. 2006). MacroH2A has two isoforms, macroH2A1 and macroH2A2 encoded by two distinct genes (Chadwick and Willard 2001, Kustatscher, Hothorn et al. 2005) (H2AFY and H2AFY2, respectively). MacroH2A1 has two alternative spliced variants, macroH2A1.1 and macroH2A1.2, that differ by only one exon in the macro domain (Pehrson, Costanzi et al. 1997). MacroH2A variants are mostly associated with inactive X chromosomes in female mammals (Chadwick and Willard 2001), centrosomes (Rasmussen, Mastrangelo et al. 2000, Mermoud, Tassin et al. 2001) and inactive genes, and are transcriptionally repressive in nature. However, ChIP-chip studies revealed that apart from

being enriched in transcriptionally repressed genes, mH2A also positively regulates the transcription of 12% of active genes in humans (Gamble, Frizzell et al. 2010). Similar to other histone variants, mH2A also undergoes post-translational modifications. The macrodomain of macroH2A is poly-ADP ribosylated (Kustatscher, Hothorn et al. 2005, Timinszky, Till et al. 2009) and the serine residue in its linker domain is phosphorylated in a cell cycle-dependent manner (Bernstein, Muratore-Schroeder et al. 2008).

Another H2A variant is the mammalian-specific variant H2A.Bbd (Barr Body Deficient) (Chadwick and Willard 2001) which has an approximately 50% sequence identity with canonical histone H2A (Gonzalez-Romero, Mendez et al. 2008). The nucleosomes containing H2A.Bbd is mostly enriched within actively transcribed genes (Gonzalez-Romero, Mendez et al. 2008). It is also associated with spliceosome components, particularly those in the U2 snRNP (Tolstorukov, Goldman et al. 2012). Its interaction with DNA is weaker and binds to shorter segments (118 bp) (Bao, Konesky et al. 2004). H2A.Bbd depleted cells have a genome-wide change in gene expression involving down-regulation of transcription and aberrant mRNA splicing patterns (Tolstorukov, Goldman et al. 2012). In *Candida albicans*, a pathogenic yeast, an unconventional H2A variant, H2A.1 has been recently identified (Brimacombe, Burke et al. 2019) which lacks the conserved serine/threonine phosphorylation site at position 121. H2A.1 aids in ploidy modulation in diploid and tetraploid mating products. In strains that lack the noncanonical histone H2A, the chromosome loss rate is lower than wild-type in aneuploidy-inducing growth conditions, suggesting the presence of H2A promotes chromosome instability (Brimacombe, Burke et al. 2019).

Table 1-2 List of core histone H2A variants.

All known core histone H2A variants and their cell cycle stage-specific expression, functions and knockout phenotype are summarized. ND- Not determined, RC- Replication coupled, RI- Replication independent. Adapted from (Maze, Noh et al. 2014).

Histone	Cell cycle Stage Specific expression	Location	Function	Knockout phenotype
H2A	RC	Throughout the nucleus	Core histone	ND
H2AX	RI	Throughout the nucleus	DNA repair	Male infertility
H2A.Z	RI	Throughout the nucleus	Cell cycle regulation, gene silencing in telomeres, gene activation	Embryonic lethality
macroH2A	Possibly RI	Inactive X Chromosome, centrosomes and inactive genes	Gene silencing	Brain malformation in zebrafish
H2ABbd	RI	Actively transcribed genes, spliceosome components	Gene activation	Down-regulation of transcription and aberrant mRNA splicing patterns

Histone H2B

Histone H2B is relatively less diverse in terms of variants than H2A due to its position constraints in the nucleosome. H2B variants play a very specialized role in chromatin compaction and transcription repression, especially during gametogenesis (Green, Collas et al. 1995). There are no reports of H2B variants in somatic cell lineages to date. In sea urchin, there is evidence of a sperm-specific H2B variant, that has a repeated tail motif binding to the minor groove of DNA, thus contributing to the tight packing of DNA

in sperm heads (Green and Poccia 1989, Green, Collas et al. 1995). Two other testis specific H2B variants have been reported: hTSH2B (Zalensky, Siino et al. 2002) and H2BFWT (Churikov, Siino et al. 2004) (**Table 1-3, Figure 1.4**).

Table 1-3 List of core histone H2B variants.

All histone H2B variants identified till date and their cell cycle stage-specific expression, functions and knockout phenotype are summarized. ND- Not determined, RC- Replication coupled, RI- Replication independent. Adapted from (Maze, Noh et al. 2014).

Histone	Cell cycle stage specific expression	Location	Function	Knockout phenotype
H2B	RC	Throughout the nucleus	Core histone	ND
hTSH2B	RI	Acrosomes, sperm- specific	Chromatin-to-nucleoprotamine transition	ND
H2BFWT	Possibly RI	Sperm nuclei associated with telomeric chromatin, primate- specific	may have telomere-associated functions	ND

Histone H3

Histone H3 is one of the most slowly evolving core histones compared to H2A and H2B (Malik and Henikoff 2003). In yeasts, there is only one non-centromeric histone H3 (H3.3 like) involved in both RC and RI nucleosome assemblies. In mammals, seven H3 variants have been identified to date. H3.1 and H3.2 (Luger, Mader et al. 1997, Schones, Cui et al. 2008) are the canonical histone H3. The variant histone H3 includes H3.3 (Franklin and Zweidler 1977, Ahmad and Henikoff 2002, Mito, Henikoff et al. 2005, Wirbelauer, Bell et al. 2005, Mito, Henikoff et al. 2007, Goldberg, Banaszynski et al. 2010) and centromere-specific variant histone H3 (CENP-A) (Palmer, O'Day et al. 1987, Palmer, O'Day et al. 1991, Sullivan, Hechenberger et al. 1994). Others include testis-specific histone, H3.1t (Witt, Albig

et al. 1996) and primate-specific variant, H3.X and H3.Y (Wiedemann, Mildner et al. 2010) **(Table 1-4, Figure 1.4)**.

H3.1 and H3.2 differ by a single amino acid at position 96, which does not confer functional divergence to the variants. H3.3 differs from H3.2 by four amino acids (at positions 31, 87, 89 and 90) and H3.1 by five amino acids (at position 31 and 87-90) with position 31 located in the N-terminal tail and positions 87, 89, and 90 located in the $\alpha 2$ helix of the histone-fold domain (reviewed in (Maze, Noh et al. 2014). The amino acids at position 87-90 in canonical H3 are the critical residues for preventing its replication-independent deposition, as observed in *Drosophila* (Ahmad and Henikoff 2002) **(Figure 1.4)**. In mammalian cells, the serine residue at position 31 in H3.3 can be phosphorylated. Phosphorylation at S31 has been shown to regulate gene expression by enhancing acetylation of enhancers in both embryonic stem (mES) cells and differentiated cells in mice (Hake, Garcia et al. 2005, Martire, Gogate et al. 2019, Sitbon, Boyarchuk et al. 2020). In addition, introducing any mutation in H3.3 to resemble canonical H3.2 alters its genome-wide enrichment patterns in mES cells (Goldberg, Banaszynski et al. 2010). H3.3 is enriched both at transcriptionally active and repressed regions in the genome. In *Drosophila* and mammals, H3.3 is observed at the gene body of transcribed genes and promoters of both active and inactive genes (Sakai, Schwartz et al. 2009). H3.3 plays a passive role by compensating for the evicted nucleosome as the transcriptional machinery progresses in highly transcribed genes. It also contributes to “active transcriptional memory” by maintaining a continuous nucleosome turnover that allows accessibility of regulatory elements to the corresponding promoters, as observed in *Xenopus* (Ng and Gurdon 2008). However, it is dispensable in maintaining the transcriptional memory in *Drosophila* embryos and mES cells (Goldberg, Banaszynski et al. 2010). Apart from transcriptionally active regions, H3.3 is also found to be enriched at telomeres and pericentromeric heterochromatin in mES cells, mouse embryonic fibroblasts and in somatic cells (Wong, Ren et al. 2009, Goldberg, Banaszynski et al. 2010, Lewis, Elsaesser et al. 2010, Santenard, Ziegler-Birling et al. 2010). In germ cells, H3.3 is enriched during the first male meiotic prophase involved in meiotic sex chromosome inactivation (van der Heijden, Derijck et al. 2007), leading to sex-linked gene inactivation. It is also preferentially

incorporated in the sperm nucleus prior to zygote formation when the protamines are evicted, leading to germline remodeling observed in *Drosophila* (Loppin, Bonnefoy et al. 2005), mammals (Torres-Padilla, Bannister et al. 2006) and plants. In addition, mutations of H3.3K27, not H3K27, leads to chromosome segregation defects (Santenard, Ziegler-Birling et al. 2010).

One of the defining features of a eukaryotic chromosome is the centromeres. Centromeres are structurally and functionally specialized regions that act as the site of spindle microtubule attachment during mitosis. In most organisms, the centromere identity is determined by the presence of nucleosomes containing the H3 histone variant, (CENP-A) encoded by *CSE4* in *S. cerevisiae*, *cnp1* + in *S. pombe*, *CID* in *D. melanogaster*, *HCP-3* in *C. elegans*, and *CENP-A* in *H. sapiens* (Palmer, O'Day et al. 1987, Palmer, O'Day et al. 1990, Palmer, O'Day et al. 1991, Sullivan 2001, McKinley and Cheeseman 2016). Centromeric histone H3 is indispensable in all organisms as its depletion leads to aberrant kinetochore formation and chromosome missegregation. Centromeric histone H3, in contrast to canonical histone H3, undergoes rapid evolution in sequence. They have a highly diverged and shorter N-terminal tail, and a relatively less divergent HFD (50-60% identity). Within HFD, there is a CENP-A targeting domain (CATD) (Black, Brock et al. 2007, Black, Jansen et al. 2007) contributing to a more rigid structure (Black, Foltz et al. 2004) relative to that region in canonical H3. CATD acts as the recognition site of centromere-specific chaperone protein, Holiday junction-recognizing protein (HJURP) (Dunleavy, Roche et al. 2009, Foltz, Jansen et al. 2009).

H3.Y is mostly associated with transcriptionally active regions around the TSS, forming relaxed chromatin (Wiedemann, Mildner et al. 2010). H3.Y is involved in regulating expression of genes involved in cell cycle control in response to stress stimuli, leading to the reduction of cell growth.

H3t replaces canonical H3 in the early stages of spermatogenesis. The expression of meiotic genes is altered in the absence of H3t leading to weakened entry into meiosis. Nucleosomes containing H3t are loosely bound compared to nucleosomes containing H3.1 indicating a possible role of H3t in chromatin remodeling processes during

spermatogenesis, such as in the histone–protamine exchange (Tachiwana, Kagawa et al. 2010, Ueda, Harada et al. 2017). H3.5 is a hominid-specific histone variant expressed in human seminiferous tubules and is accumulated around transcription start site (TSS) (Schenk, Jenke et al. 2011, Urahama, Harada et al. 2016). Similar to H3t, H3.5 nucleosomes are quite unstable and observed during the first step of spermatogenesis and are probably involved in the chromatin reorganization process during sperm maturation.

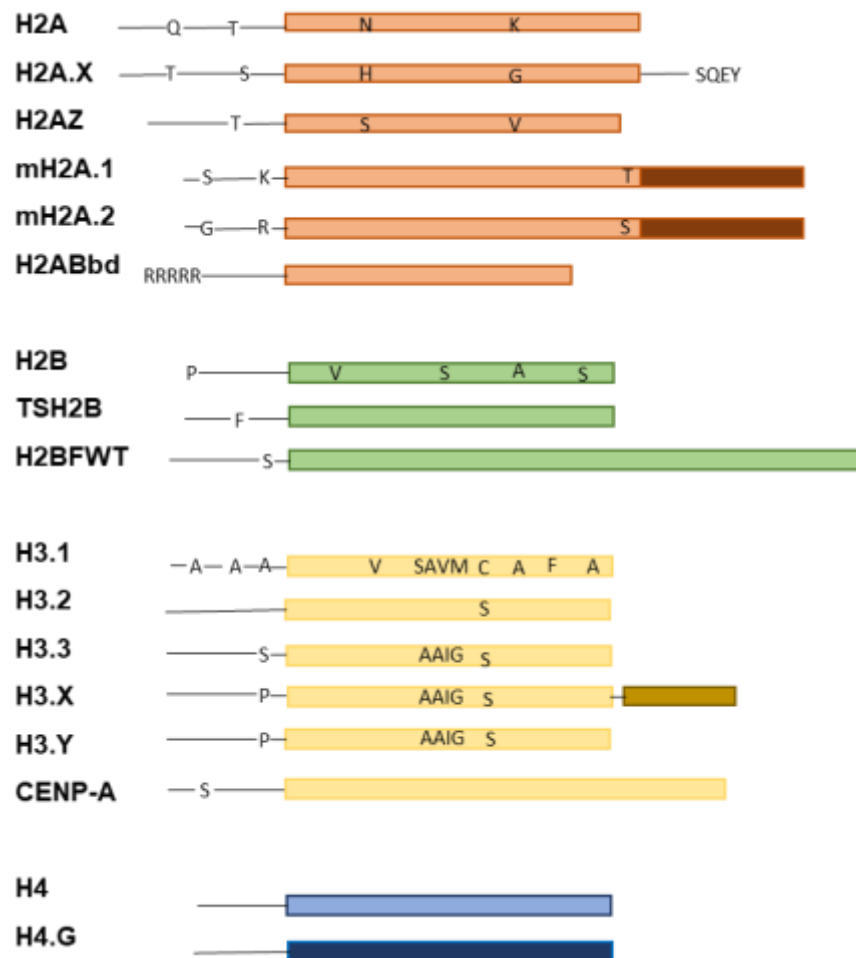


Figure 1.4 Core histone variants in humans.

Line diagrams of histones with variant-specific amino acid residues indicated. Variants that have markedly diverged from their canonical counterparts are marked in different shades of color (for example, histone H3-like centromeric protein A (CENP-A)). Modified from (Maze, Noh et al. 2014). H4G has high sequence divergence between variants, so specific amino acid differences are not indicated.

Table 1-4 List of core histone H3 variants.

All known core histone H3 variants and their cell cycle stage-specific expression, functions and knockout phenotype are summarized. ND- Not determined, RC- Replication coupled, RI- Replication independent. Adapted from (Maze, Noh et al. 2014).

Histone	Cell cycle stage specific expression	Location	Function	Knockout phenotype
H3.1 H3.2	RC	Throughout the nucleus	Core histone	
H3.3	RI	Gene body and promoter region of transcribed genes, telomeres and pericentric heterochromatin	Epigenetic reprogramming, regulating the transcription of active and silent genes	Adult infertility in <i>Drosophila</i> and H3.3A-gene-trap and H3.3B-knockout mice
CENP-A	RI	Centromere	Chromosome segregation	Embryonic lethality at E3.5–E8.5 in mice
H3t	RI	in differentiating spermatogonia Testis specific	Essential for spermatogenesis	ND
H3.X	Possibly RI	Primate specific, expressed in neurons	ND	ND
H3.Y	Possibly RI	Primate specific, expressed in brain cells, in osteosarcoma cells	ND	Knockdown affects genes involved in cell cycle control and cell growth
H3.5	Possibly RI	Hominid specific, expressed in seminiferous tubules in euchromatin	Chromatin reorganization during sperm maturation	ND

Histone H4

Histone H4 is one of the slowest evolving core histones (Malik and Henikoff 2003), and there were no reports of sequence variants of histone H4 in higher eukaryotes for a long time. In lower eukaryotes such as *Trypanosomes* and some urochordates, H4 variants have been found.

In a recent study, a hominid specific histone H4 variant has been identified, H4G (Long, Sun et al. 2019) (**Table 1-5**). H4G lacks five amino acids in the C-terminal region compared to canonical H4, the region required for cell viability in yeast. It has 85% sequence identity with the canonical H4 amino acid sequence. H4G is overexpressed in tumor stage-dependent manner in breast cancer patients, and it enhances rDNA transcription.

Table 1-5 List of core histone H4 variants.

Histone H4 variants identified till date and its properties and functions are summarized. ND- Not determined, RI- Replication independent. Adapted and modified from (Maze, Noh et al. 2014).

Histone	Cell cycle stage specific expression	Location	Function	Knockout phenotype
H4G	Possibly RI	Hominid specific, nucleolar localization, overexpressed in breast cancer cells	Regulates rRNA and protein synthesis	Reduced cell growth

Nucleosome occupancy and regulation of gene expression

The nucleosomal arrangement across genes acts as a barrier for RNA polymerase II (RNAPII)-mediated transcription (Saunders, Core et al. 2006). Therefore, RNAPII recruits additional factors to gain access and thus overcomes this barrier. Besides, the non-uniform

distribution of nucleosomes poses an additional challenge for RNAPII to function. Promoter regions of genes have a reduced occupancy of nucleosomes, whereas the coding region has variable occupancy depending on the transcription status of a gene. These nucleosome-depleted regions (NDRs) are usually characterized by the presence of poly (dA:dT) tracks [except *S. pombe* (Lantermann, Straub et al. 2010), which disfavor nucleosome formation (Ramachandran and Henikoff 2015)]. The NDRs are usually flanked on either side by well-positioned nucleosomes. The downstream +1 nucleosome is highly positioned covering the transcription start site (TSS), which determines the precise positioning of nearby nucleosomes, with nucleosomes density phasing out as we move away from the TSS. The position and the composition of histones in the +1 nucleosome are crucial factors for movement of RNAPII through the gene body and binding of transcription factors (Lai and Pugh 2017). Studies at the promoter regions indicate that the RNAPII interacts differently with the proximal and distal face of the nucleosome while transcription. This skewed interaction has a direct correlation with the asymmetrical positioning of histone variants and their marks within specific nucleosomes (Rhee, Bataille et al. 2014). The nucleosomes are also the site of PTMs and remodeling upon transcription initiation. The transcription factors and the ATP-dependent remodelers are crucial for the maintenance of NDRs as well (Whitehouse, Rando et al. 2007, Hartley and Madhani 2009).

Evolution of histones in eukaryotes

The evolutionary origin of eukaryotic histones can be traced back to the archaeal histones hinting towards archaea being either ancestral state or sister due to its structural conservation. The packaging of nucleosomes in the last eukaryotic common ancestor (LECA) is similar to those of eukaryotes in terms of the presence of histone tails, PTMs of histone tails, and variant histones such as centromeric histone H3 at centromeres (Alva and Lupas 2019). Proteins with HFD are observed in all three domains; bacteria, archaea, and eukaryotes. In contrast to octamer of histones in eukaryotes, archaea contain homologs of H3 and H4 proteins. Archaea can form both homodimers and heterodimers of histones. Archaeal histones consist of a single HFD, and no N-terminal or C-terminal tails (Malik and Henikoff 2003). These histones mostly folded as homodimers polymerize to form tetramers wrapped around 60 bp of DNA or more forming “hypernucleosomes” (Mattioli,

Bhattacharyya et al. 2017). The structural backbone of an archaeal histone dimer can be superimposed to H2A-H2B dimer or to H3-H4 dimer in eukaryotic histones to 2-Å resolution suggesting that although four eukaryotic core histones lack sequence similarity to each other and to archaeal histones, they are structurally identical. In certain species of archaea, tandemly located HFD pairs are constrained to fold together thus giving rise to doublet form of histones. In *Haloferax volcanii*, such doublets further dimerize to form a four HFD like structure which is regularly spaced on a chromosome. Such stages are considered to be the intermediate stage between archaeal and eukaryotic histones promoting the diversification of four core histone families (Ammar, Torti et al. 2012, Talbert, Meers et al. 2019).

A series of evidence suggest that viruses can be the precursor of eukaryotic histones. The giant viruses belonging to the family *Marseilleviridae* encode divergently transcribing HFD doublets that form heterodimers, and these HFDs have unstructured tails, resembling eukaryotic core histone pairs. Therefore, it is plausible that there was a common ancestor of eukaryotic and viral histones (e.g. *Marseilleviridae*) before the eukaryotic histone variants diverged (Erives 2017). *Marseilleviridae* have either acquired these doublet histones from proto-eukaryotes to protect the viral genome from host nucleases or from archaea to package the viral genome in capsids. Thus, eukaryotic nucleosomes might have been acquired from archaea or giant viruses (*Marseilleviridae*) but initially histones might have been selected to package DNA or silence nucleases or transposable elements. All eukaryotes have homologs of core histones.

In case of linker histone H1, which lacks HFD, an independent origin is observed as it is not identified in LECA, archaea, but its carboxy-terminal is found in bacteria. The characteristic winged-helix domain of H1 is found in animals and plants but is absent in several protist groups, indicating an independent acquisition of this domain in animal, fungal, and plant lineages (Kasinsky, Lewis et al. 2001).

Chaperones and their role in the incorporation of histone variants

Histone chaperones are proteins associated with deposition of histones onto DNA and involved in their transfer, but not a part of the final product (nucleosome) (Gurard-Levin, Quivy et al. 2014, Mattioli, D'Arcy et al. 2015, Hammond, Stromme et al. 2017). They mostly carry an acidic patch or histone binding domain to interact with histones (Laskey, Honda et al. 1978). They prevent aberrant DNA- histone interactions in functionally specialized regions (centromere and telomere). Apart from histone deposition they play diverse functions in histone folding (Campos, Fillingham et al. 2010), stabilizing the soluble pool of histones (Cook, Gurard-Levin et al. 2011), influencing histone enzyme interactions (Parthun, Widom et al. 1996, Han, Zhou et al. 2007, Campos, Fillingham et al. 2010), and promoting histone exchange (Belotserkovskaya, Oh et al. 2003, Adkins, Howar et al. 2004, Groth, Corpet et al. 2007). Chaperones were initially identified in *X. laevis* oocytes with H2A-H2B dimers (Laskey, Honda et al. 1978). Chaperones can act as nucleosome assembly factors or can have specificity for particular histones. They can also differ in their loading timing in the DNA.

There are chaperones for H3-H4, H2A-H2B dimers, and those specific for H2A, H2B, H3 variants (**Table 1-6**). Chaperones specific for variants recognize the solvent exposed residues of the variant histones. There are general histone chaperones, nuclear autoantigenic sperm protein (NASP) and anti-silencing factor 1 (Asf1) for H3 containing nucleosomes (both canonical and variant) (Natsume, Eitoku et al. 2007, Bowman, Koide et al. 2017), and Nap1 for H2A-H2B dimer. There is a remarkable diversity among histone chaperones, including lack of any common domain. NASP occurs in two forms: Somatic NASP, expressed ubiquitously, and testicular NASP expressed in testis and ovary. NASP has H3-H4 chaperone activity *in vitro* (Wang, Gao et al. 2008, Osakabe, Tachiwana et al. 2010). Hif1, the homolog of NASP in *S. cerevisiae* (Poveda, Pamblanco et al. 2004) and Sim3 in *Schizosacharomyces pombe* (Dunleavy, Pidoux et al. 2007), respectively, have been reported to have *in vivo* chaperone activity. NASP maintains the H3-H4 reservoir in the cell by balancing between histone protection and degradation by autophagy (Richardson, Batova et al. 2000).

Asf1 is the most conserved H3-H4 chaperone and was identified as a transcriptional derepressor in yeast (English, Adkins et al. 2006). Asf1 can coordinate the process of histone incorporation during replication fork progression. They can regulate (a) *de novo* histone deposition by handing over newly synthesized H3.1-H4 dimers to CAF-1 (a canonical H3 chaperone) (Tyler, Collins et al. 2001, Mello, Sillje et al. 2002) or (b) by recycling the old histones with Mcm2-7 helicase to evict old histones and redistribute in daughter strands. Asf1 interacts, along with CAF-1 or HIRA, to channelize the deposition of canonical and variant histone H3 in distinct deposition pathways (Natsume, Eitoku et al. 2007).

Biochemical analysis of soluble histone complexes suggests the presence of CAF-1 with the replication coupled H3.1 variant (Liu, Roemer et al. 2012, Liu, Roemer et al. 2016); HIRA (Ahmad and Henikoff 2002, Tagami, Ray-Gallet et al. 2004) and death domain-associated protein (DAXX) with the replication-independent variant H3.3 (Drane, Ouararhni et al. 2010, Lewis, Elsaesser et al. 2010). Besides this HJURP (Scm3 in yeast) is associated with the centromeric H3 variant CENP-A (Foltz, Jansen et al. 2009). CAF-1 is the H3.1-H4 histone specific chaperone coupled to DNA replication and repair (Smith and Stillman 1989). CAF-1 is composed of three subunits: p150, p60, and RbAp48 (p48) in human cells (Cac1, Cac2, and Cac3 in yeast) (Kaufman, Kobayashi et al. 1995). The large subunit, p150, interacts with PCNA to promote DNA synthesis coupled deposition (Shibahara and Stillman 1999). This interaction is facilitated by the phosphorylation of p150 by Cdc7/ Dbf4. The CAF-1 dimerization by p150 subunit promotes H3-H4 tetramerization (Quivy, Grandi et al. 2001). CAF-1 has high rates of sequence divergence; however, they are functionally conserved.

HIRA is an H3.3-specific chaperone that deposits during interphase, independent of DNA replication. The yeast HIRA complex consists of Hir1p, Hir2p, Asf1p, Hir3p, and Hpc2p. Human HIRA resembles in sequence to that of Hir1p and Hir2p of yeast, and bioinformatic analyses have revealed ubinuclein 1 (UBN1) and calcineurin-binding protein1 (CABIN1) in humans to be the orthologs of Hpc2p and Hir3p (Banumathy, Somaiah et al. 2009). The HIRA complex mediates H3.3 localization at bivalent promoters, active promoters, and transcribed gene bodies. The HIRA complex interacts with H3.3 via

its UBN1 subunit that binds preferentially to H3.3 G90 residue (Elsaesser and Allis 2010, Ricketts, Frederick et al. 2015, Ricketts and Marmorstein 2017). Mutation of this residue abrogates the interaction. In budding yeast, CAF-1 and HIRA compensate for each other's function. There is crosstalk in HIRA and CAF-1 deposition pathways in human cells. HIRA can bind to naked DNA and can interact with RNAPII, hinting towards its recruitment at transcription start sites.

DAXX is another H3.3 chaperone (Drane, Ouararhni et al. 2010, Goldberg, Banaszynski et al. 2010, Lewis, Elsaesser et al. 2010) involved in loading at regulatory regions during neuronal activation in calcium- and calcineurin-dependent phosphorylation manner. DAXX can associate with the chromatin remodeler, α -thalassemia/ mental retardation X-linked (ATRX) protein, and thus can be recruited to specific genomic loci (Dhayalan, Tamas et al. 2011, Eustermann, Yang et al. 2011, Iwase, Xiang et al. 2011). The DAXX/ ATRX complex interacts with the unique residues at 87-90 position in H3.3 and deposits this histone variant at pericentromeres, telomeres, and repetitive elements (Liu, Xiong et al. 2012). Taken together, DAXX and HIRA act as chaperones for the same histone variant but play different roles by interacting with various cellular machinery.

HJURP is another centromere histone H3 specific chaperone involved in the loading of CENP-A in epigenetically defined centromeres (Dunleavy, Roche et al. 2009, Foltz, Jansen et al. 2009). HJURP was initially identified as the protein that binds to Holliday junctions (recombination intermediates) *in vitro*. The newly synthesized CENP-A is deposited at centromeres during late telophase and early G1 in human cells (Jansen, Black et al. 2007). This deposition timing overlaps with the localization of HJURP at centromeres. Experiments in chromatin fibers to identify the centromeric specific location of H3.3 during replication suggested that H3.3 may act as a placeholder and is later replaced to CENP-A by HJURP-dependent manner (Dunleavy, Almouzni et al. 2011).

Table 1-6 List of histone chaperones identified till date.

Their homologs in yeast, corresponding histones and functions of chaperones are enlisted. Adapted and modified from (Hammond, Stromme et al. 2017) and (Gurard-Levin, Quivy et al. 2014).

Histone chaperone	<i>S. cerevisiae</i> homologue (s)	Histone preference	Function
Anti-silencing function 1 A/B (ASF1A/B)	Anti-silencing function 1 (Asf1)	H3.1-, H3.2-, H3.3-H4	Histone donor to CAF-1 and HIRA
Minichromosome maintenance protein 2 (MCM2)	Minichromosome maintenance protein 2 (Mcm2)	CENP-A-, H3.1-, H3.2-, H3.3-H4	Co-chaperoning of H3-H4 dimer with ASF1
Retinoblastoma associated protein 46 (RbAp46)	Histone acetyltransferase 2 (Hat2)	H3-H4	Component of HAT1 holoenzyme, binds to histone H4, aids in acetylation of H4
Heat shock protein 90A/B (HSP90A and HSP90B)	Heat shock cognate (Hsc82), Heat shock protein 82 (Hsp82)	H1, H2A, H2B, H3, H4	Folding of translated H3-H4 protein
Heat shock cognate 70 (HSC70)	Stress-seventy subfamily A (Ssa1, Ssa2, Ssa3, Ssa4)	H1, H2A, H2B, H3, H4	Involved in histone (H3-H4) protein folding
Somatic nuclear autoantigenic sperm protein (sNASP)	Hat1 interacting factor (Hif1)	H3.1-, H3.2-, H3.3-H4, H1	maintain a soluble reservoir of mature H3-H4, stabilizes soluble H3-H4 pools by assisting with histone folding and by protecting H3-H4 from degradation by chaperone-mediated autophagy
Importin 4 (IPO4)	ND	H3.1-, H3.2-, H3.3-H4	Import of histones in the nucleus
Suppressor of Ty 6 (SPT6)	Suppressor of Ty (Spt6)	H3-H4	Transcription initiation and elongation

ND	Regulator of Ty 1 transposition 106 (Rtt106)	H3-H4	Heterochromatin silencing
ND	Chaperone for Htz1/H2A-H2B dimer 1 (Chz1)	H2A.Z-H2B	H2A.Z incorporation by SWR1
Holliday junction recognition protein (HJURP)	Suppressor of chromosome missegregation 3 (Scm3)	CENP-A-H4 (Cse4-H4)	Deposition factor involved in centromeric maintenance
Patient SE translocation (SET)	Vacuolar protein sorting 75 (Vps75)	H3-H4	Assists Asf1 in loading
Nucleosome assembly protein 1-like (NAP1L1-6)	Nucleosome assembly protein (Nap1)	H2A-, H2A.Z-H2B, H3-H4, H1	Cytosolic-nuclear transport, replication, transcription
Nucleophosmin 1 (NPM1)	ND	H3-H4, CENP-A-H4, H1	Plays role in chromatin remodeling, and mitosis as well as in DNA repair, replication and transcription
Nucleoplasmin 2 (NPM2)	ND	H2A-H2B	
Nucleoplasmin 3 (NPM3)	ND	ND	
Nucleolin (NCL)	ND	H2A-H2B, H1	
CAF-1 (Chromatin assembly factor 1) complex	Chromatin assembly complex 1 (Cac1), Chromatin assembly complex 2 (Cac2), Chromatin assembly complex 3 (Cac3)	H3.1-H4	Aids in DNA synthesis coupled deposition, replication, DNA repair
Retinoblastoma associated protein 48 (RbAp48)	Multi-copy suppressor of IRA1 (Msi1)	H3.1-, H3.2-, H3.3-H4	Component of the CAF-1 complex
Histone regulation A (HIRA)	Histone regulation (Hir1, Hir2, Hir3, Histone periodic control; Hpc2)	H3.3-H4	Aids in DNA synthesis independent deposition.
Suppressor of Ty 16 (SPT16)	Suppressor of Ty 16 (Spt16)	H2A-H2B, H3-H4	Component of the FACT complex

Structure-specific recognition protein 1 (SSRP1)	PO11 binding 3 (Pob3)-non- histone protein 6 (Nhp6A/B)	H2A-H2B, H3-H4	Component of the FACT complex, transcription elongation, regulation of chromatin remodeling
Death domain-associated protein 6 (DAXX)	ND	H3.3-H4	DNA synthesis independent deposition factor, role in telomere maintenance, ribosomal DNA, pericentric heterochromatin
Alpha-thalassemia/mental retardation syndrome X-linked (ATRX)	ND	H3.3-H4	DNA synthesis independent deposition factor in combination with DAXX, role in telomere and pericentric heterochromatin maintenance

Candida albicans

Candida albicans is a diploid budding yeast (Riggsby, Torres-Bauza et al. 1982) belonging to phylum Ascomycota and subphylum Saccharomycotina. It is one of the most abundant fungal species in the human microbiota, as well as the most prevalent fungal pathogen (Fisher, Gurr et al. 2020). It primarily colonizes various sites of the host body asymptotically, mostly in the skin, mouth, gastrointestinal and genitourinary tracts of healthy individuals (Noble, Gianetti et al. 2017). However, any variation in the host immunity, stress or other resident microbiota can lead to overgrowth of *C. albicans*, giving rise to varying degrees of infections ranging from superficial mucosal to hematogenously disseminated candidiasis. Despite being a commensal, it can even proliferate in healthy people to cause restricted infections in the skin, nails, and mucous membranes.

CUG clade species

In the phylum Ascomycota, a group of fungi underwent a genetic code deviation where the CUG codon encodes predominantly for serine instead of universal leucine (Santos and Tuite 1995). These constitute the CUG clade species. Until 2016, the only known example of codon reassignment in the nuclear genome of eukaryotes was the reassignment of CUG from leucine to serine in a clade of budding yeasts that includes *Candida albicans* (Kawaguchi, Honda et al. 1989, Moura, Paredes et al. 2010). In 2016, the second reassignment of the CUG codon to alanine was observed in *Pachysolen tannophilus* (Muhlhausen, Findeisen et al. 2016, Riley, Haridas et al. 2016). Recently a systemic analysis of 52 yeast species belonging to the CUG clade in which reassignment of the CUG codon has occurred was carried out (Krassowski, Coughlan et al. 2018). This classified the CUG clade species as Ala, Ser1, Ser2, Leu1, and Leu2 clades as well as paraphyletic outgroup taxa (Leu0) with the standard code. There are two models proposing the mechanism of codon reassignment during the course of evolution: ambiguous intermediate model, and unassigned codon model (Sengupta and Higgs 2015). In the ambiguous intermediate model, a codon undergoes a transition phase during which it can be translated to both the amino acids, old and new. This ambiguity can arise due to anticodon misreading or competition between two competing nonambiguous tRNAs, eventually producing cells with a mixture of proteins with different amino acids at each site (Massey, Moura et al. 2003). In the unassigned codon model, out of the 64 codons, tRNA for a corresponding codon is either lost or becomes nonfunctional, making the codon untranslatable. The tRNA for any other amino acid, when undergoes a mutation, later captures the unassigned codon. This reassignment of the CUG codon from Leu to Ser occurred 170 million years ago (Fitzpatrick, Logue et al. 2006). A single tRNA with CAG anticodon decodes the CUG codon as serine in these species. However, this tRNA is generally charged with serine (97%). Still, it is also mischarged with leucine (3%) *in vivo* in certain species like *Candida zeylanoides* making CUG codon “polysemous” (Suzuki, Ueda et al. 1997) and thus providing evidence for the ambiguous intermediate theory. Sequence analyses of tRNAs and their introns from *Candida* species suggest that this ambiguous tRNA (tRNA_{CAGSer}) emerged before the divergence of *Saccharomyces* and *Candida* genera and competed with the wild-type

tRNA_{CAGLeu} for CUG codons during mRNA decoding. The ancestor of *Saccharomyces* spp. lost this tRNA (tRNA_{CAGSer}) retaining the universal genetic code, while the ancestor of the CUG clade lost the corresponding tRNA_{CAGLeu} thus coding for serine instead of leucine. Comparative genomics studies to identify the origin of 17,000 CUG codons present in the *C. albicans* genome suggest that this code deviation resulted in a massive mutational change of CUGs to UUG or UUA Leu codons (Massey, Moura et al. 2003). The CUG codons present in extant CUG clade species have evolved relatively recently from codons encoding serine or amino acids with similar chemical properties rather than the Leu codon (Massey, Moura et al. 2003).

In the course of evolution of budding yeast, the CUG codon was reassigned in three independent events in three separate branches of Saccharomycotina, giving rise to five different clades; Ala, Ser1, Ser2, Leu1, and Leu2 clades. The Ser1 clade includes many pathogenic *Candida* species such as *C. albicans*, *C. tropicalis*, and extends till *Babjeviella* (Shen, Opulente et al. 2018) **(Figure 1.5)**. The Ser2 clade constitutes of two genera *Ascoidea* and *Saccharomycopsis*. The Ser2 clade is the sister to the Leu1 clade, which contains *Saccharomyces cerevisiae*, *Cyberlindnera*, and *Wickerhamomyces*. There are unique tRNAs carrying anticodon for CUG in Ser1, Ser2, and Ala1 clade species. These novel tRNAs arise as a result of mutations of preexisting tRNAs of serine and alanine. The tRNA_{CAGSer} molecule of Clade 1 has a G at position 37, which is at 3' of the anticodon, whereas Ser2 clade species contain an A at position 37. In *C. albicans*, a G at this position is responsible for the misincorporation of leucine in 3% of the genome. Except for *B. inositovora*, this G at position 37 is conserved across all the Ser1 clade species. Like other CUG clades, Ser2 clade species have two tRNAs to read CUGs, both for serine and leucine, although mass spectrometry analyses suggest they code mostly for serine. This observation also supports the ambiguous intermediate model of codon evolution. The Ser2 clade is at the final stage of evolution since *Ascoidea rubescens*, a member of the Ser2 clade, have lost the tRNA_{CAGLeu} gene, whereas the remaining four clades have both the tRNAs. Studies suggest that misincorporation of leucine can alter various attributes in *C. albicans* such as morphogenesis, phenotypic switching, and adhesion (Miranda, Rocha et al. 2007). Thus, CUG codon ambiguity generates protein diversity within the cell, which can be

advantageous to asexual microorganisms (Miranda, Silva-Dias et al. 2013). However, this independent parallel reassigment of the CUG codon in five clades indicates that this CUG codon reassigment is driven by the natural selection against the tRNAs and not by the outcome of proteomic changes.

An emerging hypothesis is that the tRNA_{CAG}Leu is cleaved by toxins secreted by virus-like elements (VLEs). VLEs are cytoplasmic linear DNA plasmids that code for a toxin and an antitoxin. There are examples of toxin secreted by *Kluyveromyces lactis* (Leu1 clade) known to cleave tRNA^{Glu}(UUC) and from strains of *Millerozyma acaciae* and *Debaryomyces robertsiae* (Ser1 clade) to cleave tRNA^{Gln}(UUG). BLAST searches have identified such VLE-like plasmids in Leu2 and Ser2 clade species as well (Frank and Wolfe 2009, Satwika, Klassen et al. 2012). Thus, the hypothesis suggests that the VLEs infected and lowered the cellular pool of leucine tRNAs. The response from the yeast lineages was either by changing the genetic code or by acquiring new resistant tRNAs while retaining the universal code. Thus, this CUG codon reassigment might be a drastic mechanism of defense response by host (yeasts) against an infectious agent (Krassowski, Coughlan et al. 2018).

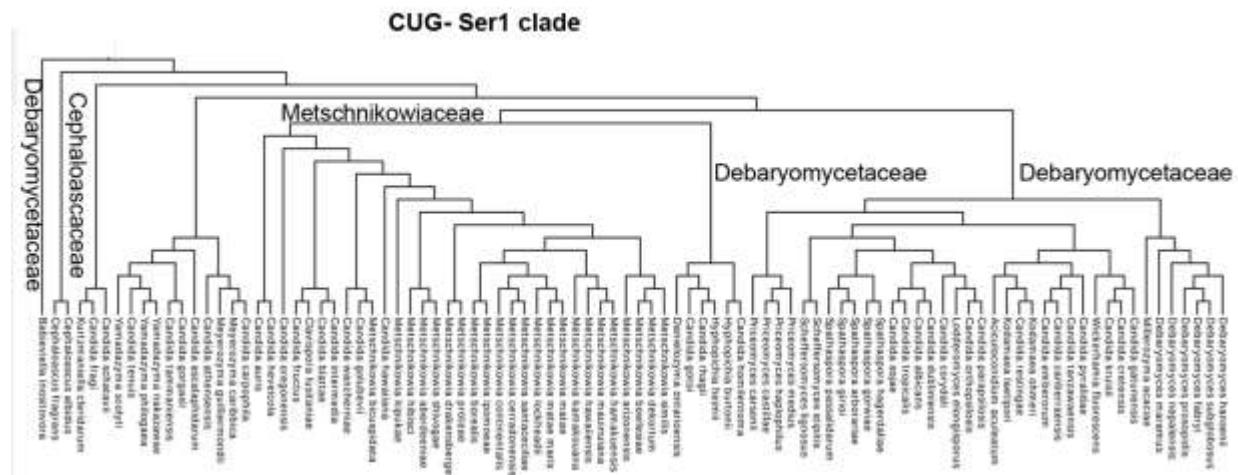


Figure 1.5 Phylogenetic tree depicting the CUG clade species. 94 fungal species are listed in this phylogenetic tree. The CUG-Ser1 clade contains species from the families Debaryomycetaceae, Metschnikowiaceae, and Cephaloascaceae (listed here). Other CUG clades include the CUG-Ser2 clade consisting of families Ascoideaceae and Saccharomycopsidaceae; and the CUG-Ala clade which includes several taxa in need of reassigment (not listed here). Adapted and modified from (Shen, Opulente et al. 2018).

Pathogenic traits of *C. albicans*

A number of virulence factors and fitness attributes modulate the ability of *C. albicans* to infect diverse host niches. These anatomical niches differ drastically in terms of pH, nutrient sources and availability, and oxygen content. Phenotypic transitions, the expression of adhesins and invasins on the cell surface, thigmotropism, biofilm formation, and the secretion of hydrolytic enzymes are the major virulence factors (**Figure 1.6**). In addition, the ability of the organism to adapt to fluctuations to environmental pH, nutrient availability, and robust stress response mechanisms enhance its fitness to changing environmental conditions (Mayer, Wilson et al. 2013).

pH is known to modulate the morphological forms wherein low pH (<7) favors yeast form of growth, while high pH (>7) is required for hyphal growth in *C. albicans* (Odds 1985, Sudbery 2011). Starvation, the presence of serum or N-acetylglucosamine, physiological temperature, and CO₂ also induce the formation of hyphae (Sudbery 2011). The pH of human blood and tissues is moderately alkaline (pH 7.4), while the pH of the digestive tract, depending on its location, ranges from very acidic (pH 2) to alkaline (pH 8), and the pH of the vagina is acidic (pH 4.78). Neutral to alkaline pH causes severe stress to *C. albicans*. *C. albicans* have cell surface proteins like β -glycosidases to adapt to changing pH. It can also control extracellular pH by alkalization of the environment during nutrient scarcity (Vylkova, Carman et al. 2011).

C. albicans has a specialized group of proteins known as adhesins that mediate adherence to other cells, biotic, and abiotic surfaces (Sundstrom 2002, Verstrepen and Klis 2006). The ability of *C. albicans* to adhere via adhesins is a crucial and first step in host invasion and biofilm formation. Most of the adhesins are cell surface proteins. *C. albicans* adhesins include three gene families: agglutinin-like sequence (ALS) protein family, which consists of eight members (Als1–7 and Als9), Hwp family and Hyr. Hwp family consists of Hwp1, Hwp2, Eap1 and Rbt1. Hwp1 is a hypha-associated GPI-linked protein that facilitates covalent linkage between *C. albicans* hyphae to host cells (Staab,

Bradway et al. 1999). Apart from cell surface adherence, Hwp1 and Als3 have also been reported to be involved in biofilm formation (Nobile, Schneider et al. 2008).

C. albicans hypha invades into host cells using two mechanisms: induced endocytosis and active penetration (Zakikhany, Naglik et al. 2007, Naglik, Moyes et al. 2011). Induced endocytosis is mediated by the specialized proteins on the cell surface (invasins) that mediate binding to host ligands and are thus engulfed by the host cells. It is mainly dependent on host activities. Two invasins identified so far are Als3 and Ssa1 (Zakikhany, Naglik et al. 2007, Sun, Solis et al. 2010). On the other hand, active penetration is a fungal-driven process that requires viable *C. albicans* hypha but not host activity. There are certain unidentified host factors involved in active penetration. Fungal adhesion and physical forces are considered to be the key players in penetration (Wachtler, Wilson et al. 2011). Secreted hydrolases are also believed to contribute to active penetration (Wachtler, Wilson et al. 2011). Secreted hydrolases also increase the efficiency of extracellular nutrient acquisition by hydrolyzing host proteins (Naglik, Moyes et al. 2011). *C. albicans* expresses three different classes of secreted hydrolases: proteases, phospholipases, and lipases. Sap proteins are encoded by a family of 10 *SAP* genes. The level of Sap activity is correlated to virulence in *C. albicans* (Naglik, Challacombe et al. 2003).

Another pathogenic trait of *C. albicans* is its ability to form biofilms (Fanning and Mitchell 2012). Both abiotic and biotic cell surfaces are prone to biofilm formation. It is a stepwise process involving adherence of yeast cells to a substrate, proliferation of yeast cells, emergence of hyphal and pseudohyphal cells, formation of extracellular matrix material and, finally, dispersion of yeast cells from biofilms to seed new sites (Nobile, Fox et al. 2012). *C. albicans* biofilms have an additional advantage to free-floating cells as they do not trigger the production of reactive oxygen species (ROS) and are impervious to killing by neutrophils (Xie, Thompson et al. 2012).

Contact sensing by *C. albicans* to both biotic and abiotic surfaces is crucial for successful pathogenicity (Kumamoto 2008). On coming in contact with a surface, yeast cells switch to hyphal growth form and can even invade the substratum in mucosal membranes. Contacts with a solid surface also promote biofilm formation. Ridged surfaces give rise to

the directional hyphal formation. This property of *C. albicans* is essential for epithelial cell damage and virulence.

C. albicans is exposed to various nutrient sources when it colonizes in the gut and also during infection at multiple sites of the body. However, it can utilize all the host-derived nutrient sources, glucose, lipids, proteins, and amino acids, depending on the niche (Brock 2009). Metal acquisition such as zinc is crucial in certain stages of *C. albicans* infection (Citiulo, Jacobsen et al. 2012). Copper and manganese are also required for fungal growth. Besides being able to adapt to these changing nutrients, it also responds to the host and pathogen-induced changes by switching to hyphal or a hypervirulent form. In essence, the pathogenic traits of *C. albicans*, especially its ability to switch forms, makes it a successful pathogen.

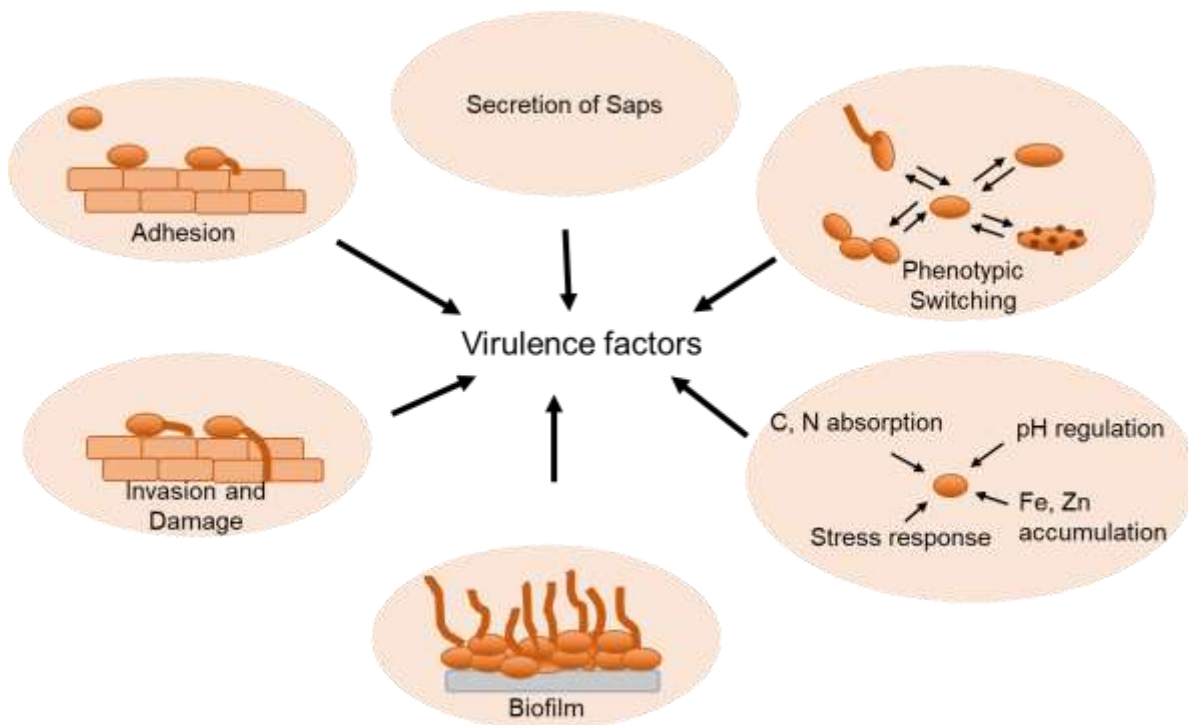


Figure 1.6 Outline of the pathogenic traits of *C. albicans*.

C. albicans yeast cells adhere to host surfaces by the expression of adhesins. Contact to the host cell surface induces yeast to hypha transition. The fungus penetrates the host cells by adhesion, followed by the application of physical forces and secretion of fungal hydrolases to break down the barriers. The yeast cells also attach to abiotic (e.g., catheters) or biotic (host cells) surfaces that can give rise to the formation of biofilms. Phenotypic plasticity also influences the adaptation to host niche and biofilm formation in *C. albicans*. In

addition, secretion of Saps contributes to virulence of the organism. Besides these virulence factors, several fitness traits such as metabolic flexibility and uptake of different compounds as carbon (C) and nitrogen (N) sources, and essential trace metals including iron (Fe), zinc (Zn), copper (Cu) and manganese (Mn) contribute to maintenance of fungal pathogenicity.

Morphological plasticity of *C. albicans*

Many human fungal pathogens including *C. albicans*, *Histoplasma capsulatum*, and *Coccidioides immitis* switch between different morphological forms. These transitions are crucial for virulence. Nine distinct cell shapes have already been observed in *C. albicans* arising due to environmental cues (Kadosh 2017). These different morphological forms are associated with various niches and also vary in their propensity to adapt to virulent or pathogenic lifestyle (Noble, Gianetti et al. 2017). Among these transitions, yeast to hyphal transition is most extensively characterized (Lo, Kohler et al. 1997); (Braun and Johnson 1997) (Braun, Head et al. 2000) (Saville, Lazzell et al. 2003); (Carlisle, Banerjee et al. 2009) (Gow, Brown et al. 2002) (Figure 1.7).

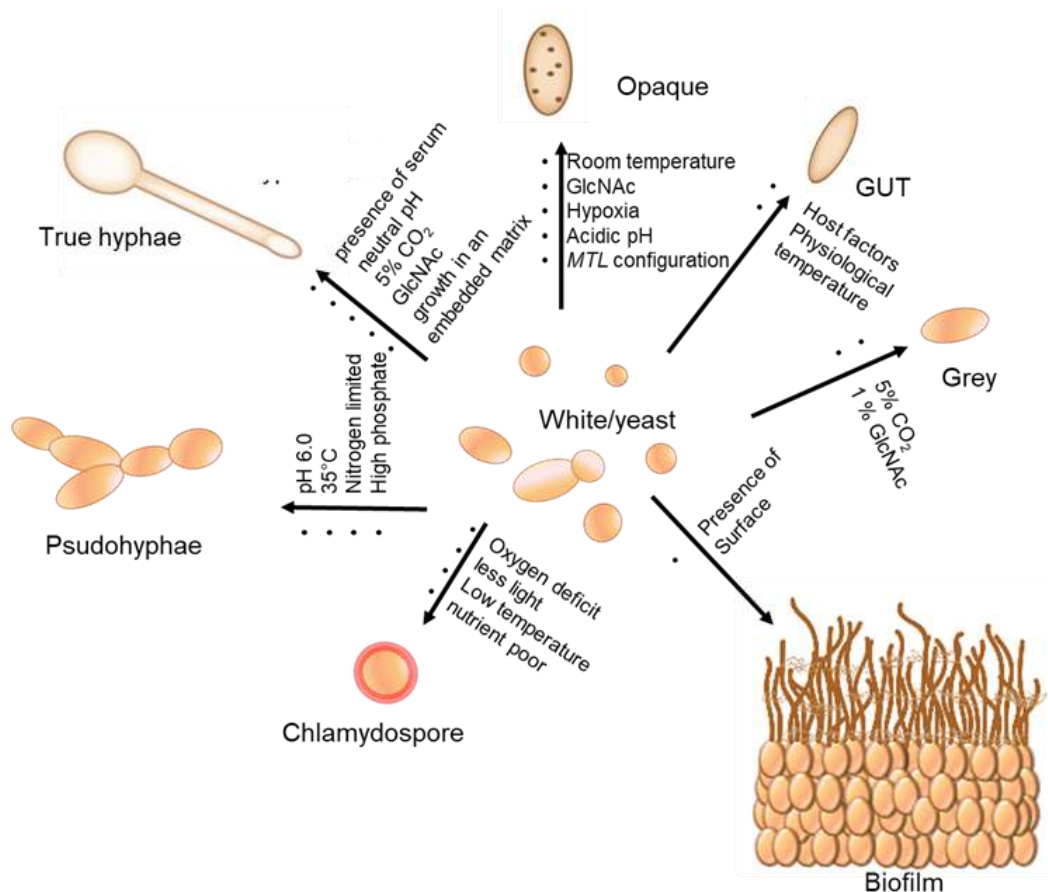


Figure 1.7 Phenotypic transitions in *C. albicans*.

C. albicans cells switch reversibly between yeast (also known as white (**a**/ α)), hyphae, and pseudohyphae under diverse host niches. Chlamydoconidia are produced from the terminal (suspensor) cells of multicellular hyphae or pseudohyphae under harsh growth conditions. Other yeast-like elongated phenotypes include opaque, gray and GUT. *C. albicans* mating-type-like (*MTL*) loci, *MTLa* ('**a**') or *MTL α* (' α ') cells switch between white (**a** or α) and opaque (**a** or α) phenotypes. White (**a** or α) cells resemble typical white (**a**/ α) yeasts, while opaque (**a** or α) cells are elongated and have 'pimple' structures on their cell surface. GUT cells represent a commensal form of *C. albicans* in the GI tract of individuals. *C. albicans* also can give rise to a multicellular community like structure in the form of biofilms.

Switching between yeast and hypha

Yeast cells, also known as 'white' cells, are unicellular and round-to-oval in shape (Odds 1985, Sudbery, Gow et al. 2004). They reproduce by budding and the nuclear division occurs at the junction of mother-daughter cell. After cytokinesis, as the progeny cells detach completely from the mother cells and thus yeasts are considered to be unicellular (solitary). In contrast, hyphal cells are long, filamentous with parallel walls, and lack constrictions at septal junctions (Sudbery 2011). Following cytokinesis, hyphal cells remain attached to each other, thus giving rise to a multicellular branched filamentous structure. There are several *in vitro* conditions known to induce these transitions. There is another morphological form termed pseudohyphae, which shares properties of both yeast and hyphae. The nuclear division occurs at the mother-daughter junction like yeast cells, but cells remain attached after cytokinesis, similar to hyphae (Sudbery, Gow et al. 2004). Although unlike hyphae, the junctions are demarcated by visible indentations in pseudohyphae and cells do not have parallel walls.

Previously, yeast cells were considered as commensals, whereas hyphal forms are more virulent. Hyphal cells are invasive in solid media, express several virulence specific factors such as adhesin like proteins (Hwp1), agglutinins (Als3) (Mayer, Wilson et al. 2013), antioxidant defense proteins (Sod5) (Martchenko, Alarco et al. 2004) and tissue degrading enzymes (Saps) (Naglik, Challacombe et al. 2003). During the transition from commensal to the pathogen, hyphal cells acquire trace metals like iron and zinc from a host

(Citiulo, Jacobsen et al. 2012). It also escapes phagocytosis by piercing the macrophage membrane (Krysan, Sutterwala et al. 2014).

Hypha bring about the damage by a cytolytic toxin called Candidalysin, a peptide generated from a parent protein, Ece1 (Wilson, Naglik et al. 2016). *ECE1* is one of the members of the core filamentation network in *C. albicans* and is highly expressed during hyphae formation (Birse, Irwin et al. 1993). Candidalysin intercalates and permeabilizes target epithelial membranes inducing cell lysis. The deletion of the Candidalysin-encoding region only from the *ECE1* gene was unable to activate or damage epithelial cells *in vitro* and show attenuated virulence in two *in vivo* models of mucosal infection (Moyes, Wilson et al. 2016). Thus, hyphal cells can actively penetrate the tissue by Candidalysin whereas yeast cells colonize the surface without mounting any immune response. However, in disseminated candidiasis, all three morphological forms (yeast, hyphae and pseudohyphae) are essential for successful infection. Mutants locked in any phase are unable to infect the host, thus proving that phenotypic transition among these three forms is the crucial player in *C. albicans*-host interaction and pathogenesis.

Chlamydospores are rounder than yeast cells and possess thick walls. They are formed by suspensor cells, found at the termini of hyphal filaments in response to starvation or hypoxia (Staib and Morschhauser 2007). The actual biological function of chlamydospores still remains elusive. Although they are readily induced *in vitro*, they are rarely found at the sites of infection. Nuclear division occurs in the suspensor cell, followed by the migration of one of the progeny nuclei to the nascent chlamydospore while remains attached to its mother cell.

White opaque gray transition

The ability to undergo white-opaque transition depends on the homozygosity of the mating type locus (*MTL*). The majority (90%) of *C. albicans* strains are unable to undergo switching due to heterozygosity at the *MTL* locus (*MTL α* / *MTL α*) (Slutsky, Staebell et al. 1987, Soll, Morrow et al. 1993, Johnson 2003, Lockhart, Daniels et al. 2003). *MTL* heterozygous strains are unable to switch due to the presence of the heterodimeric **a1** / **α 2**

repressor (Miller and Johnson 2002, Lohse and Johnson 2009). This is formed from the proteins encoded by the *MTL* locus, a1 protein by the *MTLa* locus, and the $\alpha 2$ protein encoded by the *MTL α* locus. The white opaque transition is a prerequisite to the sexual mating in *C. albicans* (Hull, Raisner et al. 2000). White (**a/a** or α/α) cells are yeast cells that form round, shiny, domed colonies on solid media. In room temperature, white cells occasionally (1 out of 10000) switch into opaque cells (Lockhart, Daniels et al. 2003). Opaque cells are elongated, oblong, have prominent vacuoles, and pimples on the surface. Their colonies are slightly darker and flattened compared to white cell colonies (Slutsky, Staebell et al. 1987, Johnson 2003). White and opaque cells differ in mating abilities (opaque cells are mating competent), interaction with host immune system (opaque cells are resistant to phagocytosis), colonization on host epithelial tissue, and sensitivity to filament inducing signals (Miller and Johnson 2002). The expression of approximately 1000 genes is altered as cells switch from white to opaque form. There are several environmental factors affecting the switching frequency. The presence of N-acetylglucosamine (Huang, Yi et al. 2010), hypoxia and acidic pH promote white to opaque transition whereas glucose, low levels of CO₂ (Huang, Srikantha et al. 2009), alkaline pH and mammalian body temperature reverses the cells from opaque to white form (Lohse and Johnson 2016). The actual biological relevance of white opaque transition is its ability to mate. When opaque **a** and α -cells come in close proximity, they secrete pheromones, inducing cell cycle arrest and form polarized mating projections (shmoo), leading to nuclear fusion to produce tetraploid **a**/ α cells. White (**a** or α) cells are speculated to have a special role in mating by the formation of sexual biofilm that brings the mating competent opaque cells in close proximity (Daniels, Srikantha et al. 2006, Soll and Daniels 2016). Since the majority of *C. albicans* strains are heterozygous, they are mating incompetent and undergo clonal reproduction, however the additional requirement of *C. albicans* to undergo a phenotypic transition before mating remains a mystery.

Gray cells are smaller than conventional yeast form, lack pimples on the surface of cells, and mate with at a very low frequency (in between that of white and opaque cells) (Tao, Du et al. 2014). In other words, it represents an intermediate morphology between white and opaque form. *MTL a/a* or α/α strains can switch to opaque as well as gray form

in 1% N-acetylglucosamine, as a sole carbon source, and 5% CO₂. Interestingly, *MTL a/α* is also capable of switching to gray forms in nutrient-rich conditions. Gray cells show differences in global gene expression in comparison to white and opaque cells in secreted aspartyl protease (Sap) activity and infection ability in *ex vivo* tongue infection model (Tao, Du et al. 2014).

White-GUT transition

Gastrointestinally induced transition (GUT) cells were identified in a screen of factors mediating fungal commensalism in the GI tract (Pande, Chen et al. 2013). GUT cells were isolated by laboratory-induced overexpression of the *WOR1*, the master regulator of white-opaque switching in the mammalian gastrointestinal (GI) tract. After ten days of incubation of *WOR1* overexpressed cells, a subpopulation of cells was obtained, which differed in cell and colony morphology from yeast or opaque cells (Pande, Chen et al. 2013). GUT cells are elongated in appearance similar to opaque cells, lack pimples, are stable at body temperature, and show a lower mating efficiency. GUT cells are more fit than white or opaque cells in the gastrointestinal commensal model and less virulent in the mouse bloodstream infection model. However, the GUT cells require specific host signals to maintain phenotype, which still remains unidentified.

Planktonic-biofilm transition

Primarily the planktonic form of *C. albicans* majorly consists of yeast, pseudohyphal, and hyphal cells, depending on the cues in a free-floating environment. Whereas biofilms are a three dimensional (3-D) community of cells interacting with each other, encapsulated in an extracellular matrix that develops on solid surfaces in the environment and within mammalian hosts (Chandra, Kuhn et al. 2001, Kumamoto 2002, Ramage, Saville et al. 2005, Fox and Nobile 2012, Nobile, Fox et al. 2012, Sardi, Scorzoni et al. 2013, Zhu, Wang et al. 2013, Nobile and Johnson 2015, Gulati and Nobile 2016, Soll and Daniels 2016, Noble, Gianetti et al. 2017, Lohse, Gulati et al. 2018). Biofilms are much more relevant in the natural environment than suspension culture. *C. albicans* produces highly structured biofilms that adhere to the solid surface or at the air-liquid interface, and differ in properties from their free-floating counterparts. *C. albicans* biofilms form on both biotic

and abiotic surfaces. The primary sites of *C. albicans* biofilm formation on biotic surfaces include mucosal surfaces, the oral and vaginal epithelia (Ganguly and Mitchell 2011), and abiotic surfaces include urinary and central venous catheters, pacemakers, mechanical heart valves, joint prostheses, contact lenses, and dentures (Douglas 2003, Gulati and Nobile 2016). Upon colonization, *Candida* biofilm has the ability to disseminate in the bloodstream and lead to invasive systemic infections in tissues and organs. Biofilms are highly resistant to conventional drugs, mechanical perturbations, chemical stresses, and host immune system, thus acting as a reservoir of the pathogen. Biofilms contain cells in different morphological forms including yeast cells, pseudohyphal cells, and hyphal cells. There are four temporal stages in *C. albicans* biofilm formation (**Figure 1.8 A**) (a) adherence of yeast cells to a substrate and colonization (b) growth and proliferation of yeast cells to form a basal layer of anchoring cells (microcolonies) (c) growth of pseudohyphae and hyphae cells associated with the production of extracellular matrix resulting in the formation of a complex network of several layers of cells and (d) dispersal of yeast cells from the biofilm to colonize new sites (Nobile and Johnson 2015, Lohse, Gulati et al. 2018). The majority of the knowledge of *C. albicans* biofilm formation comes for *in-vitro* studies and *in vivo* systems as well (Nobile, Fox et al. 2012). The ability of the organism to develop biofilm on several substrates and a wide range of media indicates its robustness in biofilm formation at a wide range of environmental conditions.

Extensive studies have been carried out on the genetic control of biofilm development in *C. albicans*. To date, 50 transcriptional regulators and 101 nonregulatory genes have been identified to have roles in biofilm formation (Nobile, Fox et al. 2012) (Fox, Bui et al. 2015). In 2012, an extensive screening of the transcription factor deletion library identified a network of transcription factors controlling the development of *C. albicans* biofilms (Nobile, Fox et al. 2012). The network comprises of six master transcriptional regulators, Bcr1, Tec1, Ndt80, Efg1, Brg1, and Rob1. Each of these master regulators autoregulate and control the expression of the other remaining master regulators, resulting in a complex, intertwined regulatory network that was proven by ChIP-chip and genome-wide expression analysis. These master regulators directly bind to the promoters and directly or indirectly regulate the expression of 1,000 target genes approximately (Fox and

Nobile 2012). Orthology mapping of these target genes indicates that most of them are relatively “young,” suggesting that biofilm formation in *C. albicans* is a recently acquired trait in evolutionary timescales. This network was further expanded, and three more master regulators Gal4, Rfx2 and Flo8, were included (Fox, Bui et al. 2015). In addition to the nine master regulators, 44 transcriptional regulators have been identified relevant in at least in certain stages or growth condition of *C. albicans* biofilm formation. Most of these regulators are bound by at least one of the nine master regulators directly (Nobile, Fox et al. 2012).

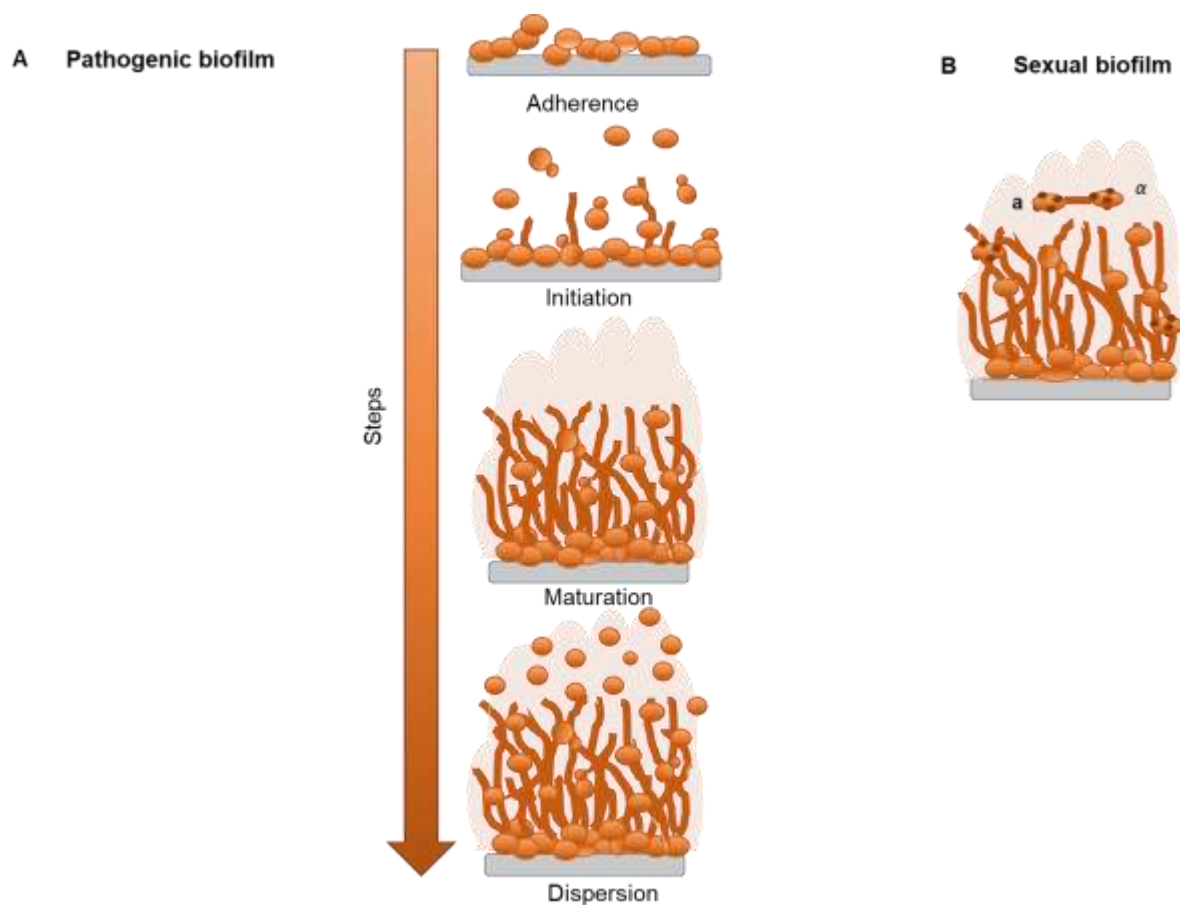


Figure 1.8 Different types of biofilm in *C. albicans*

A. Pathogenic biofilms are initiated when **a/α** yeast cells attach to a solid substrate, proliferate to form microcolonies, followed by the appearance of hyphae and pseudohyphae, which then get encapsulated in an extracellular matrix. During dispersion yeast cells detach to seed a new site. **B.** *MTLa* and *MTLα* white cells also form sexual biofilms. These biofilms differ from conventional biofilms in permeability, decreased resistance to antibiotics and host immune cells, and promotion of chemotropism between

opaque *MTLa* and *MTL α* cells. It is hypothesized that a primary function of white cell biofilms is to facilitate the mating between sexually competent *MTLa* and *MTL α* opaque cells.

Types of biofilm formation in *C. albicans*

Most of the clinical isolates of *C. albicans* are heterozygous (**a/ α**) at the mating type-like (*MTL*) locus and are capable of forming biofilms on both abiotic surfaces and biotic surfaces. These are termed as “conventional ” or “pathogenic” biofilms (Nobile and Johnson 2015) (**Figure 1.8 A**). *C. albicans* can also form biofilms when cells are homozygous or hemizygous (**a/a, a/ Δ , α / α , or α / Δ**) at the *MTL* locus. These are “sexual” biofilms (Park, Daniels et al. 2013) (**Figure 1.8 B**). These biofilms can be induced by the addition of pheromones of the opposite mating type or through the co-culturing of cells of the opposite mating types (Daniels, Srikantha et al. 2006). They are less thick and dense than conventional biofilms (25% thinner) and serve as a matrix to support genetic exchange between mating-competent opaque cells (Soll and Daniels 2016). The sexual biofilms arise when a minority of opaque cells appear by spontaneous switching in a white cell population and release the pheromone of the opposite mating type. The opaque cells within the relatively thinner sexual biofilm form mating projections while maintaining the pheromone gradient, thus having an ideal environment for mating. Therefore, sexual biofilms can induce mating and genetic diversity in specialized niches of the host body (the skin) that support white-opaque switching. Sexual biofilms are more penetrable than conventional ones. They are structurally similar but functionally distinct. Conventional and sexual biofilms are regulated by diverse transcriptional networks and signaling pathways. The signaling pathway that induces the formation of the conventional biofilm is the Ras1/cAMP pathway that includes Cdc35, Tpk2, and an unknown receptor. The sexual biofilm is triggered by a MAPK cascade initiated by the pheromone receptors Ste2 or Ste3 (Yi, Sahni et al. 2011, Huang, Huang et al. 2019). In the conventional biofilm pathway, Ras1 activation leads to cAMP production, and increased concentrations of cAMP stimulate PKA to induce the transcriptional network (Huang, Huang et al. 2019). The conventional biofilm network consists of nine core transcription regulators: Tec1, Ndt80, Rob1, Brg1, Bcr1, Efg1, Flo8,

Gal4, and Rfx2 (Nobile, Fox et al. 2012) (**Figure 1.9**). The sexual biofilm is regulated by four of the nine core transcription factors: Bcr1, Rob1, Brg1, and Tec1 and another transcription factor, Cph1 not involved in conventional biofilm (Lin, Kabrawala et al. 2013). Thus, although conventional and sexual biofilm differ phenotypically and are under distinct transcriptional regulation, they give rise to similar phenotypes, indicating that they may be specific for defined environmental conditions.

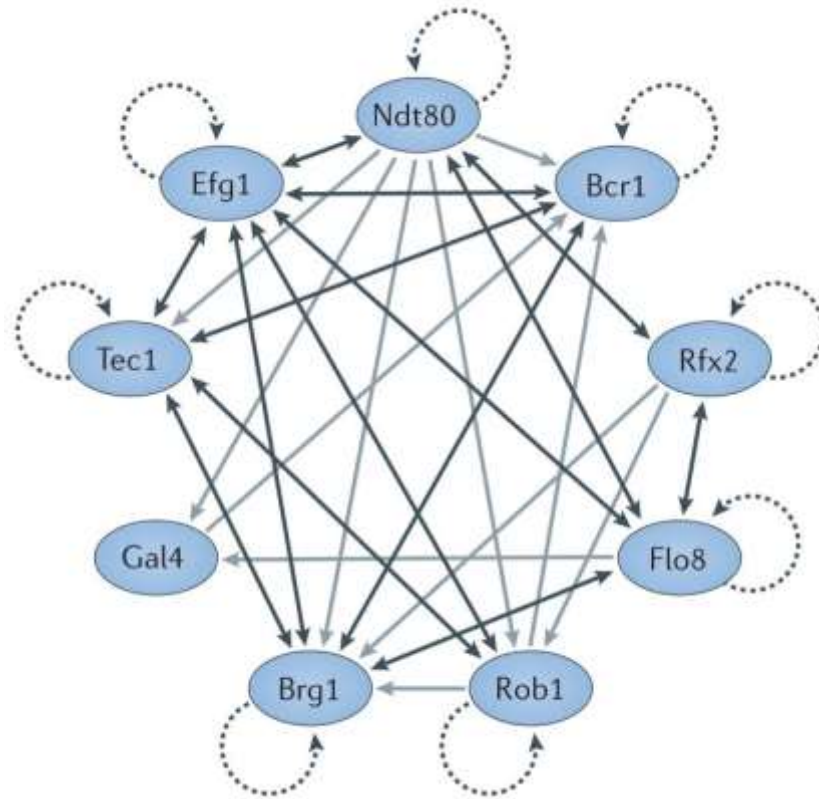


Figure 1.9 The core transcriptional biofilm circuit in *Candida albicans*.

Among the 50 transcription factors controlling biofilm formation in *C. albicans*, nine TFs (Ndt80, Bcr1, Rfx2, Flo8, Rob1, Brg1, Gal4, Tec1, and Efg1) are the 'core' set of regulators. Chromatin immunoprecipitation experiments indicate these TFs autoregulate themselves (indicated by dotted arrows) or directly bind the other and regulate the activity of each other (indicated by double-headed dark grey arrows), or directly bind and control the expression of other regulators (indicated by single-headed light grey arrows) (Lohse, Gulati et al. 2018).

Steps in biofilm formation

Adhesion

The first step of biofilm formation is adhesion, where cells attach to each other (cell-cell adhesion) and also to surfaces (cell-substrate adhesion). This step is crucial for all subsequent stages of biofilm development. Adherence of *C. albicans* to inert surfaces or biological materials is one of the significant contributors to its virulence. On initial interactions with biotic surfaces (host), the fungal cell wall plays a crucial role in host-pathogen interactions. The cell wall contains various components involved in adherence, known as adhesins (Nobile and Mitchell 2005) (Nobile, Nett et al. 2006). The cell wall is dynamic and regulates its composition and reorganizes itself based on environmental conditions (Chaffin 2008). The fungal cell wall consists of three types of polysaccharides: D-glucose, N-acetyl D-glucosamine, and D-mannose forming chitins and glucans (Tronchin, Pihet et al. 2008). The major cell wall proteins are mannoproteins (30-50% of dry weight). There are two major classes of mannoproteins: GPI proteins, such as the adhesins Als1 and Als3, distributed in the outer cell wall layer and linked to β -glucans by their GPI anchor. The second class constitutes of proteins encoded by members of the PIR (proteins with internal repeats) gene family, which are localized throughout the inner cell wall and linked covalently to β -1,3-glucans (Tronchin, Pihet et al. 2008). Als1 and Als3 belong to the Agglutinin like-sequence (ALS) gene family. They have high sequence similarity and functional redundancy. They both can interact with Hwp1 to promote cell-to-cell adhesion (Sundstrom 2002, Nobile, Nett et al. 2006). Other members of the Hwp family that are required for biofilm development include Hwp2, Rbt1, Eap1, and Ywp1. Other cell-wall proteins such as Pga1 and members of the Sap family were initially identified as direct or indirect regulators of adhesion to human cell lines or in cell-cell adhesion. Eap1, a cell wall protein, was found to regulate adhesion to polystyrene surface in *C. albicans*. The step of adhesion can be temporally classified as initial cell attachment and adhesion maintenance. Adhesins such as Hyr1, Eap1, Hwp2, and Ihd1 regulate both these steps of adhesion, whereas Als1/Als3 is mainly involved in initial attachment. In addition, null mutants of *EFG1* and *BCR1* do not differ in initial adhesion but are defective for adhesion maintenance. The yeast-specific cell wall protein Ywp1 negatively regulates the adherence of yeast cells.

The deletion of *YWP1* increases adherence in a biofilm model that contains only yeast cells (when grown at low temperature), and overexpression of Ywp1 inhibits adherence. However, recently it has been shown that the absence of Ywp1 increases initial cell attachment but lower adhesion maintenance (McCall et al. 2019).

As the free-floating *C. albicans* cells come in contact with the substrate, they form weak interactions inducing cell rolling. This step is followed by an initial attachment to the substrate regulated by several adhesin proteins, preventing the movement of cells. Then the cell enters into a decision making of either to detach from the substrate and disperse or commit to the present location and maintain adhesion depending on the environmental signaling. Long-term maintenance of adhesion is partially controlled by Ywp1, while an unknown mechanism regulates dispersion (Tronchin, Pihet et al. 2008). Another factor contributing to adherence is cell surface hydrophobicity. Hyphal cells are more hydrophobic than yeast cells. The outer fungal cell wall layer is fibrillar. However, the fibrillar conformation of cell wall changes with morphological changes in *C. albicans* (Lopez-Ribot, Casanova et al. 1991). They are short and aggregated on the surface of hydrophobic cells, whereas they are longer, evenly spaced, and radiating on the surface of hydrophilic cells.

Fungal cells have a rigid cell wall, and they lack appendages, which may help them to sense a surface/ substrate. However, as yeast cells come in contact with a polystyrene surface, a differential gene expression profile is initiated from planktonic cells when grown under otherwise similar conditions after 30 min of incubation. The genes involved in cysteine and methionine biosynthesis are up-regulated; the drug efflux pump genes *CDR1* and *MDR1* are up-regulated in the early stages of biofilm development within 6 h of surface contact. Using the fluorescent marker-based assay, activities of promoters of *CDR1* and *MDR1* have been shown to increase within 15–30 min after adherence of cells to a glass slide (Mateus, Crow et al. 2004). This change in gene expression profile correlates well with the well-established phenomenon of increased drug resistance of biofilm cells. MAP kinase Mkc1 is activated in response to surface contacts. The level of Mkc1 phosphorylation is higher when cells are grown on a variety of surfaces than in planktonic cultures. Mkc1 also plays a role in biofilm development and cell wall integrity (Kumamoto 2005) .

A library of transcription factors (TFs) mutants was screened for altered cell-substrate adherence by an *in vitro* quantitative flow-cell assay (Finkel, Xu et al. 2012). About 30 TFs were identified to be essential for adhesion to a silicone substrate under these flow conditions (**Figure 1.10**). Out of these 30 TFs, four (Bcr1, Ace2, Snf5, and Arg81) were also required for *in vitro* biofilm formation (on polystyrene microtiter plates with shaking) (Finkel, Xu et al. 2012). Thus, the genetic requirements for biofilm formation by *C. albicans* vary from one step to the next. Among these TFs, Bcr1 is one of the master regulators of biofilm formation in *C. albicans in vitro* and *in vivo*. It also regulates several cell surface-associated genes such as *HYR1*, *HWP1*, *CHT2*, *ECE1*, *RBT5*, *ALS1*, and *ALS3* (Nobile and Mitchell 2005, Nobile, Andes et al. 2006, Homann, Dea et al. 2009). It positively promotes adherence but is not required for hyphal formation (Nobile, Andes et al. 2006). Thus, Bcr1-mediated adherence is critical for biofilm formation. Interestingly, Bcr1 is an Ace2-redundant TF because they share several target genes (Finkel, Xu et al. 2012). Ace2 is also a TF involved in morphogenesis (Mulhern, Logue et al. 2006). Absence of *ACE2* in *C. albicans* results in defects in cell separation, increased pseudohyphal growth, enhanced invasion of agar media and avirulence in mice model of systemic candidiasis (Kelly, MacCallum et al. 2004). The deletion of *ACE2* severely compromises adherence and biofilm formation *in vitro*. Ace2, like Bcr1, is also dispensable during hyphal morphogenesis in normoxic conditions (Mulhern, Logue et al. 2006, Desai, van Wijlick et al. 2015). Ace2 regulates several cell wall components, such as glucanases and GPI-anchored proteins (Mulhern, Logue et al. 2006). Bcr1 and Ace2 control several Regulation of Ace2 and morphogenesis (RAM) pathway genes (Finkel, Xu et al. 2012, Saputo, Kumar et al. 2014). RAM is a well-conserved pathway that modulates cell separation, polarized growth, and cell integrity in yeast (Song, Cheon et al. 2008). Cbk1 is a kinase, a member of the NDR/LATS kinase family, which is the main effector of the RAM signaling network. In *C. albicans*, the putative Cbk1 targets identified were Ace2 (3 sites), Bcr1 (2 sites), Nrg1 (3 sites), and Zap1 (3 sites) (Gutierrez-Escribano, Zeidler et al. 2012). Thus, Cbk1 regulates biofilm formation by acting on these TFs that are crucial for different stages of biofilm development in *C. albicans*. Expression of several Ace2 target genes including *SCW11* and *CHT2* depends on Cbk1 (Gutierrez-Escribano, Gonzalez-Novo et al. 2011). Thus, the role of

Ace2 and its dependency on Bcr1 in regulating adherence and biofilm formation remains underexplored.

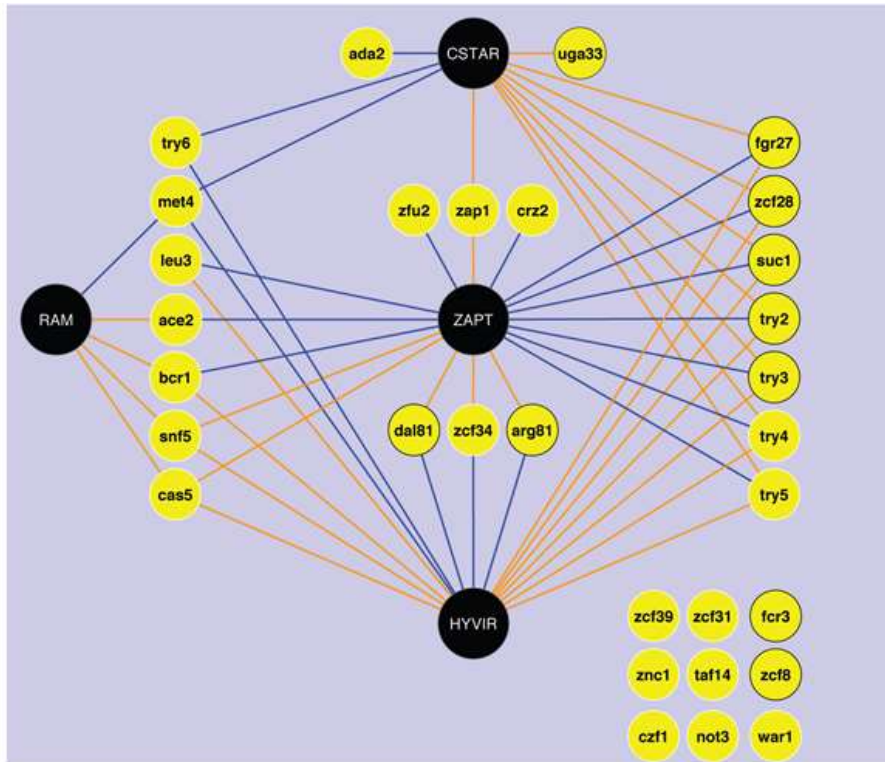


Figure 1.10 Schematic of transcriptional network of 30 adherence regulators in *C. albicans*.

The TFs involved in adherence are in yellow circles, and they regulate four clusters of target genes (in black circles) 1. hyphal growth or virulence, HYVIR. 2. Regulation of Ace2 and polarized morphogenesis (RAM), targets of Ace2, which are also regulated by Cbk1, Snf5, Cas5, Bcr1, and Met4. 3. ZAPT: known Zap1 targets. 4. CSTAR: Cell surface targets of adherence regulators. Additional small clusters of co-regulated genes did not have unifying functional or structural features. Yellow circles with black borders include those adherence regulators whose defects in adherence can be rescued by *ZAP1* overexpression. Blue lines denote negative regulation and orange lines positive regulation (Finkel, Xu et al. 2012).

Initiation

The next step of biofilm formation includes cell proliferation and initiation of filamentation of adhered cells. The cells give rise to microcolonies by anchoring the basal layer of cells. The adhered cells then filament to form hyphae. The hyphal cells contribute to the structural framework for biofilm and also act as a scaffold for other yeast,

pseudohyphae, and hyphal cells. Several transcriptional regulators contributing to hyphal formation and maintenance include Tec1, Ndt80, Efg1, and Rob1 (Schweizer, Rupp et al. 2000, Ramage, VandeWalle et al. 2002, Nobile, Fox et al. 2012, Nobile and Johnson 2015). Thus, hyphal formation and the self-adhesion and adhesion to other morphological forms are crucial for biofilm development.

Maturation

As the biofilm matures, extracellular matrix (ECM) is formed in the biofilm containing secretions from *C. albicans* cells along with environmental aggregates and lysed host cells. ECM encompasses the yeast, hyphal, and pseudohyphal cells and provides protection from the host immune system and antifungal drugs. It also contributes to the 3-dimensional architectural stability of the biofilm. ECM consists of glycoproteins (55%), carbohydrates (25%), lipids (15%), and nucleic acids (5%) (Pierce, Vila et al. 2017). There are two regulators known for biofilm matrix production in *C. albicans*: Rlm1 (Nett, Sanchez et al. 2011) and Zap1 (Nobile, Nett et al. 2009). Deletion of *RLM1* leads to reduced extracellular matrix levels whereas, the removal of *ZAP1* contributes to an increased accumulation of extracellular matrix by up-regulating two glucoamylase enzymes, Gca1, and Gca2.

Dispersal

C. albicans cells are dispersed continuously from the biofilm. Although the dispersed yeast cells morphologically resemble the planktonic yeast cells, they vary in their properties (Uppuluri, Chaturvedi et al. 2010). They have an increased adherence capacity and biofilm formation propensity. They also exhibit hypervirulence in mice model of systemic candidiasis. Three transcriptional regulators, Nrg1, Pes1, and Ume6, have been identified to be critical for dispersal of *C. albicans* biofilm cells (Uppuluri, Pierce et al. 2010). Hsp90, a molecular chaperone, is also known to regulate biofilm dispersal, as its depletion leads to a dramatic reduction in the number of dispersed cells from a biofilm (Robbins, Uppuluri et al. 2011). Another cell wall protein Ywp1, known to play a role in adhesion, also contributes to biofilm dispersion, as its deletion reduces dispersal and

increases biofilm adhesiveness in *C. albicans* (Granger, Flenniken et al. 2005, Granger 2012).

Histone H3 variants in *C. albicans*

Previous studies have identified the presence of histone H3 variants in *C. albicans* (Rai, Singha et al. 2019). This histone H3 variant varies from the core canonical histone H3, and also from the variant histone H3 present in other fungal phyla, Basidiomycota and Zoopagomycota. In *C. albicans*, *HHT2* (ORF 19.1853) and *HHT21* (ORF 19.1061) are present in clusters and code for an identical polypeptide, the canonical histone H3 (**Figure 1.11 A and B**). The *HHT1* gene is located outside the histone cluster (ORF 19.6791) and encodes for the variant histone H3, which differs at positions 31, 32, and 80 in the amino acid sequence when compared with the canonical H3 sequence (**Figure 1.11 A**). The variant histone H3 has valine, serine and serine residue at 31st, 32nd, and 80th position respectively whereas the canonical histone H3 has serine, threonine, and threonine at the corresponding positions. The variations at these three positions in the histone H3 variant are conserved in most of the CUG clade species. Thus, this histone variant possibly has evolved independently in the CUG clade and was termed as H3V^{CTG}. H3V^{CTG} is expressed in all morphological forms of *C. albicans* tested, yeast, hyphae, and pseudohyphae (**Figure 1.11 C**). However, it is expressed at lower levels as compared to canonical histone H3 in the cell. Localization studies indicate a scattered distribution pattern of H3V^{CTG} as compared to a uniform distribution of canonical histone H3 in the nucleus (**Figure 1.11 E**). H3V^{CTG} is not essential for the survival of *C. albicans* in rich media in laboratory-grown conditions (Rai, Singha et al. 2019) (**Figure 1.11 D**). It can partially fulfill the functions of canonical histone H3 in the absence of canonical histone H3 genes, possibly by assembling into the nucleosomes to support the growth of *C. albicans*.

Approximately 1/5th (1048 genes) of all *C. albicans* genes are altered in the absence of H3V^{CTG} in planktonic growth form. Biofilm, transcription, and cell cycle are the significantly altered pathway as revealed by genome-wide transcriptome profiling of the H3V^{CTG} null mutant. Transcription of a majority of biofilm-induced genes is up-regulated, whereas biofilm-repressed genes are down-regulated when cells lack H3V^{CTG}. Several

biofilm regulators such as adhesins and GPI-anchored cell wall proteins are up-regulated in H3V^{CTG} null mutants. In addition, hyphal specific secreted aspartyl proteases, *SAP5*, and *SAP6* genes, which are also involved in biofilm formation, are up-regulated in the H3V^{CTG} mutant as well. The biofilm pathway is again affected in the absence of H3V^{CTG} in the biofilm-inducing conditions of *C. albicans*. H3V^{CTG} represses biofilm growth and favors the planktonic growth form of *C. albicans*. Biofilm formation is enhanced in the absence of H3V^{CTG} at 30°C and 37°C (*in vitro*) and in rat venous catheter model (*in vivo*) as compared to wild-type (**Figure 1.11 F**). Biofilm formation is derepressed even at temperatures (30°C) not conducive to biofilm growth. Null H3V^{CTG} cells also exhibit hyperfilamentation on solid surfaces and enhanced colony wrinkling than the wild-type. The biofilm defects associated with some of its master regulators, namely, Bcr1, Tec1, and Ndt80, are significantly rescued in cells lacking H3V^{CTG}. So, H3V^{CTG} represses the biofilm gene circuit in both planktonic and biofilm conditions. However, the mechanism by which this novel histone H3 variant, H3V^{CTG} modulates the biofilm regulatory circuitry remains unclear.

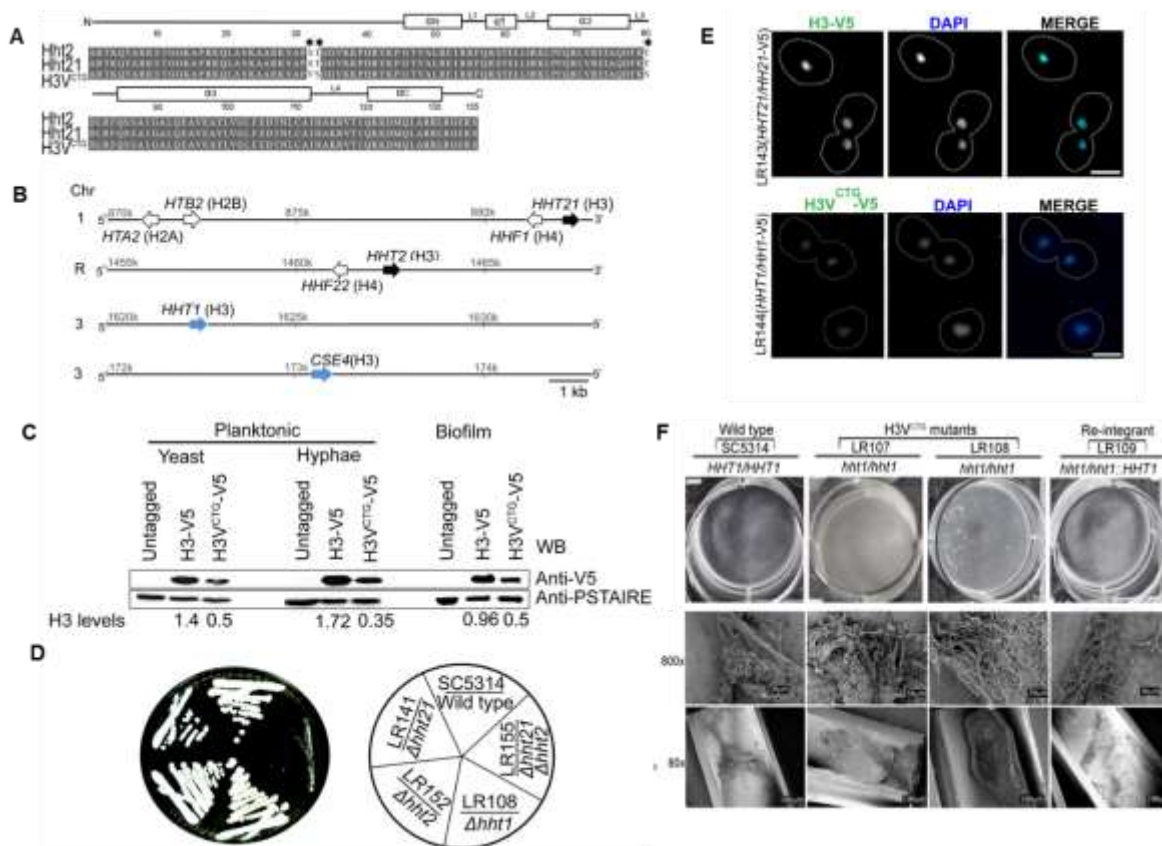


Figure 1.11 A nonessential histone H3 variant, H3V^{CTG}, represses the biofilm gene circuit.

A Amino acid sequence alignment of histone H3 proteins coded by *HHT2*, *HHT21*, and *HHT1* in *C. albicans*. Amino acid changes in the sequence among these histone H3 variants are marked by an asterisk, and identical amino acids are shaded. **B**. Cartoon representation of the locations of histone H3 genes and histone gene clusters on various chromosomes of *C. albicans*. **C**. Expression levels of *C. albicans* histone H3 proteins monitored by western blot analysis in the planktonic (yeast and hyphae) and biofilm growth conditions. **D**. Variant histone H3 null mutant has no growth defects in rich media (YPD plates) and grown at 30 °C for 3 days. **E**. Subcellular localization of the canonical histone H3 or the variant H3 in the yeast form of *C. albicans*. **F**. *In vitro* and *in vivo* biofilm assay in 6-well polystyrene plates and rat venous catheter model respectively showing enhanced biofilm formation than wild-type (Rai, Singha et al. 2019).

Rationale of the present study

C. albicans is a polymorphic fungus and is capable of undergoing high frequency morphological transitions. These transitions involve global changes in transcription profile in response to environmental cues. One of the morphological transitions in *C. albicans* is the ability of forming biofilms both *in vitro* and *in vivo*. Biofilms are a multidimensional drug resistant community of cells consisting of different cell types and distinct development stages, analogous to the evolution of multicellularity in higher eukaryotes to some extent. The formation of biofilm in *C. albicans* involves substantial changes in the genome (1/6th of the total genes are affected) (Nobile, Fox et al. 2012) (Fox, Bui et al. 2015). Chromatin factors majorly contribute to such dramatic alterations in the genome. While the transcriptional regulation during the formation of biofilms has been substantially studied, the modulation at the chromatin level during this process is less understood.

One of the key chromatin modulators, histone H3 variants (H3V^{CTG}), was previously identified exclusively in the CUG clade of ascomycetes including *C. albicans*. Histone H3 variants have been extensively studied in metazoans for their role in embryonic development and germ cell differentiation processes. Considering the conserved role of histone H3 variants in higher eukaryotes, their occurrence in yeasts is unprecedented. However, the evolution of H3V^{CTG} in CUG clade along with the formation of robust biofilm in the absence of H3V^{CTG} in *C. albicans* prompted us to identify the molecular mechanism by which H3V^{CTG} regulates the planktonic to biofilm transition in the current study. We aim to dissect the predisposition of H3V^{CTG} to the biofilm gene promoters at different growth forms.

Histone variants acquire specialized function of regulating gene expression by several modes. These include variant-specific amino acids and their corresponding chaperone machinery that facilitate the selective deposition of histones and enrichment at specific loci. Any mutation in these specific residues and associated chaperones cause developmental defects and disease in humans. Hence, we attempted to understand the contribution of each of the three variant-specific amino acids in H3V^{CTG} in acquiring this novel function of controlling the biofilm gene circuit in *C. albicans*. In addition, to identify

the specific chaperone machinery associated with H3V^{CTG} regulating its biased incorporation, we also investigated the possible loading factors of H3V^{CTG}.

Several chaperones for core and variant histone H3 including CAF-1, HIRA, DAXX and ATRX complexes have been identified till date. However, the selectivity of these chaperones for specific histone variants is only observed in higher eukaryotes. For instance, in *S. cerevisiae*, both CAF-1 and HIRA homologs are present but no histone H3 variants and CAF-1 and HIRA been shown to compensate for each other's' function. Whereas in mammalian cells CAF-1 is involved in canonical H3 loading whereas HIRA, DAXX, ATRX are involved in loading of histone H3 variants. *C. albicans* represents an intermediate stage between yeasts and higher eukaryotes in terms of functional specialization of chaperones and evolution of histone variants. *C. albicans* possess histone H3 variants (H3V^{CTG}) and both CAF-1 and HIRA homologs. So, it is plausible that there might be a rewiring in function of existing chaperones or the appearance of a new chaperone specific for H3V^{CTG}. Thus, we sought to identify chaperone specific to H3V^{CTG} by screening the existing chaperone homologs in *C. albicans*.

Biofilms are dynamic structures whose development over time is orchestrated by a string of factors. Gene expression profiling of H3V^{CTG} mutants suggest that the genes involved in each step of biofilm development are altered. We were interested in understanding the contribution of H3V^{CTG} in each of these steps. In an attempt to address its role, we chose adhesion, the first step of the biofilm pathway in this study.

Summary of the present study

The first part of the thesis describes the occupancy of two forms of histone H3, canonical H3 and variant H3 (H3V^{CTG}), at the promoter of biofilm-related genes at different modes of growth of *C. albicans*. The occupancy of H3V^{CTG} is significantly higher than canonical histone H3 at the promoters of biofilm-related genes when the cells are grown in the planktonic mode of growth. Further, the occupancy of H3V^{CTG} to the promoters of biofilm-related genes is reduced during the transition from the planktonic to biofilm mode of growth, whereas the levels of canonical histone H3 remain unchanged. The occupancy of variant histone H3 to the gene body of biofilm-related genes also decreases when cells

transit from planktonic to biofilm conditions. We also studied the occupancy of one of the biofilm master regulators, Bcr1, to the promoters of biofilm-related genes by ChIP-qPCR analysis. The binding of Bcr1 to the promoters of these genes increases in the absence of H3V^{CTG} in the planktonic conditions. Thus, our results suggest that H3V^{CTG} possibly limits access of biofilm gene-specific transcription factors to the promoters of biofilm-related genes in the planktonic mode of growth.

To study the contribution of each of the three amino acid residues that differ between variant and canonical histone H3 proteins, we generated single-point mutant strains at each of the positions 31, 32, and 80 of H3V^{CTG} to that of the canonical histone H3 sequence. We do not observe any significant differences in biofilm formation or the extent of filamentation between wild-type and single point-mutant strains. The double mutant at positions 31 and 32 of H3V^{CTG} exhibits an enhanced biofilm and hyper-filamentation phenotype, similar to that of the null mutants of H3V^{CTG}. Thus, our results indicate that, co-occurrence of amino acid residues at positions 31 and 32 is essential for functioning of H3V^{CTG}. The expression of biofilm-specific genes is higher in double point mutants as compared to each of the single mutants or the wild-type as obtained by qPCR analysis. The occupancy of Bcr1 also increases in the presence of double point mutants of H3V^{CTG} suggesting that co-occurrence of amino acids at position 31 and 32 are critical for H3V^{CTG} function.

We further analyze the presence of these residues at position 31 and 32 across the CUG clade species. Of 124 fungal species from the CUG clade analyzed, we find that variability of amino acid is allowed to alanine instead of valine only at position 31 in families Cephalosporiaceae and Metschnikowiaceae. At position 32, however, serine to threonine transition is observed in two members of Metschnikowiaceae. Interestingly, in none of the species across the CUG clade, both the residues at positions 31 (valine) and 32 (serine) are simultaneously found to be variant. This analysis further confirms the importance of co-occurrence of valine and serine at positions 31 and 32 respectively for the proper function of H3V^{CTG}.

Further we aim to identify the chaperones specific for H3V^{CTG} which might be responsible for its skewed loading at the biofilm gene promoters. To address this, we screen the available chaperone mutants of *C. albicans* for filamentation and biofilm phenotype. *cac2* (a subunit of CAF-1 complex) mutants produces more robust biofilm and exhibit enhanced filamentation on solid surfaces as compared to wild type. In other words, *cac2* mutants mimic the H3V^{CTG} null mutants in *C. albicans* hinting towards Cac2 being the probable chaperone for H3V^{CTG}. To further ascertain our claim, we studied the occupancy of H3V^{CTG} in the absence of Cac2 and observed a decrease in occupancy of H3V^{CTG} at the biofilm gene promoters in a *cac2* null background.

In the second part of the thesis, we address the temporal regulation of biofilm formation by H3V^{CTG}. To delineate the role of H3V^{CTG} in adhesion, we choose a transcription factor, Ace2, known to regulate cell adherence in *C. albicans*. The deletion of H3V^{CTG} in the *ace2* null mutant background leads to partial but significant rescue of the ability of cells to adhere to the solid surface and thereby biofilm-forming defects in *C. albicans*. Global transcriptome analysis of *ace2* and *hht1* double null mutants in adhered conditions reveal significant alterations in gene expression as compared to *ace2* null mutants. In order to identify the possible genes that might have been involved in rescuing the adherence defect associated with *ace2* null mutants, first, we identified the Ace2-mediated genes involved in adherence. We then examined the status of the expression of these genes in *ace2* and *hht1* double null mutants grown under identical conditions. Our analysis suggests that a major rewiring occurs at the level of gene expression as 37% (145 out of 392) of Ace2-regulated adherence genes are altered when H3V^{CTG} is deleted in an *ace2* null background. In-depth analysis by qPCR validates that several adhesins are overexpressed in *ace2* and *hht1* double null mutants bringing back the rescue of the phenotype. In addition, our analysis identifies several previously unidentified putative adhesion factors in *C. albicans*. The majority of adhesion factors in *C. albicans* have no common signature sequences. Thus, our analysis extends the repertoire of genes involved in adherence in *C. albicans*. A better understanding of the process of adhesion is an important prerequisite to identify fungal specific proteins that are crucial for adhesion and, thus, can be targeted to inhibit biofilm formation by *C. albicans*.

Chapter 2 Results

Mechanism by which H3V^{CTG} regulates biofilm formation in *Candida albicans*

Introduction

The structural organization of chromatin and its plasticity spatiotemporally regulates global gene expression. Consequently, this dynamic nature of chromatin determines the fate of a cell in response to specific cellular or environmental signals. Contrary to the genetic information, the inherent plasticity of chromatin ensures that the effects are reversible and can lead to genome reprogramming. In eukaryotic cells, nucleosomes are the fundamental repeating unit of chromatin. A nucleosome consists of 147 base pairs (bp) of DNA wrapped around an octamer of histone proteins, containing two copies of each of the four core histones: histone H2A, histone H2B, histone H3, and histone H4. These core histones vary in form and function and can determine the timing of gene expression to ensure the faithful transmission of DNA through cell division (Ahmad and Henikoff 2002, Schwartz and Ahmad 2005). Thus, the incorporation of these variant histones can alter the chromatin landscape. The variants of histones differ from their canonical counterparts by a few amino acids or by the presence of additional large domains (Earnshaw and Rothfield 1985, Palmer, O'Day et al. 1991, Pehrson and Fried 1992, Black, Foltz et al. 2004). The variant histones classify chromatin into functional domains in multiple ways: (a) by modifying the nucleosome structure and its stability (Bonisch and Hake 2012), (b) by recruiting variant-specific molecular machinery (Nakatani, Ray-Gallet et al. 2004), and/or (c) by distinct post-translational modifications (McKittrick, Gafken et al. 2004). The functions of histone H3 variants have been extensively studied in diverse contexts including the regulation of gene expression, maintenance of totipotent chromatin (Boskovic, Eid et al. 2014, Gaume and Torres-Padilla 2015), meiotic sex chromosome activation (van der Heijden, Derijck et al. 2007), and neuronal stem cell differentiation (Xia and Jiao 2017). Although histone H3 variants are universally present in multicellular eukaryotes, their presence in the fungal systems remained largely unexplored.

C. albicans is an opportunistic fungal pathogen and is one of the significant contributors to nosocomial infections (Jarvis 1995). It primarily behaves as a commensal in the digestive tract, oral cavity, and the genital regions of healthy individuals (Kennedy and Volz 1985, Achkar and Fries 2010, Ganguly and Mitchell 2011, Kumamoto 2011). However, *C. albicans* can switch to a pathogenic lifestyle when the host immune system gets

compromised causing life-threatening systemic infections (Weig, Gross et al. 1998). *C. albicans* is polymorphic in nature, and it undergoes high-frequency phenotypic transitions like yeast to opaque, GUT, gray, hyphae, pseudohyphae, biofilms and vice versa (Noble, Gianetti et al. 2017). These phenotypic transitions occur in a short time scale and are associated with global changes in the gene expression profile in response to cues from the host niche. *C. albicans* also can form a three-dimensional community of surface-associated structures called biofilms (Kumamoto 2002, Fox, Bui et al. 2015, Nobile and Johnson 2015). Biofilms are drug-resistant and are one of the prevalent states of this organism in natural settings.

Histone H3 variants in *C. albicans*

Previous studies from our laboratory identified a histone H3 variant in *C. albicans* (Rai, Singha et al. 2019). In *C. albicans*, two genes, *HHT21* and *HHT2*, encode an identical canonical histone H3 protein while *HHT1* codes for a variant protein with changes in three amino acids at positions 31, 32 and 80 respectively (Rai, Singha et al. 2019). *C. albicans* belongs to the CUG-Ser1 clade in the phylum Ascomycota in which the CUG codon has been reassigned to code for serine instead of leucine on most occasions. The presence of histone H3 variants were found to be restricted to only CUG clade members among all the sequenced species of the phylum Ascomycota. Hence, it was named as H3V^{CTG} (Rai, Singha et al. 2019).

The homozygous null mutant of H3V^{CTG} is viable, suggesting its non-essentiality for survival in the rich media in laboratory-grown conditions. Global transcriptome analysis of the null mutant of H3V^{CTG} reveals significant alterations in gene expression of pathways associated with biofilm, transcription, and cell cycle when compared to the wild-type. The absence of H3V^{CTG} triggers filamentation in solid surfaces but has no effect in liquid media. In-depth analysis by qPCR validates that several biofilm-induced/repressed genes are over-expressed/repressed in the H3V^{CTG} null mutant in the planktonic condition itself. Phenotypic assays indicate that biofilm formation is enhanced in H3V^{CTG} mutants both *in vitro* (polystyrene plates) and *in vivo* (rat catheter) conditions.

The present study aims to address how a non-specific global DNA binding protein, H3V^{CTG} regulates a large number of genes involved in a specific phenotypic process like biofilm growth. Further, we assess the contribution of the variant-specific amino acids in H3V^{CTG} function, if any.

Occupancy of H3V^{CTG} is higher at the promoter of biofilm genes in planktonic as compared to biofilm growth conditions

To delineate the mechanism by which H3V^{CTG} regulates biofilm formation, we tested the occupancy of H3V^{CTG} at the promoter of biofilm genes. The regions tested for binding of H3V^{CTG} or canonical H3 (Hht21) were chosen from known binding regions of key biofilm regulators to the promoter of biofilm specific target genes (Nobile et al. 2012). We performed ChIP-qPCR at the promoter of ten biofilm genes, which were affected in the transcription profiling in the absence of H3V^{CTG}. The promoter of an uncharacterized ORF, Orf19.8740 was used to normalize the binding efficiency of the canonical and variant histone H3 molecules in the different growth forms. This particular ORF was chosen as its expression was unaltered in the genome-wide transcriptome study of H3V^{CTG} null mutant (Rai, Singha et al. 2019) as well as in the previously published report of genes altered during the planktonic to biofilm growth transition (Nobile, Fox et al. 2012). The untagged parent strain SN148 was used as a control to calculate the background enrichment. The promoters of biofilm-induced genes (*BMT7*, *CAN1*, *ECE1*, *HWP1*, *HGT2*, *JEN2*, and *SAP5*), biofilm-repressed genes (*NRG1* and *YWP1*), and also of an uncharacterized gene (Orf19.7380), to which five of the six biofilm master regulators bind, was used to study the occupancy of one of the canonical H3 (Hht21) or variant histone H3 (H3V^{CTG}). Our analyses revealed that in LR144 (*HHT1/HHT1-V5*), the occupancy of H3V^{CTG} was significantly higher at the promoters of biofilm-related genes compared to that of the canonical histone H3 in LR143 (*HHT21/HHT21-V5*) when the cells were grown in the planktonic mode of growth (**Figure 2.1 A**). Thus, we hypothesize that higher occupancy of H3V^{CTG} at the promoters of biofilm genes may prevent the access of transcription factors at the promoters, thereby repressing the expression of genes involved in biofilm formation.

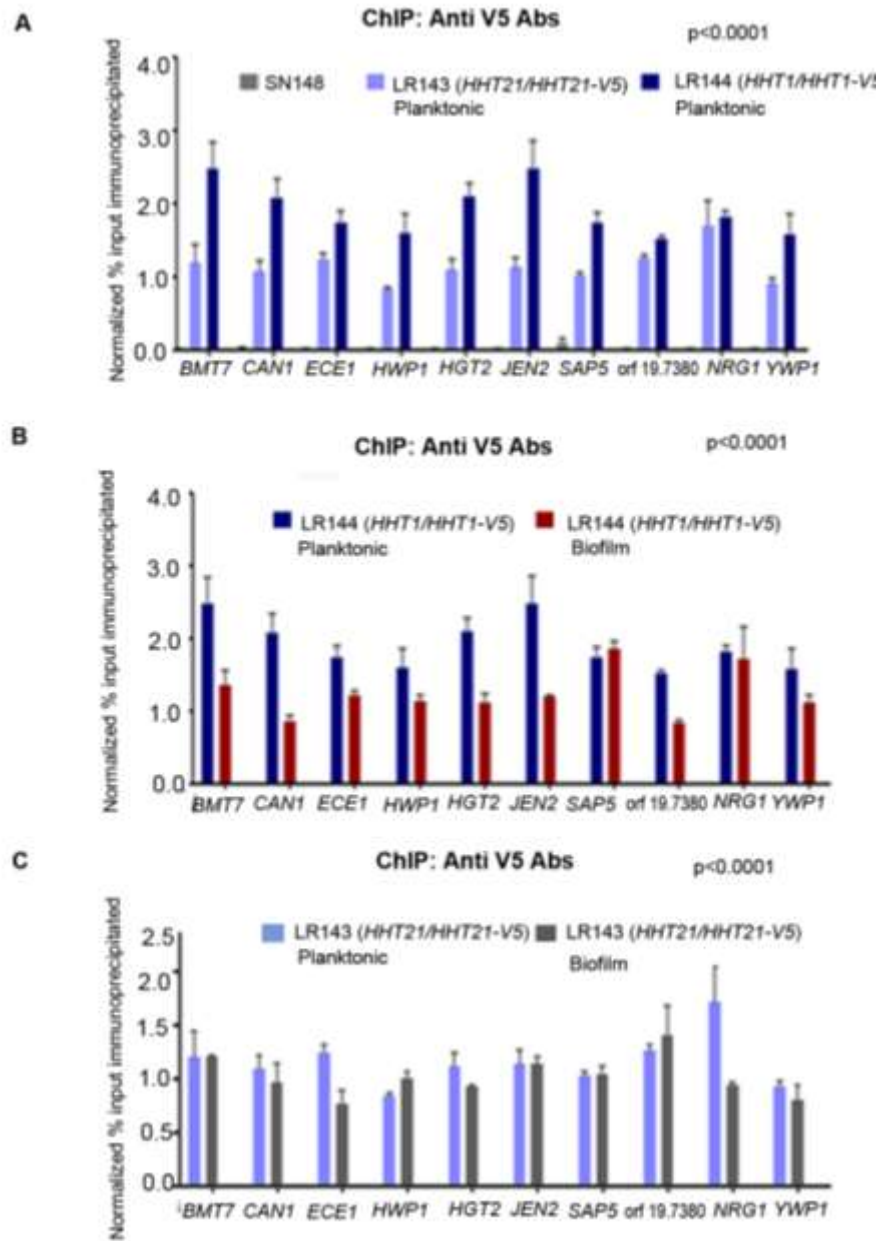


Figure 2.1 Variant histone H3 limits the access of transcription modulators to promoters of biofilm-related genes.

A. ChIP assays with anti-V5 antibodies were performed in cells of LR143 (*HHT21/HHT21-V5*) and LR144 (*HHT1/HHT1-V5*) expressing a V5-tagged canonical histone H3 or variant histone H3 grown in planktonic conditions. The input and IP DNA fractions were analyzed by qPCR (quantitative PCR) with gene-specific promoter primer pairs for binding of either canonical histone H3 or H3V^{CTG}. The qPCR was also performed with untagged strain to detect the background DNA elution in the ChIP assay. The enrichment of canonical histone H3 or H3V^{CTG} to the promoters of biofilm-related genes was normalized with Orf19.874 and is represented as a normalized percent input IP in the y-axis. **B.** Similarly, ChIP assays with anti-V5 antibodies were performed in LR144 (*HHT1/HHT1-V5*) cells grown as a

biofilm. The enrichment of H3V^{CTG} to the promoters of biofilm genes was compared in both planktonic (data procured from the Figure 2.1 A) and biofilm conditions and is represented as a normalized percent input IP in the y-axis. C. ChIP assays with anti-V5 antibodies were performed in LR143 (*HHT21/HHT21-V5*) cells grown in planktonic and biofilm conditions. The enrichment of H3-V5 to the promoters of biofilm genes was compared in both planktonic and biofilm conditions and is represented as a normalized percent input IP in the y-axis. The x-axis indicates the biofilm genes whose promoter regions were assayed for binding. Error bars indicate standard error of Mean (SEM). The values from three independent ChIP experiments, each performed with three technical replicates were plotted. A two-way ANOVA test was performed to determine statistical significance. Primer sequences are listed in Table 6.2.

Occupancy of H3V^{CTG} at the promoter and gene body of biofilm genes decreases as the cell switches from planktonic to biofilm condition

Preferential occupancy of H3V^{CTG} to the promoters of biofilm genes prompted us to examine the occupancy of H3V^{CTG} as the cells undergo a morphological transition from the free-floating planktonic to biofilm form. The occupancy of H3V^{CTG} at the promoters was analyzed in LR144 (*HHT1/HHT1-V5*) in both planktonic and biofilm growth conditions at the same ten biofilm gene promoters analyzed previously. Except at *SAP5* and *NRG1* promoters, a significant drop in the binding of H3V^{CTG} to the promoters of biofilm genes was observed during the transition from planktonic to biofilm growth, indicating that the binding of H3V^{CTG} is more efficient at the majority of the promoters of biofilm genes during the planktonic condition (**Figure 2.1 B**). As the cells transit to the biofilm mode, the promoters are depleted of H3V^{CTG} nucleosomes, leading to an increased expression of biofilm-related genes. Similar to the promoters, we also observed a drop of H3V^{CTG} at the gene bodies (*JEN2*, *ECE1*, and *HWP1*) in the biofilm mode as compared to planktonic growth conditions (**Figure 2.2**). Thus, we observe that there is an overall depletion of H3V^{CTG} levels at both the coding regions and promoters of biofilm genes in the biofilm mode of growth.

It has been demonstrated previously that the induction of transcription is correlated with nucleosome depletion at the upstream activating sequence (UAS) regions in *Saccharomyces cerevisiae* (Prelich and Winston 1993). Therefore, to substantiate our claim, we tested the overall total H3 levels at these ten promoters in both planktonic and biofilm

mode in wild-type (SC5314) cells using anti H3 antibodies. We observed a decline in total H3 levels at the promoters of *BMT7*, *CAN1*, *ECE1*, *HGT2*, *JEN2*, *SAP5*, and *NRG1* in biofilm conditions indicative of nucleosome depleted regions providing access to transcription factors that regulate biofilm specific gene expression (**Figure 2.3**).

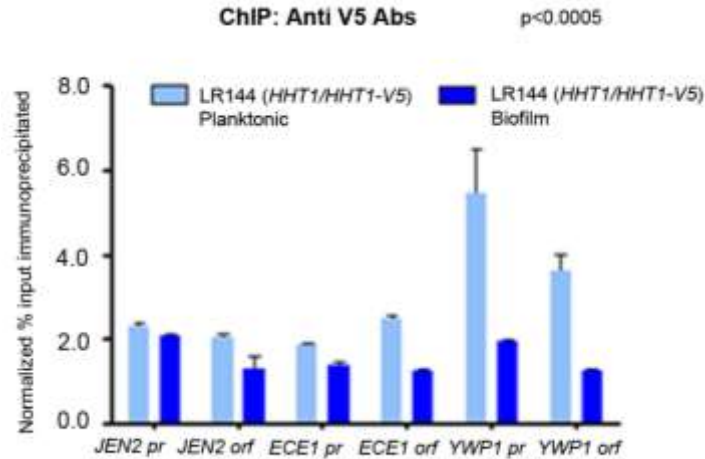


Figure 2.2 The binding of H3V^{CTG} drops at the promoter and gene bodies of biofilm genes in biofilm conditions.

ChIP assays with anti-V5 antibodies were performed in the strain LR144 (*HHT1/HHT1-V5*) grown in planktonic and biofilm state. The input and IP DNA fractions were analyzed by qPCR at the three promoters and gene bodies of biofilm genes. The enrichment of H3V^{CTG} was calculated and normalized with Orf19.874 and is represented as a normalized percent input IP in the y-axis. The x-axis indicates the biofilm genes whose promoter regions and gene bodies were assayed for binding. Error bars indicate standard error of Mean (SEM). The values from three independent ChIP experiments, each performed with three technical replicates were plotted. A two-way ANOVA test was performed to determine statistical significance. Primer sequences are listed in Table 6.2.

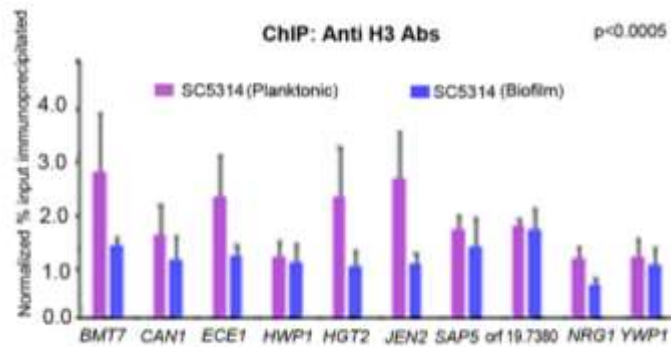


Figure 2.3 Total histone H3 levels at the promoter of biofilm genes decline as the cells transit from the planktonic to biofilm mode of growth in *C. albicans*.

The binding of total H3 was examined in wild-type (SC5314) cells grown in planktonic and biofilm conditions. ChIP assays were performed with anti-H3 antibodies, and the input and IP DNA fractions were analyzed by qPCR with ten primer pairs from promoters of the biofilm genes for the binding of H3. The enrichment of H3 was calculated and normalized with Orf19.874 and is represented as a normalized percent input IP in the y-axis. The x-axis indicates the biofilm genes whose promoter regions were assayed for binding. Error bars indicate standard error of Mean (SEM). The values from three independent ChIP experiments, each performed with three technical replicates were plotted. A two-way ANOVA test was performed to determine statistical significance. Primer sequences are listed in Table 6.2.

Occupancy of canonical H3 is unaltered during the planktonic to biofilm growth transition

It is plausible that there is an overall drop in the occupancy of histone H3 at the promoters of biofilm genes during the planktonic-biofilm growth transition rather than a preferential decrease of H3V^{CTG} binding. This led us to investigate the binding of canonical H3 at the promoters of biofilm genes during the planktonic-biofilm transition. For this, the occupancy of one of the V5 tagged canonical histone H3 genes (LR143, *HHT21/HHT21-V5*) at the promoters of biofilm-related genes (*BMT7*, *CAN1*, *ECE1*, *HGT2*, *HWP1*, *JEN2*, *SAP5*, orf19.7380, *YWP1*, and *NRG1*) was examined. The levels of canonical H3 at the promoter of biofilm genes were unaltered irrespective of the growth condition of *C. albicans* cells- planktonic or biofilm (**Figure 2.1 C**). This trend in the occupancy of canonical H3 was not similar to that of H3V^{CTG} binding at the promoters of biofilm relevant genes between planktonic and biofilm conditions. Thus, our studies reveal that the expression of biofilm genes is modulated by the differential binding of H3V^{CTG} to the promoter of each of the biofilm genes at distinct growth states (planktonic and biofilm) rather than by overall histone H3 levels.

Occupancy of biofilm specific transcription factor Bcr1 is increased at the promoter of biofilm genes in H3V^{CTG} null mutant in the planktonic condition of growth

Based on our previous observations, we proposed that depletion of H3V^{CTG} might provide access to transcription factors at the promoters of biofilm genes. To test this

hypothesis, we analyzed the occupancy of Bcr1, a master regulator of biofilm formation at the promoters of biofilm-related genes. We performed ChIP-qPCR analysis in the wild-type (CJN1785, *BCR1-Myc/BCR1*) and the H3V^{CTG} null mutant expressing myc-tagged Bcr1 (LR133, *BCR1-Myc/BCR1 hht1/hht1*). Binding of Bcr1-myc was analyzed on the promoters of a set of genes that showed an altered (up-regulation or down-regulation) expression in the H3V^{CTG} mutant by ChIP-qPCR. Our results confirm that the absence of H3V^{CTG} enhances the binding of the biofilm master regulator Bcr1 to the promoters of these genes in the planktonic conditions (**Figure 2.4**). These results were in accordance with the transcriptome profiling of H3V^{CTG}, further strengthening the fact that H3V^{CTG} plays a significant role in repressing the biofilm promoting gene network during planktonic growth in *C. albicans*.

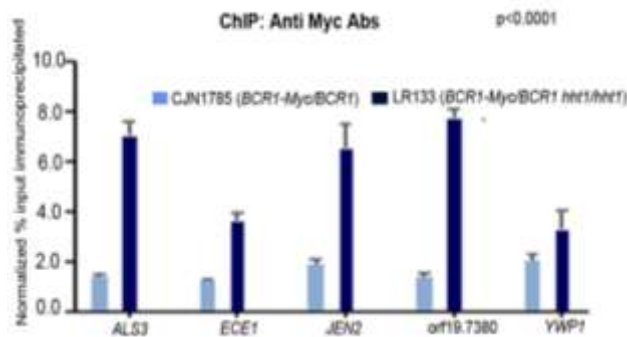


Figure 2.4 Variant histone H3 restricts the access of transcription factors to the biofilm gene promoters.

The binding of one of the master regulators of biofilm, Bcr1, was examined either in the presence or in the absence of H3V^{CTG} in the planktonic conditions. ChIP assays were performed with anti-myc antibodies in both CJN1785 (*BCR1-Myc/BCR1*) and LR133 (*BCR1-Myc/BCR1 hht1/hht1*) expressing Bcr1-myc. The input and IP DNA fractions were analyzed by qPCR with primers from gene-specific promoter primer pairs for binding of Bcr1. The enrichment of Bcr1-myc was calculated and normalized with Orf19.874 and is represented as a normalized percent input IP in the y-axis. The x-axis indicates the biofilm genes whose promoter regions were assayed for binding. Error bars indicate standard error of Mean (SEM). The values from three independent ChIP experiments, each performed with three technical replicates were plotted. A two-way ANOVA test was performed to determine statistical significance. Primer sequences are listed in Table 6.2.

Co-occurrence of amino acid residues at position 31 and 32 is essential for the function of variant histone H3

The H3V^{CTG} differs from canonical H3 in three amino acids at positions 31, 32, and 80 from valine, serine and serine to serine, threonine and threonine, respectively. We were interested to know the functional significance of each of the three amino acid residues that differ between the variant and canonical histone H3. To understand this, we generated single-point mutant strains of H3V^{CTG}, where each position was individually mutated to that of the canonical histone H3 sequence resulting in the strains RS103 (*hht1/hht1::HHT1^{V31S}*), RS105 (*hht1/hht1::HHT1^{S32T}*) and RS107 (*hht1/hht1::HHT1^{S80T}*) (**Figure 2.5 A**). We did not observe any significant differences in filamentation on the solid surface or biofilm formation between wild-type (SC5314) and point-mutant strains (RS103, *hht1/hht1::HHT1^{V31S}*, RS105, *hht1/hht1::HHT1^{S32T}* and RS107, *hht1/hht1::HHT1^{S80T}*) (**Figure 2.5 B and C and Figure 2.6**).

Further, we also generated a double point mutant in which the amino acids at positions 31 and 32 of H3V^{CTG} were changed to the amino acid residues similar to those of the canonical histone H3 at the corresponding positions (RS109, *hht1/hht1::HHT1^{V31S, S32T}*). The double point mutant (RS109, *hht1/hht1::HHT1^{V31S, S32T}*) showed significantly more biomass and hyperfilamentation phenotype, identical to that of the H3V^{CTG} null mutant (**Figure 2.5 B and C and Figure 2.6**). The extent of filamentation was also observed to be higher at the level of colonies derived from a single cell (**Figure 2.7**). Thus the inability of double point mutant (RS109, *hht1/hht1::HHT1^{V31S, S32T}*) to rescue the phenotype of H3V^{CTG} null mutant suggests that the co-occurrence of amino acid residues at positions 31 and 32 is essential for variant histone H3 to function as a biofilm repressor during the planktonic growth. It also confirms that the phenotype of null mutants of variant H3 (H3V^{CTG}) is associated explicitly with variant histone H3 and not with the global levels of histone H3.

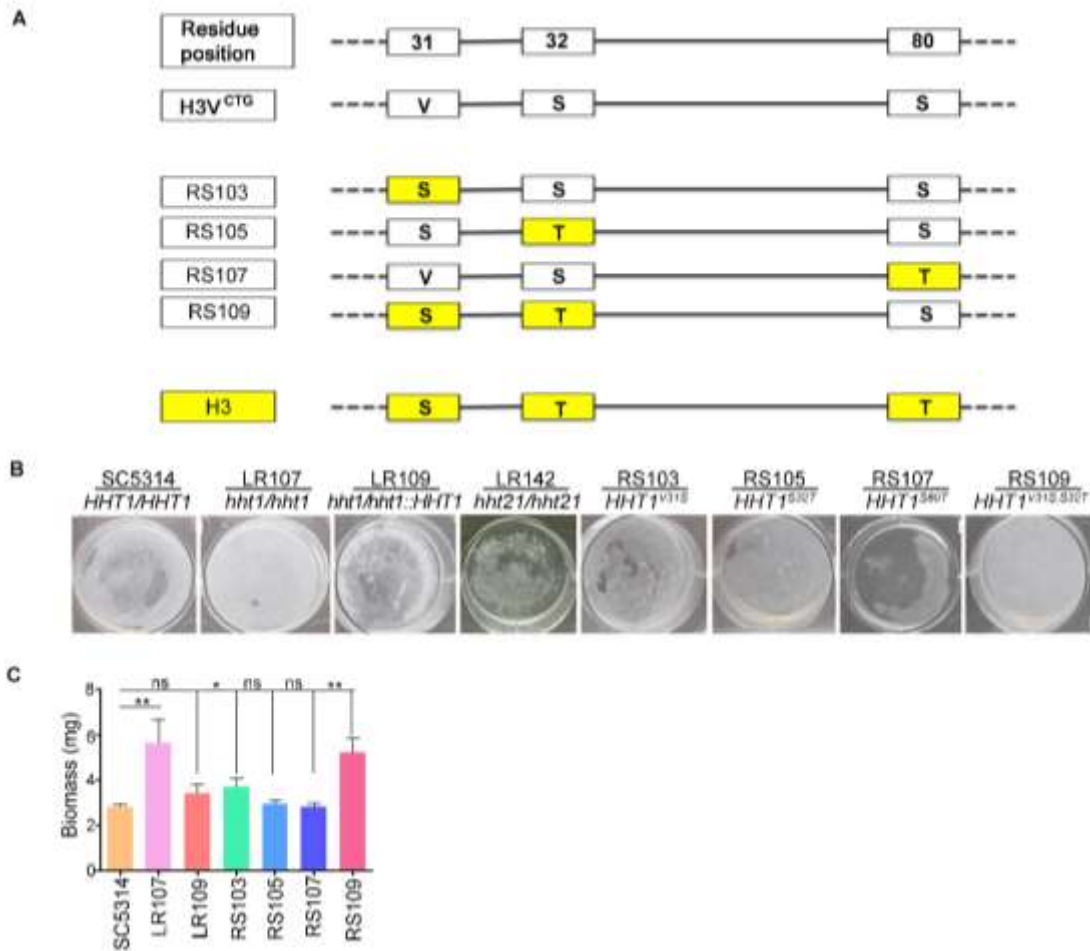


Figure 2.5 Co-occurrence of valine and serine at 31 and 32 position is critical for the biofilm repressive function of H3V^{CTG} in *C. albicans*.

A. Schematics represent various point-mutant strains constructed by changing amino acid residues at positions 31, 32, and 80 of variant histone H3 to that of the canonical histone H3. **B.** Wild-type (SC5314), LR107 (*hht1/hht1*), LR109 (*hht1/hht1::HHT1*), RS103 (*hht1/hht1::HHT1^{V31S}*), RS105 (*hht1/hht1::HHT1^{S32T}*), RS107 (*hht1/hht1::HHT1^{S80T}*), and RS109 (*hht1/hht1::HHT1^{V31S,S32T}*) were allowed to form biofilm in YPDU for 48 h at 37°C; wells were washed to remove the nonadherent cells and photographed. **C.** Biomass dry weights of the wild-type (SC5314), LR107 (*hht1/hht1*), LR109 (*hht1/hht1::HHT1*), RS103 (*hht1/hht1::HHT1^{V31S}*), RS105 (*hht1/hht1::HHT1^{S32T}*), RS107 (*hht1/hht1::HHT1^{S80T}*), and RS109 (*hht1/hht1::HHT1^{V31S,S32T}*) grown as biofilm in YPDU at 37°C for 48 h.

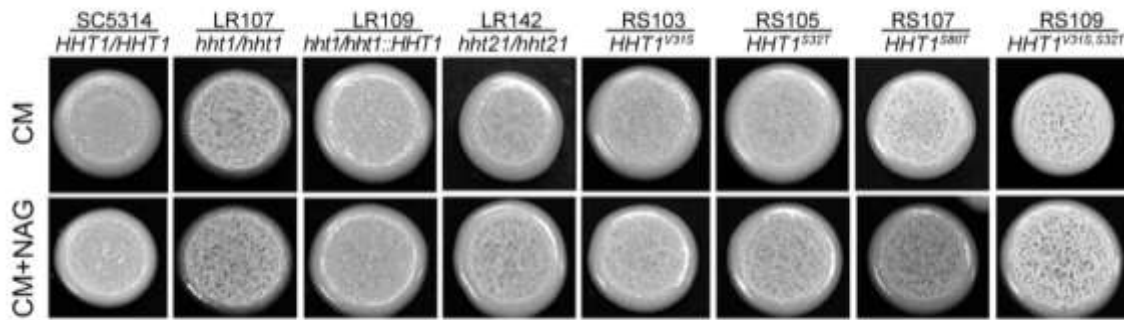


Figure 2.6 Amino acid residues valine, and serine at 31 and 32 position are essential for the filamentation function of H3V^{CTG} in *C. albicans*

Wild-type (SC5314), LR107 (*hht1/hht1*), LR109 (*hht1/hht1::HHT1*), LR142 (*hht21/hht21*), RS103 (*hht1/hht1::HHT1^{V31S}*), RS105 (*hht1/hht1::HHT1^{S32T}*), RS107 (*hht1/hht1::HHT1^{S80T}*), and RS109 (*hht1/hht1::HHT1^{V31S, S32T}*) were spotted on synthetic dextrose media complemented with essential amino acids (CM) agar plates, and CM+NAG (synthetic dextrose with 1 mM N-acetyl glucosamine) agar plates, and incubated for 72 h at 37°C.

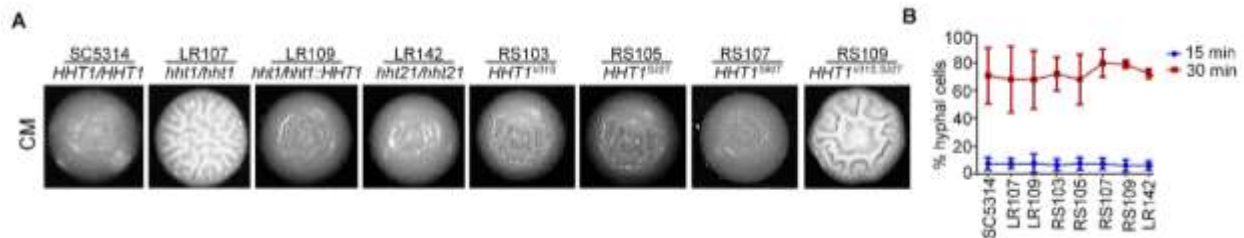


Figure 2.7 The filamentation phenotype of H3V^{CTG} mutants is observed at a single-cell level.

Wild-type (SC5314), LR107 (*hht1/hht1*), LR109 (*hht1/hht1::HHT1*), LR142 (*hht21/hht21*), RS103 (*hht1/hht1::HHT1^{V31S}*), RS105 (*hht1/hht1::HHT1^{S32T}*), RS107 (*hht1/hht1::HHT1^{S80T}*), and RS109 (*hht1/hht1::HHT1^{V31S, S32T}*) **A.** plated for single colonies and monitored for filament formation after 48 h at 37°C **B.** allowed to form filaments in liquid YPD with 10% FBS at 37°C. The proportion of hyphal cells formed by these strains after 15 and 30 mins of induction is plotted.

A copy of H3V^{CTG} with mutations at position 31 and 32 could not complement H3V^{CTG} function

Our studies show that the double point mutants of H3V^{CTG} at positions 31 and 32 (RS109, *hht1/hht1::HHT1^{V31S, S32T}*) mimic the phenotype of H3V^{CTG} null mutant (LR107 and

LR108, *hht1/hht1*) (**Figure 2.5 B and C and Figure 2.6**). Earlier reports suggest that the expression of biofilm genes is induced in H3V^{CTG} null mutant in planktonic growth *in vitro* (Rai, Singha et al. 2019). Interestingly, we observed that similar to H3V^{CTG} null mutants (LR107 and LR108, *hht1/hht1*), in double point mutants of H3V^{CTG} at 31 and 32 positions (RS109 and RS110, *hht1/hht1::HHT1^{V31S, S32T}*), the expression of a subset of critical biofilm-related genes was altered, as validated by qPCR analysis (**Figure 2.8**). Thus, our study suggests that the amino acid residues at positions 31 and 32 of H3V^{CTG} fine-tune the maintenance of the planktonic growth by repressing the biofilm growth-promoting gene circuitry.

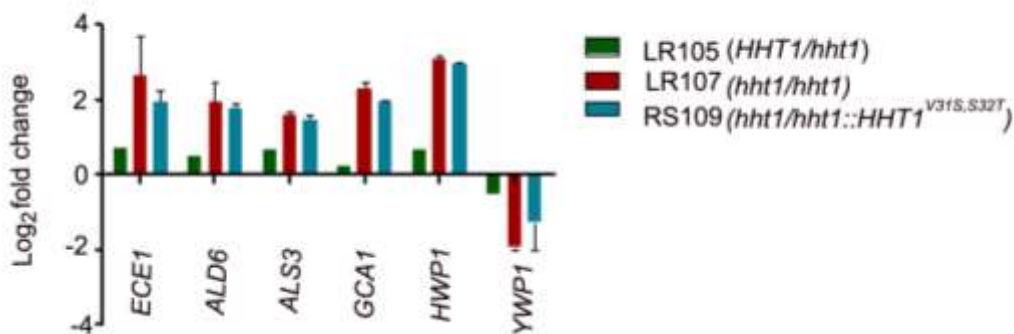


Figure 2.8 Mutation of H3V^{CTG} at positions 31, 32 induces the biofilm gene circuitry during the planktonic mode.

Expression of biofilm-related genes was examined by qPCR analysis with the cells of LR105 (*HHT1/hht1*), LR107 (*hht1/hht1*) and RS109 (*hht1/hht1::HHT1^{V31S, S32T}*) grown in YPDU under planktonic conditions. ΔC_t values were derived after normalizing of expression of biofilm genes with that of actin. $\Delta\Delta C_t$ values were calculated for relative expression of biofilm-related genes in the H3V^{CTG} null mutants compared with the wild-type. The values from three independent qPCR experiments were plotted. A t-test was performed to determine statistical significance. Primer sequences are listed in Table 6.2.

Occupancy of a biofilm specific transcription factor, Bcr1 is increased at the promoters of biofilm relevant genes in the presence of a full-length protein with mutations at position 31 and 32 of H3V^{CTG}

Previously we have shown that the accessibility of Bcr1 to the promoters of biofilm-related genes is enhanced in the absence of H3V^{CTG} as compared to wild-type in the

planktonic mode of growth. Since the double point mutants of H3V^{CTG} at positions 31 and 32 (RS109, *hht1/hht1::HHT1^{V31S, S32T}*) phenocopies H3V^{CTG} null mutant (LR107 and LR108, *hht1/hht1*), we examined whether the occupancy of Bcr1 is also affected in the presence of double point mutant of H3V^{CTG}, when present as a single copy in the cell (RS112, *BCR1-Myc/BCR1 hht1/hht1::HHT1^{V31S, S32T}*). Since the single point mutants of H3V^{CTG} (RS103, *hht1/hht1::HHT1^{V31S}*, RS105, *hht1/hht1::HHT1^{S32T}* and RS107, *hht1/hht1::HHT1^{S80T}*) shows phenotypes compared to that of wild-type strain in terms of biofilm formation, we assessed the Bcr1 enrichment at the promoters of biofilm genes in one of the single point mutant strains (RS111, *BCR1-Myc/BCR1 hht1/hht1::HHT1^{V31S}*) for comparative analysis. ChIP analysis of Bcr1 density in the double point mutant strains of H3V^{CTG} (RS112, *BCR1-Myc/BCR1 hht1/hht1::HHT1^{V31S, S32T}*) revealed that the binding of Bcr1 was increased at the promoters of *JEN2*, *ECE1*, *ALS3*, *YWP1* and Orf19.7380 as compared to wild-type (**Figure 2.9 A**). The binding of Bcr1 to the biofilm gene promoters was unaltered in the single point mutant strains (RS111, *BCR1-Myc/BCR1 hht1/hht1::HHT1^{V31S}*) as compared to wild-type (CJN1785, *BCR1-Myc/BCR1*) (**Figure 2.9 B**). Thus, the occupancy of Bcr1 in the single- and double-point mutant strains of H3V^{CTG} corroborated their respective filamentation and biofilm phenotype.

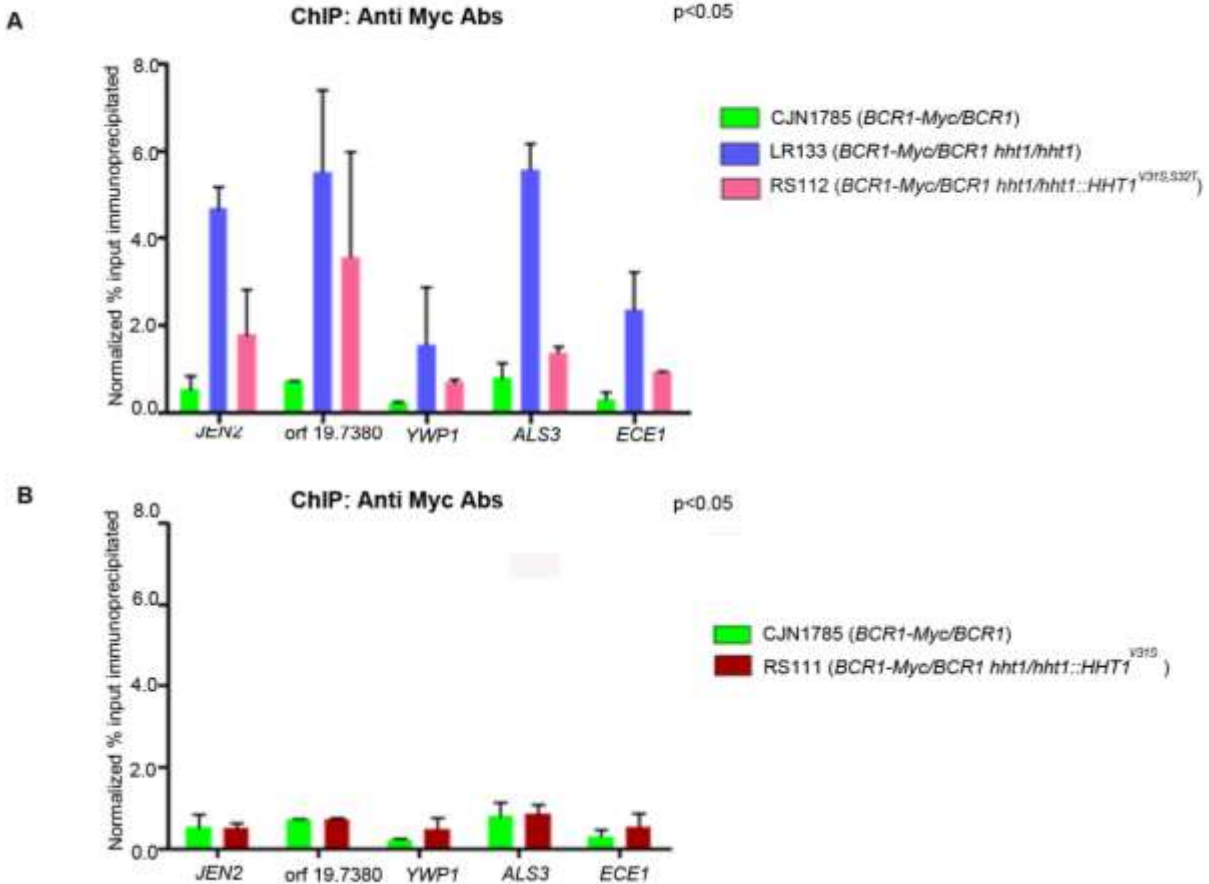


Figure 2.9 Occupancy of Bcr1 is increased at the promoter of biofilm genes in double point mutants.

A. ChIP assays were performed with anti-myc antibodies in the cells of wild-type (C.JN1785, *BCR1-Myc/BCR1*), H3V^{CTG} null mutant, LR133 (*BCR1-Myc/BCR1 hht1/hht1*) and double point-mutant strain at position 31 and 32, RS112 (*BCR1-Myc/BCR1 hht1/hht1::HHT1^{V31S,S32T}*). **B.** Similarly, ChIP assays were performed with anti-myc antibodies in point-mutant strain at position 31, RS111 (*BCR1-Myc/BCR1 hht1/hht1::HHT1^{V31S}*). The enrichment of Bcr1-myc at the promoter of biofilm genes was compared to wild-type (C.JN1785, *BCR1-Myc/BCR1*). The input and IP DNA fractions were analyzed by qPCR with primers from promoters of the biofilm genes for the binding of Bcr1-myc. The enrichment of Bcr1-myc was calculated and normalized with Orf19.874 and is represented as a normalized percent input IP in the y-axis. The x-axis indicates the biofilm genes whose promoter regions were assayed for binding. Error bars indicate standard error of Mean (SEM). The values from three independent ChIP experiments, each performed with three technical replicates were plotted. A two-way ANOVA test was performed to determine statistical significance. Primer sequences are listed in Table 6.2.

Occupancy of the double point mutant H3V^{CTG} (Hht1^{V31S, S32T}) decreases at the promoter of biofilm genes

Since the double point mutant of H3V^{CTG} (RS109, *hht1/hht1::HHT1^{V31S, S32T}*) imitated the phenotype of the H3V^{CTG} null mutant (LR107, *hht1/hht1*), we investigated the loading of this mutated H3V^{CTG} at the promoters of biofilm genes. We epitope-tagged the double point mutant of H3V^{CTG} in a strain of *C. albicans* where it was the only copy of the variant H3 present in the cell (RS113, *hht1/hht1::HHT1^{V31S, S32T}-V5*). We then performed ChIP-qPCR at the promoters of the biofilm genes, which were affected in the transcription profiling in the absence of H3V^{CTG}. We observed a decrease in the binding of the mutated H3V^{CTG} at the promoter of *CAN1*, *BMT7*, *HWP1*, *YWP1*, *orf19.7380* and *SAP5* (Figure 2.10). This observation alludes to the fact that residues at positions 31 and 32 are critical for localization of H3V^{CTG}, thereby explaining the biofilm specific defects upon mutation of these residues in H3V^{CTG}.

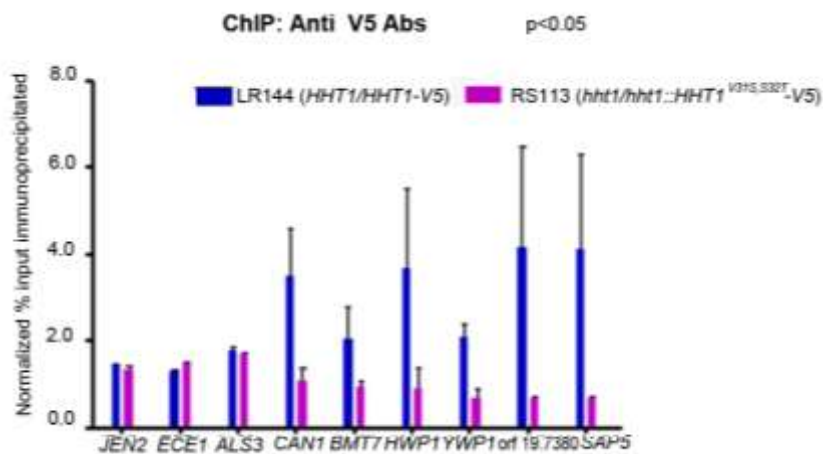


Figure 2.10 Occupancy of the double point mutants of H3V^{CTG} decreases at the promoter of biofilm genes.

ChIP assays with anti-V5 antibodies were performed in cells of LR144 (*HHT1/HHT1-V5*) and RS113 (*hht1/hht1::HHT1^{V31S, S32T}-V5*) expressing a V5-tagged variant histone H3 or double point mutant histone H3 (Hht1^{V31S, S32T}) grown in planktonic conditions. The input and IP DNA fractions were analyzed by qPCR with gene-specific promoter primer pairs for binding of either H3V^{CTG} or mutated H3V^{CTG}. The enrichment of H3V^{CTG} or mutated H3V^{CTG} was calculated and normalized with Orf19.874 and is represented as a normalized percent input IP in the y-axis. The x-axis indicates the biofilm genes whose promoter regions were assayed for binding. Error bars indicate standard error of mean (SEM). The values from 3

independent ChIP experiments, each performed with three technical replicates were plotted. A two-way ANOVA test was performed to determine statistical significance. Primer sequences are listed in Table 6.2.

Conservation of variant-specific residues of H3V^{CTG} across the CUG clade species in Ascomycota

C. albicans and related *Candida* species comprise the CUG clade in which the tRNA corresponding to CUG codon codes for serine instead of leucine majority of the time. Recent investigations on the genome of yeast species have identified three independent events involving the reassignment of CUG codons from universal leucine to alanine once and twice to serine (Krassowski, Coughlan et al. 2018). Therefore, based on different translations of the CUG codon, there are five monophyletic groups (clade): Ala, Ser1, Ser2, Leu1, and Leu2 clades, as well as a paraphyletic outgroup taxa (Leu0) with the standard code. *C. albicans* belongs to the Ser1 clade, which also contains many pathogenic *Candida* species and extends till *Babjeviella* (Shen, Opulente et al. 2018). The Ser2 clade consists of the genera *Ascoidea* and *Saccharomyopsis*. Ser2 clade species, however contain few CUG codons in their conserved genes (Krassowski, Coughlan et al. 2018). The Ser2 clade is the sister clade of the Leu1 clade, which contains *Saccharomyces cerevisiae*.

We analyzed the genomes of species belonging to the CUG clade to study the presence of histone H3 variants and their amino acid sequence conservation. The genome sequence information of 94 members of the CUG-Ser1 clade is available (Shen, Opulente et al. 2018). H3V^{CTG} could not be detected in the members of CUG-Ala, CUG-Ser2, CUG-Leu1, and Leu2 clades. However, across the CUG-Ser1 clade species, the presence of H3V^{CTG} was ubiquitous except in *Babjeviella inositovera* (**Figure 2.11**). An in-depth analysis of the amino acid sequence composition of H3V^{CTG} in the species within the CUG-Ser1 clade revealed the following: (1) In family Debaromycetaceae to which *C. albicans* belongs, the amino acid residues at positions 31, 32, and 80 are conserved as valine, serine, and serine respectively. (2) However, in the Metschnikowiaceae family of the CUG-Ser1 clade, in the majority of species of *Metschnikowia* (*M. aberdeeniae*, *M. arizonensis*, *M. bicuspidata*, *M. borealis*, *M. bowlesiae*, *M. cerradonensis*, *M. continentalis*, *M. dekortum*, *M. drakensbergensis*,

M. hamakuensis, *M. hawaiiensis*, *M. hibisci*, *M. ipomoeae*, *M. kamakouana*, *M. kipukae*, *M. lockheadii*, *M. matae*, *M. matae maris*, *M. mauiuiana*, *M. proteae*, *M. santaceciliae*, *M. shivogae* and *M. similis*), *Meyerozyma* genera (*M. caribbica* and *M. guilliermondii*) and *Candida caprophila*, there were variations in amino acid residues at position 31 (alanine instead of valine) or 32 (threonine instead of serine) (**Table 2-1**). While substitutions were observed independently at either of these positions, we did not detect any histone H3 variant that showed variation at both amino acid positions, 31 and 32. Taken together with the phenotype obtained in RS109 (*hht1/hht1::HHT1^{V31S, S32T}*) and these analyses suggest that the co-occurrence of amino acid residues at positions 31 and 32 is critical for the function of H3V^{CTG} as a biofilm regulator in *C. albicans*.

Overall, our studies suggest that the presence of a single copy of H3V^{CTG} with mutations at 31st and 32nd position phenocopies the genetic deletion of H3V^{CTG} inducing the biofilm gene circuitry and hyperfilamentation on the solid surface. Co-immunoprecipitation studies in human cell lines indicate that mutation of variant-specific residues of H3.3 (AAIG at 87-90 instead of SAVM) diminishes the interaction of its specific chaperone, DAXX (Elsasser, Huang et al. 2012). We have also shown that mutation of amino acid residues at positions 31 and 32 of H3V^{CTG} inhibits its occupancy at the promoter of biofilm genes (**Figure 2.10**). Taken together, it is possible that these H3V^{CTG} specific amino acid residues at positions 31 and 32, might be crucial in the loading of H3V^{CTG} to the biofilm gene promoters, or they may also carry variant-specific modifications with restricted assembly into particular chromatin domains.

To test if the residues at positions 31 and 32 of H3V^{CTG} might contribute to differential chaperone recognition and incorporation at distinct genomic regions (biofilm promoters), we analyzed the phenotype of already identified histone H3 chaperone mutants in *C. albicans*. CAF-1 and HIRA complexes are chaperones involved in recruiting canonical and variant histone H3, respectively, to distinct genomic locations. Cac2, a subunit of CAF-1, is involved in the recruitment of canonical/DNA synthesis coupled (DSC) histone H3 to chromatin by associating with replication machinery. Hir1, a subunit of the HIRA complex, is involved in the recruitment of variant/DNA synthesis independent (DSI) histone H3 to chromatin. We examined the phenotype of previously reported mutants of



Figure 2.11 Phylogenetic tree depicting conservation of variant-specific residues of H3V^{CTG} across CUG-Ser1 clade of ascomycetes.

Out of 332 fungal species sequenced (Chen *et al.*, 2018), 94 members from CUG-Ser1 clade were analyzed for the presence of H3V^{CTG}.

Table 2-1 Table representing the conservation/divergence of amino acid residues at a particular position in H3 variants of the CUG-Ser1 clade species.

Any divergence in amino acid sequence at 31, 32 and 80 position of H3V^{CTG} from “ VSS ” is highlighted (T- threonine in blue and A- alanine in yellow).

Organism	Amino acid residues of H3V ^{CTG}		
	31	32	80
<i>Aciculoconidium aculeatum</i>	V	S	S
<i>Babjeviella inositovora</i>	x	x	x
<i>Candida albicans</i>	V	S	S
<i>Candida ascalaphidarum</i>	V	S	S
<i>Candida athensensis</i>	V	S	S
<i>Candida auris</i>	V	S	S
<i>Candida blattae</i>	V	S	S
<i>Candida canberraensis</i>	V	S	S
<i>Candida carpophila</i>	V	T	S
<i>Candida corydali</i>	V	S	S
<i>Candida cretensis</i>	V	S	S
<i>Candida dubliniensis</i>	V	S	S
<i>Candida emberorum</i>	V	S	S
<i>Candida fragi</i>	V	S	S
<i>Candida fructus</i>	V	S	S
<i>Candida gatunensis</i>	V	S	S
<i>Candida golubevii</i>	V	S	S
<i>Candida gorgasii</i>	V	S	S
<i>Candida gotoi</i>	V	S	S
<i>Candida hawaiiiana</i>	A	S	S
<i>Candida homilentoma</i>	V	S	S
<i>Candida intermedia</i>	V	S	S
<i>Candida kruisii</i>	V	T	S
<i>Candida oregonensis</i>	V	S	S
<i>Candida orthopsilosis</i>	V	S	S
<i>Candida parapsilosis</i>	V	S	S
<i>Candida pyralidae</i>	V	S	S
<i>Candida restingae</i>	V	S	S
<i>Candida rhagii</i>	V	S	S
<i>Candida schatavii</i>	V	S	S
<i>Candida sojae</i>	V	S	S
<i>Candida tammaniensis</i>	V	S	S
<i>Candida tanzawaensis</i>	V	S	S
<i>Candida tenuis</i>	V	S	S
<i>Candida tropicalis</i>	V	S	S
<i>Candida wancherniae</i>	V	S	S
<i>Cephaloascus albidus</i>	T	S	S
<i>Cephaloascus fragrans</i>	T	S	S

<i>Clavispora lusitaniae</i>	V	S	S
<i>Danielozyma ontarioensis</i>	V	S	S
<i>Debaryomyces fabryi</i>	V	S	S
<i>Debaryomyces hansenii</i>	V	S	S
<i>Debaryomyces maramus</i>	V	S	S
<i>Debaryomyces nepalensis</i>	V	S	S
<i>Debaryomyces prosopidis</i>	V	S	S
<i>Debaryomyces subglobosus</i>	V	S	S
<i>Hyphopichia burtonii</i>	V	S	S
<i>Hyphopichia heimii</i>	V	S	S
<i>Kodamaea laetipori</i>	V	S	S
<i>Kodamaea ohmeri</i>	V	S	S
<i>Kurtzmaniella cleridarum</i>	V	S	S
<i>Lodderomyces elongisporus</i>	V	S	S
<i>Metschnikowia aberdeeniae</i>	A	S	S
<i>Metschnikowia arizonensis</i>	A	S	S
<i>Metschnikowia bicuspidata</i>	V	S	S
<i>Metschnikowia borealis</i>	A	S	S
<i>Metschnikowia bowlesiae</i>	A	S	S
<i>Metschnikowia cerradonensis</i>	A	S	S
<i>Metschnikowia continentalis</i>	A	S	S
<i>Metschnikowia dekortum</i>	A	S	S
<i>Metschnikowia drakensbergensis</i>	A	S	S
<i>Metschnikowia hamakuensis</i>	A	S	S
<i>Metschnikowia hawaiiensis</i>	A	S	S
<i>Metschnikowia hibisci</i>	A	S	S
<i>Metschnikowia ipomoeae</i>	A	S	S
<i>Metschnikowia kamakouana</i>	A	S	S
<i>Metschnikowia kipukae</i>	A	S	S
<i>Metschnikowia lockheadii</i>	A	S	S
<i>Metschnikowia matae</i>	A	S	S
<i>Metschnikowia matae maris</i>	A	S	S
<i>Metschnikowia mauinuiana</i>	A	S	S
<i>Metschnikowia proteae</i>	A	S	S
<i>Metschnikowia santaceciliae</i>	A	S	S
<i>Metschnikowia shivogae</i>	A	S	S
<i>Metschnikowia similis</i>	A	S	S
<i>Meyerozyma caribbica</i>	V	T	S
<i>Meyerozyma guilliermondii</i>	V	T	S
<i>Millerozyma acaciae</i>	V	S	S
<i>Priceomyces carsonii</i>	V	S	S
<i>Priceomyces castillae</i>	V	S	S
<i>Priceomyces haplophilus</i>	V	S	S
<i>Priceomyces medius</i>	V	S	S
<i>Scheffersomyces lignosus</i>	V	S	S
<i>Scheffersomyces stipitis</i>	V	S	S
<i>Spathaspora arborariae</i>	V	S	S

<i>Spathaspora girioi</i>	V	S	S
<i>Spathaspora gorwiae</i>	V	S	S
<i>Spathaspora hagerdaliae</i>	V	S	S
<i>Spathaspora passalidarum</i>	V	S	S
<i>Wickerhamia fluorescens</i>	V	S	S
<i>Yamadazyma nakazawae</i>	V	S	S
<i>Yamadazyma philogaea</i>	V	S	S
<i>Yamadazyma scolyti</i>	V	S	S

each of these chaperone complexes (Cac2 for CAF-1 and Hir1 for HIRA) for biofilm formation assuming that the cognate chaperone mutant will mimic the phenotype of H3V^{CTG} null mutants (LR107 and LR108, *hht1/hht1*).

***cac2* mutants mimic the hyperfilamentation phenotype of H3V^{CTG} null mutant**

The deletion mutants of *cac2* (CA-MT363, *cac2/cac2*) and *hir1* (CA-MT376, *hir1/hir1*) in *C. albicans* were tested for filamentation in solid media surface. In the media conditions tested, the null mutants of *cac2* (CA-MT363, *cac2/cac2*) exhibited higher colony wrinkling than wild-type (SC5314) in both complete media and YPDU (**Figure 2.12 A**). The *hir1* null mutants (CA-MT376, *hir1/hir1*) in *C. albicans* have previously been reported to be defective in filamentation (Jenull, Tscherner et al. 2017) and were found to be less filamentous in the media conditions tested for our experiment as well (**Figure 2.12 A**). We also observed that *cac2* null mutants (CA-MT363, *cac2/cac2*) formed a robust biofilm than the wild-type (**Figure 2.12 B**) phenocopying the H3V^{CTG} null mutants in *C. albicans*. On the other hand, the mutants of the HIRA complex, a known variant H3 (H3.3) specific chaperone in *Xenopus* (Prochasson, Florens et al. 2005) and humans (Ray-Gallet, Quivy et al. 2002, Nakatani, Ray-Gallet et al. 2004, Tagami, Ray-Gallet et al. 2004) shows a phenotype contrasting to that of H3V^{CTG} null mutants in *C. albicans*. Based on these observations, we posit that Cac2, a subunit of the canonical H3 chaperone complex CAF-1 in many organisms, could be the probable chaperone for variant histone H3, H3V^{CTG} in *C. albicans*.

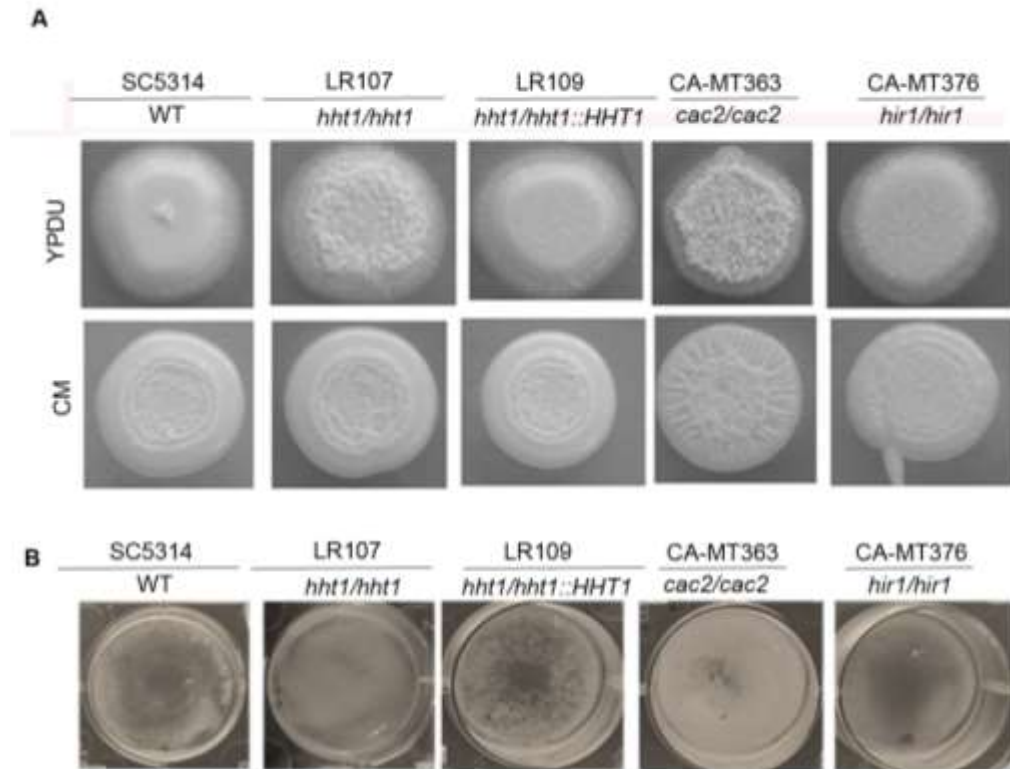


Figure 2.12 *cac2* null mutants mimic the hyperfilamentation and enhanced biofilm formation phenotype of the H3V^{CTG} null mutant.

Wild-type (SC5314), LR107 (*hht1/hht1*), LR109 (*hht1/hht1::HHT1*), CA-MT363 (*cac2/cac2*) and CA-MT376 (*hir1/hir1*) were monitored for **A.** filament formation for 48 h at 37°C in YPDU and CM plates and **B.** biofilm formation after 48 h at 37°C.

H3V^{CTG} levels at the promoter of biofilm genes are reduced in the absence of Cac2

To further assess the contribution of these chaperones in recruiting histone H3 variants in *C. albicans*, we epitope-tagged both canonical (RS501, *cac2/cac2* HHT21/HHT21-V5) and variant histone H3 (RS502, *cac2/cac2* HHT1/HHT1-V5) in *cac2* null mutant background independently. We then examined the alteration in the occupancy of canonical histone H3 or its variant in the absence of Cac2. We observed that the occupancy of H3V^{CTG} at the promoter of biofilm genes decreases in the absence of Cac2 in planktonic condition (**Figure 2.13 A**). The trend of canonical histone binding was reversed entirely in the case of absence of Cac2 (**Figure 2.13 B**). The occupancy of canonical H3 increased in the absence of Cac2. These observations hint towards the possibility of a functional divergence during the chaperone assignment of H3V^{CTG} in *C. albicans*.

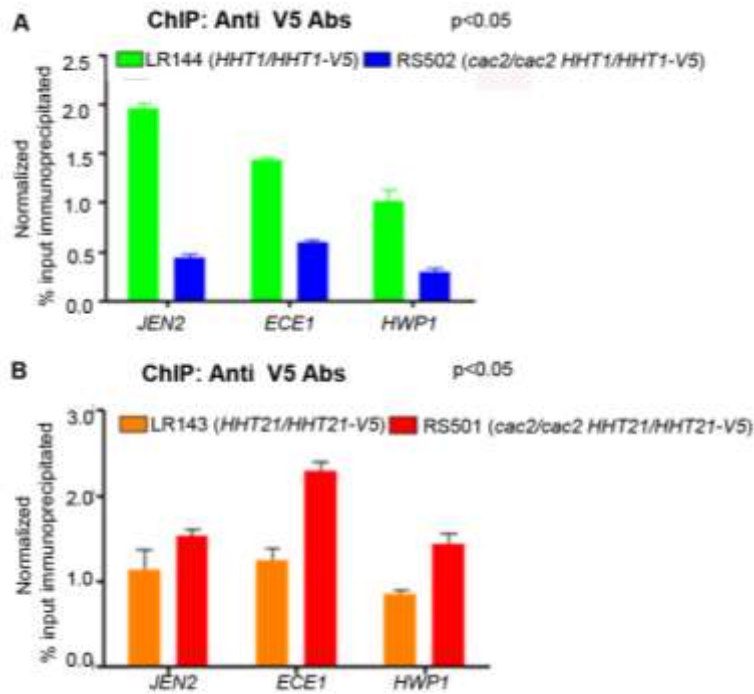


Figure 2.13 Reduction of H3V^{CTG} levels in the absence of Cac2.

A. ChIP assays with anti-V5 antibodies were performed in cells of LR144 (*HHT1/HHT1-V5*) and RS502 (*cac2/cac2 HHT1/HHT1-V5*) expressing a V5-tagged variant histone H3 in wild-type background and *cac2* null mutant background respectively grown in planktonic conditions. **B.** ChIP assays with anti-V5 antibodies were performed in cells of LR143 (*HHT21/HHT21-V5*) and RS501 (*cac2/cac2 HHT21/HHT21-V5*) expressing a V5-tagged canonical histone H3 in wild-type background and *cac2* null mutant background respectively. The input and IP DNA fractions were analyzed by qPCR with gene-specific promoter primer pairs for binding of H3V^{CTG} (Hht1) or canonical histone H3 (Hht21). The enrichment of canonical histone H3 or H3V^{CTG} was calculated and normalized with Orf19.874. The enrichment of canonical histone H3 or H3V^{CTG} to the promoters of biofilm-related genes is represented as a normalized percent input IP in the y-axis. The x-axis indicates the biofilm genes whose promoter regions were assayed for binding. Error bars indicate standard error of mean (SEM). The values from three independent ChIP experiments, each performed with three technical replicates were plotted. A two-way ANOVA test was performed to determine statistical significance. Primer sequences are listed in Table 6.2.

Chapter 3

Temporal regulation of biofilm development by variant histone H3 in *C. albicans*

Introduction

Our existing knowledge of histone H3 variants in *C. albicans* indicates that H3V^{CTG} acts as a major regulator of the biofilm gene circuitry. The genome-wide transcriptome data of the H3V^{CTG} null mutant indicates altered expression of a subset of critical biofilm-related genes. However, the step(s) at which H3V^{CTG} regulates biofilm development in *C. albicans* remain(s) unclear.

Biofilm formation can be broadly divided into four steps: (a) adherence of yeast cells to biotic/abiotic substrate, (b) initiation of a basal layer of microcolonies of yeast cells along with the appearance of hyphal and pseudohyphal cells, (c) maturation where the cells get entrapped in the extracellular matrix and (d) dispersion where yeast cells detach from the biofilm to seed at new sites (Chandra, Kuhn et al. 2001, Kumamoto 2002, Ramage, Saville et al. 2005, Sardi, Scorzoni et al. 2013, Zhu, Wang et al. 2013, Nobile and Johnson 2015, Gulati and Nobile 2016, Soll and Daniels 2016, Noble, Gianetti et al. 2017, Lohse, Gulati et al. 2018). There is an interconnected network involving ~1200 genes regulating this phenotypic transition. Nine master regulators (Bcr1, Tec1, Ndt80, Efg1, Brg1, Rfx2, Gal4, Flo8, and Rob1) (Nobile, Fox et al. 2012, Fox, Bui et al. 2015) for biofilm formation have been identified to date.

In an attempt to delineate the step(s) at which the variant histone H3, H3V^{CTG} regulate(s) biofilm development in *C. albicans*, we chose to investigate its possible role in its first step, on cell surface adherence. In a screen of transcription factor (TF) mutants affecting cell-substrate adherence, 30 TFs were identified to be essential for the process. Among these 30 TFs, four of them, namely Bcr1, Ace2, Snf5, and Arg81, had an additional role in biofilm formation *in vitro* (on polystyrene microtiter plates with shaking). For example, adherence to plastic surfaces is severely compromised in the absence of one of these regulators, Ace2 (Kelly, MacCallum et al. 2004). The *ace2* null mutant cells form biofilms with a strikingly different morphology as compared to wild-type cells in *C. albicans* (Kelly, MacCallum et al. 2004). In addition, another adherence and biofilm master regulator, Bcr1, shares several common targets of RAM (Regulation of Ace2 and

morphogenesis) pathway with Ace2. The RAM pathway is known to control biofilm formation in *C. albicans* (Finkel, Xu et al. 2012).

Previously we demonstrated that in the absence of H3V^{CTG}, one of the master regulators of biofilm development, such as Bcr1 gains access to the promoter of biofilm specific genes in planktonic conditions and regulates their expression. Besides, genome-wide expression data of the H3V^{CTG} (*hht1/hht1*) null mutant showed a trend of up-regulated expression of adhesins, including *ALS3* and *HWP1*. Based on these observations, we hypothesize that in the absence of Ace2, Bcr1 may not gain access to promoters of the biofilm specific genes due to the presence of H3V^{CTG}, and hence they exhibit adhesion and biofilm defects. However, in the absence of both Ace2 and H3V^{CTG}, Bcr1 might gain access to the promoter of biofilm specific genes and might be able to rescue the defects related to adhesion and biofilm formation associated with the *ace2* single mutant. This would also verify whether adhesion is one of the steps in biofilm development that is regulated by H3V^{CTG}. To address this possibility, we sought to study the genetic interaction between *ACE2* and *HHT1*.

Substrate adherence defects of *ace2* null cells of *C. albicans* is partially rescued in *ace2* and *hht1* double null mutant cells

Previous reports suggest that biofilm-forming defects of the *bcr1* null mutant is rescued by the overexpression of *ALS3* and partially rescued by overexpression of other target genes of Bcr1, like *ALS1*, *ECE1* or *HWP1*. Overexpression of common eight target genes (*ORF19.3337*, *ALS1*, *TPO4*, *ORF19.4000*, *EHT1*, *HYR1*, *HWP1*, and *CAN2*) regulated by six master regulators of biofilm formation (Bcr1, Tec1, Ndt80, Efg1, Brg1, and Rob1) show significant restoration of biofilm formation to varying degrees depending on the target gene-mutant combination (Nobile, Fox et al. 2012). Several adhesins, including *ALS3*, *ECE1* and *HWP1*, were up-regulated in the H3V^{CTG} null mutant. Moreover, H3V^{CTG} was found to bind to the promoters of many of the biofilm-related genes, possibly to inhibit biofilm growth and to promote planktonic growth. Thus, we examined the extent of adhesion and biofilm formation in the absence of both an adhesion regulator Ace2 and a biofilm repressor H3V^{CTG}. In addition, *ace2* null mutants have been shown to severely hamper biofilm formation (Kelly, MacCallum et al. 2004). To test whether the deletion of

H3V^{CTG} can rescue adhesion and biofilm defects of *ace2* null cells, we deleted both copies of *HHT1* (H3V^{CTG}) in RS404 (*ace2/ace2*) and examined both adhesion properties and biofilm-forming ability of the double mutants, RS408, RS409 (*ace2/ace2 hht1/hht1*) in YNB medium. Three different assays were performed (a) optical density measurements 90 min post adhesion (**Figure 3.1 A**), (b) metabolic activity by XTT assay (**Figure 3.1 B**), and (c) CFU counting by plating adhered cells 90 min post adhesion (**Figure 3.1 C**). In all the three assays, we observed that the deletion of *HHT1* in the *ace2* null cells led to significant rescue of the ability of cells to adhere to the solid surface. This rescue in phenotype was further observed in biofilm formation (**Figure 3.2 A**). Although the distinct morphology in biofilm formed by *ace2* null mutants (RS404) was still observed in RS408, RS409 (*ace2/ace2 hht1/hht1*) mutants, there was a significant increase in both adhesion and biofilm as quantified by biomass and optical density measurements (**Figure 3.2 B and C**). Taken together, we conclude that the deletion of histone H3V^{CTG} rescued adhesion and biofilm-forming defects associated with *ace2* null mutants.

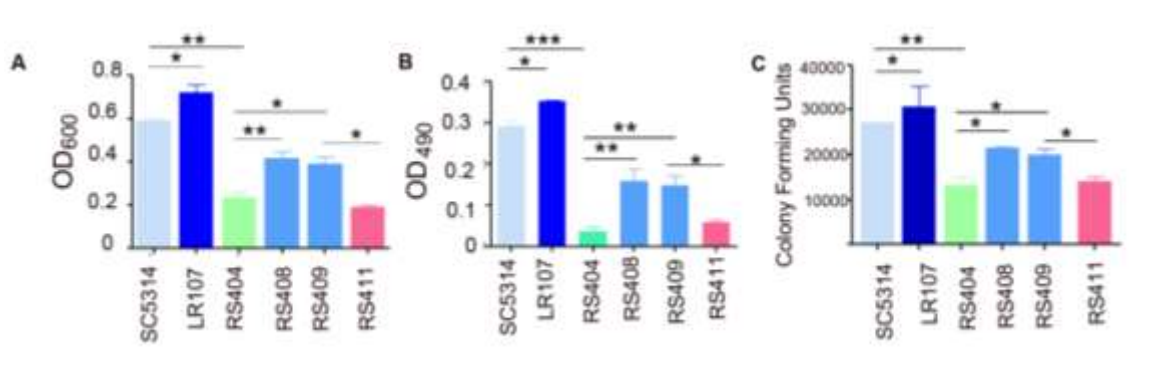


Figure 3.1 The deletion of H3V^{CTG} rescues the adherence defects associated with *ace2* null mutants in *C. albicans*.

SC5314 (wild-type), LR107 (*hht1/hht1*), RS404 (*ace2/ace2*), RS408, RS409 (*ace2/ace2 hht1/hht1*) and RS411 (*ace2/ace2 hht1/hht1::HHT1*) were allowed to adhere in six-well polystyrene plates in YNB+500 mM gal for 90 min at 37°C. The wells were washed to remove the nonadherent cells, and adhered cells were quantified by **A.** crystal violet staining **B.** XTT assay to measure the metabolic activity of adhered yeast cells **C.** CFU counting by plating of the adhered cells. Results from three independent experiments were considered for the statistical analysis. Statistical significance (p-value) was calculated with a Student's two-tailed unpaired t-test and is represented by the asterisks (*p-value ≤ 0.05, **p-value ≤ 0.01, ***p-value ≤ 0.001).

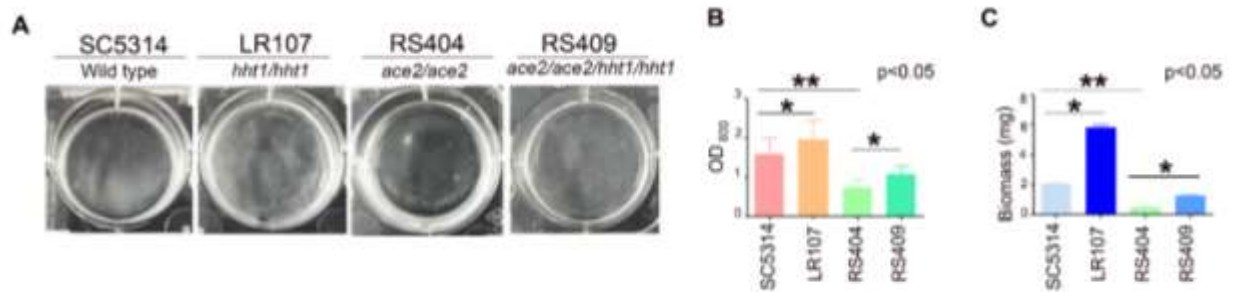


Figure 3.2 The deletion of variant histone H3V^{CTG} rescues biofilm defects in *ace2* null mutants in *C. albicans*.

A. SC5314, LR107 (*hht1/hht1*), RS404 (*ace2/ace2*) and RS409 (*ace2/ace2 hht1/hht1*) were allowed to form biofilms in YNB+500 mM gal for 48 h at 37°C; wells were washed to remove the nonadherent cells and photographed. The experiment was repeated thrice. **B.** Biofilm formation was quantified using the standard optical density assay by measuring OD₆₀₀ of the cells adhered to the bottom of the plates. Data are the mean of three independent wells per condition. Error bars represent the standard deviation. **C.** Quantification of the dry biomass weights of the biofilms grown in YNB at 37°C measured in three independent experiments. Statistical significance (p-value) was calculated with a Student’s two-tailed unpaired t-test and is represented by the asterisks (*p-value ≤ 0.05, **p-value ≤ 0.01, ***p-value ≤ 0.001).

Identification of genes involved in Ace2 mediated adherence

A genome-wide comparative transcriptome analysis was carried out to understand the genes/pathways that are altered by the absence of H3V^{CTG}, resulting in the partial rescue of the *ace2* null mutant phenotype in the *ace2 hht1* double null mutants. The gene expression profiles of two biological replicates of each of these strains were determined: LR107 and LR108 (*hht1/hht1*), RS404 and RS405 (*ace2/ace2*) and RS408 and RS409 (*ace2/ace2 hht1/hht1*). Two independent colonies of the parental strain SC5314 (*ACE2/ACE2 HHT1/HHT1*) were taken as a control. These strains were grown in yeast nitrogen base (YNB) supplemented with 500 mM galactose and allowed to adhere for 90 min in the serum coated polystyrene plates at 37°C. mRNA was isolated from each of these strains and their transcriptome profile was determined.

Ace2 is a well-characterized transcription factor that plays roles in morphogenesis (cell separation and cytokinesis), metabolic pathways such as lipid metabolism, glycolysis, mitochondrial activity, adherence, and virulence (Kelly, MacCallum et al. 2004, Mulhern,

Logue et al. 2006). However, previous transcriptome studies on *ace2* null mutants were performed in yeast and hyphal conditions. Our present work is focused on understanding the role of Ace2 in cell adherence on a solid surface, a key step in biofilm formation. Therefore, the expression studies were carried out in an adhered condition for 90 min.

The transcriptome profiling of RS404, RS405 (*ace2/ace2*) revealed that approximately one-third of all *C. albicans* genes (2,041 genes) had altered expression (fold change > 1.5, $p < 0.05$) in the adhered condition. Out of these altered genes, 1244 genes were up-regulated, whereas the remaining 797 genes were down-regulated in null mutants of *ace2* compared with the wild-type (**Figure 3.3 A**). Previous reports on the transcriptome study of *ace2* null cells grown in conditions that favor yeast form had identified 645 genes (FDR of 0.9%) with altered expression when compared to the wild-type (Mulhern, Logue et al. 2006). The current transcriptome study on the *ace2* null mutant thus reveals an extended repertoire of genes being regulated by Ace2 in adhered condition. A total of 206 genes were found to be common between the two data sets (planktonic/yeast and adhered condition) in the absence of Ace2 (**Figure 3.3 B**). The common ones include genes involved in cell separation, cytokinesis, and lipid metabolism.

Subsequently, a detailed investigation of the additional genes regulated by Ace2 in the adhered condition was carried out to identify Ace2-mediated adherence specific genes (AcASGs). The altered gene-sets (2041 genes) in the *ace2* null mutant (RS404, *ace2/ace2*) was compared with previously published results of genes known to be expressed differentially (978 genes) during planktonic to adherence mode of growth (Fox, Bui et al. 2015) (NCBI accession No.GSE61143) (**Figure 3.3 C**). The analyses revealed that out of the 978 differentially expressed genes involved in the planktonic to adherence transition (**right panel**), expression of 392 genes was altered by Ace2 (AcASGs) (**left panel**), of which 190 genes were up-regulated, and 202 genes were down-regulated when Ace2 is absent. Of note, about 40% of adhesion genes are regulated by Ace2.

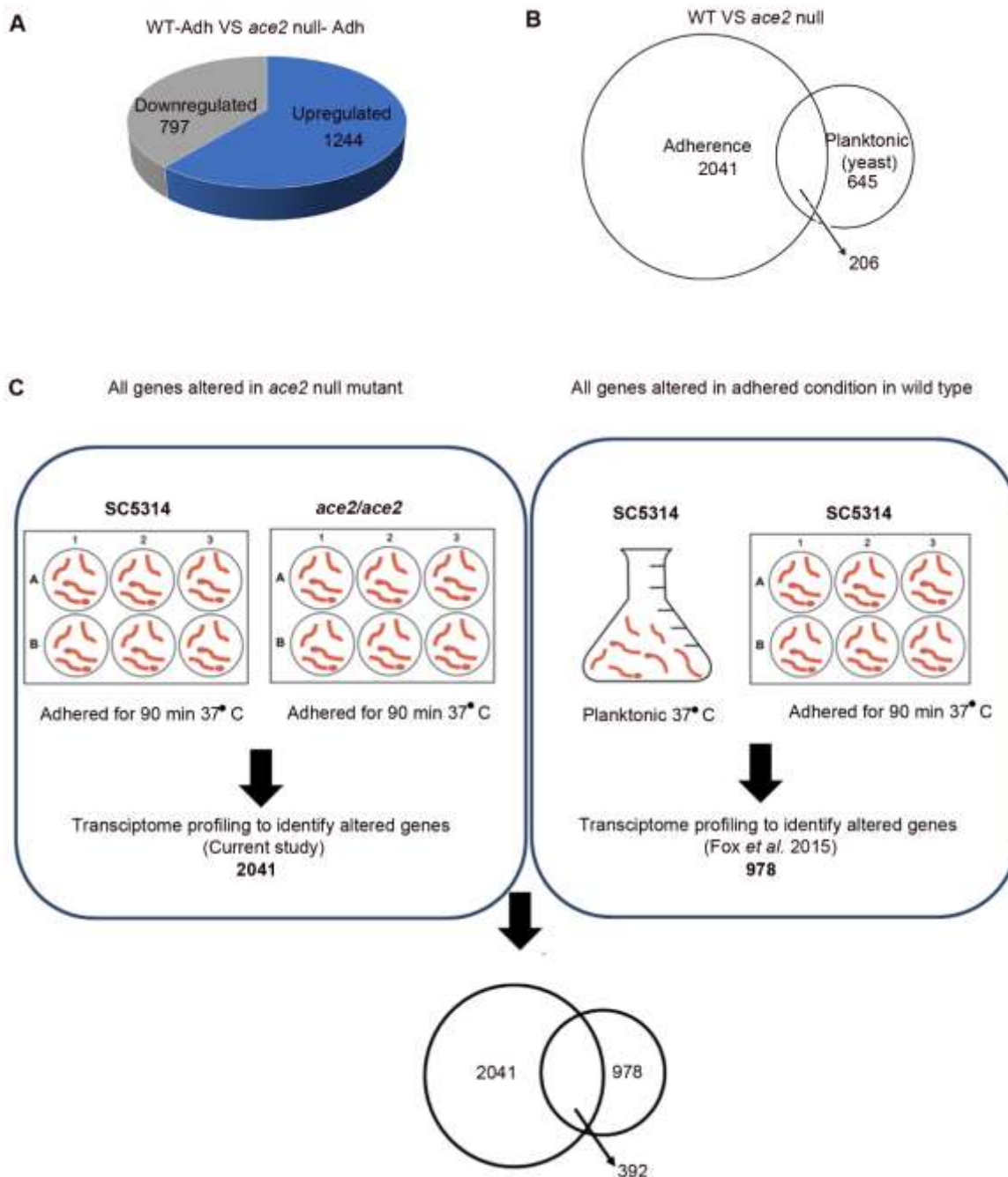


Figure 3.3 Identification of Ace2 mediated adherence specific genes (AcASGs).

A. Global gene expression array analysis was performed in the wild-type SC5314 (*ACE2/ACE2*) and RS404 (*ace2/ace2*) grown in YNB media in the adhered mode of growth for 90 min. The pie chart represents the total number of differentially expressed genes in *ace2* null mutants. **B.** Genome-wide expression data were compared to identify the common genes that are altered both in planktonic and adhered growth conditions in the *ace2* null mutants and represented as a Venn diagram. A total of 206 genes are common between these two data sets (represented by an arrow). **C.** Identification of Ace2 regulated

adherence specific genes (AcASGs) by comparison of genome-wide expression data of *ace2* null mutants (RS404, *ace2/ace2*) in adhered condition (left panel) and genes altered during planktonic to adhesion transition (right panel). A total of 392 genes (indicated by an arrow) are common between these two data sets represented in the form of a Venn diagram.

Global gene expression array analysis of the double mutant of *ace2* and *hht1* reveals the up-regulation of adherence genes compared to *ace2* null mutant

More than one third (392) of the 978 genes involved in adhesion are regulated by Ace2. Adhesion is a critical step for successful biofilm development. Earlier the null mutant of *HHT1*-encoded H3V^{CTG} has been shown to form more robust biofilms than the wild-type. Having shown partial rescue of biofilm defects associated with *ace2* mutant in the double mutant cells of *hht1 ace2*, we were curious to identify the genes involved in the partial rescue of adhesion. We compared the transcriptionally altered gene-sets of RS408 and RS409 (*ace2/ace2 hht1/hht1*) to RS404 (*ace2/ace2*) in the adhered condition of growth (**Figure 3.4 A**). About 318 genes were differentially up-regulated and 814 genes down-regulated in RS408 and RS409 (*ace2/ace2 hht1/hht1*) mutant cells as compared to RS404 (*ace2/ace2*) (**Figure 3.4 B**). Functional categorization of up- and down-regulated genes suggested that the biofilm gene circuit was the most significantly altered pathway due to *HHT1* deletion in the *ace2* null mutant. This observation suggests that the absence of H3V^{CTG} relieves the repression of the biofilm genes in *ace2* null mutants, allowing partial rescue of phenotypic defects in *ace2/ace2 hht1/hht1* double mutants. Previous reports suggested that biofilm-forming defects of various factors, including master regulators of biofilm formation (Bcr1, Tec1, Ndt80, Efg1, Brg1, and Rob1) are rescued wholly or partially by the overexpression of their target genes. For example, overexpression of either *ALS3*, *ECE1*, or *HWP1* partially rescues the biofilm defects in the *bcr1* null mutant (Nobile, Andes et al. 2006). Overexpression of *ACE2* also rescued adherence and biofilm defects in *snf5* (a chromatin remodeler) null mutants (Finkel, Xu et al. 2012). Similarly, increased expression of biofilm target genes was observed in RS408, RS409 (*ace2/ace2 hht1/hht1*) double mutants when compared to RS404 (*ace2/ace2*). In RS408, RS409 (*ace2/ace2 hht1/hht1*) a significant up-regulation in the expression of several adhesins such as *ALS2*, *ALS3*, *ALS4*, and genes involved in adherence, *HWP1*, *ECE1*, *ZFU2* was observed. In addition,

the expression of several adherence regulators such as Pho8, Djp1, Cdc19, Pgi1, which are generally induced upon adherence of *C. albicans* to polystyrene, were also up-regulated in RS408, RS409 (*ace2/ace2 hht1/hht1*) as compared to RS404 (*ace2/ace2*).

The down-regulated genes include various uncharacterized ORFs and cell wall proteins (Rbe1) that are normally repressed during planktonic to biofilm transition. On the other hand, slight down-regulation (\log_2 fold change -0.4-0.8) in the expression of few other adhesins belonging to *ALS* family such as *ALS5*, *ALS6* and *ALS7* was observed in RS408, RS409 (*ace2/ace2 hht1/hht1*). Nevertheless, the roles of these genes as adhesins remain elusive. The expression of *ALS6* is reported to be unaffected in response to microtiter plates (used in our experimental condition), and *ALS7* is known to be down-regulated in the biofilm mode of growth. Furthermore, adherence regulators such as Try6 were down-regulated in RS408, RS409 (*ace2/ace2 hht1/hht1*) as well, accounting for the partial rescue of defects.

Expression of each of *ALS3*, *ECE1*, *HWP1*, and *ZFU2* genes was analyzed by qPCR and was found to be higher in RS408, RS409 (*ace2/ace2 hht1/hht1*) than RS404 (*ace2/ace2*) (**Figure 3.4 C**). Thus, microarray data, together with qPCR analysis, confirmed that H3V^{CTG} represses the adherence genes in the planktonic state of *C. albicans*.

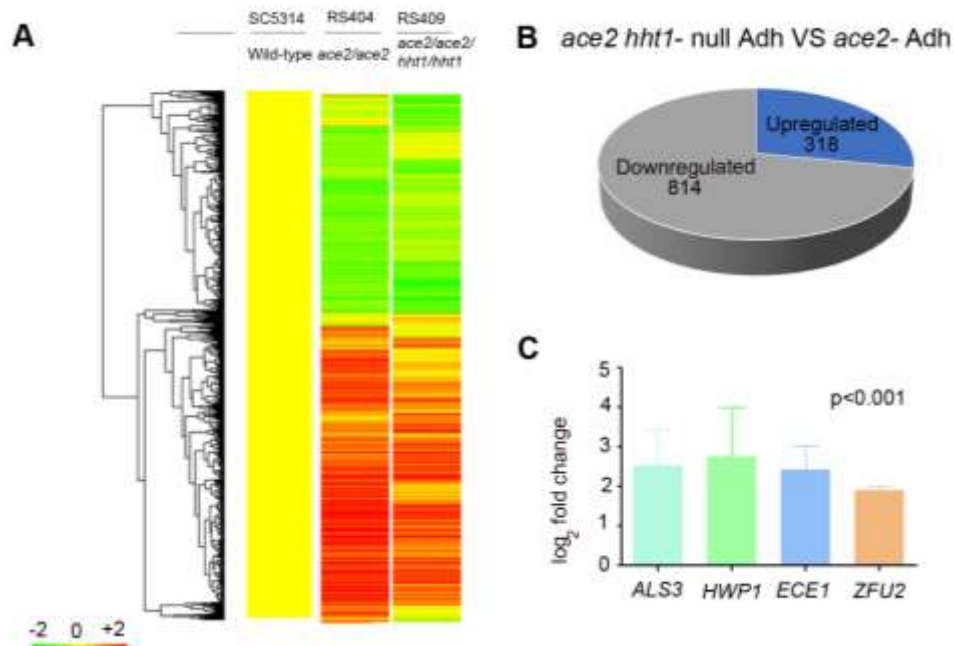


Figure 3.4 Gene expression profile of *ace2* and *hht1* double mutant reveals a differential expression pattern compared to *ace2* null mutant.

A. Comparison of expression data (≥ 1.5 fold difference with $p \leq 0.05$) of genes from wild-type (SC5314), LR107 (*hht1/hht1*), RS404 (*ace2/ace2*) and RS408 (*ace2/ace2 hht1/hht1*) are illustrated as heat-map. **B.** Global gene expression array analysis was performed in RS404 (*ace2/ace2*) and RS408 (*ace2/ace2 hht1/hht1*) and grown in YNB media in adhered mode of growth for 90 min. The pie chart represents the total number of differentially expressed genes in RS409 (*ace2/ace2 hht1/hht1*) with respect to RS404 (*ace2/ace2*). **C.** qPCR analysis was performed for adhesins (*ALS3*, *HWP1*, *ECE1*) and transcription factors (*ZFU2*) in RS404 (*ace2/ace2*) and RS409 (*ace2/ace2 hht1/hht1*) grown in YNB +500 mM galactose under adhered conditions. ΔC_t values were derived after normalization of expression of the gene of interest with that of actin, and $\Delta\Delta C_t$ values were calculated for relative expression of adhesin genes in the double mutants of *ace2 hht1* as compared to the single mutant of *ace2*.

Having shown that deletion of H3V^{CTG} influences the amplitude of adhesins in RS408, RS409 (*ace2/ace2 hht1/hht1*), we wanted to determine the transcriptional status of all those genes in RS408, RS409 (*ace2/ace2 hht1/hht1*) double mutants that were fine-tuned in response to substrate adhesion stimuli and are regulated by Ace2. We have previously identified 392 Ace2-mediated planktonic to adherence transition genes

(AcASGs) (**Figure 3.3 A**) of which 190 adherence-specific genes were up-regulated and 202 adherence specific genes were down-regulated in the absence of Ace2.

Comparative transcriptome analysis of *ace2 hht1* double mutant (RS408 and RS409, *ace2/ace2 hht1/hht1*) with AcASGs was carried out. The analyses revealed quantitatively contrasting transcriptional responses of adherence specific genes in *ace2 hht1* double null mutants (RS408 and RS409, *ace2/ace2 hht1/hht1*) when compared to *ace2* null mutants (RS404, *ace2/ace2*). For instance, 190 genes (AcASGs) were differentially up-regulated in RS404 (*ace2/ace2*) in adhered condition giving rise to the adherence and biofilm defects as compared to wild-type. Approximately 1/2 (47%) of these up-regulated AcASGs were down-regulated in RS408, RS409 (*ace2/ace2 hht1/hht1*) in comparison to RS404 (*ace2/ace2*). Of the remaining up-regulated AcASGs, the transcript levels of 47% of genes were restored to the wild-type levels by the deletion of H3V^{CTG} in RS404 (*ace2/ace2*) cells. Similarly, 202 genes were differentially down-regulated in RS404 (*ace2/ace2*) when compared to wild-type contributing to the phenotypic defects. Approximately 1/4th (28%) of these down-regulated AcASGs were up-regulated in RS408, RS409 (*ace2/ace2 hht1/hht1*) mutants with respect to RS404 (*ace2/ace2*). In the remaining down-regulated AcASGs, the transcript levels of 65% of genes were restored to the wild-type levels by the deletion of H3V^{CTG} in RS404 (*ace2/ace2*) cells. So, the transcriptional amplitude of both activated and repressed Ace2 mediated adherence gene (AcASGs) sets drastically change upon loss of H3V^{CTG} in the absence of Ace2. The expression levels of AcASGs in RS404 (*ace2/ace2*) relative to those of the wild-type (left column) and RS408, RS409 (*ace2/ace2 hht1/hht1*) relative to the RS404 (*ace2/ace2*) (right column) are represented in the form of a heat map (**Figure 3.5, 3.6**). The up-, down- and unaffected AcASGs in RS408, RS409 (*ace2/ace2 hht1/hht1*) are clustered in three individual heat maps.

The transcriptionally altered AcASGs consist of mostly uncharacterized genes and cannot be categorized under any functionally relevant GO terms. These genes can serve as strong candidates of adherence regulators in *C. albicans*. Further characterization of these genes will increase the repertoire of regulators involved in cell-substrate adherence, a medically relevant condition in *C. albicans*. Thus, our analyses hints towards an additional level of regulation implemented by H3V^{CTG} in repressing adhesion in *C. albicans*.

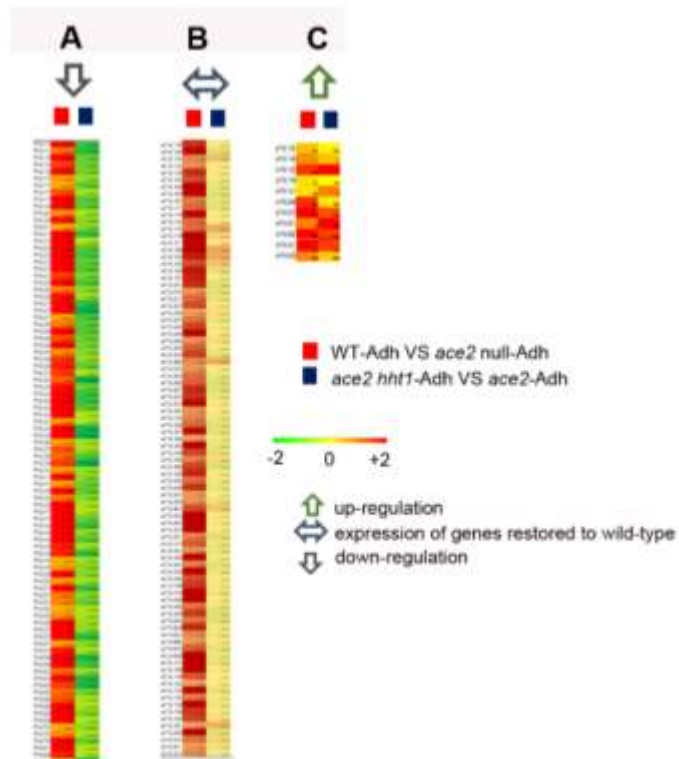


Figure 3.5 Transcriptional circuit of adherence induced genes is rewired upon the deletion of H3V^{CTG} in the *ace2* null mutant.

Analysis of transcriptional status of AcASGs that were up-regulated in RS404 (*ace2/ace2*) when compared to wild-type [marked by a red box]. Gene identifications and descriptions were obtained from Candida Genome Database (CGD). The differentially expressed genes in RS408, RS409 (*ace2/ace2 hht1/hht1*) [marked by a blue box] have been clustered with the corresponding altered gene in RS404 (*ace2/ace2*). The arrows at top represent the expression level of the cluster of genes in RS408, RS409 (*ace2/ace2 hht1/hht1*) mutants relative to Rs404 (*ace2/ace2*). **A.** ↑ up-regulated, **B.** ↓ down-regulated **C.** ↔ expression of genes restored to the levels of wild-type.

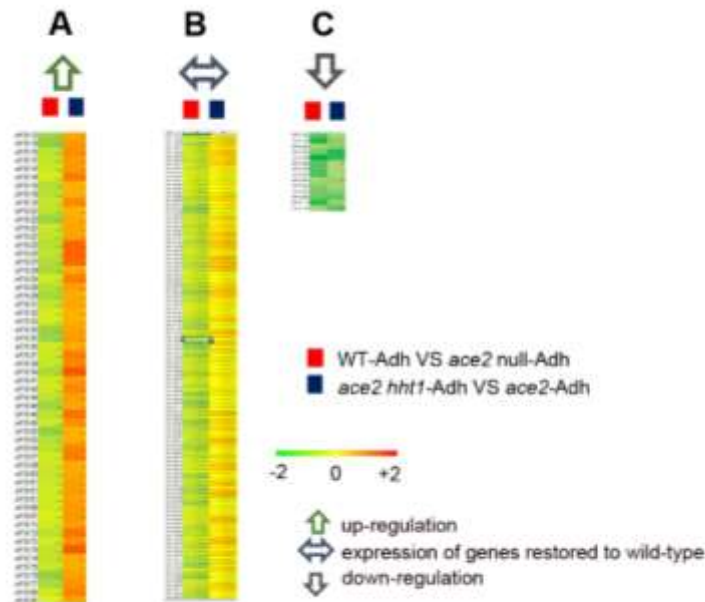


Figure 3.6 The transcriptome profile of down-regulated genes in *ace2* null mutants is rewired upon the deletion of H3V^{CTG}.

Analysis of the transcriptional status of AcASGs that were down-regulated in RS404 (*ace2/ace2*) when compared to wild-type [marked by a red box]. Gene identifications and descriptions were obtained from CGD. The differentially expressed genes in RS408, RS409 (*ace2/ace2 hht1/hht1*) [marked by a blue box] have been clustered with the corresponding RS404 (*ace2/ace2*) altered gene. The arrows at top represent the expression level of the cluster of genes in RS408, RS409 (*ace2/ace2 hht1/hht1*) mutants relative to RS404 (*ace2/ace2*). **A.** ↑ up-regulated, **B.** ↓ down-regulated **C.** ↔ expression of genes restored to the levels of wild-type.

Chapter 4 Discussion

C. albicans is an opportunistic fungal pathogen and the most prevalent fungal species of the human microbiota. It is capable of forming biofilms on abiotic and biotic surfaces. Although the regulation of the formation of biofilms at the transcriptional level has been extensively studied, limited reports are available on the regulation of this process at the chromatin level.

Occupancy of H3V^{CTG} at the promoter of biofilm genes determines the morphological growth transitions in *C. albicans*

In the present study, we examined the binding of the histone H3 variant (H3V^{CTG}) and a canonical histone H3 protein (Hht21) (**Figure 4.1 A**) at the promoters of biofilm-related genes in *C. albicans* by ChIP-qPCR analysis. H3V^{CTG} constitutes the minor fraction (approximately one third) of the total cellular pools of histone H3 in different modes of growth: yeast, hyphal and biofilm (Rai, Singha et al. 2019) (**Figure 4.1 B**). Despite its lower levels in cells, the occupancy of H3V^{CTG} is higher at the promoters of biofilm relevant genes compared to canonical histone H3 in the planktonic mode of growth. The occupancy of H3V^{CTG} is significantly reduced at these promoters during the transition of *C. albicans* cells from planktonic to biofilm growth mode. However, the levels of canonical H3 at these promoters remain the same irrespective of whether the cells are in free-floating planktonic or biofilm mode (**Figure 4.1 B and C**). In addition, there is an overall dip in the total histone H3 binding at the promoters of biofilm genes i.e., the promoter regions are depleted of nucleosomes. Similar to the promoter regions, the occupancy of H3V^{CTG} also declines at the gene bodies. Many eukaryotes, like the budding yeast, *Drosophila* and mammalian cells share similar attributes of nucleosome displacement and transcriptional activation to that of *C. albicans* (Lee, Shibata et al. 2004, Chow, Georgiou et al. 2005, Mito, Henikoff et al. 2005). In *Saccharomyces cerevisiae*, nucleosomes are depleted from active gene promoters leading to transcriptional activation genome-wide *in vivo*. Any variation caused in the transcriptional program globally due to some stress/ factors such as heat shock or a change in carbon source may lead to depletion of nucleosomes at induced promoters and increased nucleosome occupancy at repressed promoters (Lee, Shibata et al. 2004). This local depletion of nucleosomes thus acts as sites for transcription factor binding and induction of expression of genes. In *Drosophila*, H3.3 is enriched at the

promoter regions and gene bodies of many active genes and the promoters of active genes are continually replaced by histone variant H3.3 containing nucleosomes (Schwartz and Ahmad 2005). In mammalian cells, H3.3/H2A.Z containing nucleosomes serve as placeholders for 'nucleosome-free regions' which would otherwise be occupied by stable nucleosomes, allowing transcription factors to gain access (Jin and Felsenfeld 2007). This phenomenon is observed in active promoters as well as enhancers and insulator regions in mammalian cells. The biofilm gene circuitry in *C. albicans* consists of about 55 transcriptional regulators modulating each other's expression and ~1000 target genes (Nobile, Fox et al. 2012, Lohse, Gulati et al. 2018). Hence, the planktonic to biofilm transition alters about 1/6th of the *C. albicans* genome. The preferential binding of H3V^{CTG} to the promoters of biofilm-related genes, depletion of H3V^{CTG} at the promoters during the planktonic-biofilm transition along with enhanced biofilm formation (*in vitro* and *in vivo*) (Rai, Singha et al. 2019) associated with H3V^{CTG} null mutant cells together indicate that H3V^{CTG} acts as a negative regulator of biofilm development. We posit that H3V^{CTG} might have evolved to constrain the pathogenic traits of *C. albicans* so that it emerges as a successful commensal.

Our experimental data suggested that H3V^{CTG} makes chromatin less accessible to biofilm transcription modulators. In its absence, biofilm specific transcription factors (TFs) turn on the biofilm gene circuitry. Genetic studies in *D. melanogaster* suggests that the default state of homeotic genes is the silent state. Polycomb group proteins (PcGs) are responsible for maintaining the silent state and trithorax group proteins (trxGs) for active state at specific sites (Cleard, Moshkin et al. 2006, Ringrose and Paro 2007). TrxGs alter chromatin and associate with DNase I hypersensitive sites suggesting that they maintain the active state by making chromatin continuously accessible to TFs. The simplest model for TF accessibility proposes that TFs compete and displace nucleosomes for DNA binding. The TFs gain access to their DNA template in short periods during nucleosome turnover events. Local accessibility increases with the increasing concentration of TFs, allowing other TFs and cofactors to stabilize the accessible state. This mechanism does not involve any direct interaction between TFs and nucleosomes and is thus passive. This model is applicable only in euchromatin because nucleosome turnover rates within heterochromatic

regions are inadequate to support the requisite exchange. This has been proven by *in vitro* experiments where Rous sarcoma virus internal enhancer binding factor (IBF) factor (C/EBP β) competes with histones for binding at distal regulatory regions (Svaren, Klebanow et al. 1994, Di Stefano, Collombet et al. 2016). In metastatic cells, TF NFIB competes with histones to bind to weakly accessible binding sites in primary tumors and initiates metastatic gene expression (Lone, Shukla et al. 2013). In zebrafish, zygotic gene transcription begins with the exclusion of histones by TFs (Amodeo, Jukam et al. 2015, Joseph, Palfy et al. 2017). To test this model, we studied the binding of Bcr1, a master regulator of biofilm formation, to the promoters of the biofilm-related genes in *C. albicans*. The results indicate an enhanced promoter binding of Bcr1 in the absence of H3V^{CTG}, thus proving that binding of a biofilm specific transcription factor Bcr1 is occluded by the presence of histone H3 variant, H3V^{CTG} in *C. albicans*. This study helps in understanding chromatin changes mediated by a histone H3 variant to regulate one of the most dramatic morphological transitions in a medically important human fungal pathogen. Further investigations on other biofilm-specific transcriptional regulators and their interplay with H3V^{CTG} would identify additional regulatory pathways. In addition, genome-wide studies on the binding of H3V^{CTG} would provide the nucleosome landscape in planktonic and biofilm conditions.

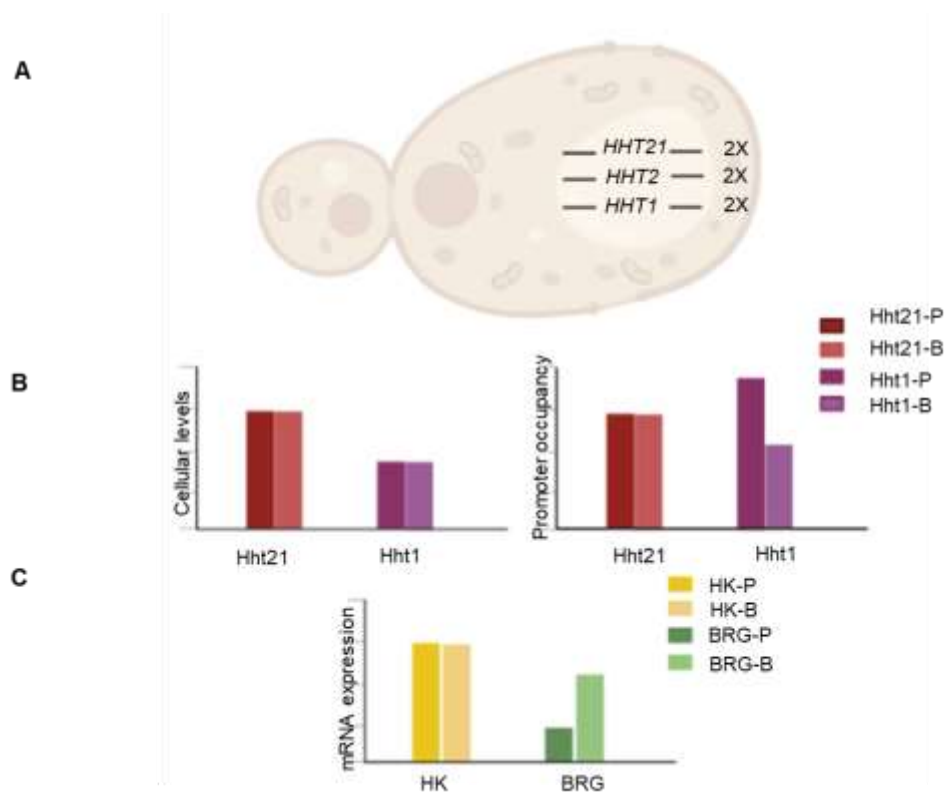


Figure 4.1 The CUG Ser1 clade-specific histone H3 variant evolved as the molecular switch of morphological growth transitions in *C. albicans*.

A. In *C. albicans*, *HHT2* (*ORF 19.1853*) and *HHT21* (*ORF 19.1061*) code for an identical polypeptide, the canonical histone H3, whereas *HHT1* (*ORF 19.6791*) encodes a variant protein differing at positions 31, 32, and 80 in the amino acid sequence. **B.** The variant histone H3 (Hht1) is less abundant in the cellular pool than its canonical form in *C. albicans* (left graph). Relative occupancy of the canonical histone H3 remains unaltered on the promoters of several biofilm-related genes tested in planktonic and biofilm cells (right graph). On the other hand, occupancy of the variant histone H3, H3V^{CTG}, is significantly higher on the promoters of the same set of biofilm genes in the planktonic cells compared with those grown in the biofilm conditions. **C.** The biofilm relevant genes (BRGs) (~1200) is expressed differentially in planktonic and biofilm mode. In the presence of environmental inducers, the expression of BRGs are up-regulated. Based on experimental evidence, we posit that the variant histone H3 containing nucleosomes make biofilm gene promoters less accessible for binding of transcription modulators (transcription activators or repressors) of biofilm-related genes. When H3V^{CTG} levels drop, biofilm transcription modulators gain access and bind to the promoters to modulate the genetic circuitry to favor the biofilm mode of growth.

Variant specific amino acid residues of H3V^{CTG} are indispensable for its repressive behavior on biofilm growth

Investigations on the inherent bias that drives H3V^{CTG} to specific loci and identifying the histone chaperone complexes involved in its deposition are crucial in understanding the unique enrichment patterns of H3V^{CTG}. Several factors such as differences in the amino acid composition and histone modifications unique to each variant, may contribute to biased incorporation. In flies, unique amino acids in canonical H3 prevent its replication-independent incorporation (Ahmad and Henikoff 2002). In mammalian cells, the variant-specific serine residue at position 31 in H3.3 on phosphorylation contributes to its distinct localization pattern compared to canonical H3 (Hake, Garcia et al. 2005). In addition, Gly90 of H3.3 dictates its binding to UBN1 (Ubinuclein-1, a subunit of HIRA chaperone complex) (Ricketts, Frederick et al. 2015) or DAXX (another H3 chaperone) (Elsasser, Huang et al. 2012) by diverse mechanisms. In mouse embryonic stem cells, the variant-specific residues are the key factors in determining their genome-wide enrichment patterns (Goldberg, Banaszynski et al. 2010).

In *C. albicans*, mutational analysis of variant-specific residues reveals that changes at two of the three positions (31 and 32) in the histone H3 core induce the biofilm gene circuitry (**Figure 4.2**). The alteration of the variant-specific residues simultaneously at 31 and 32 positions of H3V^{CTG} to that of canonical H3 residues yield phenotypes similar to those associated with the H3V^{CTG} null mutant i.e., in the presence of a copy of H3V^{CTG} with mutations at 31 and 32 position as the only source of H3V^{CTG} in cell cannot complement H3V^{CTG} function. However, any alteration of variant-specific residues individually can complement H3V^{CTG} function, and phenocopies the H3V^{CTG} add back mutant. In all other sequenced CUG clade species as well, variations in amino acid residues from the H3V^{CTG} sequence are observed only on either of these two positions (31 or 32) but not together. Thus, the co-occurrence of amino acid residues at positions 31 and 32 controls the repressive role of H3V^{CTG} in biofilm formation. Such specificity of occurrence of amino acid residues could be explained if these positions in H3V^{CTG} make contacts with a variant-specific assembly factor or bind to accessory proteins, which affect the functioning of a general nucleosome assembly factor. Hence, it is relevant to think that these two

consecutive H3V^{CTG} specific amino acids residues can either act as chaperone recognition site or may facilitate H3V^{CTG} to interact with distinct nucleosome assembly machinery.

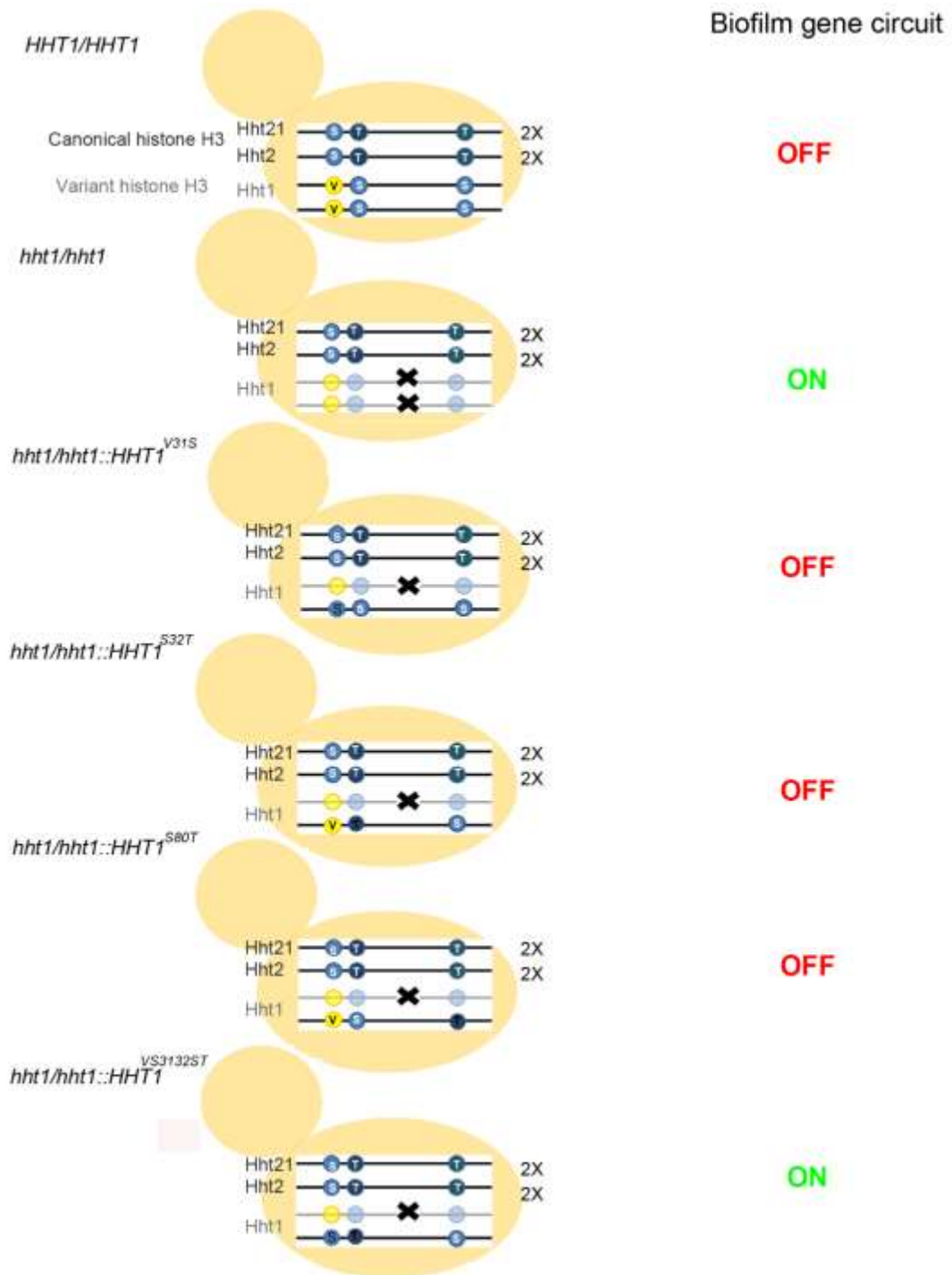


Figure 4.2 Co-occurrence of amino acid residues at 31 and 32 positions of H3V^{CTG} is essential for its function.

Schematic of the strains developed to assay the role of variant specific amino acid residues of H3V^{CTG} in biofilm formation. Wild type Hht1 and Hht1 with point-mutants (as mentioned in each cartoon yeast cell) were constructed by changing the amino acid residues at positions 31, 32, and 80 of the variant histone H3 (Hht1) to that of the canonical histone H3 sequence and integrating them at native locus in a *hht1* null background. The impact of these mutations on the biofilm gene circuit is depicted as ON/OFF.

Cac2, a member of CAF-1 complex is a putative chaperone for H3V^{CTG}

CAF-1 and HIRA are the two well-known conserved chaperone complexes involved in the incorporation of canonical and variant histone H3, respectively, at the first step of nucleosome assembly. CAF-1 is not essential in *S. cerevisiae* (Kaufman, Kobayashi et al. 1997) and in *Arabidopsis* (Varas, Santos et al. 2017). However the mutants in *S. cerevisiae* show increased UV sensitivity (Kaufman, Kobayashi et al. 1997), reduced gene silencing at telomeres (Monson, de Bruin et al. 1997) and mating loci (Enomoto and Berman 1998) and gross chromosomal rearrangements (Myung, Pennaneach et al. 2003) and developmental and differentiation defects in *Arabidopsis*. In mice (Hatanaka, Inoue et al. 2015) and *Drosophila* (Song, He et al. 2007), CAF-1 is essential. The mutants exhibit embryonic lethality at the 16-celled stage in mice and hemizygous lethality in *Drosophila*. Structural studies of CAF-1 in budding yeast reveal that among the three subunits, Cac1 is involved in histone binding by an acidic 50 amino acid stretch. The Cac2 subunit is essential for productive histone binding in association with Cac1. Cac2 is indispensable for nucleosome assembly by CAF-1 in budding yeast (Mattiroli, Bhattacharyya et al. 2017).

In *C. albicans*, *CAC2* is not essential for viability, and Cac2 have a conserved role in response to genotoxic, UV, and thermal stress (Stevenson and Liu 2013). Hir1, a subunit of HIRA complex is also dispensable, but have a conserved role in histone gene repression (Stevenson and Liu 2013). Hir1 also have an additional function in fungal morphogenesis with mutants showing reduced filamentation in solid and liquid media compared to wild-type (Jenull, Tscherner et al. 2017). The role of CAF-1 in fungal morphogenesis prior to our study remained underexplored. Our results suggest that in the absence of Cac2, cells are

hyperfilamentous and form enhanced biofilm than wild-type *C. albicans* cells. This observation indicates the acquisition of an unconventional function of CAF-1 in *C. albicans*. *cac2* null mutants phenocopy the *hht1* null mutants in both inducing biofilm formation and solid surface filamentation. In addition, the occupancy of H3V^{CTG} is reduced at the promoters of biofilm genes in the absence of Cac2 whereas the occupancy of canonical H3 is unaffected. In light of the existing evidence and the results obtained in our study, CAF-1 emerges as the putative H3V^{CTG} chaperone in *C. albicans*. Future studies on the physical interaction of CAF-1 and H3V^{CTG} would verify this assumption. Further, the specificity of Cac2 to H3V^{CTG} remains unclear. Thus, the contribution of variant-specific amino acids of H3V^{CTG} and its interaction with CAF-1 needs to be explored (**Figure 4.3**).

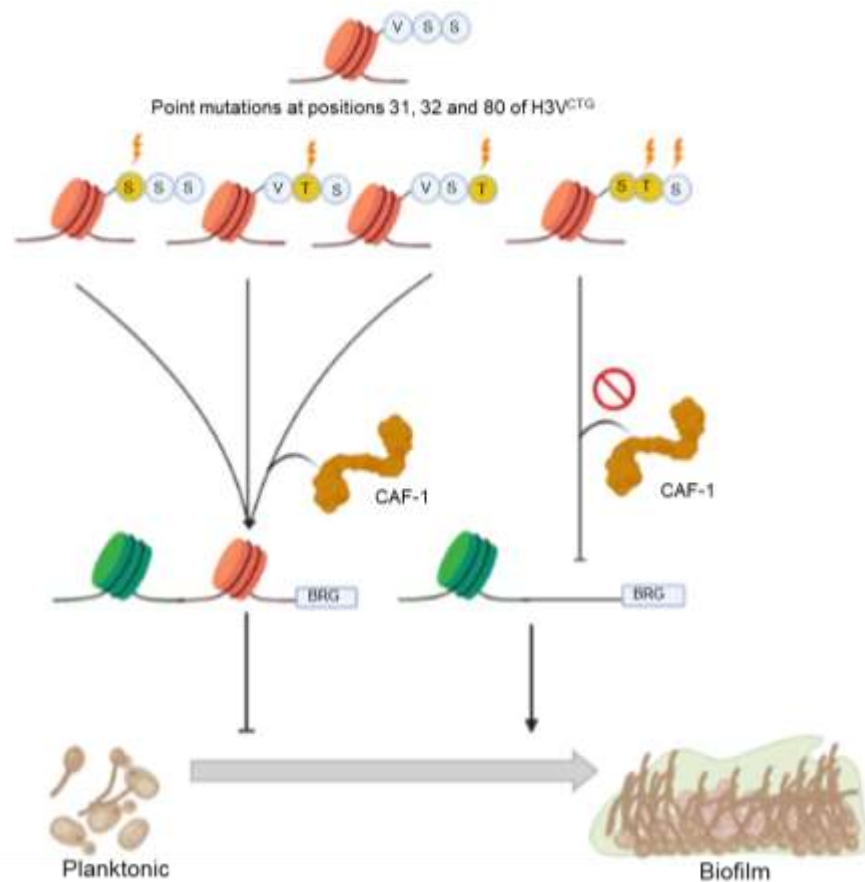


Figure 4.3 Variant specific amino acid residues in H3V^{CTG} might determine its interaction with chaperones.

The biofilm gene circuit is modulated by H3V^{CTG} (in red) and more specifically, by the co-occurrence of two amino acids at 31 and 32 positions (in blue circles) in the planktonic state as determined by mutational analysis. On screening the known chaperone mutants for histone H3, a subunit of the CAF-1 chaperone complex, Cac2 was identified as the putative chaperone for H3V^{CTG}. We hypothesize that Cac2 is probably specific to H3V^{CTG} via interactions with its unique amino acid residues.

Absence of H3V^{CTG} rescues defects in *ace2* null mutants

Ace2 is a zinc finger transcription factor and its deletion results in cell separation defects, increased invasion into solid agar, reduced adherence to plastic surfaces, avirulence in the mouse model of disseminated candidiasis and reduced biofilms with a distinctly different morphology from wild-type cells (Kelly, MacCallum et al. 2004). In this study, we have shown that the effect of the absence of a morphogenetic transcription factor like Ace2 can be rescued partially by the deletion of H3V^{CTG}. The deletion of H3V^{CTG} in *ace2* null mutant causes enhanced biofilm formation as compared to the parent *ace2* null mutant. We postulate that the nucleosomes containing H3V^{CTG} prevent the binding of Ace2 to genes of biofilm formation during planktonic growth. Ace2 acts as a positive regulator for adhesion and biofilm formation. Thus, it is possible that in the absence of H3V^{CTG}, binding of Ace2 to target genes required for morphogenesis is enhanced. This inverse correlation in phenotype suggests that H3V^{CTG} plays an antagonistic role in the biofilm regulatory circuitry compared to that of Ace2. In light of the existing evidence of up-regulated expression of adhesins in H3V^{CTG} null mutants and the results obtained in the present study, we posit that H3V^{CTG} possibly blocks the binding sites of Ace2 and other biofilm specific transcription factors in planktonic state giving rise to the phenotypic defects in *ace2* null mutants. However, in the absence of H3V^{CTG}, Ace2 binding sites are accessible to other transcription factors, thereby showing rescue in adhesion and biofilm defects (**Figure 4.4**). Ace2 is known to share several common targets of RAM (Regulation of Ace2 and morphogenesis) pathway with Bcr1 (Finkel, Xu et al. 2012).

We identified the Ace2-mediated adherence gene (AcASG) sets to identify those that are coregulated by H3V^{CTG} and are possibly involved in adherence. A significant rewiring was observed in the transcriptional response of the *ace2 hht1* double null mutant cells

when compared to *ace2* null mutants. The expression of about 37% (146 out of 392) of AcASGs was found to be reversed in the double mutants of *ace2* and *hht1* as compared to *ace2* null cells. The trend was observed for both transcriptionally activated and repressed genes. Most of these genes are uncharacterized, and future studies on the characterization of these genes will add to the existing knowledge of regulators involved in cell-substrate adherence.

In metazoans, histone H3 variants play a key role in the development and differentiation processes of embryonic stem cells (Tanaka, Kunath et al. 2002). During cellular differentiation, stem cells undergo selective activation and silencing of lineage-specific genes. Similar to metazoans, H3V^{CTG} might have evolved to govern the morphogenetic switch in unicellular organisms such as yeast of the CTG clade. In conclusion, we envision that H3V^{CTG} constrains the pathogenic attributes of *C. albicans*, perhaps to enhance its success as a commensal by regulating the expression of genes involved in one of the most dramatic morphological growth transitions required for virulence/pathogenesis.

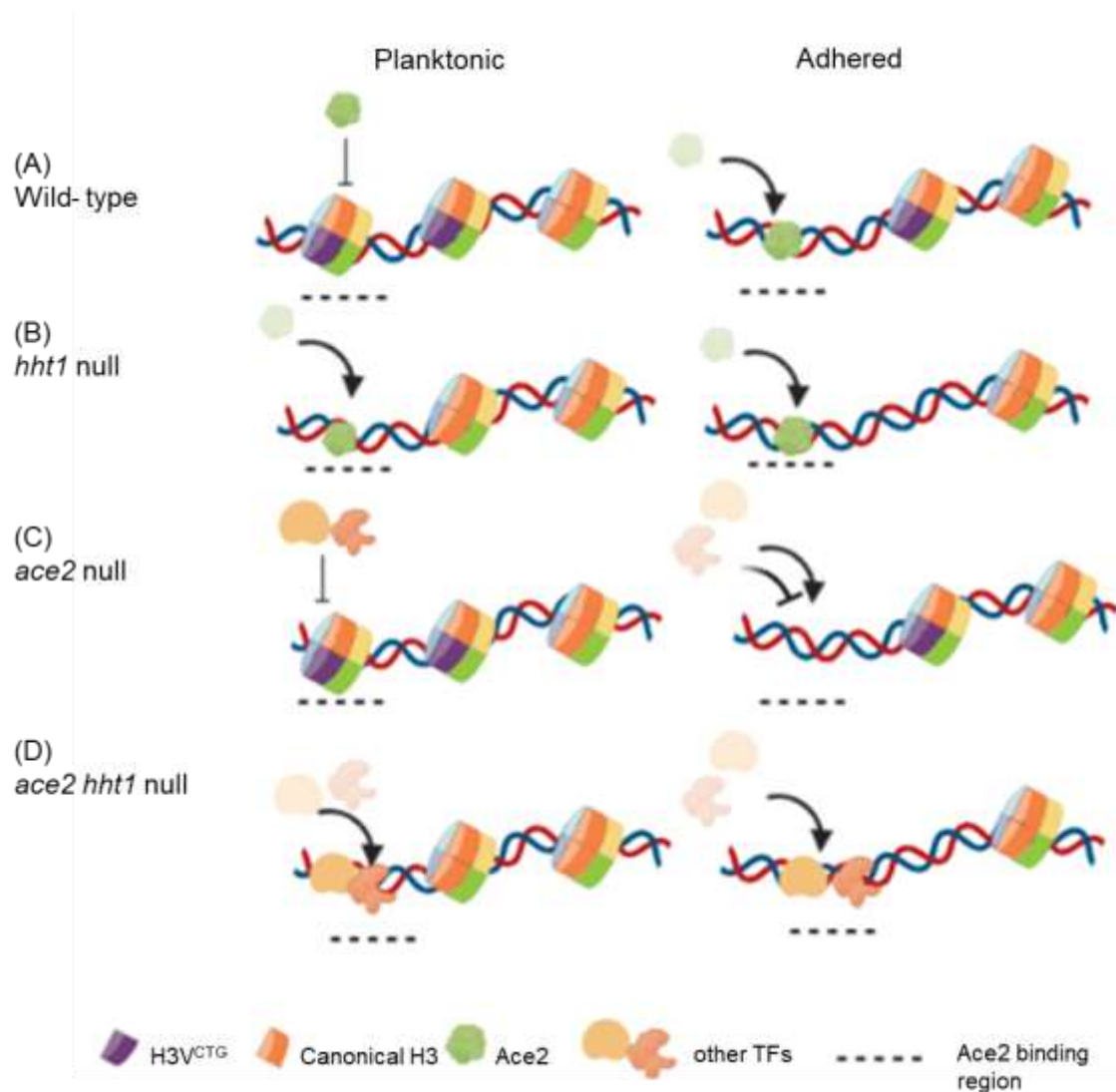


Figure 4.4 A proposed mechanism depicting H3V^{CTG} acting as a molecular switch of morphological growth transitions (planktonic-biofilm) in *C. albicans*.

A. In the wild-type cells, H3V^{CTG} prevents the binding of transcription factor Ace2 to its respective gene promoters in the planktonic growth condition inhibiting the expression of adherence specific genes (AcASGs). In contrast, during the adhered condition, as the levels of H3V^{CTG} goes down, Ace2 gains access to these sites and binds to these promoters to induce the expression of AcASGs. **B.** In the absence of H3V^{CTG}, Ace2 can bind to the promoter regions of AcASGs and induce their expression in both planktonic and adhered growth conditions. **C.** In the absence of Ace2, AcASGs are not induced giving rise to adhesion and biofilm defects. In addition, H3V^{CTG} also remains bound to the promoters of AcASGs, making them inaccessible for binding by other TFs. Thus, AcASGs are repressed in both planktonic and adhered growth conditions. **D.** However, in the absence of both H3V^{CTG} and Ace2, some other transcription factors probably bind to the promoters and induce the expression of ASGs in both planktonic as well as adhered conditions and subsequently show a partial rescue of adherence and biofilm defects.

Chapter 5 Materials and Methods

Strains and primers

All the yeast strains used for the study are enlisted in Table 6.1. The oligonucleotide primers used have been tabulated in Table 6.2.

Buffers and solutions used

All of the buffers and solutions used in this study were prepared in autoclaved double distilled water with analytical grade reagents. Solutions were stored at room temperature unless stated otherwise.

1. TE Buffer (10x)- 100 mM Tris (pH=8.0 or 7.5 as required for the assay), 10 mM EDTA
2. LiOAc/ TE solution- 0.1 M LiOAc (pH=7.5), 1x-TE (pH=7.5)
3. PEG solution- 0.1 M LiOAc (pH=7.5), 1xTE (pH=7.5), 42 % (w/v) PEG3350
4. Phosphate buffered saline (10x)- 80 g NaCl, 2 g KCl, 14.4 g Na₂HPO₄, 2.4 g KH₂PO₄ for 1 L water (pH=7.4)
5. Genomic DNA extraction buffer for *C. albicans*- 2% TritonX-100, 1% SDS, 100 mM NaCl, 10 mM Tris-Cl (pH=8.0), 1 mM EDTA
6. Cell lysis buffer- 0.1 N NaOH, 1% SDS
7. SDS sample loading buffer (5x)- 30% Glycerol, 10% SDS, 250 mM Tris-Cl (pH=6.8), 0.02% bromophenol blue, 5% 2-mercaptoethanol* (* added fresh)
8. SDS-PAGE tank buffer (10x)- 30 g Tris base, 144 g glycine, 10 g SDS for 1 L buffer.

Buffers for chromatin immunoprecipitation (Buffers 9- 16)

9. Spheroplasting buffer- 40 mM Citric acid, 0.01 M EDTA, 1.2 M Sorbitol supplemented with 20 mg/ mL lysing enzymes from *Trichoderma harzianum* (Sigma)
10. Buffer I- 0.25% Triton X-100, 10 mM EDTA, 0.5 mM EGTA, 10 mM Na-HEPES pH=6.5
11. Buffer II- 200 mM NaCl, 1 mM EDTA, 0.5 mM EGTA, 10 mM Na-HEPES pH=6.5

12. Lysis buffer- 50 mM HEPES pH=7.4, 1% Triton X-100, 140 mM NaCl, 0.1% Na-deoxycholate, 1 mM EDTA supplemented with 1xPIC (Protease Inhibitor Cocktail); always freshly prepared
13. Low salt wash buffer- 0.1% SDS, 1% Triton X-100, 2 mM EDTA, 20 mM Tris pH=8.0, 150 mM NaCl (storage at 4°C)
14. High salt wash buffer- 0.1% SDS, 1% Triton X-100, 2 mM EDTA, 20 mM Tris pH=8.0, 500 mM NaCl (storage at 4°C)
15. LiCl wash buffer- 0.25 M LiCl, 1% NP-40, 1% Na-deoxycholate, 1 mM EDTA, 10 mM Tris pH=8.0 (storage at 4°C)
16. Elution buffer- 0.1 M NaHCO₃, 1% SDS (always freshly prepared)
17. CloNAT Nourseothricin- 100 mg/mL solution in autoclaved double distilled water
18. Ampicillin- 100 mg/mL solution in autoclaved double distilled water
19. Chloramphenicol- 34 mg/mL solution in 100% ethanol

Reagents for biofilm assay

20. Fetal Bovine Serum- Invitrogen (Catalog No. 10270-106)
21. Six-well plate- corning costar (Catalog No. 3516)
22. XTT (sodium 3'-[1-[(phenylamino)-carbonyl]-3,4-tetrazolium]-bis(4-methoxy-6-nitro)benzene-sulfonic acid hydrate)- Sigma (Catalog No. X4626)
23. Crystal Violet Solution- Merck (Catalog No. V5265)

Antibodies and affinity beads

Resource	Description	Source	Catalog No.	Additional information
Antibody	anti-H3 (rabbit polyclonal)	Abcam	ab1791	ChIP (5 µL per 500 µL IP fraction)
Antibody	anti-V5 (mouse monoclonal)	Invitrogen	R960-25	ChIP (2 µL per 500 µL IP fraction)

				Western Blot(WB) (1:5000)
Antibody	Anti-c-Myc (mouse monoclonal)	Calbiochem	OP 10	ChIP (25 μ L per 500 μ L IP fraction)
Antibody	anti-mouse IgG HRP (goat polyclonal)	Abcam	ab97023	WB (1:10000)
Affinity beads	Protein-A sepharose beads	Sigma	P3391	ChIP (20 μ L per 500 μ L fraction)

Media, growth conditions and transformation

C. albicans strains were grown in YPDU (1% yeast extract, 2% peptone, 2% dextrose, and 100 μ g/ml uridine) at 30°C. For biofilm assays, YPDU, Spider media (1% peptone, 1% yeast extract, 1% mannitol, 0.5% NaCl, and 0.2% K₂HPO₄) (LIU et al. 1994) and YNB (yeast nitrogen base) + 500 mM galactose were used at 37°C. The filamentation assays were performed with complete media, and complete media containing 1 mM N-acetylglucosamine. Each strain was diluted to an OD₆₀₀ of 0.080, spotted on the plate containing above-mentioned media, and incubated for 2-3 days at 30°C and photographed. Transformation of *C. albicans* was performed by the lithium acetate mediated transformation technique, as described previously (Baum, Sanyal et al. 2002). Transformants were either selected on synthetic media (2% dextrose, 1% YNB and auxotrophic supplements) for auxotrophic markers or on YPD with 100 μ g/ml nourseothricin for NAT^R transformants.

Strain construction

Construction of *C. albicans* strains expressing *HHT1* V5 and *HHT21* V5 tag

To tag the endogenous copy of *HHT21* (LR143), the Ca*HHT21*-V5 cassette was amplified using pLSR107 as a template, with two long primers: the forward primer (1061V5IFP) containing homology to the last codons of the Ca*HHT21ORF* and the reverse primer (1061SDSRP) bearing homology to 3' UTR.

To tag the endogenous copy of *HHT1* (LR144), the Ca*HHT1*-V5 cassette was amplified using pLSR108 as a template with two long primers: the forward primer (6791V52LFP) containing homology to Ca*HHT1* and the reverse primer (6791DSNAT1RP) homologous to 3' UTR (**Figure 5.1**).

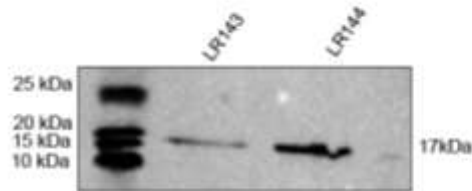


Figure 5.1 Western blot confirmation for V5 epitope tagging of *HHT1* and *HHT21* in LR143 and LR144.

Whole-cell lysates from strains LR143 (*HHT21/HHT21-V5*), LR144 (*HHT1/HHT1-V5*) were separated by SDS-PAGE using 12% gels. The proteins were transferred onto nitrocellulose membranes and probed with anti-V5 antibodies for immunoblot analysis. LR143 and LR144 are positive for V5 tagging (expected band size 17 kDa).

Construction of *C. albicans* strain expressing Bcr1-myc in the *hht1* null mutant background

Strain LR133 (*BCR1-Myc/BCR1 hht1/hht1*) was constructed by deleting both the alleles of *HHT1* in the strain CJN1785 (*BCR1-Myc/BCR1*) using the *SAT1*-flipper cassette from pSLR103 (Rai, Singha et al. 2019). The plasmid was digested with *KpnI* and *SacI* before the transformation. Deletions were confirmed by PCR (**Figure 5.2**).

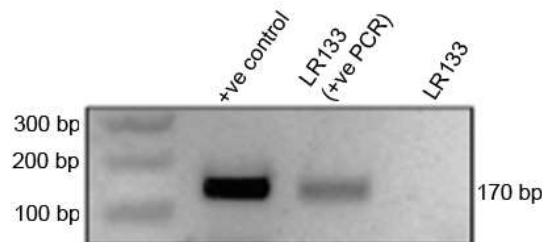


Figure 5.2 Confirmation of *HHT1* deletion in LR133.

The genomic DNA was isolated from strains SC5314, LR133 (*BCR1-Myc/BCR1 hht1/hht1*), and PCR amplified using HHT1FP and HHT1RP. LR133 was negative for ORF-specific PCR, indicating the deletion of *HHT1* ORF (170 bp). Lane corresponding to LR133 (+ve PCR)

represents PCR with a different set of primers in the same genomic DNA to check the integrity of genomic DNA, +ve - positive control (wild-type).

Construction of *C. albicans* strain expressing point mutants of *HHT1*

To generate single point mutants at positions 31 (RS103 and RS104), 32 (RS105 and RS106) and 80 (RS107 and RS108) and double point mutants at position 31 and 32 (RS109 and RS110) of *HHT1*, LR108 (*hht1/hht1*) was complemented at the native locus with the mutated alleles of *HHT1*; *HHT1*^{V31S} (RS103 and RS104), *HHT1*^{S32T} (RS105 and RS106), *HHT1*^{S80T} (RS107 and RS108) or *HHT1*^{V31S, S32T} (RS109 and RS110) from plasmids pRS103, pRS105, pRS106, and pRS104, respectively. Plasmids were digested with *Apa*I and *Sac*I prior to transformation. Transformants were selected for nourseothricin (NAT) resistance, and the reintegration of the mutated allele of *HHT1* at the right locus was confirmed by PCR (Figure 5.3).

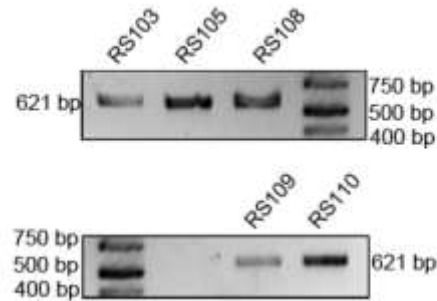


Figure 5.3 Confirmation of integration of mutated *HHT1* ORF at position 31, 32 and 80 in RS103, RS105, RS108, RS109 and RS110.

The genomic DNA was isolated from strains RS103 (*hht1/hht1::HHT1*^{V31S}), RS105 (*hht1/hht1::HHT1*^{S32T}), RS108 (*hht1/hht1::HHT1*^{S80T}), RS109 (*hht1/hht1::HHT1*^{V31S, S32T}) and RS110 (*hht1/hht1::HHT1*^{V31S, S32T}), and PCR amplified using RA1 and NATRP. Strains RS103, RS105, RS108, RS109 and RS110 are positive for integration PCR (621 bp).

Construction of the *C. albicans* strain expressing Bcr1-myc in the *hht1/hht1::HHT1*^{V31S, S32T} mutant background

To tag Bcr1 with Myc epitope in RS111 (*hht1/hht1::HHT1*^{V31S}) and RS112 (*hht1/hht1::HHT1*^{V31S, S32T}), the mutated allele of *HHT1*^{V31S} or *HHT1*^{V31S, S32T} from plasmids pRS103 and pRS104 was transformed in LR133 (*BCR1-Myc/BCR1 hht1/hht1*) background.

The plasmids were digested with *ApaI* and *SacI* before the transformation. Deletions were confirmed by PCR (**Figure 5.4**).

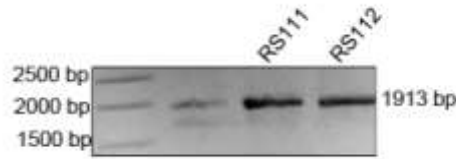


Figure 5.4 Confirmation of integration of mutated *HHT1* ORF at positions 31, 32, and 80 in RS111, and RS112.

The genomic DNA was isolated from strains RS111 (*hht1/hht1::HHT1^{V31S}*) and RS112 (*hht1/hht1::HHT1^{V31S, S32T}*), and PCR amplified using 6791FP and NATRP. RS111 and RS112 are positive for integration PCR (1913 bp).

Construction of *C. albicans* strain expressing V5-tagged allele of mutated *HHT1* (*HHT1^{V31S, S32T}*) at 31 and 32 position

To tag the point mutated copy of *HHT1^{V31S, S32T}* (RS113, RS114, RS115; *hht1/hht1::HHT1^{V31S, S32T-V5}*), the C-terminus of Ca*HHT1* was amplified using pLSR108 as a template with two long primers: the forward primer (6791V52LFP) containing homology to Ca*HHT1* and the reverse primer (RS235) homologous to 3' UTR. The amplified Ca*HHT1-V5* cassette was then used to transform RS109 (*hht1/hht1::HHT1^{V31S, S32T}*) to tag *HHT1^{V31S, S32T}* (RS113, RS114, RS115, *hht1/hht1::HHT1^{V31S, S32T-V5}*) (**Figure 5.5**).



Figure 5.5 Western blot confirmation for V5 epitope tagging of point mutants of *HHT1* at 31 and 32 positions in RS113, RS114, RS115.

Whole-cell lysates from strains RS113 (*hht1/hht1::HHT1^{V31S, S32T-V5}*), RS114 (*hht1/hht1::HHT1^{V31S, S32T-V5}*), and RS115 (*hht1/hht1::HHT1^{V31S, S32T-V5}*) were separated by SDS-PAGE using 12% gels. The proteins were transferred onto nitrocellulose membranes and probed with anti-V5 antibodies for immunoblot analysis. RS113, RS114 and RS115 are desired transformants for V5 tagging (expected band size 17 kDa).

Construction of the *C. albicans* strain expressing V5-tagged allele of *HHT1* and *HHT21* in the *cac2* null mutant background

To tag the endogenous copy of *HHT21* in CA-MT363 (*cac2/cac2*) to generate RS501 (*cac2/cac2 HHT21/HHT21-V5*), the Ca*HHT21*-V5 cassette was amplified using pLSR107 as a template, with two long primers: the forward primer (1061V5IFP) containing homology to the last codons of the coding region of Ca*HHT21* and the reverse primer (1061SDSRP) bearing homology to 3' UTR. To tag the endogenous copy of *HHT1* in CA-MT363 (*cac2/cac2*) to generate RS502 (*cac2/cac2 HHT1/HHT1-V5*), the Ca*HHT1*-V5 cassette was amplified using pLSR108 as a template and two long primers: the forward primer (6791V52LFP) containing homology to Ca*HHT1* and the reverse primer (6791DSNAT1RP) homologous to 3' UTR (**Figure 5.6**).

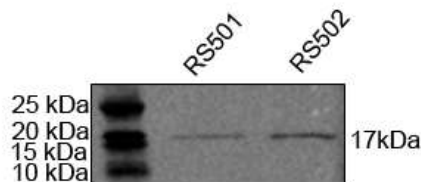


Figure 5.6 Western blot confirmation for V5 epitope tagging of *HHT1* and *HHT21* in *cac2* null mutant background.

Whole-cell lysates from strains RS501 (*cac2/cac2 HHT21/HHT21-V5*) and RS502 (*cac2/cac2 HHT1/HHT1-V5*) were separated by SDS-PAGE using 12% gels. The proteins were transferred onto nitrocellulose membranes and probed with anti-V5 antibodies for immunoblot analysis. RS501 (*cac2/cac2 HHT21/HHT21-V5*) and RS502 (*cac2/cac2 HHT1/HHT1-V5*) are desired transformants for V5 tagging (17 kDa).

Construction of null mutants of *ace2* of *C. albicans*

Null mutants of *ace2*, RS404 and RS405 (*ace2/ace2*) were constructed using SC5314 as the parent strain. The *SAT1*-flipper cassette flanked by upstream and downstream sequences of *ACE2* (pRS401) was digested with *SacI* and *KpnI* and transformed into SC5314. Transformants were selected for nourseothricin (NAT) resistance. The deletion of one copy of *ACE2* was confirmed by PCR in two independent clones, RS400 and RS401. To recycle the marker, cells were grown in maltose-containing medium lacking NAT, as described in (Reuss, Vik et al. 2004). The loss of *SAT1* (NAT-sensitive) was confirmed by

streaking cells on YPD and nourseothricin-containing YPD plates; two clones were selected (RS402 and RS403). To delete the remaining allele of *ACE2*, the same *SAT1*-flipper cassette was used to transform RS402 and RS403. Two independent clones bearing *ace2* null mutations, RS404 and RS405, were PCR confirmed (**Figure 5.7**).



Figure 5.7 Confirmation of *ACE2* deletion in RS404, RS405.

The genomic DNA was isolated from strains RS404 (*ace2/ace2*), RS405 (*ace2/ace2*) RS408, RS409, and PCR amplified using RS178 and RS179. RS404 and RS405 were positive for deletion cassette integration (750 bp). ORF-specific PCR did not yield any amplicon for RS404, RS405 (339 bp).

Construction of double null mutants of *ace2* and *hht1* of *C. albicans*

Double null mutants of *ace2* and *hht1*, RS408 and RS409 (*ace2/ace2 hht1/hht1*) were constructed using LR107 (*hht1/hht1*) as the parent strain. The *SAT1*-flipper cassette flanked by upstream and downstream sequences of *ACE2* (pRS401) was digested with *SacI* and *KpnI* and transformed into LR107 (*hht1/hht1*). Transformants were selected for NAT resistance. The deletion of one copy of *HHT1* was confirmed by PCR in two independent clones, RS406 (*ace2/ACE2*) and RS407 (*ace2/ACE2*). To recycle the marker, cells were grown in maltose-containing medium lacking nourseothricin, as described in (Reuss, Vik et al. 2004). The loss of *SAT1* was confirmed by streaking cells on YPD and nourseothricin-containing YPD plates. To delete the remaining allele of *ACE2*, the same *SAT1*-flipper cassette was used to transform. Two independent clones bearing *hht1* and *ace2* null mutations, RS408 and RS409 (*ace2/ace2 hht1/hht1*), were confirmed by PCR (**Figure 5.8**).

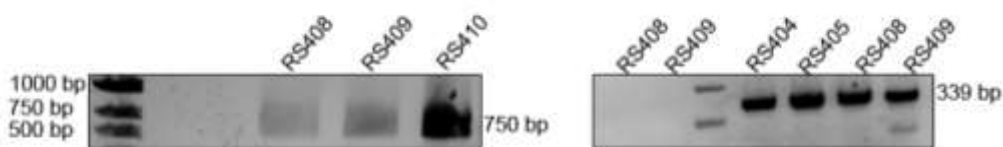


Figure 5.8 Confirmation of *ACE2* deletion in RS408, RS409 by PCR.

The genomic DNA was isolated from strains RS408 (*ace2/ace2 hht1/hht1*), RS409 (*ace2/ace2 hht1/hht1*), RS410 (*ace2/ace2 hht1/hht1*) and PCR amplified using RS178 and RS179. RS408, RS409, and RS410 were positive for cassette integration (750 bp). ORF-specific PCR did not yield any amplicon for RS408, RS409 (339 bp).

Construction of add-back strain of *HHT1* ORF in double mutants of *ace2* and *hht1* of *C. albicans*

Double mutants of *ace2* and *hht1*, RS410 (*ace2/ace2 hht1/hht1*) were transformed with pLSR103 (pSFS2a backbone with *HHT1* ORF and homology from the promoter and 3' UTR regions) and the integration of the *HHT1* ORF in RS411 (*ace2/ace2 hht1/hht1::HHT1*), RS412 (*ace2/ace2 hht1/hht1::HHT1*) at the native locus was confirmed by PCR (**Figure 5.9**).



Figure 5.9 Confirmation of *HHT1* reintegration in RS411, RS412 by PCR.

The genomic DNA was isolated from strains RS411 (*ace2/ace2 hht1/hht1::HHT1*), RS412 (*ace2/ace2 hht1/hht1::HHT1*) and PCR amplified using HHT1FP and HHT1RP. RS411 and RS412 gave the desired amplicon (170 bp).

Construction of plasmids

Construction of pLSR107

A 269 bp fragment having *ORF19.1061* and downstream sequences with V5 sequence in the forward cloning primers was PCR amplified and cloned into pBluescript KSII (-) having the *HIS1* sequence at *SacI/SacII* sites. The cassette was confirmed by restriction digestion.

Construction of pLSR108

A 451 bp fragment having *ORF19.6791* and downstream sequences with V5 sequence in the forward cloning primers were PCR amplified and cloned into pBluescript KSII (-) having *HIS1* sequences at *SacI/SacII* sites. The cassette was confirmed by restriction digestion.

Construction of pRS107

A 501 bp fragment having 3' ÚTR sequence of *ORF19.6791* was PCR amplified and cloned into pSFS2a at *SacI/SacII* sites. The cassette was confirmed by restriction digestion.

Construction of pRS103, pRS104, pRS105, pRS106, and pRS401

The *HHT1* coding region was mutated by overlap PCR using primers sdm1fp, sdm1rp (V31S, in pRS103), primers RS181 and RS182 (V31S, S32T, in pRS104), primers RS211 and RS212 (S32T, pRS105), or primers RS233 and RS234 (S80T, in pRS106). A 1656 bp fragment containing the mutated ORFs was cloned into the *Apal/XhoI* sites of pRS107. Clones were confirmed by restriction analysis and, the presence of the mutation was confirmed by Sanger sequencing.

Construction of pRS401

A 350 bp fragment having the upstream sequence of *ACE2* and 310 bp downstream of *ACE2* were PCR amplified with primers RS164, RS165, and RS166, RS167 respectively. The upstream fragment was cloned in pSFS2A digested with *KpnI* and *XhoI*; the downstream fragment was inserted in the resulting plasmid digested with *SacI* and *SacII*.

***E. coli* competent cells preparation and transformation**

Competent cells of DH5 α were prepared by the PEG method (Chung et al 1989). Cells from an overnight grown culture were seeded at 1% into flasks containing LB media and grown at 37°C. Cells were chilled on ice when the OD₆₀₀ reached 0.3-0.5. Cells were harvested by centrifugation at 2500 rpm for 5 min at 4°C. Cell pellet from 50 mL culture was gently resuspended in 2 mL of ice-cold TSS buffer (2xLB, 10% (w/v) PEG3350, 100 mM MgCl₂, 5% (v/v) DMSO). Aliquots of 100 μ L were made and snap-frozen using liquid N₂. For transformation, the desired amount of plasmid or ligation product (in not more

than 10 μ L volume) was added per tube after thawing on ice. Post addition, the tubes were tap mixed, incubated on ice for 30 min. Cells were recovered in LB media at 37°C for 45 min. Cells were then harvested, resuspended, and plated on LB plates containing the appropriate antibiotic.

Genomic DNA preparation

Between 3-5 ml of overnight grown culture was harvested, washed with autoclaved water, and resuspended in 0.2 mL extraction buffer. Cells were lysed by vortexing with 0.3 g of acid-washed glass beads and 0.2 mL of phenol: chloroform: isoamyl alcohol (25:24:1). After centrifugation at 14,000 rpm for 10 min, the supernatant was collected, and DNA was precipitated with 100% ethanol at -20°C for 1 h. The tubes were centrifuged at 14,000 rpm at 4°C, and the pellet was washed with ice-cold 70% ethanol. The pellet was air-dried and resuspended in 30 μ L of 1xTE.

Cell lysate preparation and western blot analysis

Approximately 3 OD₆₀₀ equivalent *C. albicans* cells were harvested and precipitated by 12.5 % TCA overnight at -20°C. The pellet was spun down at 13000 rpm and washed with 80% acetone. Pellet was then dried and resuspended in lysis buffer (1% SDS, 0.1N NaOH) and SDS loading dye. Samples were boiled for 5 min and electrophoresed on a 12% polyacrylamide gel. The protein was transferred by the semi-dry method for 40 min at 25 V. After the protein transfer, the blot was blocked with 5 % skimmed milk for 30 min. The blot was incubated with anti-V5 antibodies or anti-myc antibodies for 3 h. The blot was washed thrice in PBST (1X PBS + 0.05 % Tween-20) and incubated with goat anti-mouse IgG-HRP for 1 h. Following three PBST washes, the blot was developed using chemiluminescence method (SuperSignal WestPico Chemiluminescent substrate, Thermo scientific, cat no. 34080).

Chromatin Immunoprecipitation (ChIP)

Strains were grown in YPDU (50 ml for histone ChIP and 200 ml for Bcr1 ChIP) till log phase. Crosslinking was done for 15 min (for histone H3) or 120 min (for Bcr1) using formaldehyde to a final concentration of 1%, and cells were quenched using 0.135 mM glycine for 5 min at room temperature. Quenched cells were incubated in a reducing environment in the presence of 9.5 ml distilled water and 0.5 ml of β -Mercaptoethanol (HiMedia cat. no. MB041). Cells were then spheroplasted in lysing enzyme from *Trichoderma harzanium* (Sigma cat. no. L1412) in spheroplasting buffer (1 M sorbitol, 0.1 M sodium citrate, 0.01 M EDTA) for 3 h at 60 rpm in 37°C. Spheroplasts were spun and washed, followed by resuspending in 1 ml of lysis buffer (50 mM HEPES pH-7.4, 1% Triton X-100, 140 mM NaCl, 0.1% Na-deoxycholate, 1 mM EDTA). Chromatin was sheared in a Bioruptor (Diagenode) for 60 cycles of 30 s on and 30 s off. The sheared chromatin was run on a 2% agarose gel to check for the appropriate size (300-500 bp). One-tenth of the lysate was saved as the input (I), and the rest was split as two fractions- IP (+ antibody) and mock (- antibody). To the IP fraction, required concentration of antibody was added, and both tubes were incubated at 4°C overnight. Then to the + and - tubes, Protein-A beads (Sigma cat. no. P3391) were added and incubated for 8 h. The beads were then washed in low and high salt conditions and finally eluted in elution buffer (1% SDS, 0.1 M sodium bicarbonate). The eluted samples were decrosslinked at 65°C overnight and deproteinized. Following phenol-chloroform extraction, all three samples, I, +, and - were ethanol precipitated. The DNA pellet was finally resuspended in 20 μ l of MilliQ water. All three samples (I, +, -) were then subjected to semiquantitative and qPCR reactions.

ChIP-qPCR analysis

The input and IP DNA were diluted appropriately and qPCR reactions were set up using primers listed in Table 6.2. The enrichment was determined by the percentage input method. Two-way ANOVA and Bonferonni post-tests were performed to determine statistical significance. All the percent IP values represented in the graphs are the ratio of percent IP of the protein of interest (canonical/variant/total histone H3/Bcr1) at the promoters of biofilm genes to the corresponding values of the protein of

interest at the promoter of *ORF19.8740*, which was used as an internal control to estimate the efficiency of the pulldown.

RNA extraction

RNA was isolated from *C. albicans* yeast cells by growing them in YPDU to an $OD_{600}=0.5$, and 4×10^7 cells were taken for spheroplasting. Cells were pelleted down at 4000 rpm and washed with 1 ml of Y1 buffer (2.5 M sorbitol, 0.5 M EDTA pH-7.4). Cells were finally resuspended in 2 ml of Y1 buffer, 10 mg of lysing enzyme from *Trichoderma harzanium* (Sigma cat. no. L1412), and 20 μ l of β -Mercaptoethanol was added and spheroplasted at 37°C at 70 rpm. After 90% spheroplasting, spheroplasts were isolated by centrifugation at 1800 rpm for 5 min. To the spheroplasts, 1ml of TRIZOL (Invitrogen) was added, mixed vigorously, and incubated for 5 min at room temperature. Then to the above mixture, 200 μ l of chloroform was added and spun at 13000 rpm for 10 min. The upper aqueous layer was collected, and isopropanol was added for precipitation at room temperature for 30 min. It was then centrifuged at 13000 rpm for 20 min. The RNA pellet was washed, air-dried, and resuspended in 20 μ l of RNase free water.

For RNA isolation of adhered cells of *C. albicans*, RNA was isolated from *C. albicans* cells by the RNeasy mini kit (Qiagen, Cat.No.74104). Adhered cells were collected after 90 min of adhesion and were processed as same as mentioned above till the spheroplasting step. The spheroplasts were isolated by centrifugation and RNA was isolated by Qiagen Kit protocol (Cat, No.74104). Protocol is described in RNeasy Mini Handbook (Protocol yeast 1).

cDNA preparation and Reverse transcription PCR

A total of 500 ng of RNA was taken for cDNA synthesis. The reaction mixture contained 4 μ l of 5 x RT buffer (Invitrogen), 2 μ l of 10 mM of dNTP, 2 μ l of 0.1 M DTT, 2 μ l of 10 pMol of Oligo(dT) primers (Sigma, Cat. No. O-4387) and 1 μ l of M-MuLV reverse transcriptase (Fermentas, EP0732) in a final volume of 20 μ l. Reverse transcription PCR reactions were carried out at 37°C for 60 min followed by heat inactivation at 85°C for 5 min.

Quantitative PCR

Primers designed for qPCR reactions were between 100-110 bp long. Analysis of the melt curve was also performed to ensure specific amplification without any secondary non-specific amplicons. PCR was carried out in a final volume of 20 μ l using 2X Sensi Fast SYBR mix (BIO-98020). Real-time PCR analysis was carried out in i-Cycler (BIO-RAD) using the following reaction conditions: 95°C for 2 min, 95°C for 30 s, 55°C for 30 s, 72°C for 30 s for 40 cycles. Fold difference in expression of mRNA was calculated by $\Delta\Delta C_t$ method (Real-Time PCR applications guide BIO-Rad). Actin was used as the normalization control.

Gene expression microarray design and data analysis

The concentration of the RNA extracted was evaluated using Bioanalyzer (Agilent; 2100), while the purity of the RNA extracted was determined using the standard procedure for the same by measuring A_{260} and A_{280} on a Nanodrop Spectrophotometer (Thermo Scientific; 1000). The samples were labeled using Agilent Quick Amp labeling Kit (Part number: 5190-0442). A total of 500 ng of RNA was reverse transcribed using Oligo(dT) primer tagged to T7 promoter sequence. The cDNA obtained was converted to double-stranded cDNA in the same reaction. Further, the cDNA was converted to cRNA in the *in vitro* transcription step using T7 RNA polymerase enzyme and Cy3 dye was added into the reaction mix. During cRNA synthesis, Cy3 dye was incorporated into the newly synthesized strands. cRNA obtained was cleaned up using Qiagen RNeasy columns (Qiagen, Cat No: 74106). Concentration and the amount of dye incorporated were determined using Nanodrop. Samples that passed the QC for the specific activity (Minimum RNA concentration 500/ μ l and absorbance 260/280=2) were taken for hybridization. A total of 600 ng of labeled cRNA was hybridized on the array (AMADID: 29460) using the Gene Expression Hybridization Kit (Part Number 5190-0404; Agilent) in Sure hybridization Chambers (Agilent) at 65°C for 16 h. Hybridized slides were washed using Agilent Gene Expression wash buffers (Part No: 5188-5327). The hybridized, washed microarray slides were then scanned on a G 2600 D scanner (Agilent Technologies). Data extraction from images was done using Feature Extraction software v 10.7 of Agilent. Microarray data were pre-processed using Limma package

(Smyth et al., 2005) of statistical R language. Briefly, pre-processing includes (a) background correction (b) within array normalization and (c) fitting data to a linear model. Finally, an empirical Bayes moderated statistics was applied to find significant changes in the expression levels. We used a cut-off of p-value <0.05 and |fold change| >1.5 for the differential expression of mutant over wild-type to define differentially expressed genes. Differentially regulated genes were clustered using hierarchical clustering to identify significant gene expression patterns. Genes were classified based on functional annotation. Genes were annotated by using Candida Genome Database (CGD).

Biofilm assay on six-well polystyrene plates

Biofilms were grown *in vitro* in YPDU or YNB + 500 mM galactose by growing the biofilms directly on the bottom of 6-well polystyrene plates (CELLSSTAR, 657160). Biofilms were developed as described by Nobile and Mitchell (Nobile and Mitchell 2005). Strains were grown in YPD overnight at 30°C, diluted to an optical density at 600 nm (OD₆₀₀) of 0.5 in 3 ml of medium. The 6-well plates were pretreated overnight with fetal bovine serum (FBS) and washed with 2 ml PBS. The inoculated plate was incubated at 37°C for 90 min at 110 rpm agitation for the initial adhesion of cells. Plates were then washed with 2 ml PBS, and 3 ml of fresh media was added, and plates were incubated at 37°C for 48 h. To estimate the dry biomass of biofilms, biofilms were scrapped, and the content of each well was transferred to preweighed nitrocellulose filters. Biofilm-containing filters were dried overnight at 60°C and weighed. The average total biomass for each strain was calculated from 3 independent samples after subtracting the mass of the empty filter.

Quantitative adherence assay using crystal violet staining and XTT assay

Strains were grown in YPDU overnight at 30°C, diluted to an OD₆₀₀ 0.5 in 200 µl of YNB + 50 mM galactose and added to a sterile 96-well plate. The 96-well plate was previously treated with bovine serum (Gibco, Invitrogen) overnight at 37°C and washed with 1xPBS. The plate was incubated at 37°C for 2 h at 120 rpm for initial adhesion. The wells were washed with 200 µl of PBS twice and stained with 0.4 % crystal violet for

15 min. Further, each well was washed with PBS four times and immediately destained with 200 μ l of 95% ethanol for 2 h. The destained solution was diluted to the desired dilution with 95% ethanol and measured spectrophotometrically at 595 nm. The absorbance values for the controls were subtracted from the values for the test wells to minimize background interference. A similar protocol for 90 min adherence was followed for XTT assay after washing off the nonadhered cells. The quantitation was done using 2,3-bis (2-methoxy-4-nitro-5-sulfo-phenyl)-2H-tetrazolium-5-carboxanilide (XTT) reduction assay that measures the activity of mitochondrial dehydrogenase. The XTT solution (1 mg/ml) was prepared by dissolving XTT powder (Sigma) in 1xPBS, and the solution was filter-sterilized (0.22- μ m pore size filter). The XTT solution (40 μ l) was mixed with freshly prepared menadione solution (0.4 mM; 2 μ l) (Sigma) at 20:1 (v/v) immediately prior to the assay. Thereafter, PBS (158 μ l) was mixed with XTT-menadione solution (42 μ l), transferred to each well containing pre-washed cells, and incubated in the dark for 3 h at 37°C. After the incubation, the colored supernatant (100 μ l) was transferred to new microtiter plates, and the optical density of the supernatant was measured at 490 nm with a microplate reader.

Quantitative adherence assay using colony-forming unit (CFU) counting

Strains were grown in YPDU overnight at 30°C, diluted to an OD₆₀₀ 0.5 in 200 μ l of YNB+ 500 mM galactose, and added to a sterile 96-well plate. The 96-well plate was previously treated with bovine serum (Gibco, Invitrogen) overnight at 37°C and washed with 1xPBS. The plate was incubated at 37°C for 2 h at 120 rpm for initial adhesion. The wells were washed with 200 μ l of PBS twice, and the adhered cells were scraped from the bottom of the plate by scraping and repeated pipetting in 200 μ l PBS. The cells were then resuspended in various dilutions and plated on non-selective (YPDU) plates. The colonies were counted and multiplied with dilution factors. The graph contains the mean of two independent experiments.

Table 5-1 Strains used in the study

Name	Genotype	Description	Reference
SC5314	Wild type	Clinical isolate	(Aszalos, Robison et al. 1968)
SN148	<i>Δura3::imm434/Δura3::imm434</i> <i>Δhis1::hisG/Δhis1::hisG</i> , <i>Δarg4::hisG/Δarg4::hisG</i> , <i>Δleu2::hisG/Δleu2::hisG</i>	Arginine, Histidine, Leucine, Uridine Auxotroph. Derived from SC5314.	(Noble and Johnson 2005)
LR105	<i>SC5314 HHT1/Δhht1::FRT</i>	<i>HHT1</i> one copy deletion in SC5314 background	(Rai, Singha et al. 2019)
LR107	<i>SC5314 Δhht1::FRT/Δhht1::FRT</i>	<i>HHT1</i> deletion in SC5314 background	(Rai, Singha et al. 2019)
LR109	<i>SC5314 Δhht1::FRT/Δhht1::HHT1::FRT</i>	<i>HHT1</i> add back in <i>HHT1</i> null background	(Rai, Singha et al. 2019)
LR143	<i>Δura3::imm434/Δura3::imm434</i> <i>Δhis1::hisG/Δhis1::hisG</i> <i>Δarg4::hisG/Δarg4::hisG</i> <i>Δleu2::hisG/Δleu2::hisG</i> <i>HHT21/HHT21::V5-HIS1</i> <i>RPS10/rps10::URA3</i>	Hht21 V5 epitope tagged in SN148 background	This study
LR144	<i>Δura3::imm434/Δura3::imm434</i> <i>Δhis1::hisG/Δhis1::hisG</i> <i>Δarg4::hisG/Δarg4::hisG</i> <i>Δleu2::hisG/Δleu2::hisG</i> <i>HHT1/HHT1::V5-HIS1</i> <i>RPS10/rps10::URA3</i>	Hht1 V5 epitope tagged in SN148 background	This study
CJN1785	<i>Δura3::imm434/Δura3::imm434/URA3-IRO1</i> <i>Δhis1::hisG/Δhis1::hisG</i> <i>Δarg4::hisG/Δarg4::hisG</i> <i>Δleu2::hisG::pHIS1/Δleu2::hisG::BCR1-13XMyC-FRT</i>	Bcr1 myc tagged in SN152 background	(Nobile, Fox et al. 2012)
LR133	<i>Δura3::imm434/Δura3::imm434/URA3-IRO1</i> <i>Δhis1::hisG/Δhis1::hisG</i> <i>Δarg4::hisG/Δarg4::hisG</i> <i>Δleu2::hisG::pHIS1/Δleu2::hisG::BCR1-13XMyC-FRT</i> <i>hht1::FRT/hht1::NAT FLP</i>	Bcr1 myc tagged in <i>hht1/hht1</i> background	This study
RS103	<i>Δhht1::FRT/Δhht1::HHT1^{V31S} NAT-FLP</i>	<i>HHT1</i> added back with point	This study

		mutation at 31 position from valine to serine	
RS104	<i>Δhht1::FRT/Δhht1::HHT1^{V31S} NAT-FLP</i>	<i>HHT1</i> added back with point mutation at 31 position from valine to serine	This study
RS105	<i>Δhht1::FRT/Δhht1::HHT1^{S32T} NAT-FLP</i>	<i>HHT1</i> added back with point mutation at 32 position from serine to threonine	This study
RS106	<i>Δhht1::FRT/Δhht1::HHT1^{S32T} NAT-FLP</i>	<i>HHT1</i> added back with point mutation at 32 position from serine to threonine	This study
RS107	<i>Δhht1::FRT/Δhht1::HHT1^{S80T} NAT-FLP</i>	<i>HHT1</i> added back with point mutation at 80 position from serine to threonine	This study
RS108	<i>Δhht1::FRT/Δhht1::HHT1^{S80T} NAT-FLP</i>	<i>HHT1</i> added back with point mutation at 80 position from serine to threonine	This study
RS109	<i>Δhht1::FRT/Δhht1::HHT1^{VS3132ST} NAT-FLP</i>	<i>HHT1</i> added back with point mutation at 31,32 position from valine, serine to serine, threonine	This study
RS110	<i>Δhht1::FRT/Δhht1::HHT1^{VS3132ST} NAT-FLP</i>	<i>HHT1</i> added back with point mutation at 31,32 position from valine,	This study

		serine to serine, threonine	
RS111	<i>Δura3::imm434/Δura3::imm434/URA3-IRO1 Δhis1::hisG/Δhis1::hisG Δarg4::hisG/Δarg4::hisG Δleu2::hisG::pHIS1/Δleu2::hisG::BCR1-13XMyc-FRT hht1::FRT/hht1::HHT1^{V31S} NAT-FLP</i>	Bcr1 myc tagged in <i>HHT1</i> added back with point mutation at 31 position background	This study
RS112	<i>Δura3::imm434/Δura3::imm434/URA3-IRO1 Δhis1::hisG/Δhis1::hisG Δarg4::hisG/Δarg4::hisG Δleu2::hisG::pHIS1/Δleu2::hisG::BCR1-13XMyc-FRT hht1::FRT/hht1::HHT1^{VS3132ST} NAT-FLP</i>	Bcr1 myc tagged in <i>HHT1</i> added back with point mutation at 31, 32 position background	This study
RS113	<i>Δhht1::FRT/Δhht1::HHT1^{VS3132ST} V5 NAT</i>	Hht1 add back copy V5 epitope tagged where the <i>HHT1</i> gene is point mutated at 31, 32 position from valine, serine to serine, threonine	This study
CA-MT363	<i>Δcac2::FRT/Δcac2::FRT</i>	<i>CAC2</i> deleted in SC5314 background	(Tscherner, Zwolanek et al. 2015)
CA-MT376	<i>Δhir1::FRT/Δhir1::FRT</i>	<i>HIR1</i> deleted in SC5314 background	(Jenull, Tscherner et al. 2017)
RS501	<i>Δcac2::FRT/Δcac2::FRT::HHT21/HHT21::V5 NAT</i>	Hht21 V5 epitope tagged in <i>cac2/cac2</i> background	This study
RS502	<i>Δcac2::FRT/Δcac2::FRT::HHT1/HHT1::V5 NAT</i>	Hht1 V5 epitope tagged in <i>cac2/cac2</i> background	This study
RS400	<i>SC5314 Δace2NATflp/ACE2</i>	<i>ACE2</i> one copy deletion in SC5314 background with <i>SAT1</i> flipper cassette	This study
RS401	<i>SC5314 Δace2NATflp/ACE2</i>	<i>ACE2</i> one copy deletion in	This study

		SC5314 background with <i>SAT1</i> flipper cassette	
RS402	<i>SC5314 ACE2/Δace2::FRT</i>	<i>ACE2</i> one copy deletion in SC5314 background with marker recycled	This study
RS403	<i>SC5314 ACE2/Δace2::FRT</i>	<i>ACE2</i> one copy deletion in SC5314 background with marker recycled	This study
RS404	<i>SC5314 Δace2NATflp/Δace2::FRT</i>	<i>ACE2</i> both copy deletion in SC5314 background with <i>SAT1</i> flipper cassette	This study
RS405	<i>SC5314 Δace2NATflp/Δace2::FRT</i>	<i>ACE2</i> both copy deletion in SC5314 background with <i>SAT1</i> flipper cassette	This study
RS406	<i>ACE2/Δace2::FRT Δhht1::FRT/Δhht1::FRT</i>	<i>ACE2</i> one copy deletion in <i>hht1</i> null background with <i>SAT1</i> flipper cassette	This study
RS407	<i>ACE2/Δace2::FRT Δhht1::FRT/Δhht1::FRT</i>	<i>ACE2</i> one copy deletion in <i>hht1</i> null background with <i>SAT1</i> flipper cassette	This study
RS408	<i>ace2NATflp/Δace2::FRT::Δhht1::FRT/Δhht1::FRT</i>	<i>ACE2</i> both copy deletion in <i>hht1</i> null background with <i>SAT1</i> flipper cassette	This study
RS409	<i>ace2NATflp/Δace2::FRT::Δhht1::FRT/Δhht1::FRT</i>	<i>ACE2</i> both copy deletion in <i>hht1</i> null background	This study

		with <i>SAT1</i> flipper cassette	
RS410	<i>ace2NATflp/Δace2::FRT::Δhht1::FRT/Δhht1::FRT</i>	<i>ACE2</i> both copy deletion in <i>hht1</i> null background with marker recycled	This study
RS411	<i>ace2NATflp/Δace2::FRT::Δhht1::FRT/Δhht1::FRT::HHT1 NATflp</i>	<i>HHT1</i> added back in <i>ace2</i> and <i>hht1</i> null background	This study

Table 5-2 Oligonucleotides used in this study

Name	Sequence	Description
1061V52CFP	CGA GCT CTT GAG AGG TGA AAG ATC TGG TAA GCC TAT CCC TAA CCC TCT CCT CGG TCT CGA TTC TAC GTA GGT TAA GCT CGT GGC GGG	Primer for cloning and amplification of <i>HHT21</i> V5 epitope tag
1061V5CRP	TCCCCGCGGCCGGATGTTTGTTTTATTTTTC	
1061V5IFP	TAACTTGTGTGCTATCCATGCTAAGAGAGTTACCATT CA AAAGAAAGATATGCAATTAGCTAGAAGATTGAGAGG TGA AAGATCT	
6791V52CFP	CGAGCTCTTAAGAGGTGAAAGATCTGGTAAGCCTATC CC TAACCCTCTCCTCGGTCTCGATTCTACGTAAGA CAGGATAAGATAGGAT	Primer for cloning and amplification of <i>HHT1</i> V5 epitope tag
6791V5CRP	TCCCCGCGGGACTTCAAGATTATAATTAAAACA AAG	
6791V52LFP	CTAATTTATGTGCTATTCATGCTAAAAGAGTTACTTT CAAAAGAAAGATATGCAATTAGCTAGAAGATTAA GAGGTGAAAGATCT	
RS213	GTA ACTCCTCTAACGTTGTTTTCCGTTAAACAGTAA TAGCAAGTCAATTAGAATTGGGTGTGAAGCATACCCG GGGATATCAAGCTTGCCT	Reverse primer for V5 epitope tagging of <i>HHT21</i> from pBS NAT-1061
RS214	CACTCATTTGCAATTCAGTAATTTATTATTCTACTT TTTAATATTTTTCTTATGATTATCAACTCGGGCCC GGGATATCAAGCTTGCCT	Reverse primer for V5 epitope tagging of <i>HHT1</i> from pBS NAT-6791
HWP1RTFP	CCG CTC GAG TTA AGA TCT TTC ACC TC	qPCR primers for RNA expression
HWP1RTRP	GAA ATA GGA GCG ACA CTT G	
ALS3RTFP	CGC AAT CCA ATT CTG ATA CC	
ALS3RTRP	GAA TAA CAG AAC CAG ATC CG	
ECE1FP	CAA CCA GTT AAA AGA GAT GCC	
ECE1RP	TTT CTG AAA CAA TTT GAG CAG C	
YWP1FP	GTTGCTGGTGGTGTTAATGG	
YWP1RP	AAG TAC TAA TGG CAG CTT TAC C	
GCA1FP	GGT GAA TAT GAA GTT CGT CAA CC	
GCA1RP	GTA GTT GTG GCT TAC TGT TTC G	
JEN2FP	TTT ATT GGT CCT GAA AAC AGA GG	
JEN2RP	GAA TCA CCT CTG TCT TCC CTA TC	

ALD6FP	GGT AAG GCT GGT ATT ACT TTC TTG	
ALD6RP	TTG GCA TTG AAG TAG AAG GTT TC	
ACT1FP	GGTATTGTTTTGGATTCTGGTG	
ACT1RP	CAAGTCTCTACCAGCCAAATC	
HWP1PFP2	CCC TTA AAA CCG ATC AAG AAA G	ChIP- qPCR primers
HWP1PRP2	CGA GAC GAG GAC AAC AAC	
ECE1PFP2	GGT GAT GAA TGG TGA TTG AAT G	
ECE1PRP2	GTG TCA ATT TTA CGG CTT TGT	
YWP1P2FP	TTG ATA CTA TTT CCT CAA AAA GCC	
YWP1P2RP	GTT TCT AAA AGA GGC GTT GCT G	
NRG1PFP	CAT ATT GGT GTA TAA TAA TCA TC	
NRG1PRP	AAA CAA CAC CAT ACA ATG TGA CAC	
CAN1PFP	TCC GAA TTG ATA TCT CGT TTA AG	
CAN1PRP	TGG AAG AGA TGA GCC AGT GGT G	
BMT7PFP	TTG AAC TAA AAG GCT GAG CAT G	
BMT7PRP	ATA TAT GCG ATG GAT TAG TCA TC	
HGT2PFP	TTT GGT CTA GCT GGG GGG	
HGT2PRP	CAA AGC ACA CAT TAA TAT CCA GC	
SAP5PFP	ACG CAA TTT CAC CAA TTA TAG TC	
SAP5PRP	GGC AGG TTT GTA AGT AAA TAA TG	
JEN2PFP	GAG TTT TGT GTA ATG ACC AGC	
JEN2PRP	TCA CTT TGT TGT ATT TTG TGG	
Orf19.7380FP	CCT CAA TTA CCT TGC AGT AGT C	
Orf19.7380RP	CAA TCA AGT ACA GCG CAA AC	
ORF874PFP	AATCGTTGAATTTCTTCTCGC	
ORF874PRP	GAGAAATTAGTGCGGTAAAGTTG	
RS180	CCGGGGCCCGTTTTTCATCCCCAAAAATC	Primers for point mutant generation of <i>HHT1</i> at 31st, 32 nd and 80 th position
RS185	CCGCTCGAGGATTATCAACTCGGGGAC	
RS181	GCCAGAAAATCCGCCCCATCTACTGGTGGTGTCAAAA AACC	
RS182	GGTTTTTTGACACCACCAGTAGATGGGGCGGATTTTC TGCC	
Sdm1fp	GCCAGAAAATCCGCCCCATCATCCGGTGGTGTCAAAA AA	
Sdm1rp	TTTTTTTGACACCACCGGATGATGGGGCGGATTTTCTG GC	
RS186	TCCCCGCGGGACGAAGAATAATCTACTC	
RS187	CGAGCTCCATTCACACATTAATGGC	
RS211	CAGAAAATCCGCCCCAGTTACTGGTGGTGTCAAAAA CCTC	
RS212	CAGAAAATCCGCCCCAGTTACTGGTGGTGTCAAAAA CCTC	
RS233	GAGAAATTGCTCAAGATTTTAAAATGATTTAAGAT TTCAATCTTCTGC	

RS234	GCAGAAGATTGAAATCTTAAATCAGTTTTAAAATCT TGAGCAATTTCTC	
RS164	CGGGGTACCGCCACCGATGACTTTATATG	<i>ACE2</i> deletion cassette cloning primers
RS165	CCGCTCGAGGTGAAGGAGGTGCAAAAGTTG	
RS166	TCCCCGCGGGGAGAGAAGATTGCATTTTC	
RS167	CGAGCTCGGATGATGCTTCAGGATAAG	
RS177	GTGGTAGTGCAGAAATGCAC	<i>ACE2</i> deletion confirmation primers
RS178	GTCCATTCATTCAGAAGCAC	ORF specific primers for <i>ACE2</i>
RS179	GCCACCAACTGAATCTGATT	
HHT1FP	CTTCTCCTTATACTTATTTAAC	ORF specific primers for <i>HHT1</i>
HHT1RP	CCACCGGAAACTGGGGCG	
RA10	CGGAAACTGGGGCGGC	Outside cassette primer for confirmation of <i>HHT1</i> deletion
NATRP	CTATTCTCTAGAAAGTATAGGAACTTC	NAT specific primer

References

- Aszalos, A., R. S. Robison, P. Lemanski and B. Berk (1968). "Trienine, an antitumor triene antibiotic." J Antibiot (Tokyo) **21**(10): 611-615.
- Jenull, S., M. Tscherner, M. Gulati, C. J. Nobile, N. Chauhan and K. Kuchler (2017). "The *Candida albicans* HIR histone chaperone regulates the yeast-to-hyphae transition by controlling the sensitivity to morphogenesis signals." Sci Rep **7**(1): 8308.
- Nobile, C. J., E. P. Fox, J. E. Nett, T. R. Sorrells, Q. M. Mitrovich, A. D. Hernday, B. B. Tuch, D. R. Andes and A. D. Johnson (2012). "A recently evolved transcriptional network controls biofilm development in *Candida albicans*." Cell **148**(1-2): 126-138.
- Noble, S. M. and A. D. Johnson (2005). "Strains and strategies for large-scale gene deletion studies of the diploid human fungal pathogen *Candida albicans*." Eukaryot Cell **4**(2): 298-309.
- Rai, L. S., R. Singha, H. Sanchez, T. Chakraborty, B. Chand, S. Bachellier-Bassi, S. Chowdhury, C. d'Enfert, D. R. Andes and K. Sanyal (2019). "The *Candida albicans* biofilm gene circuit modulated at the chromatin level by a recent molecular histone innovation." PLoS Biol **17**(8): e3000422.
- Tscherner, M., F. Zwolanek, S. Jenull, F. J. Sedlazeck, A. Petryshyn, I. E. Frohner, J. Mavrianos, N. Chauhan, A. von Haeseler and K. Kuchler (2015). "The *Candida albicans* Histone Acetyltransferase Hat1 Regulates Stress Resistance and Virulence via Distinct Chromatin Assembly Pathways." PLoS Pathog **11**(10): e1005218.
- Achkar, J. M. and B. C. Fries (2010). "Candida infections of the genitourinary tract." Clin Microbiol Rev **23**(2): 253-273.
- Adkins, M. W., S. R. Howar and J. K. Tyler (2004). "Chromatin disassembly mediated by the histone chaperone Asf1 is essential for transcriptional activation of the yeast PH05 and PH08 genes." Mol Cell **14**(5): 657-666.
- Ahmad, K. and S. Henikoff (2002). "The histone variant H3.3 marks active chromatin by replication-independent nucleosome assembly." Mol Cell **9**(6): 1191-1200.
- Akhmanova, A. S., P. C. Bindels, J. Xu, K. Miedema, H. Kremer and W. Hennig (1995). "Structure and expression of histone H3.3 genes in *Drosophila melanogaster* and *Drosophila hydei*." Genome **38**(3): 586-600.
- Alva, V. and A. N. Lupas (2019). "Histones predate the split between bacteria and archaea." Bioinformatics **35**(14): 2349-2353.
- Ammar, R., D. Torti, K. Tsui, M. Gebbia, T. Durbic, G. D. Bader, G. Giaever and C. Nislow (2012). "Chromatin is an ancient innovation conserved between Archaea and Eukarya." Elife **1**: e00078.
- Amodeo, A. A., D. Jukam, A. F. Straight and J. M. Skotheim (2015). "Histone titration against the genome sets the DNA-to-cytoplasm threshold for the *Xenopus* midblastula transition." Proc Natl Acad Sci U S A **112**(10): E1086-1095.
- Arents, G., R. W. Burlingame, B. C. Wang, W. E. Love and E. N. Moudrianakis (1991). "The nucleosomal core histone octamer at 3.1 Å resolution: a tripartite protein assembly and a left-handed superhelix." Proc Natl Acad Sci U S A **88**(22): 10148-10152.

Arents, G. and E. N. Moudrianakis (1995). "The histone fold: a ubiquitous architectural motif utilized in DNA compaction and protein dimerization." Proc Natl Acad Sci U S A **92**(24): 11170-11174.

Azsalos, A., R. S. Robison, P. Lemanski and B. Berk (1968). "Trienine, an antitumor triene antibiotic." J Antibiot (Tokyo) **21**(10): 611-615.

Banumathy, G., N. Somaiah, R. Zhang, Y. Tang, J. Hoffmann, M. Andrade, H. Ceulemans, D. Schultz, R. Marmorstein and P. D. Adams (2009). "Human UBN1 is an ortholog of yeast Hpc2p and has an essential role in the HIRA/ASF1a chromatin-remodeling pathway in senescent cells." Mol Cell Biol **29**(3): 758-770.

Bao, Y., K. Konesky, Y. J. Park, S. Rosu, P. N. Dyer, D. Rangasamy, D. J. Tremethick, P. J. Laybourn and K. Luger (2004). "Nucleosomes containing the histone variant H2A.Bbd organize only 118 base pairs of DNA." EMBO J **23**(16): 3314-3324.

Barski, A., S. Cuddapah, K. Cui, T. Y. Roh, D. E. Schones, Z. Wang, G. Wei, I. Chepelev and K. Zhao (2007). "High-resolution profiling of histone methylations in the human genome." Cell **129**(4): 823-837.

Bednar, J., R. A. Horowitz, S. A. Grigoryev, L. M. Carruthers, J. C. Hansen, A. J. Koster and C. L. Woodcock (1998). "Nucleosomes, linker DNA, and linker histone form a unique structural motif that directs the higher-order folding and compaction of chromatin." Proc Natl Acad Sci U S A **95**(24): 14173-14178.

Belotserkovskaya, R., S. Oh, V. A. Bondarenko, G. Orphanides, V. M. Studitsky and D. Reinberg (2003). "FACT facilitates transcription-dependent nucleosome alteration." Science **301**(5636): 1090-1093.

Bernstein, E., T. L. Muratore-Schroeder, R. L. Diaz, J. C. Chow, L. N. Changolkar, J. Shabanowitz, E. Heard, J. R. Pehrson, D. F. Hunt and C. D. Allis (2008). "A phosphorylated subpopulation of the histone variant macroH2A1 is excluded from the inactive X chromosome and enriched during mitosis." Proc Natl Acad Sci U S A **105**(5): 1533-1538.

Birse, C. E., M. Y. Irwin, W. A. Fonzi and P. S. Sypherd (1993). "Cloning and characterization of ECE1, a gene expressed in association with cell elongation of the dimorphic pathogen *Candida albicans*." Infect Immun **61**(9): 3648-3655.

Black, B. E., M. A. Brock, S. Bedard, V. L. Woods, Jr. and D. W. Cleveland (2007). "An epigenetic mark generated by the incorporation of CENP-A into centromeric nucleosomes." Proc Natl Acad Sci U S A **104**(12): 5008-5013.

Black, B. E. and D. W. Cleveland (2011). "Epigenetic centromere propagation and the nature of CENP-a nucleosomes." Cell **144**(4): 471-479.

Black, B. E., D. R. Foltz, S. Chakravarthy, K. Luger, V. L. Woods, Jr. and D. W. Cleveland (2004). "Structural determinants for generating centromeric chromatin." Nature **430**(6999): 578-582.

Black, B. E., L. E. Jansen, D. R. Foltz and D. W. Cleveland (2010). "Centromere identity, function, and epigenetic propagation across cell divisions." Cold Spring Harb Symp Quant Biol **75**: 403-418.

Black, B. E., L. E. Jansen, P. S. Maddox, D. R. Foltz, A. B. Desai, J. V. Shah and D. W. Cleveland (2007). "Centromere identity maintained by nucleosomes assembled with histone H3 containing the CENP-A targeting domain." Mol Cell **25**(2): 309-322.

- Boeckmann, L., Y. Takahashi, W. C. Au, P. K. Mishra, J. S. Choy, A. R. Dawson, M. Y. Szeto, T. J. Waybright, C. Heger, C. McAndrew, P. K. Goldsmith, T. D. Veenstra, R. E. Baker and M. A. Basrai (2013). "Phosphorylation of centromeric histone H3 variant regulates chromosome segregation in *Saccharomyces cerevisiae*." Mol Biol Cell **24**(12): 2034-2044.
- Bonisch, C. and S. B. Hake (2012). "Histone H2A variants in nucleosomes and chromatin: more or less stable?" Nucleic Acids Res **40**(21): 10719-10741.
- Boskovic, A., A. Eid, J. Pontabry, T. Ishiuchi, C. Spiegelhalter, E. V. Raghu Ram, E. Meshorer and M. E. Torres-Padilla (2014). "Higher chromatin mobility supports totipotency and precedes pluripotency in vivo." Genes Dev **28**(10): 1042-1047.
- Bowman, A., A. Koide, J. S. Goodman, M. E. Colling, D. Zinne, S. Koide and A. G. Ladurner (2017). "sNASP and ASF1A function through both competitive and compatible modes of histone binding." Nucleic Acids Res **45**(2): 643-656.
- Braun, B. R., W. S. Head, M. X. Wang and A. D. Johnson (2000). "Identification and characterization of TUP1-regulated genes in *Candida albicans*." Genetics **156**(1): 31-44.
- Braun, B. R. and A. D. Johnson (1997). "Control of filament formation in *Candida albicans* by the transcriptional repressor TUP1." Science **277**(5322): 105-109.
- Brimacombe, C. A., J. E. Burke, J. Y. Parsa, S. Catania, T. R. O'Meara, J. N. Witchley, L. S. Burrack, H. D. Madhani and S. M. Noble (2019). "A natural histone H2A variant lacking the Bub1 phosphorylation site and regulated depletion of centromeric histone CENP-A foster evolvability in *Candida albicans*." PLoS Biol **17**(6): e3000331.
- Brock, M. (2009). "Fungal metabolism in host niches." Curr Opin Microbiol **12**(4): 371-376.
- Brown, D. T. (2003). "Histone H1 and the dynamic regulation of chromatin function." Biochem Cell Biol **81**(3): 221-227.
- Bruce Alberts, Alexander Johnson, Julian Lewis, Martin Raff, Keith Roberts and P. Walter. (2002). Molecular Biology of the Cell, Garland Science.
- Bustin, M., F. Catez and J. H. Lim (2005). "The dynamics of histone H1 function in chromatin." Mol Cell **17**(5): 617-620.
- Campos, E. I., J. Fillingham, G. Li, H. Zheng, P. Voigt, W. H. Kuo, H. Seepany, Z. Gao, L. A. Day, J. F. Greenblatt and D. Reinberg (2010). "The program for processing newly synthesized histones H3.1 and H4." Nat Struct Mol Biol **17**(11): 1343-1351.
- Campos, E. I. and D. Reinberg (2009). "Histones: annotating chromatin." Annu Rev Genet **43**: 559-599.
- Carlisle, P. L., M. Banerjee, A. Lazzell, C. Monteagudo, J. L. Lopez-Ribot and D. Kadosh (2009). "Expression levels of a filament-specific transcriptional regulator are sufficient to determine *Candida albicans* morphology and virulence." Proc Natl Acad Sci U S A **106**(2): 599-604.
- Chadwick, B. P. and H. F. Willard (2001). "A novel chromatin protein, distantly related to histone H2A, is largely excluded from the inactive X chromosome." J Cell Biol **152**(2): 375-384.
- Chaffin, W. L. (2008). "*Candida albicans* cell wall proteins." Microbiol Mol Biol Rev **72**(3): 495-544.

Chakravarthy, S., S. K. Gundimella, C. Caron, P. Y. Perche, J. R. Pehrson, S. Khochbin and K. Luger (2005). "Structural characterization of the histone variant macroH2A." *Mol Cell Biol* **25**(17): 7616-7624.

Chandra, J., D. M. Kuhn, P. K. Mukherjee, L. L. Hoyer, T. McCormick and M. A. Ghannoum (2001). "Biofilm formation by the fungal pathogen *Candida albicans*: development, architecture, and drug resistance." *J Bacteriol* **183**(18): 5385-5394.

Chow, C. M., A. Georgiou, H. Szutorisz, A. Maia e Silva, A. Pombo, I. Barahona, E. Dargelos, C. Canzonetta and N. Dillon (2005). "Variant histone H3.3 marks promoters of transcriptionally active genes during mammalian cell division." *EMBO Rep* **6**(4): 354-360.

Churikov, D., J. Siino, M. Svetlova, K. Zhang, A. Gineitis, E. Morton Bradbury and A. Zalensky (2004). "Novel human testis-specific histone H2B encoded by the interrupted gene on the X chromosome." *Genomics* **84**(4): 745-756.

Citiulo, F., I. D. Jacobsen, P. Miramon, L. Schild, S. Brunke, P. Zipfel, M. Brock, B. Hube and D. Wilson (2012). "Candida albicans scavenges host zinc via Pra1 during endothelial invasion." *PLoS Pathog* **8**(6): e1002777.

Cleard, F., Y. Moshkin, F. Karch and R. K. Maeda (2006). "Probing long-distance regulatory interactions in the Drosophila melanogaster bithorax complex using Dam identification." *Nat Genet* **38**(8): 931-935.

Cook, A. J., Z. A. Gurard-Levin, I. Vassias and G. Almouzni (2011). "A specific function for the histone chaperone NASP to fine-tune a reservoir of soluble H3-H4 in the histone supply chain." *Mol Cell* **44**(6): 918-927.

Daniels, K. J., T. Srikantha, S. R. Lockhart, C. Pujol and D. R. Soll (2006). "Opaque cells signal white cells to form biofilms in *Candida albicans*." *EMBO J* **25**(10): 2240-2252.

Davey, C. A., D. F. Sargent, K. Luger, A. W. Maeder and T. J. Richmond (2002). "Solvent mediated interactions in the structure of the nucleosome core particle at 1.9 a resolution." *J Mol Biol* **319**(5): 1097-1113.

Deal, R. B., C. N. Topp, E. C. McKinney and R. B. Meagher (2007). "Repression of flowering in Arabidopsis requires activation of FLOWERING LOCUS C expression by the histone variant H2A.Z." *Plant Cell* **19**(1): 74-83.

Desai, P. R., L. van Wijlick, D. Kurtz, M. Juchimiuk and J. F. Ernst (2015). "Hypoxia and Temperature Regulated Morphogenesis in *Candida albicans*." *PLoS Genet* **11**(8): e1005447.

Dhayalan, A., R. Tamas, I. Bock, A. Tattermusch, E. Dimitrova, S. Kudithipudi, S. Ragozin and A. Jeltsch (2011). "The ATRX-ADD domain binds to H3 tail peptides and reads the combined methylation state of K4 and K9." *Hum Mol Genet* **20**(11): 2195-2203.

Di Stefano, B., S. Collombet, J. S. Jakobsen, M. Wierer, J. L. Sardina, A. Lackner, R. Stadhouders, C. Segura-Morales, M. Francesconi, F. Limone, M. Mann, B. Porse, D. Thieffry and T. Graf (2016). "C/EBPalpha creates elite cells for iPSC reprogramming by upregulating Klf4 and increasing the levels of Lsd1 and Brd4." *Nat Cell Biol* **18**(4): 371-381.

Dorigo, B., T. Schalch, A. Kulangara, S. Duda, R. R. Schroeder and T. J. Richmond (2004). "Nucleosome arrays reveal the two-start organization of the chromatin fiber." *Science* **306**(5701): 1571-1573.

- Douglas, L. J. (2003). "*Candida* biofilms and their role in infection." Trends Microbiol **11**(1): 30-36.
- Drane, P., K. Ouararhni, A. Depaux, M. Shuaib and A. Hamiche (2010). "The death-associated protein DAXX is a novel histone chaperone involved in the replication-independent deposition of H3.3." Genes Dev **24**(12): 1253-1265.
- Dunleavy, E. M., G. Almouzni and G. H. Karpen (2011). "H3.3 is deposited at centromeres in S phase as a placeholder for newly assembled CENP-A in G(1) phase." Nucleus **2**(2): 146-157.
- Dunleavy, E. M., A. L. Pidoux, M. Monet, C. Bonilla, W. Richardson, G. L. Hamilton, K. Ekwall, P. J. McLaughlin and R. C. Allshire (2007). "A NASP (N1/N2)-related protein, Sim3, binds CENP-A and is required for its deposition at fission yeast centromeres." Mol Cell **28**(6): 1029-1044.
- Dunleavy, E. M., D. Roche, H. Tagami, N. Lacoste, D. Ray-Gallet, Y. Nakamura, Y. Daigo, Y. Nakatani and G. Almouzni-Pettinotti (2009). "HJURP is a cell-cycle-dependent maintenance and deposition factor of CENP-A at centromeres." Cell **137**(3): 485-497.
- Earnshaw, W. C. and N. Rothfield (1985). "Identification of a family of human centromere proteins using autoimmune sera from patients with scleroderma." Chromosoma **91**(3-4): 313-321.
- Elsaesser, S. J. and C. D. Allis (2010). "HIRA and Daxx constitute two independent histone H3.3-containing predeposition complexes." Cold Spring Harb Symp Quant Biol **75**: 27-34.
- Elsasser, S. J., H. Huang, P. W. Lewis, J. W. Chin, C. D. Allis and D. J. Patel (2012). "DAXX envelops a histone H3.3-H4 dimer for H3.3-specific recognition." Nature **491**(7425): 560-565.
- Eltsov, M., K. M. Maclellan, K. Maeshima, A. S. Frangakis and J. Dubochet (2008). "Analysis of cryo-electron microscopy images does not support the existence of 30-nm chromatin fibers in mitotic chromosomes in situ." Proc Natl Acad Sci U S A **105**(50): 19732-19737.
- English, C. M., M. W. Adkins, J. J. Carson, M. E. Churchill and J. K. Tyler (2006). "Structural basis for the histone chaperone activity of Asf1." Cell **127**(3): 495-508.
- Enomoto, S. and J. Berman (1998). "Chromatin assembly factor I contributes to the maintenance, but not the re-establishment, of silencing at the yeast silent mating loci." Genes Dev **12**(2): 219-232.
- Erives, A. J. (2017). "Phylogenetic analysis of the core histone doublet and DNA topo II genes of Marseilleviridae: evidence of proto-eukaryotic provenance." Epigenetics Chromatin **10**(1): 55.
- Eustermann, S., J. C. Yang, M. J. Law, R. Amos, L. M. Chapman, C. Jelinska, D. Garrick, D. Clynes, R. J. Gibbons, D. Rhodes, D. R. Higgs and D. Neuhaus (2011). "Combinatorial readout of histone H3 modifications specifies localization of ATRX to heterochromatin." Nat Struct Mol Biol **18**(7): 777-782.
- Fan, J. Y., D. Rangasamy, K. Luger and D. J. Tremethick (2004). "H2A.Z alters the nucleosome surface to promote HP1 α -mediated chromatin fiber folding." Mol Cell **16**(4): 655-661.
- Fanning, S. and A. P. Mitchell (2012). "Fungal biofilms." PLoS Pathog **8**(4): e1002585.
- Felsenfeld, G. and J. D. McGhee (1986). "Structure of the 30 nm chromatin fiber." Cell **44**(3): 375-377.
- Fernandez-Capetillo, O., S. K. Mahadevaiah, A. Celeste, P. J. Romanienko, R. D. Camerini-Otero, W. M. Bonner, K. Manova, P. Burgoyne and A. Nussenzweig (2003). "H2AX is required for chromatin remodeling and inactivation of sex chromosomes in male mouse meiosis." Dev Cell **4**(4): 497-508.

- Finkel, J. S., W. Xu, D. Huang, E. M. Hill, J. V. Desai, C. A. Woolford, J. E. Nett, H. Taff, C. T. Norice, D. R. Andes, F. Lanni and A. P. Mitchell (2012). "Portrait of *Candida albicans* adherence regulators." PLoS Pathog **8**(2): e1002525.
- Fisher, M. C., S. J. Gurr, C. A. Cuomo, D. S. Blehert, H. Jin, E. H. Stukenbrock, J. E. Stajich, R. Kahmann, C. Boone, D. W. Denning, N. A. R. Gow, B. S. Klein, J. W. Kronstad, D. C. Sheppard, J. W. Taylor, G. D. Wright, J. Heitman, A. Casadevall and L. E. Cowen (2020). "Threats Posed by the Fungal Kingdom to Humans, Wildlife, and Agriculture." mBio **11**(3).
- Fitzpatrick, D. A., M. E. Logue, J. E. Stajich and G. Butler (2006). "A fungal phylogeny based on 42 complete genomes derived from supertree and combined gene analysis." BMC Evol Biol **6**: 99.
- Flyamer, I. M., J. Gassler, M. Imakaev, H. B. Brandao, S. V. Ulianov, N. Abdennur, S. V. Razin, L. A. Mirny and K. Tachibana-Konwalski (2017). "Single-nucleus Hi-C reveals unique chromatin reorganization at oocyte-to-zygote transition." Nature **544**(7648): 110-114.
- Foltz, D. R., L. E. Jansen, A. O. Bailey, J. R. Yates, 3rd, E. A. Bassett, S. Wood, B. E. Black and D. W. Cleveland (2009). "Centromere-specific assembly of CENP-a nucleosomes is mediated by HJURP." Cell **137**(3): 472-484.
- Fox, E. P., C. K. Bui, J. E. Nett, N. Hartooni, M. C. Mui, D. R. Andes, C. J. Nobile and A. D. Johnson (2015). "An expanded regulatory network temporally controls *Candida albicans* biofilm formation." Mol Microbiol **96**(6): 1226-1239.
- Fox, E. P. and C. J. Nobile (2012). "A sticky situation: untangling the transcriptional network controlling biofilm development in *Candida albicans*." Transcription **3**(6): 315-322.
- Frank, A. C. and K. H. Wolfe (2009). "Evolutionary capture of viral and plasmid DNA by yeast nuclear chromosomes." Eukaryot Cell **8**(10): 1521-1531.
- Frank, D., D. Doenecke and W. Albig (2003). "Differential expression of human replacement and cell cycle dependent H3 histone genes." Gene **312**: 135-143.
- Franklin, S. G. and A. Zweidler (1977). "Non-allelic variants of histones 2a, 2b and 3 in mammals." Nature **266**(5599): 273-275.
- Fretzin, S., B. D. Allan, A. van Daal and S. C. Elgin (1991). "A *Drosophila melanogaster* H3.3 cDNA encodes a histone variant identical with the vertebrate H3.3." Gene **107**(2): 341-342.
- Gamble, M. J., K. M. Frizzell, C. Yang, R. Krishnakumar and W. L. Kraus (2010). "The histone variant macroH2A1 marks repressed autosomal chromatin, but protects a subset of its target genes from silencing." Genes Dev **24**(1): 21-32.
- Ganguly, S. and A. P. Mitchell (2011). "Mucosal biofilms of *Candida albicans*." Curr Opin Microbiol **14**(4): 380-385.
- Gaume, X. and M. E. Torres-Padilla (2015). "Regulation of Reprogramming and Cellular Plasticity through Histone Exchange and Histone Variant Incorporation." Cold Spring Harb Symp Quant Biol **80**: 165-175.
- Gelato, K. A. and W. Fischle (2008). "Role of histone modifications in defining chromatin structure and function." Biol Chem **389**(4): 353-363.
- Goldberg, A. D., L. A. Banaszynski, K. M. Noh, P. W. Lewis, S. J. Elsaesser, S. Stadler, S. Dewell, M. Law, X. Guo, X. Li, D. Wen, A. Chappier, R. C. DeKolver, J. C. Miller, Y. L. Lee, E. A. Boydston, M. C. Holmes, P.

- D. Gregory, J. M. Greally, S. Rafii, C. Yang, P. J. Scambler, D. Garrick, R. J. Gibbons, D. R. Higgs, I. M. Cristea, F. D. Urnov, D. Zheng and C. D. Allis (2010). "Distinct factors control histone variant H3.3 localization at specific genomic regions." *Cell* **140**(5): 678-691.
- Gonzalez-Romero, R., J. Mendez, J. Ausio and J. M. Eirin-Lopez (2008). "Quickly evolving histones, nucleosome stability and chromatin folding: all about histone H2A.Bbd." *Gene* **413**(1-2): 1-7.
- Gow, N. A., A. J. Brown and F. C. Odds (2002). "Fungal morphogenesis and host invasion." *Curr Opin Microbiol* **5**(4): 366-371.
- Granger, B. L. (2012). "Insight into the antiadhesive effect of yeast wall protein 1 of *Candida albicans*." *Eukaryot Cell* **11**(6): 795-805.
- Granger, B. L., M. L. Flenniken, D. A. Davis, A. P. Mitchell and J. E. Cutler (2005). "Yeast wall protein 1 of *Candida albicans*." *Microbiology* **151**(Pt 5): 1631-1644.
- Green, G. R., P. Collas, A. Burrell and D. L. Poccia (1995). "Histone phosphorylation during sea urchin development." *Semin Cell Biol* **6**(4): 219-227.
- Green, G. R. and D. L. Poccia (1989). "Phosphorylation of sea urchin histone CS H2A." *Dev Biol* **134**(2): 413-419.
- Grigoryev, S. A., G. Arya, S. Correll, C. L. Woodcock and T. Schlick (2009). "Evidence for heteromorphic chromatin fibers from analysis of nucleosome interactions." *Proc Natl Acad Sci U S A* **106**(32): 13317-13322.
- Groth, A., A. Corpet, A. J. Cook, D. Roche, J. Bartek, J. Lukas and G. Almouzni (2007). "Regulation of replication fork progression through histone supply and demand." *Science* **318**(5858): 1928-1931.
- Grover, P., J. S. Asa and E. I. Campos (2018). "H3-H4 Histone Chaperone Pathways." *Annu Rev Genet* **52**: 109-130.
- Gulati, M. and C. J. Nobile (2016). "*Candida albicans* biofilms: development, regulation, and molecular mechanisms." *Microbes Infect* **18**(5): 310-321.
- Gurard-Levin, Z. A., J. P. Quivy and G. Almouzni (2014). "Histone chaperones: assisting histone traffic and nucleosome dynamics." *Annu Rev Biochem* **83**: 487-517.
- Gutierrez-Escribano, P., A. Gonzalez-Novo, M. B. Suarez, C. R. Li, Y. Wang, C. R. de Aldana and J. Correa-Bordes (2011). "CDK-dependent phosphorylation of Mob2 is essential for hyphal development in *Candida albicans*." *Mol Biol Cell* **22**(14): 2458-2469.
- Gutierrez-Escribano, P., U. Zeidler, M. B. Suarez, S. Bachellier-Bassi, A. Clemente-Blanco, J. Bonhomme, C. R. Vazquez de Aldana, C. d'Enfert and J. Correa-Bordes (2012). "The NDR/LATS kinase Cbk1 controls the activity of the transcriptional regulator Bcr1 during biofilm formation in *Candida albicans*." *PLoS Pathog* **8**(5): e1002683.
- Hadjur, S., L. M. Williams, N. K. Ryan, B. S. Cobb, T. Sexton, P. Fraser, A. G. Fisher and M. Merkenschlager (2009). "Cohesins form chromosomal cis-interactions at the developmentally regulated IFNG locus." *Nature* **460**(7253): 410-413.
- Hake, S. B. and C. D. Allis (2006). "Histone H3 variants and their potential role in indexing mammalian genomes: the "H3 barcode hypothesis"." *Proc Natl Acad Sci U S A* **103**(17): 6428-6435.

Hake, S. B., B. A. Garcia, E. M. Duncan, M. Kauer, G. Dellaire, J. Shabanowitz, D. P. Bazett-Jones, C. D. Allis and D. F. Hunt (2006). "Expression patterns and post-translational modifications associated with mammalian histone H3 variants." J Biol Chem **281**(1): 559-568.

Hake, S. B., B. A. Garcia, M. Kauer, S. P. Baker, J. Shabanowitz, D. F. Hunt and C. D. Allis (2005). "Serine 31 phosphorylation of histone variant H3.3 is specific to regions bordering centromeres in metaphase chromosomes." Proc Natl Acad Sci U S A **102**(18): 6344-6349.

Hammond, C. M., C. B. Stromme, H. Huang, D. J. Patel and A. Groth (2017). "Histone chaperone networks shaping chromatin function." Nat Rev Mol Cell Biol **18**(3): 141-158.

Han, J., H. Zhou, Z. Li, R. M. Xu and Z. Zhang (2007). "Acetylation of lysine 56 of histone H3 catalyzed by RTT109 and regulated by *ASF1* is required for replisome integrity." J Biol Chem **282**(39): 28587-28596.

Happel, N. and D. Doenecke (2009). "Histone H1 and its isoforms: contribution to chromatin structure and function." Gene **431**(1-2): 1-12.

Hartley, P. D. and H. D. Madhani (2009). "Mechanisms that specify promoter nucleosome location and identity." Cell **137**(3): 445-458.

Harvey Lodish, Arnold Berk, S Lawrence Zipursky, Paul Matsudaira, David Baltimore and J. Darnell. (2000). Molecular Cell Biology.

Hatanaka, Y., K. Inoue, M. Oikawa, S. Kamimura, N. Ogonuki, E. N. Kodama, Y. Ohkawa, Y. Tsukada and A. Ogura (2015). "Histone chaperone CAF-1 mediates repressive histone modifications to protect preimplantation mouse embryos from endogenous retrotransposons." Proc Natl Acad Sci U S A **112**(47): 14641-14646.

Henikoff, S. and M. M. Smith (2015). "Histone variants and epigenetics." Cold Spring Harb Perspect Biol **7**(1): a019364.

Hergeth, S. P. and R. Schneider (2015). "The H1 linker histones: multifunctional proteins beyond the nucleosomal core particle." EMBO Rep **16**(11): 1439-1453.

Hoffmann, G., A. Samel-Pommerencke, J. Weber, A. Cuomo, T. Bonaldi and A. E. Ehrenhofer-Murray (2018). "A role for CENP-A/Cse4 phosphorylation on serine 33 in deposition at the centromere." FEMS Yeast Res **18**(1).

Homann, O. R., J. Dea, S. M. Noble and A. D. Johnson (2009). "A phenotypic profile of the *Candida albicans* regulatory network." PLoS Genet **5**(12): e1000783.

Huang, G., Q. Huang, Y. Wei, Y. Wang and H. Du (2019). "Multiple roles and diverse regulation of the Ras/cAMP/protein kinase A pathway in *Candida albicans*." Mol Microbiol **111**(1): 6-16.

Huang, G., T. Srikantha, N. Sahni, S. Yi and D. R. Soll (2009). "CO(2) regulates white-to-opaque switching in *Candida albicans*." Curr Biol **19**(4): 330-334.

Huang, G., S. Yi, N. Sahni, K. J. Daniels, T. Srikantha and D. R. Soll (2010). "N-acetylglucosamine induces white to opaque switching, a mating prerequisite in *Candida albicans*." PLoS Pathog **6**(3): e1000806.

Hull, C. M., R. M. Raisner and A. D. Johnson (2000). "Evidence for mating of the "asexual" yeast *Candida albicans* in a mammalian host." Science **289**(5477): 307-310.

- Iwase, S., B. Xiang, S. Ghosh, T. Ren, P. W. Lewis, J. C. Cochrane, C. D. Allis, D. J. Picketts, D. J. Patel, H. Li and Y. Shi (2011). "ATRX ADD domain links an atypical histone methylation recognition mechanism to human mental-retardation syndrome." Nat Struct Mol Biol **18**(7): 769-776.
- Izzo, A., K. Kamieniarz and R. Schneider (2008). "The histone H1 family: specific members, specific functions?" Biol Chem **389**(4): 333-343.
- Jansen, L. E., B. E. Black, D. R. Foltz and D. W. Cleveland (2007). "Propagation of centromeric chromatin requires exit from mitosis." J Cell Biol **176**(6): 795-805.
- Jarvis, W. R. (1995). "Epidemiology of nosocomial fungal infections, with emphasis on *Candida* species." Clin Infect Dis **20**(6): 1526-1530.
- Jenull, S., M. Tscherner, M. Gulati, C. J. Nobile, N. Chauhan and K. Kuchler (2017). "The *Candida albicans* HIR histone chaperone regulates the yeast-to-hyphae transition by controlling the sensitivity to morphogenesis signals." Sci Rep **7**(1): 8308.
- Jin, C. and G. Felsenfeld (2007). "Nucleosome stability mediated by histone variants H3.3 and H2A.Z." Genes Dev **21**(12): 1519-1529.
- Johnson, A. (2003). "The biology of mating in *Candida albicans*." Nat Rev Microbiol **1**(2): 106-116.
- Joseph, S. R., M. Palfy, L. Hilbert, M. Kumar, J. Karschau, V. Ziburdaev, A. Shevchenko and N. L. Vastenhouw (2017). "Competition between histone and transcription factor binding regulates the onset of transcription in zebrafish embryos." Elife **6**.
- Kadosh, D. (2017). Morphogenesis in *C. albicans*. Candida albicans: Cellular and Molecular Biology. R. Prasad. Cham, Springer International Publishing: 41-62.
- Kasinsky, H. E., J. D. Lewis, J. B. Dacks and J. Ausio (2001). "Origin of H1 linker histones." FASEB J **15**(1): 34-42.
- Kaufman, P. D., R. Kobayashi, N. Kessler and B. Stillman (1995). "The p150 and p60 subunits of chromatin assembly factor I: a molecular link between newly synthesized histones and DNA replication." Cell **81**(7): 1105-1114.
- Kaufman, P. D., R. Kobayashi and B. Stillman (1997). "Ultraviolet radiation sensitivity and reduction of telomeric silencing in *Saccharomyces cerevisiae* cells lacking chromatin assembly factor-I." Genes Dev **11**(3): 345-357.
- Kawaguchi, Y., H. Honda, J. Taniguchi-Morimura and S. Iwasaki (1989). "The codon CUG is read as serine in an asporogenic yeast *Candida cylindracea*." Nature **341**(6238): 164-166.
- Kelly, M. T., D. M. MacCallum, S. D. Clancy, F. C. Odds, A. J. Brown and G. Butler (2004). "The *Candida albicans* CaACE2 gene affects morphogenesis, adherence and virulence." Mol Microbiol **53**(3): 969-983.
- Kennedy, M. J. and P. A. Volz (1985). "Ecology of *Candida albicans* gut colonization: inhibition of *Candida* adhesion, colonization, and dissemination from the gastrointestinal tract by bacterial antagonism." Infect Immun **49**(3): 654-663.
- Koop, R., L. Di Croce and M. Beato (2003). "Histone H1 enhances synergistic activation of the MMTV promoter in chromatin." EMBO J **22**(3): 588-599.
- Kornberg, R. D. (1974). "Chromatin structure: a repeating unit of histones and DNA." Science **184**(4139): 868-871.

- Kornberg, R. D. and J. O. Thomas (1974). "Chromatin structure; oligomers of the histones." Science **184**(4139): 865-868.
- Krassowski, T., A. Y. Coughlan, X. X. Shen, X. Zhou, J. Kominek, D. A. Opulente, R. Riley, I. V. Grigoriev, N. Maheshwari, D. C. Shields, C. P. Kurtzman, C. T. Hittinger, A. Rokas and K. H. Wolfe (2018). "Evolutionary instability of CUG-Leu in the genetic code of budding yeasts." Nat Commun **9**(1): 1887.
- Krimer, D. B., G. Cheng and A. I. Skoultchi (1993). "Induction of H3.3 replacement histone mRNAs during the precommitment period of murine erythroleukemia cell differentiation." Nucleic Acids Res **21**(12): 2873-2879.
- Kruihof, M., F. T. Chien, A. Routh, C. Logie, D. Rhodes and J. van Noort (2009). "Single-molecule force spectroscopy reveals a highly compliant helical folding for the 30-nm chromatin fiber." Nat Struct Mol Biol **16**(5): 534-540.
- Krysan, D. J., F. S. Sutterwala and M. Wellington (2014). "Catching fire: *Candida albicans*, macrophages, and pyroptosis." PLoS Pathog **10**(6): e1004139.
- Ku, M., J. D. Jaffe, R. P. Koche, E. Rheinbay, M. Endoh, H. Koseki, S. A. Carr and B. E. Bernstein (2012). "H2A.Z landscapes and dual modifications in pluripotent and multipotent stem cells underlie complex genome regulatory functions." Genome Biol **13**(10): R85.
- Kumamoto, C. A. (2002). "Candida biofilms." Curr Opin Microbiol **5**(6): 608-611.
- Kumamoto, C. A. (2005). "A contact-activated kinase signals *Candida albicans* invasive growth and biofilm development." Proc Natl Acad Sci U S A **102**(15): 5576-5581.
- Kumamoto, C. A. (2008). "Molecular mechanisms of mechanosensing and their roles in fungal contact sensing." Nat Rev Microbiol **6**(9): 667-673.
- Kumamoto, C. A. (2011). "Inflammation and gastrointestinal *Candida* colonization." Curr Opin Microbiol **14**(4): 386-391.
- Kustatscher, G., M. Hothorn, C. Pugieux, K. Scheffzek and A. G. Ladurner (2005). "Splicing regulates NAD metabolite binding to histone macroH2A." Nat Struct Mol Biol **12**(7): 624-625.
- Lai, W. K. M. and B. F. Pugh (2017). "Understanding nucleosome dynamics and their links to gene expression and DNA replication." Nat Rev Mol Cell Biol **18**(9): 548-562.
- Lantermann, A. B., T. Straub, A. Stralfors, G. C. Yuan, K. Ekwall and P. Korber (2010). "Schizosaccharomyces pombe genome-wide nucleosome mapping reveals positioning mechanisms distinct from those of *Saccharomyces cerevisiae*." Nat Struct Mol Biol **17**(2): 251-257.
- Laskey, R. A., B. M. Honda, A. D. Mills and J. T. Finch (1978). "Nucleosomes are assembled by an acidic protein which binds histones and transfers them to DNA." Nature **275**(5679): 416-420.
- Leach, T. J., M. Mazzeo, H. L. Chotkowski, J. P. Madigan, M. G. Wotring and R. L. Glaser (2000). "Histone H2A.Z is widely but nonrandomly distributed in chromosomes of *Drosophila melanogaster*." J Biol Chem **275**(30): 23267-23272.
- Lee, C. K., Y. Shibata, B. Rao, B. D. Strahl and J. D. Lieb (2004). "Evidence for nucleosome depletion at active regulatory regions genome-wide." Nat Genet **36**(8): 900-905.
- Lennox, R. W. and L. H. Cohen (1988). "The production of tissue-specific histone complements during development." Biochem Cell Biol **66**(6): 636-649.

- Lewis, P. W., S. J. Elsaesser, K. M. Noh, S. C. Stadler and C. D. Allis (2010). "Daxx is an H3.3-specific histone chaperone and cooperates with ATRX in replication-independent chromatin assembly at telomeres." Proc Natl Acad Sci U S A **107**(32): 14075-14080.
- Lin, C. H., S. Kabrawala, E. P. Fox, C. J. Nobile, A. D. Johnson and R. J. Bennett (2013). "Genetic control of conventional and pheromone-stimulated biofilm formation in *Candida albicans*." PLoS Pathog **9**(4): e1003305.
- Liu, C. P., C. Xiong, M. Wang, Z. Yu, N. Yang, P. Chen, Z. Zhang, G. Li and R. M. Xu (2012). "Structure of the variant histone H3.3-H4 heterodimer in complex with its chaperone DAXX." Nat Struct Mol Biol **19**(12): 1287-1292.
- Liu, W. H., S. C. Roemer, A. M. Port and M. E. Churchill (2012). "CAF-1-induced oligomerization of histones H3/H4 and mutually exclusive interactions with Asf1 guide H3/H4 transitions among histone chaperones and DNA." Nucleic Acids Res **40**(22): 11229-11239.
- Liu, W. H., S. C. Roemer, Y. Zhou, Z. J. Shen, B. K. Dennehey, J. L. Balsbaugh, J. C. Liddle, T. Nemkov, N. G. Ahn, K. C. Hansen, J. K. Tyler and M. E. Churchill (2016). "The Cac1 subunit of histone chaperone CAF-1 organizes CAF-1-H3/H4 architecture and tetramerizes histones." Elife **5**.
- Lo, H. J., J. R. Kohler, B. DiDomenico, D. Loebenberg, A. Cacciapuoti and G. R. Fink (1997). "Nonfilamentous *C. albicans* mutants are avirulent." Cell **90**(5): 939-949.
- Lockhart, S. R., K. J. Daniels, R. Zhao, D. Wessels and D. R. Soll (2003). "Cell biology of mating in *Candida albicans*." Eukaryot Cell **2**(1): 49-61.
- Lohse, M. B., M. Gulati, A. D. Johnson and C. J. Nobile (2018). "Development and regulation of single- and multi-species *Candida albicans* biofilms." Nat Rev Microbiol **16**(1): 19-31.
- Lohse, M. B. and A. D. Johnson (2009). "White-opaque switching in *Candida albicans*." Curr Opin Microbiol **12**(6): 650-654.
- Lohse, M. B. and A. D. Johnson (2016). "Identification and Characterization of Wor4, a New Transcriptional Regulator of White-Opaque Switching." G3 (Bethesda) **6**(3): 721-729.
- Lone, I. N., M. S. Shukla, J. L. Charles Richard, Z. Y. Peshev, S. Dimitrov and D. Angelov (2013). "Binding of NF-kappaB to nucleosomes: effect of translational positioning, nucleosome remodeling and linker histone H1." PLoS Genet **9**(9): e1003830.
- Long, M., X. Sun, W. Shi, A. Yanru, S. T. C. Leung, D. Ding, M. S. Cheema, N. MacPherson, C. J. Nelson, J. Ausio, Y. Yan and T. Ishibashi (2019). "A novel histone H4 variant H4G regulates rDNA transcription in breast cancer." Nucleic Acids Res **47**(16): 8399-8409.
- Lopez-Ribot, J. L., M. Casanova, J. P. Martinez and R. Sentandreu (1991). "Characterization of cell wall proteins of yeast and hydrophobic mycelial cells of *Candida albicans*." Infect Immun **59**(7): 2324-2332.
- Loppin, B., E. Bonnefoy, C. Anselme, A. Laurencon, T. L. Karr and P. Couble (2005). "The histone H3.3 chaperone HIRA is essential for chromatin assembly in the male pronucleus." Nature **437**(7063): 1386-1390.
- Luger, K., M. L. Dechassa and D. J. Tremethick (2012). "New insights into nucleosome and chromatin structure: an ordered state or a disordered affair?" Nat Rev Mol Cell Biol **13**(7): 436-447.

Luger, K., A. W. Mader, R. K. Richmond, D. F. Sargent and T. J. Richmond (1997). "Crystal structure of the nucleosome core particle at 2.8 Å resolution." *Nature* **389**(6648): 251-260.

Malik, H. S. and S. Henikoff (2003). "Phylogenomics of the nucleosome." *Nat Struct Biol* **10**(11): 882-891.

Mannironi, C., W. M. Bonner and C. L. Hatch (1989). "H2A.X, a histone isoprotein with a conserved C-terminal sequence, is encoded by a novel mRNA with both DNA replication type and polyA 3' processing signals." *Nucleic Acids Res* **17**(22): 9113-9126.

Martchenko, M., A. M. Alarco, D. Harcus and M. Whiteway (2004). "Superoxide dismutases in *Candida albicans*: transcriptional regulation and functional characterization of the hyphal-induced SOD5 gene." *Mol Biol Cell* **15**(2): 456-467.

Martire, S., A. A. Gogate, A. Whitmill, A. Tafessu, J. Nguyen, Y. C. Teng, M. Tastemel and L. A. Banaszynski (2019). "Phosphorylation of histone H3.3 at serine 31 promotes p300 activity and enhancer acetylation." *Nat Genet* **51**(6): 941-946.

Marzluff, W. F., P. Gongidi, K. R. Woods, J. Jin and L. J. Maltais (2002). "The human and mouse replication-dependent histone genes." *Genomics* **80**(5): 487-498.

Massey, S. E., G. Moura, P. Beltrao, R. Almeida, J. R. Garey, M. F. Tuite and M. A. Santos (2003). "Comparative evolutionary genomics unveils the molecular mechanism of reassignment of the CTG codon in *Candida* spp." *Genome Res* **13**(4): 544-557.

Mateus, C., S. A. Crow, Jr. and D. G. Ahearn (2004). "Adherence of *Candida albicans* to silicone induces immediate enhanced tolerance to fluconazole." *Antimicrob Agents Chemother* **48**(9): 3358-3366.

Mattiroli, F., S. Bhattacharyya, P. N. Dyer, A. E. White, K. Sandman, B. W. Burkhardt, K. R. Byrne, T. Lee, N. G. Ahn, T. J. Santangelo, J. N. Reeve and K. Luger (2017). "Structure of histone-based chromatin in Archaea." *Science* **357**(6351): 609-612.

Mattiroli, F., S. D'Arcy and K. Luger (2015). "The right place at the right time: chaperoning core histone variants." *EMBO Rep* **16**(11): 1454-1466.

Mayer, F. L., D. Wilson and B. Hube (2013). "*Candida albicans* pathogenicity mechanisms." *Virulence* **4**(2): 119-128.

Maze, I., K. M. Noh, A. A. Soshnev and C. D. Allis (2014). "Every amino acid matters: essential contributions of histone variants to mammalian development and disease." *Nat Rev Genet* **15**(4): 259-271.

McKinley, K. L. and I. M. Cheeseman (2016). "The molecular basis for centromere identity and function." *Nat Rev Mol Cell Biol* **17**(1): 16-29.

McKittrick, E., P. R. Gafken, K. Ahmad and S. Henikoff (2004). "Histone H3.3 is enriched in covalent modifications associated with active chromatin." *Proc Natl Acad Sci U S A* **101**(6): 1525-1530.

Mello, J. A., H. H. Sillje, D. M. Roche, D. B. Kirschner, E. A. Nigg and G. Almouzni (2002). "Human Asf1 and CAF-1 interact and synergize in a repair-coupled nucleosome assembly pathway." *EMBO Rep* **3**(4): 329-334.

Meneghini, M. D., M. Wu and H. D. Madhani (2003). "Conserved histone variant H2A.Z protects euchromatin from the ectopic spread of silent heterochromatin." *Cell* **112**(5): 725-736.

Mermoud, J. E., A. M. Tassin, J. R. Pehrson and N. Brockdorff (2001). "Centrosomal association of histone macroH2A1.2 in embryonic stem cells and somatic cells." *Exp Cell Res* **268**(2): 245-251.

Miller, M. G. and A. D. Johnson (2002). "White-opaque switching in *Candida albicans* is controlled by mating-type locus homeodomain proteins and allows efficient mating." *Cell* **110**(3): 293-302.

Miranda, I., R. Rocha, M. C. Santos, D. D. Mateus, G. R. Moura, L. Carreto and M. A. Santos (2007). "A genetic code alteration is a phenotype diversity generator in the human pathogen *Candida albicans*." *PLoS One* **2**(10): e996.

Miranda, I., A. Silva-Dias, R. Rocha, R. Teixeira-Santos, C. Coelho, T. Goncalves, M. A. Santos, C. Pina-Vaz, N. V. Solis, S. G. Filler and A. G. Rodrigues (2013). "*Candida albicans* CUG mistranslation is a mechanism to create cell surface variation." *MBio* **4**(4).

Mito, Y., J. G. Henikoff and S. Henikoff (2005). "Genome-scale profiling of histone H3.3 replacement patterns." *Nat Genet* **37**(10): 1090-1097.

Mito, Y., J. G. Henikoff and S. Henikoff (2007). "Histone replacement marks the boundaries of cis-regulatory domains." *Science* **315**(5817): 1408-1411.

Monson, E. K., D. de Bruin and V. A. Zakian (1997). "The yeast Cac1 protein is required for the stable inheritance of transcriptionally repressed chromatin at telomeres." *Proc Natl Acad Sci U S A* **94**(24): 13081-13086.

Moura, G. R., J. A. Paredes and M. A. Santos (2010). "Development of the genetic code: insights from a fungal codon reassignment." *FEBS Lett* **584**(2): 334-341.

Moyes, D. L., D. Wilson, J. P. Richardson, S. Mogavero, S. X. Tang, J. Wernecke, S. Hofs, R. L. Gratacap, J. Robbins, M. Runglall, C. Murciano, M. Blagojevic, S. Thavaraj, T. M. Forster, B. Hebecker, L. Kasper, G. Vizcay, S. I. Iancu, N. Kichik, A. Hader, O. Kurzai, T. Luo, T. Kruger, O. Kniemeyer, E. Cota, O. Bader, R. T. Wheeler, T. Gutschmann, B. Hube and J. R. Naglik (2016). "Candidalysin is a fungal peptide toxin critical for mucosal infection." *Nature* **532**(7597): 64-68.

Muhlhausen, S., P. Findeisen, U. Plessmann, H. Urlaub and M. Kollmar (2016). "A novel nuclear genetic code alteration in yeasts and the evolution of codon reassignment in eukaryotes." *Genome Res* **26**(7): 945-955.

Mulhern, S. M., M. E. Logue and G. Butler (2006). "*Candida albicans* transcription factor Ace2 regulates metabolism and is required for filamentation in hypoxic conditions." *Eukaryot Cell* **5**(12): 2001-2013.

Myung, K., V. Pennaneach, E. S. Kats and R. D. Kolodner (2003). "Saccharomyces cerevisiae chromatin-assembly factors that act during DNA replication function in the maintenance of genome stability." *Proc Natl Acad Sci U S A* **100**(11): 6640-6645.

Nagata, T., T. Kato, T. Morita, M. Nozaki, H. Kubota, H. Yagi and A. Matsushiro (1991). "Polyadenylated and 3' processed mRNAs are transcribed from the mouse histone H2A.X gene." *Nucleic Acids Res* **19**(9): 2441-2447.

Naglik, J. R., S. J. Challacombe and B. Hube (2003). "*Candida albicans* secreted aspartyl proteinases in virulence and pathogenesis." *Microbiol Mol Biol Rev* **67**(3): 400-428, table of contents.

Naglik, J. R., D. L. Moyes, B. Wachtler and B. Hube (2011). "*Candida albicans* interactions with epithelial cells and mucosal immunity." *Microbes Infect* **13**(12-13): 963-976.

- Nakatani, Y., D. Ray-Gallet, J. P. Quivy, H. Tagami and G. Almouzni (2004). "Two distinct nucleosome assembly pathways: dependent or independent of DNA synthesis promoted by histone H3.1 and H3.3 complexes." Cold Spring Harb Symp Quant Biol **69**: 273-280.
- Natsume, R., M. Eitoku, Y. Akai, N. Sano, M. Horikoshi and T. Senda (2007). "Structure and function of the histone chaperone CIA/ASF1 complexed with histones H3 and H4." Nature **446**(7133): 338-341.
- Nett, J. E., H. Sanchez, M. T. Cain, K. M. Ross and D. R. Andes (2011). "Interface of *Candida albicans* biofilm matrix-associated drug resistance and cell wall integrity regulation." Eukaryot Cell **10**(12): 1660-1669.
- Ng, R. K. and J. B. Gurdon (2008). "Epigenetic memory of an active gene state depends on histone H3.3 incorporation into chromatin in the absence of transcription." Nat Cell Biol **10**(1): 102-109.
- Nobile, C. J., D. R. Andes, J. E. Nett, F. J. Smith, F. Yue, Q. T. Phan, J. E. Edwards, S. G. Filler and A. P. Mitchell (2006). "Critical role of Bcr1-dependent adhesins in *C. albicans* biofilm formation in vitro and in vivo." PLoS Pathog **2**(7): e63.
- Nobile, C. J., E. P. Fox, J. E. Nett, T. R. Sorrells, Q. M. Mitrovich, A. D. Hernday, B. B. Tuch, D. R. Andes and A. D. Johnson (2012). "A recently evolved transcriptional network controls biofilm development in *Candida albicans*." Cell **148**(1-2): 126-138.
- Nobile, C. J. and A. D. Johnson (2015). "Candida albicans Biofilms and Human Disease." Annu Rev Microbiol **69**: 71-92.
- Nobile, C. J. and A. P. Mitchell (2005). "Regulation of cell-surface genes and biofilm formation by the *C. albicans* transcription factor Bcr1p." Curr Biol **15**(12): 1150-1155.
- Nobile, C. J., J. E. Nett, D. R. Andes and A. P. Mitchell (2006). "Function of *Candida albicans* adhesin Hwp1 in biofilm formation." Eukaryot Cell **5**(10): 1604-1610.
- Nobile, C. J., J. E. Nett, A. D. Hernday, O. R. Homann, J. S. Deneault, A. Nantel, D. R. Andes, A. D. Johnson and A. P. Mitchell (2009). "Biofilm matrix regulation by *Candida albicans* Zap1." PLoS Biol **7**(6): e1000133.
- Nobile, C. J., H. A. Schneider, J. E. Nett, D. C. Sheppard, S. G. Filler, D. R. Andes and A. P. Mitchell (2008). "Complementary adhesin function in *C. albicans* biofilm formation." Curr Biol **18**(14): 1017-1024.
- Noble, S. M., B. A. Gianetti and J. N. Witchley (2017). "Candida albicans cell-type switching and functional plasticity in the mammalian host." Nat Rev Microbiol **15**(2): 96-108.
- Noble, S. M. and A. D. Johnson (2005). "Strains and strategies for large-scale gene deletion studies of the diploid human fungal pathogen *Candida albicans*." Eukaryot Cell **4**(2): 298-309.
- Odds, F. C. (1985). "Morphogenesis in *Candida albicans*." Crit Rev Microbiol **12**(1): 45-93.
- Osakabe, A., H. Tachiwana, T. Matsunaga, T. Shiga, R. S. Nozawa, C. Obuse and H. Kurumizaka (2010). "Nucleosome formation activity of human somatic nuclear autoantigenic sperm protein (sNASP)." J Biol Chem **285**(16): 11913-11921.
- Ouararhni, K., R. Hadj-Slimane, S. Ait-Si-Ali, P. Robin, F. Miettton, A. Harel-Bellan, S. Dimitrov and A. Hamiche (2006). "The histone variant mH2A1.1 interferes with transcription by down-regulating PARP-1 enzymatic activity." Genes Dev **20**(23): 3324-3336.

- Palmer, D. K., K. O'Day and R. L. Margolis (1990). "The centromere specific histone CENP-A is selectively retained in discrete foci in mammalian sperm nuclei." Chromosoma **100**(1): 32-36.
- Palmer, D. K., K. O'Day, H. L. Trong, H. Charbonneau and R. L. Margolis (1991). "Purification of the centromere-specific protein CENP-A and demonstration that it is a distinctive histone." Proc Natl Acad Sci U S A **88**(9): 3734-3738.
- Palmer, D. K., K. O'Day, M. H. Wener, B. S. Andrews and R. L. Margolis (1987). "A 17-kD centromere protein (CENP-A) copurifies with nucleosome core particles and with histones." J Cell Biol **104**(4): 805-815.
- Pande, K., C. Chen and S. M. Noble (2013). "Passage through the mammalian gut triggers a phenotypic switch that promotes *Candida albicans* commensalism." Nat Genet **45**(9): 1088-1091.
- Park, Y. N., K. J. Daniels, C. Pujol, T. Srikantha and D. R. Soll (2013). "Candida albicans forms a specialized "sexual" as well as "pathogenic" biofilm." Eukaryot Cell **12**(8): 1120-1131.
- Parthun, M. R., J. Widom and D. E. Gottschling (1996). "The major cytoplasmic histone acetyltransferase in yeast: links to chromatin replication and histone metabolism." Cell **87**(1): 85-94.
- Pehrson, J. R., C. Costanzi and C. Dharia (1997). "Developmental and tissue expression patterns of histone macroH2A1 subtypes." J Cell Biochem **65**(1): 107-113.
- Pehrson, J. R. and V. A. Fried (1992). "MacroH2A, a core histone containing a large nonhistone region." Science **257**(5075): 1398-1400.
- Phair, R. D., P. Scaffidi, C. Elbi, J. Vecerova, A. Dey, K. Ozato, D. T. Brown, G. Hager, M. Bustin and T. Misteli (2004). "Global nature of dynamic protein-chromatin interactions in vivo: three-dimensional genome scanning and dynamic interaction networks of chromatin proteins." Mol Cell Biol **24**(14): 6393-6402.
- Pierce, C. G., T. Vila, J. A. Romo, D. Montelongo-Jauregui, G. Wall, A. Ramasubramanian and J. L. Lopez-Ribot (2017). "The *Candida albicans* Biofilm Matrix: Composition, Structure and Function." J Fungi (Basel) **3**(1).
- Pina, B. and P. Suau (1987). "Changes in histones H2A and H3 variant composition in differentiating and mature rat brain cortical neurons." Dev Biol **123**(1): 51-58.
- Poveda, A., M. Pamblanco, S. Tafrov, V. Tordera, R. Sternglanz and R. Sendra (2004). "Hif1 is a component of yeast histone acetyltransferase B, a complex mainly localized in the nucleus." J Biol Chem **279**(16): 16033-16043.
- Prelich, G. and F. Winston (1993). "Mutations that suppress the deletion of an upstream activating sequence in yeast: involvement of a protein kinase and histone H3 in repressing transcription in vivo." Genetics **135**(3): 665-676.
- Probst, A. V., E. Dunleavy and G. Almouzni (2009). "Epigenetic inheritance during the cell cycle." Nat Rev Mol Cell Biol **10**(3): 192-206.
- Prochasson, P., L. Florens, S. K. Swanson, M. P. Washburn and J. L. Workman (2005). "The HIR corepressor complex binds to nucleosomes generating a distinct protein/DNA complex resistant to remodeling by SWI/SNF." Genes Dev **19**(21): 2534-2539.

- Quivy, J. P., P. Grandi and G. Almouzni (2001). "Dimerization of the largest subunit of chromatin assembly factor 1: importance in vitro and during *Xenopus* early development." EMBO J **20**(8): 2015-2027.
- Rai, L. S., R. Singha, H. Sanchez, T. Chakraborty, B. Chand, S. Bachellier-Bassi, S. Chowdhury, C. d'Enfert, D. R. Andes and K. Sanyal (2019). "The *Candida albicans* biofilm gene circuit modulated at the chromatin level by a recent molecular histone innovation." PLoS Biol **17**(8): e3000422.
- Ramachandran, S. and S. Henikoff (2015). "Replicating Nucleosomes." Sci Adv **1**(7).
- Ramage, G., S. P. Saville, D. P. Thomas and J. L. Lopez-Ribot (2005). "*Candida* biofilms: an update." Eukaryot Cell **4**(4): 633-638.
- Ramage, G., K. VandeWalle, J. L. Lopez-Ribot and B. L. Wickes (2002). "The filamentation pathway controlled by the Efg1 regulator protein is required for normal biofilm formation and development in *Candida albicans*." FEMS Microbiol Lett **214**(1): 95-100.
- Ramakrishnan, V. (1997). "Histone H1 and chromatin higher-order structure." Crit Rev Eukaryot Gene Expr **7**(3): 215-230.
- Rangasamy, D., I. Greaves and D. J. Tremethick (2004). "RNA interference demonstrates a novel role for H2A.Z in chromosome segregation." Nat Struct Mol Biol **11**(7): 650-655.
- Rasmussen, T. P., M. A. Mastrangelo, A. Eden, J. R. Pehrson and R. Jaenisch (2000). "Dynamic relocalization of histone MacroH2A1 from centrosomes to inactive X chromosomes during X inactivation." J Cell Biol **150**(5): 1189-1198.
- Ray-Gallet, D., J. P. Quivy, C. Scamps, E. M. Martini, M. Lipinski and G. Almouzni (2002). "HIRA is critical for a nucleosome assembly pathway independent of DNA synthesis." Mol Cell **9**(5): 1091-1100.
- Redon, C., D. Pilch, E. Rogakou, O. Sedelnikova, K. Newrock and W. Bonner (2002). "Histone H2A variants H2AX and H2AZ." Curr Opin Genet Dev **12**(2): 162-169.
- Reuss, O., A. Vik, R. Kolter and J. Morschhauser (2004). "The *SAT1* flipper, an optimized tool for gene disruption in *Candida albicans*." Gene **341**: 119-127.
- Rhee, H. S., A. R. Bataille, L. Zhang and B. F. Pugh (2014). "Subnucleosomal structures and nucleosome asymmetry across a genome." Cell **159**(6): 1377-1388.
- Richardson, R. T., I. N. Batova, E. E. Widgren, L. X. Zheng, M. Whitfield, W. F. Marzluff and M. G. O'Rand (2000). "Characterization of the histone H1-binding protein, NASP, as a cell cycle-regulated somatic protein." J Biol Chem **275**(39): 30378-30386.
- Ricketts, M. D., B. Frederick, H. Hoff, Y. Tang, D. C. Schultz, T. Singh Rai, M. Grazia Vizioli, P. D. Adams and R. Marmorstein (2015). "Ubinuclein-1 confers histone H3.3-specific-binding by the HIRA histone chaperone complex." Nat Commun **6**: 7711.
- Ricketts, M. D. and R. Marmorstein (2017). "A Molecular Prospective for HIRA Complex Assembly and H3.3-Specific Histone Chaperone Function." J Mol Biol **429**(13): 1924-1933.
- Riggsby, W. S., L. J. Torres-Bauza, J. W. Wills and T. M. Townes (1982). "DNA content, kinetic complexity, and the ploidy question in *Candida albicans*." Mol Cell Biol **2**(7): 853-862.
- Riley, R., S. Haridas, K. H. Wolfe, M. R. Lopes, C. T. Hittinger, M. Goker, A. A. Salamov, J. H. Wisecaver, T. M. Long, C. H. Calvey, A. L. Aerts, K. W. Barry, C. Choi, A. Clum, A. Y. Coughlan, S. Deshpande, A. P.

- Douglass, S. J. Hanson, H. P. Klenk, K. M. LaButti, A. Lapidus, E. A. Lindquist, A. M. Lipzen, J. P. Meier-Kolthoff, R. A. Ohm, R. P. Otilar, J. L. Pangilinan, Y. Peng, A. Rokas, C. A. Rosa, C. Scheuner, A. A. Sibirny, J. C. Slot, J. B. Stielow, H. Sun, C. P. Kurtzman, M. Blackwell, I. V. Grigoriev and T. W. Jeffries (2016). "Comparative genomics of biotechnologically important yeasts." Proc Natl Acad Sci U S A **113**(35): 9882-9887.
- Ringrose, L. and R. Paro (2007). "Polycomb/Trithorax response elements and epigenetic memory of cell identity." Development **134**(2): 223-232.
- Robbins, N., P. Uppuluri, J. Nett, R. Rajendran, G. Ramage, J. L. Lopez-Ribot, D. Andes and L. E. Cowen (2011). "Hsp90 governs dispersion and drug resistance of fungal biofilms." PLoS Pathog **7**(9): e1002257.
- Robinson, P. J., L. Fairall, V. A. Huynh and D. Rhodes (2006). "EM measurements define the dimensions of the "30-nm" chromatin fiber: evidence for a compact, interdigitated structure." Proc Natl Acad Sci U S A **103**(17): 6506-6511.
- Robinson, P. J. and D. Rhodes (2006). "Structure of the '30 nm' chromatin fibre: a key role for the linker histone." Curr Opin Struct Biol **16**(3): 336-343.
- Rogakou, E. P., D. R. Pilch, A. H. Orr, V. S. Ivanova and W. M. Bonner (1998). "DNA double-stranded breaks induce histone H2AX phosphorylation on serine 139." J Biol Chem **273**(10): 5858-5868.
- Routh, A., S. Sandin and D. Rhodes (2008). "Nucleosome repeat length and linker histone stoichiometry determine chromatin fiber structure." Proc Natl Acad Sci U S A **105**(26): 8872-8877.
- Sakai, A., B. E. Schwartz, S. Goldstein and K. Ahmad (2009). "Transcriptional and Developmental Functions of the H3.3 Histone Variant in Drosophila." Current Biology **19**(21): 1816-1820.
- Santenard, A., C. Ziegler-Birling, M. Koch, L. Tora, A. J. Bannister and M. E. Torres-Padilla (2010). "Heterochromatin formation in the mouse embryo requires critical residues of the histone variant H3.3." Nat Cell Biol **12**(9): 853-862.
- Santos, M. A. and M. F. Tuite (1995). "The CUG codon is decoded in vivo as serine and not leucine in *Candida albicans*." Nucleic Acids Res **23**(9): 1481-1486.
- Saputo, S., A. Kumar and D. J. Krysan (2014). "Efg1 directly regulates ACE2 expression to mediate cross talk between the cAMP/PKA and RAM pathways during *Candida albicans* morphogenesis." Eukaryot Cell **13**(9): 1169-1180.
- Sardi, J. C. O., L. Scorzoni, T. Bernardi, A. M. Fusco-Almeida and M. J. S. Mendes Giannini (2013). "Candida species: current epidemiology, pathogenicity, biofilm formation, natural antifungal products and new therapeutic options." J Med Microbiol **62**(Pt 1): 10-24.
- Satwika, D., R. Klassen and F. Meinhardt (2012). "Repeated capture of a cytoplasmic linear plasmid by the host nucleus in *Debaryomyces hansenii*." Yeast **29**(3-4): 145-154.
- Saunders, A., L. J. Core and J. T. Lis (2006). "Breaking barriers to transcription elongation." Nat Rev Mol Cell Biol **7**(8): 557-567.
- Saville, S. P., A. L. Lazzell, C. Monteagudo and J. L. Lopez-Ribot (2003). "Engineered control of cell morphology in vivo reveals distinct roles for yeast and filamentous forms of *Candida albicans* during infection." Eukaryot Cell **2**(5): 1053-1060.

- Schenk, R., A. Jenke, M. Zilbauer, S. Wirth and J. Postberg (2011). "H3.5 is a novel hominid-specific histone H3 variant that is specifically expressed in the seminiferous tubules of human testes." Chromosoma **120**(3): 275-285.
- Schlissel, M. S. and D. D. Brown (1984). "The transcriptional regulation of *Xenopus* 5s RNA genes in chromatin: the roles of active stable transcription complexes and histone H1." Cell **37**(3): 903-913.
- Schones, D. E., K. Cui, S. Cuddapah, T. Y. Roh, A. Barski, Z. Wang, G. Wei and K. Zhao (2008). "Dynamic regulation of nucleosome positioning in the human genome." Cell **132**(5): 887-898.
- Schwartz, B. E. and K. Ahmad (2005). "Transcriptional activation triggers deposition and removal of the histone variant H3.3." Genes Dev **19**(7): 804-814.
- Schweizer, A., S. Rupp, B. N. Taylor, M. Rollinghoff and K. Schroppel (2000). "The TEA/ATTS transcription factor CaTec1p regulates hyphal development and virulence in *Candida albicans*." Mol Microbiol **38**(3): 435-445.
- Seitan, V. C., A. J. Faure, Y. Zhan, R. P. McCord, B. R. Lajoie, E. Ing-Simmons, B. Lenhard, L. Giorgetti, E. Heard, A. G. Fisher, P. Flicek, J. Dekker and M. Merckenschlager (2013). "Cohesin-based chromatin interactions enable regulated gene expression within preexisting architectural compartments." Genome Res **23**(12): 2066-2077.
- Sengupta, S. and P. G. Higgs (2015). "Pathways of Genetic Code Evolution in Ancient and Modern Organisms." J Mol Evol **80**(5-6): 229-243.
- Sevilla, A. and O. Binda (2014). "Post-translational modifications of the histone variant H2AZ." Stem Cell Res **12**(1): 289-295.
- Shen, X. X., D. A. Opulente, J. Kominek, X. Zhou, J. L. Steenwyk, K. V. Buh, M. A. B. Haase, J. H. Wisecaver, M. Wang, D. T. Doering, J. T. Boudouris, R. M. Schneider, Q. K. Langdon, M. Ohkuma, R. Endoh, M. Takashima, R. I. Manabe, N. Cadez, D. Libkind, C. A. Rosa, J. DeVirgilio, A. B. Hulfachor, M. Groenewald, C. P. Kurtzman, C. T. Hittinger and A. Rokas (2018). "Tempo and Mode of Genome Evolution in the Budding Yeast Subphylum." Cell **175**(6): 1533-1545 e1520.
- Shibahara, K. and B. Stillman (1999). "Replication-dependent marking of DNA by PCNA facilitates CAF-1-coupled inheritance of chromatin." Cell **96**(4): 575-585.
- Sitbon, D., E. Boyarchuk, F. Dingli, D. Loew and G. Almouzni (2020). "Histone variant H3.3 residue S31 is essential for *Xenopus* gastrulation regardless of the deposition pathway." Nat Commun **11**(1): 1256.
- Slutsky, B., M. Staebell, J. Anderson, L. Risen, M. Pfaller and D. R. Soll (1987). ""White-opaque transition": a second high-frequency switching system in *Candida albicans*." J Bacteriol **169**(1): 189-197.
- Smith, S. and B. Stillman (1989). "Purification and characterization of CAF-I, a human cell factor required for chromatin assembly during DNA replication in vitro." Cell **58**(1): 15-25.
- Soll, D. R. and K. J. Daniels (2016). "Plasticity of *Candida albicans* Biofilms." Microbiol Mol Biol Rev **80**(3): 565-595.
- Soll, D. R., B. Morrow and T. Srikantha (1993). "High-frequency phenotypic switching in *Candida albicans*." Trends Genet **9**(2): 61-65.

- Song, Y., S. A. Cheon, K. E. Lee, S. Y. Lee, B. K. Lee, D. B. Oh, H. A. Kang and J. Y. Kim (2008). "Role of the RAM network in cell polarity and hyphal morphogenesis in *Candida albicans*." Mol Biol Cell **19**(12): 5456-5477.
- Song, Y., F. He, G. Xie, X. Guo, Y. Xu, Y. Chen, X. Liang, I. Stagljar, D. Egli, J. Ma and R. Jiao (2007). "CAF-1 is essential for *Drosophila* development and involved in the maintenance of epigenetic memory." Dev Biol **311**(1): 213-222.
- Staab, J. F., S. D. Bradway, P. L. Fidel and P. Sundstrom (1999). "Adhesive and mammalian transglutaminase substrate properties of *Candida albicans* Hwp1." Science **283**(5407): 1535-1538.
- Staib, P. and J. Morschhauser (2007). "Chlamydospore formation in *Candida albicans* and *Candida dubliniensis*--an enigmatic developmental programme." Mycoses **50**(1): 1-12.
- Stevenson, J. S. and H. Liu (2013). "Nucleosome assembly factors *CAF-1* and *HIR* modulate epigenetic switching frequencies in an H3K56 acetylation-associated manner in *Candida albicans*." Eukaryot Cell **12**(4): 591-603.
- Sudbery, P., N. Gow and J. Berman (2004). "The distinct morphogenic states of *Candida albicans*." Trends Microbiol **12**(7): 317-324.
- Sudbery, P. E. (2011). "Growth of *Candida albicans* hyphae." Nat Rev Microbiol **9**(10): 737-748.
- Sullivan, K. F. (2001). "A solid foundation: functional specialization of centromeric chromatin." Curr Opin Genet Dev **11**(2): 182-188.
- Sullivan, K. F., M. Hechenberger and K. Masri (1994). "Human CENP-A contains a histone H3 related histone fold domain that is required for targeting to the centromere." J Cell Biol **127**(3): 581-592.
- Sun, J. N., N. V. Solis, Q. T. Phan, J. S. Bajwa, H. Kashleva, A. Thompson, Y. Liu, A. Dongari-Bagtzoglou, M. Edgerton and S. G. Filler (2010). "Host cell invasion and virulence mediated by *Candida albicans* Ssa1." PLoS Pathog **6**(11): e1001181.
- Sundstrom, P. (2002). "Adhesion in *Candida* spp." Cell Microbiol **4**(8): 461-469.
- Suzuki, T., T. Ueda and K. Watanabe (1997). "The 'polysemous' codon--a codon with multiple amino acid assignment caused by dual specificity of tRNA identity." EMBO J **16**(5): 1122-1134.
- Svaren, J., E. Klebanow, L. Sealy and R. Chalkley (1994). "Analysis of the competition between nucleosome formation and transcription factor binding." J Biol Chem **269**(12): 9335-9344.
- Tachiwana, H., W. Kagawa, A. Osakabe, K. Kawaguchi, T. Shiga, Y. Hayashi-Takanaka, H. Kimura and H. Kurumizaka (2010). "Structural basis of instability of the nucleosome containing a testis-specific histone variant, human H3T." Proc Natl Acad Sci U S A **107**(23): 10454-10459.
- Tagami, H., D. Ray-Gallet, G. Almouzni and Y. Nakatani (2004). "Histone H3.1 and H3.3 complexes mediate nucleosome assembly pathways dependent or independent of DNA synthesis." Cell **116**(1): 51-61.
- Talbert, P. B. and S. Henikoff (2010). "Histone variants--ancient wrap artists of the epigenome." Nat Rev Mol Cell Biol **11**(4): 264-275.
- Talbert, P. B., M. P. Meers and S. Henikoff (2019). "Old cogs, new tricks: the evolution of gene expression in a chromatin context." Nat Rev Genet **20**(5): 283-297.

- Tanaka, T. S., T. Kunath, W. L. Kimber, S. A. Jaradat, C. A. Stagg, M. Usuda, T. Yokota, H. Niwa, J. Rossant and M. S. Ko (2002). "Gene expression profiling of embryo-derived stem cells reveals candidate genes associated with pluripotency and lineage specificity." Genome Res **12**(12): 1921-1928.
- Tao, L., H. Du, G. Guan, Y. Dai, C. J. Nobile, W. Liang, C. Cao, Q. Zhang, J. Zhong and G. Huang (2014). "Discovery of a "white-gray-opaque" tristable phenotypic switching system in *Candida albicans*: roles of non-genetic diversity in host adaptation." PLoS Biol **12**(4): e1001830.
- Terme, J. M., B. Sese, L. Millan-Arino, R. Mayor, J. C. Izpisua Belmonte, M. J. Barrero and A. Jordan (2011). "Histone H1 variants are differentially expressed and incorporated into chromatin during differentiation and reprogramming to pluripotency." J Biol Chem **286**(41): 35347-35357.
- Thatcher, T. H. and M. A. Gorovsky (1994). "Phylogenetic analysis of the core histones H2A, H2B, H3, and H4." Nucleic Acids Res **22**(2): 174-179.
- Timinszky, G., S. Till, P. O. Hassa, M. Hothorn, G. Kustatscher, B. Nijmeijer, J. Colombelli, M. Altmeyer, E. H. Stelzer, K. Scheffzek, M. O. Hottiger and A. G. Ladurner (2009). "A macrodomain-containing histone rearranges chromatin upon sensing PARP1 activation." Nat Struct Mol Biol **16**(9): 923-929.
- Tolstorukov, M. Y., J. A. Goldman, C. Gilbert, V. Ogryzko, R. E. Kingston and P. J. Park (2012). "Histone variant H2A.Bbd is associated with active transcription and mRNA processing in human cells." Mol Cell **47**(4): 596-607.
- Torres-Padilla, M. E., A. J. Bannister, P. J. Hurd, T. Kouzarides and M. Zernicka-Goetz (2006). "Dynamic distribution of the replacement histone variant H3.3 in the mouse oocyte and preimplantation embryos." Int J Dev Biol **50**(5): 455-461.
- Tost, J. (2009). "DNA methylation: an introduction to the biology and the disease-associated changes of a promising biomarker." Methods Mol Biol **507**: 3-20.
- Tronchin, G., M. Pihet, L. M. Lopes-Bezerra and J. P. Bouchara (2008). "Adherence mechanisms in human pathogenic fungi." Med Mycol **46**(8): 749-772.
- Tscherner, M., F. Zwolanek, S. Jenull, F. J. Sedlazeck, A. Petryshyn, I. E. Frohner, J. Mavrianos, N. Chauhan, A. von Haeseler and K. Kuchler (2015). "The *Candida albicans* Histone Acetyltransferase Hat1 Regulates Stress Resistance and Virulence via Distinct Chromatin Assembly Pathways." PLoS Pathog **11**(10): e1005218.
- Tyler, J. K., K. A. Collins, J. Prasad-Sinha, E. Amiot, M. Bulger, P. J. Harte, R. Kobayashi and J. T. Kadonaga (2001). "Interaction between the *Drosophila* CAF-1 and ASF1 chromatin assembly factors." Mol Cell Biol **21**(19): 6574-6584.
- Ueda, J., A. Harada, T. Urahama, S. Machida, K. Maehara, M. Hada, Y. Makino, J. Nogami, N. Horikoshi, A. Osakabe, H. Taguchi, H. Tanaka, H. Tachiwana, T. Yao, M. Yamada, T. Iwamoto, A. Isotani, M. Ikawa, T. Tachibana, Y. Okada, H. Kimura, Y. Ohkawa, H. Kurumizaka and K. Yamagata (2017). "Testis-Specific Histone Variant H3t Gene Is Essential for Entry into Spermatogenesis." Cell Rep **18**(3): 593-600.
- Updike, D. L. and S. E. Mango (2006). "Temporal regulation of foregut development by HTZ-1/H2A.Z and PHA-4/FoxA." PLoS Genet **2**(9): e161.
- Uppuluri, P., A. K. Chaturvedi, A. Srinivasan, M. Banerjee, A. K. Ramasubramaniam, J. R. Kohler, D. Kadosh and J. L. Lopez-Ribot (2010). "Dispersion as an important step in the *Candida albicans* biofilm developmental cycle." PLoS Pathog **6**(3): e1000828.

- Uppuluri, P., C. G. Pierce, D. P. Thomas, S. S. Bubeck, S. P. Saville and J. L. Lopez-Ribot (2010). "The transcriptional regulator Nrg1p controls *Candida albicans* biofilm formation and dispersion." Eukaryot Cell **9**(10): 1531-1537.
- Urahama, T., A. Harada, K. Maehara, N. Horikoshi, K. Sato, Y. Sato, K. Shiraishi, N. Sugino, A. Osakabe, H. Tachiwana, W. Kagawa, H. Kimura, Y. Ohkawa and H. Kurumizaka (2016). "Histone H3.5 forms an unstable nucleosome and accumulates around transcription start sites in human testis." Epigenetics Chromatin **9**: 2.
- van der Heijden, G. W., A. A. Derijck, E. Posfai, M. Giele, P. Pelczar, L. Ramos, D. G. Wansink, J. van der Vlag, A. H. Peters and P. de Boer (2007). "Chromosome-wide nucleosome replacement and H3.3 incorporation during mammalian meiotic sex chromosome inactivation." Nat Genet **39**(2): 251-258.
- Varas, J., J. L. Santos and M. Pradillo (2017). "The Absence of the Arabidopsis Chaperone Complex CAF-1 Produces Mitotic Chromosome Abnormalities and Changes in the Expression Profiles of Genes Involved in DNA Repair." Front Plant Sci **8**: 525.
- Verstrepen, K. J. and F. M. Klis (2006). "Flocculation, adhesion and biofilm formation in yeasts." Mol Microbiol **60**(1): 5-15.
- Vignali, M. and J. L. Workman (1998). "Location and function of linker histones." Nat Struct Biol **5**(12): 1025-1028.
- Vylkova, S., A. J. Carman, H. A. Danhof, J. R. Collette, H. Zhou and M. C. Lorenz (2011). "The fungal pathogen *Candida albicans* autoinduces hyphal morphogenesis by raising extracellular pH." mBio **2**(3): e00055-00011.
- Wachtler, B., D. Wilson, K. Haedicke, F. Dalle and B. Hube (2011). "From attachment to damage: defined genes of *Candida albicans* mediate adhesion, invasion and damage during interaction with oral epithelial cells." PLoS One **6**(2): e17046.
- Wang, Q., F. Gao, W. S. May, Y. Zhang, T. Flagg and X. Deng (2008). "Bcl2 negatively regulates DNA double-strand-break repair through a nonhomologous end-joining pathway." Mol Cell **29**(4): 488-498.
- Weber, C. M. and S. Henikoff (2014). "Histone variants: dynamic punctuation in transcription." Genes Dev **28**(7): 672-682.
- Weig, M., U. Gross and F. Muhlschlegel (1998). "Clinical aspects and pathogenesis of *Candida* infection." Trends Microbiol **6**(12): 468-470.
- Whitehouse, I., O. J. Rando, J. Delrow and T. Tsukiyama (2007). "Chromatin remodelling at promoters suppresses antisense transcription." Nature **450**(7172): 1031-1035.
- Widom, J. (1998). "Chromatin structure: linking structure to function with histone H1." Curr Biol **8**(22): R788-791.
- Wiedemann, S. M., S. N. Mildner, C. Bonisch, L. Israel, A. Maiser, S. Matheisl, T. Straub, R. Merkl, H. Leonhardt, E. Kremmer, L. Schermelleh and S. B. Hake (2010). "Identification and characterization of two novel primate-specific histone H3 variants, H3.X and H3.Y." J Cell Biol **190**(5): 777-791.
- Wilson, D., J. R. Naglik and B. Hube (2016). "The Missing Link between *Candida albicans* Hyphal Morphogenesis and Host Cell Damage." PLoS Pathog **12**(10): e1005867.

- Wirbelauer, C., O. Bell and D. Schubeler (2005). "Variant histone H3.3 is deposited at sites of nucleosomal displacement throughout transcribed genes while active histone modifications show a promoter-proximal bias." Genes Dev **19**(15): 1761-1766.
- Witt, O., W. Albig and D. Doenecke (1996). "Testis-specific expression of a novel human H3 histone gene." Exp Cell Res **229**(2): 301-306.
- Wong, L. H., H. Ren, E. Williams, J. McGhie, S. Ahn, M. Sim, A. Tam, E. Earle, M. A. Anderson, J. Mann and K. H. Choo (2009). "Histone H3.3 incorporation provides a unique and functionally essential telomeric chromatin in embryonic stem cells." Genome Res **19**(3): 404-414.
- Woodcock, C. L. and S. Dimitrov (2001). "Higher-order structure of chromatin and chromosomes." Curr Opin Genet Dev **11**(2): 130-135.
- Woodcock, C. L., A. I. Skoultchi and Y. Fan (2006). "Role of linker histone in chromatin structure and function: H1 stoichiometry and nucleosome repeat length." Chromosome Res **14**(1): 17-25.
- Wu, J. I., J. Lessard and G. R. Crabtree (2009). "Understanding the words of chromatin regulation." Cell **136**(2): 200-206.
- Wu, R. S., S. Tsai and W. M. Bonner (1982). "Patterns of histone variant synthesis can distinguish G0 from G1 cells." Cell **31**(2 Pt 1): 367-374.
- Xia, W. and J. Jiao (2017). "Histone variant H3.3 orchestrates neural stem cell differentiation in the developing brain." Cell Death Differ **24**(9): 1548-1563.
- Xie, Z., A. Thompson, T. Sobue, H. Kashleva, H. Xu, J. Vasilakos and A. Dongari-Bagtzoglou (2012). "Candida albicans biofilms do not trigger reactive oxygen species and evade neutrophil killing." J Infect Dis **206**(12): 1936-1945.
- Yi, S., N. Sahni, K. J. Daniels, K. L. Lu, T. Srikantha, G. Huang, A. M. Garnaas and D. R. Soll (2011). "Alternative mating type configurations (a/alpha versus a/a or alpha/alpha) of Candida albicans result in alternative biofilms regulated by different pathways." PLoS Biol **9**(8): e1001117.
- Yuen, K. C., B. D. Slaughter and J. L. Gerton (2017). "Condensin II is anchored by TFIIC and H3K4me3 in the mammalian genome and supports the expression of active dense gene clusters." Sci Adv **3**(6): e1700191.
- Zakikhany, K., J. R. Naglik, A. Schmidt-Westhausen, G. Holland, M. Schaller and B. Hube (2007). "In vivo transcript profiling of *Candida albicans* identifies a gene essential for interepithelial dissemination." Cell Microbiol **9**(12): 2938-2954.
- Zalensky, A. O., J. S. Siino, A. A. Gineitis, I. A. Zalenskaya, N. V. Tomilin, P. Yau and E. M. Bradbury (2002). "Human testis/sperm-specific histone H2B (hTSH2B). Molecular cloning and characterization." J Biol Chem **277**(45): 43474-43480.
- Zeitlin, S. G., C. M. Barber, C. D. Allis and K. F. Sullivan (2001). "Differential regulation of CENP-A and histone H3 phosphorylation in G2/M." J Cell Sci **114**(Pt 4): 653-661.
- Zhu, Z., H. Wang, Q. Shang, Y. Jiang, Y. Cao and Y. Chai (2013). "Time course analysis of *Candida albicans* metabolites during biofilm development." J Proteome Res **12**(6): 2375-2385.
- Zlatanova, J., S. H. Leuba and K. van Holde (1998). "Chromatin fiber structure: morphology, molecular determinants, structural transitions." Biophys J **74**(5): 2554-2566.

Zofall, M., T. Fischer, K. Zhang, M. Zhou, B. Cui, T. D. Veenstra and S. I. Grewal (2009). "Histone H2A.Z cooperates with RNAi and heterochromatin factors to suppress antisense RNAs." Nature **461**(7262): 419-422.

List of publications

1. A Surprising Role for the Sch9 Protein Kinase in Chromosome Segregation in *Candida albicans* (2015) Neha Varshney, Alida Schaekel, **Rima Singha**, Tanmoy Chakraborty, Lasse van Wijlick, Joachim F. Ernst and Kaustuv Sanyal. vol. 199 no. 3 671-674.
2. Epigenetic determinants of phenotypic plasticity in *Candida albicans* (2018) Laxmi Shanker Rai, **Rima Singha**, Priya Brahma, Kaustuv Sanyal vol. 32, Issue 1 10-19.
3. The *Candida albicans* biofilm gene circuit modulated at the chromatin level by a recent molecular histone innovation (2019) Laxmi Shanker Rai, **Rima Singha**, Hiram Sanchez, Tanmoy Chakraborty, Bipin Chand, Sophie Bachellier-Bassi, Shantanu Chowdhury, Christophe d'Enfert, David R. Andes, Kaustuv Sanyal [10.1371/journal.pbio.3000422](https://doi.org/10.1371/journal.pbio.3000422)

A Surprising Role for the Sch9 Protein Kinase in Chromosome Segregation in *Candida albicans*

Neha Varshney,^{*,1} Alida Schaekel,^{†,‡,1} Rima Singha,^{*} Tanmoy Chakraborty,^{*,2} Lasse van Wijlick,^{†,‡} Joachim F. Ernst,^{†,‡,3} and Kaustuv Sanyal^{*,3}

^{*}Molecular Mycology Laboratory, Jawaharlal Nehru Centre for Advanced Scientific Research, Jakkur, Bangalore 560064, India, and

[†]Department Biologie, Molekulare Mykologie and [‡]Manchot Graduate School Molecules of Infection, Heinrich-Heine-Universität, Düsseldorf 40225, Germany

ORCID ID: 0000-0002-6611-4073 (K.S).

ABSTRACT The AGC kinase Sch9 regulates filamentation in *Candida albicans*. Here, we show that Sch9 binding is most enriched at the centromeres in *C. albicans*, but not in *Saccharomyces cerevisiae*. Deletion of CaSch9 leads to a 150- to 750-fold increase in chromosome loss. Thus, we report a previously unknown role of Sch9 in chromosome segregation.

KEYWORDS kinase, Sch9, centromere, chromosome segregation, kinetochore

TARGET of rapamycin complex 1 (TORC1) is a major regulator of cell growth and a nutrient sensor in all eukaryotic cells. In the pathogenic yeast *Candida albicans*, the AGC kinase Sch9, one of the direct downstream targets of TORC1, represses filamentation in hypoxia and under high CO₂ conditions. Sch9 performs distinct functions in growth and morphogenesis depending on the availability of O₂ and CO₂ (Stichternoth *et al.* 2011). Earlier studies indicated that absence of Sch9 increases the chronological life span of *Saccharomyces cerevisiae* (Fabrizio *et al.* 2001). However, *sch9* mutant cells of *C. albicans* have a reduced longevity only under normoxic conditions and not under hypoxic conditions (Stichternoth *et al.* 2011).

In this study, we sought to determine the genomic binding sites of the HA-tagged Sch9 protein by ChIP on chip (ChIP-chip) experiments under normoxia as well as hypoxia with and

without elevated CO₂ levels in *C. albicans*. Remarkably, the major binding peaks of Sch9 coincided with the centromere (*CEN*) regions. Centromeric Sch9 binding was observed under normoxia (Figure 1A) as well as under hypoxia with or without 6% CO₂ (Figure 1B). Under all conditions, a few reproducible Sch9 binding peaks occurred outside the *CEN* regions as well (not shown). The ChIP-chip data were validated by semiquantitative (data not shown) and quantitative PCR (qPCR) analysis using *CEN5*- and *CEN7*-specific primers (Figure 1C).

Enrichment of Sch9 binding at *CEN* regions led us to examine its possible role in the stability of the kinetochore, a multiprotein complex formed on the *CEN* DNA. The centromere–kinetochore complex plays a central role in the microtubule–kinetochore-mediated process of chromosome segregation. First, we analyzed the nuclear morphology in wild-type (CAI4) and mutant cells (CAS1 and CCS3) (strain construction, Southern confirmation, and genotype of strains are described in the Supporting Information, File S1, Figure S1 and Table S1, respectively). Except for a marginal increase in proportion of large-budded cells (at G2/M stage) with the unsegregated nucleus in the *sch9* mutant cells (CAS1 and CCS3) as compared to the wild type (CAI4), no significant difference was evident (Figure S2). A marginal increase observed in the proportion of large-budded mutant cells having an unsegregated nuclear mass as compared to wild type is insignificant, since the wild-type cells also showed unsegregated DNA mass, as expected, during the pre-anaphase stage of the cell cycle. Moreover, a significant delay in G1 in the *sch9* mutant added to the complexity of analysis. Like *S. cerevisiae*, centromeres are clustered

Copyright © 2015 by the Genetics Society of America
doi: 10.1534/genetics.114.173542

Manuscript received December 11, 2014; accepted for publication January 6, 2015; published Early Online January 15, 2015.

Supporting information is available online at <http://www.genetics.org/lookup/suppl/doi:10.1534/genetics.114.173542/-/DC1>.

ChIP-chip data have been deposited at http://www.candidagenome.org/download/systematic_results/Chakraborty_2014/.

¹These authors contributed equally to this work.

²Present address: Department of Microbiology, University of Szeged, Ko'ze'pfasor, Szeged, Hungary 672.

³Corresponding authors: Department Biologie, Molekulare Mykologie, Heinrich-Heine-Universität Düsseldorf, Universitätsstr. 1/Geb. 26.12, 40225 Düsseldorf, Germany. E-mail: joachim.ernst@uni-duesseldorf.de; Molecular Mycology Laboratory, Molecular Biology and Genetics Unit, Jawaharlal Nehru Centre for Advanced Scientific Research, Jakkur, Bangalore 560064, India. E-mail: sanyal@jncasr.ac.in

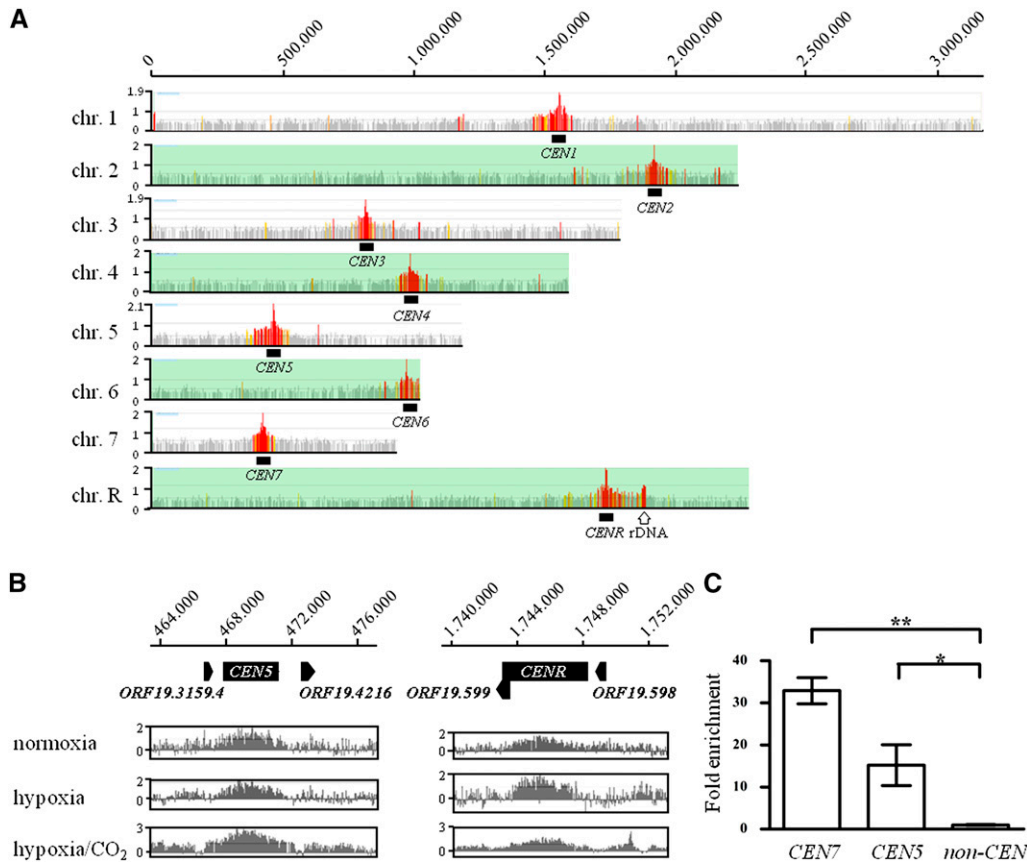


Figure 1 Genomic localization of the Sch9 kinase. The ChIP-chip procedure was carried out essentially as described previously (Lassak *et al.* 2011; Schaeckel *et al.* 2013). *C. albicans* genomic tiling microarrays (NimbleGen) were probed pair-wise by immunoprecipitated chromatin of a strain expressing HA-tagged Sch9 (AF1006) and the corresponding control strain (CAS1). Two independent cultures were assayed for each combination of strains. (A) An overview of Sch9 binding. Significant binding peaks were calculated by the NimbleScan software (NimbleGen) and color-coded according to their FDR values in red [false discovery rate (FDR) ≤ 0.05], orange (FDR ≤ 0.1), yellow (FDR 0.1–0.2), and gray (FDR > 0.2). Significant Sch9-binding peaks were detected at centromeres by genomic ChIP-chip on all *C. albicans* chromosomes. In addition, a significant peak occurred at the rDNA locus (open arrow). (B) Examples for centromeric binding of Sch9 at *CEN5* and *CEN7*. Scaled log₂ ratios of cells grown in normoxia and hypoxia with or without 6% CO₂ are shown. Note that Sch9 enrichment was obtained for cells grown under normoxia or hypoxia conditions. (C) Enrichment at *CEN7*, *CEN5*, and the noncentromeric region was analyzed using qPCR. qPCR analysis reveals the mean fold enrichment of Sch9 at the centromeres obtained in two independent ChIP experiments (\pm SD) relative to the no-tag control and normalized to the input samples. The calculation was done with two biological replicates (two ChIP samples), and each measurement was performed in triplicate. Significant difference was observed in Sch9 recruitment at the *CEN5* and *CEN7* region ($P < 0.05$) and ($P < 0.01$), respectively (shown by asterisks).

throughout the cell cycle in *C. albicans* (Roy *et al.* 2011; Sanyal and Carbon 2002; Thakur and Sanyal 2012). Depletion of an essential kinetochore protein leads to centromere declustering and delocalization of the centromere-specific histone Cse4 in *C. albicans* (Thakur and Sanyal 2012). However, we found neither centromere declustering nor any significant change in the centromeric histone Cse4 levels at the kinetochore (Cse4-GFP intensity) in wild-type (strain 8675) and *sch9* mutant (strain 8675T) strains (Figure 2A). To further investigate the role of Sch9 in Cse4 localization at the centromeres, we performed Cse4-ChIP assays with wild-type (J200) and mutant cells (J200T). We analyzed enrichment of Cse4 at *CEN5* and *CEN7* regions both by semiquantitative (Figure S3) and qPCR (Figure 2B) (primer sequences are listed in Table S2). Cse4 binding was found to be similar at the centromeres in the presence or absence of Sch9. Thus, Sch9 does not seem to play a direct role in Cse4-mediated kinetochore integrity in *C. albicans*.

Many kinetochore proteins play crucial but nonessential roles in the process of chromosome segregation (Sanyal *et al.* 1998; Ortiz *et al.* 1999; Poddar *et al.* 1999; Ghosh *et al.* 2001; Measday *et al.* 2002). The centromeric localization of Sch9 prompted us to examine whether Sch9 plays a role in high-fidelity chromosome segregation. One or both of the alleles of *SCH9* were deleted from the diploid genome of the *C. albicans*

wild-type strain RM1000AH, which was previously used to study chromosome loss (Sanyal *et al.* 2004). Each homolog of chromosome 7 is marked by the auxotrophic marker *HIS1* or *ARG4* in RM1000AH (Figure 3A). The strains were confirmed by Southern blot analysis (Figure S1). We previously reported that the natural rate of loss of a chromosome in wild-type *C. albicans* (SN148) is $< 5 \times 10^{-4}$ /cell/generation (Mitra *et al.* 2014). Two independent null (*sch9/sch9*) mutant strains (RMKS2A and RMKS2B) exhibited a 150- to 750-fold increase in chromosome loss as compared to the spontaneous rate of loss of a chromosome (Figure 3B). Even heterozygous (*SCH9/sch9*) mutants of *SCH9* (RMKS1A and RMKS1B) exhibited chromosome loss at a rate higher than the wild type (Figure 3B). This high rate of chromosome loss is comparable to the loss rate exhibited by several *S. cerevisiae* kinetochore mutants. The role of Sch9 in chromosome segregation was further validated by re-integrating the *SCH9* ORF, including its native promoter and terminator sequences at the *RPS10* locus. While the chromosome loss was completely suppressed in re-integrants (RMKS1AR and RMKS1BR) generated in the *SCH9/sch9* mutant background (RMKS1A and RMKS1B), a reduced rate of loss was observed in re-integrants (RMKS2AR and RMKS2BR) in the *sch9/sch9* null mutant background (RMKS2A and RMKS2B) (Figure 3C). While this assay measures the loss of

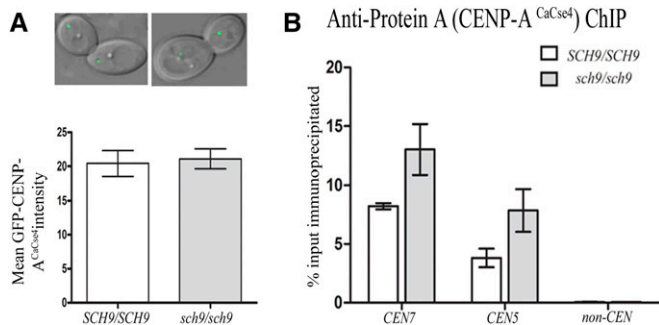


Figure 2 Sch9 is not required for Cse4-mediated kinetochore stability. (A) Microscopy images showing Cse4-GFP signal intensities in wild-type 8675 (*CSE4-GFP/CSE4;SCH9/SCH9*) and mutant 8675T (*CSE4-GFP/CSE4;sch9/sch9*). *C. albicans* wild-type and mutant strains where *CSE4* is GFP-tagged were grown overnight at 30° under normoxic conditions in YPDU (1% yeast extract, 2% peptone, 2% dextrose supplemented with 10mg/100ml uridine) and washed with water, and images were taken using a confocal laser-scanning microscope (LSM 510 META, Carl Zeiss). The brightest GFP signal in each cell was determined using the Image J software as described before (Roy *et al.* 2011). Briefly, an equal area from each cell was selected. The average pixel intensity was measured and corrected for the background by subtracting the lowest pixel intensity value in the field from the average. Then the mean GFP intensity was measured using the Image J software and the graph was plotted using Graph Pad Prism. Measurement was taken from 45 cells in each case. The experiment was performed twice. Standard error of mean (t-test) was used to calculate statistical significance ($P < 0.05$). For strain construction (see Supporting Information). (B) Cse4 localization at the centromere is not affected by absence of Sch9. Standard ChIP assays were performed on strains CAKS102 (*CSE4-TAP/CSE4;SCH9/SCH9*) and J200T (*CSE4-TAP/Cse4;sch9/sch9*) (grown at 30° under normoxic conditions) using anti-Protein A antibodies. Enrichment at *CEN7*, *CEN5*, and the noncentromeric region was analyzed by qPCR. PCR using total DNA (T) or ChIP DNA fractions with (+) or without (-) antibodies was performed. qPCR analysis revealed the enrichment of Cse4 at the centromere as a percentage of the total chromatin input, and values were plotted as mean of triplicates \pm SD. No significant difference was observed in CaCse4 recruitment at the *CEN5* and *CEN7* region ($P > 0.05$). Percentage input was calculated as $100 \times 2^{\Delta[\text{adjusted input} - \text{Ct(IP)}]}$ (Mukhopadhyay *et al.* 2008).

heterozygosity, the loss of an unlinked single nucleotide polymorphism (SNP) on chromosome 7 along with the loss of a marker gene on the same chromosome could determine the loss of the entire chromosome. We observed that SNPs on chromosome 7 in the strains used in this study are absent, as compared to another *C. albicans* strain reported previously (Forche *et al.* 2009). However, binding of Sch9 to all centromeres combined with a higher rate of loss of the marker gene by the homozygous and heterozygous mutants led us to conclude that absence of Sch9 indeed increases the rate of chromosome loss. This confirms the critical role of Sch9 in the high-fidelity process of chromosome segregation.

To verify if centromere DNA binding of the Sch9 kinase also occurs in other yeast species outside the *Candida*-specific CTG clade, we carried out a genome-wide ChIP-chip experiment to localize HA-tagged ScSch9 (Pascual-Ahuir and Proft 2007) in *S. cerevisiae*. No detectable binding of ScSch9 to any centromere region was found. However, as in *C. albicans*, the ribosomal DNA (rDNA) locus showed significant ScSch9 binding in *S. cerevisiae* (data not shown). We conclude that Sch9

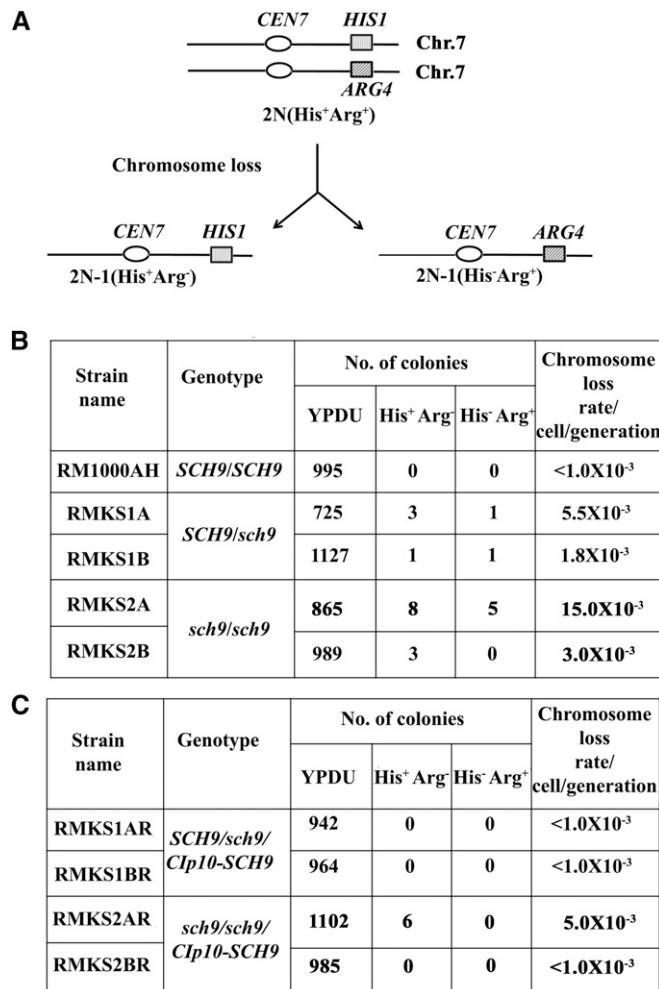


Figure 3 Chromosome loss assay. (A) Schematic of chromosome loss assay. (B and C) The chromosome loss assay was performed with two independent transformants of both mutants and revertants, as described before (Sanyal *et al.* 2004). The numbers indicate the summation of colonies patched in independent experiments. Briefly, the strains were grown for ~20 generations on YPDU medium at 30° under normoxic conditions. Subsequently, ~1000 cells were plated on YPDU agar plates for each transformant and incubated at 30° for 2 days. The single colonies were patched on YPDU, SD minimal medium (SD) without arginine (CM-arg), and SD without histidine (CM-his). The chromosome loss rate was calculated by the number of colonies that were unable to grow on selective media divided by the total number of colonies grown on nonselective media.

binding to centromeres is not a general feature among Hemiascomycetes fungi and may have arisen specifically in *C. albicans*, a member of the CTG clade, while binding to rDNA remained conserved. It would be tempting to speculate that the association of Sch9 with centromeres might have arisen specifically in the CTG clade. Nevertheless, Sch9 is important for growth in both *S. cerevisiae* and *C. albicans* (Pascual-Ahuir and Proft 2007; Stichternoth *et al.* 2011).

Rapid fungal growth requires effective biosynthetic, metabolic, and regulatory activities of cells. Nutrient abundance is signaled by the Tor1 pathway via the Sch9 AGC kinase. Thus, the remarkable strong binding of Sch9 to centromeres could be related to effective chromosomal replication. Incidentally,

deletion of a centromere-proximal replication origin leads to a moderate increase in chromosome loss (Mitra *et al.* 2014). In addition, phospho-regulation of kinetochore proteins by kinases (such as Aurora B kinase/polo-like kinase 1) has been shown to be critical for proper chromosome segregation (Shang *et al.* 2003; McKinley and Cheeseman 2014). Unlike short 125-bp, genetically determined, sequence-specific point centromeres of *S. cerevisiae*, *C. albicans* chromosomes contain unique sequence-independent epigenetically specified regional centromeres (Sanyal *et al.* 2004; Baum *et al.* 2006; Thakur and Sanyal 2013). While the targets of this AGC kinase Sch9 are largely unknown, centromere binding of this protein selectively in *C. albicans* but not in *S. cerevisiae* provides new insights of functional evolution of a protein in organisms having different types of centromeres.

Acknowledgments

This work was supported by a grant from the Department of Biotechnology, Government of India, and intramural funding from the Jawaharlal Nehru Centre for Advanced Scientific Research (to K.S.) and by grants from the Jürgen Manchot Stiftung Düsseldorf (to A.S. and L.v.W.) and the ERA-NET PathoGenoMics project OXYstress (to J.F.E.). N.V. and R.S. are supported by fellowships from the Council of Scientific and Industrial Research and University Grants Commission (Government of India), respectively.

Literature Cited

- Baum, M., K. Sanyal, P. K. Mishra, N. Thaler, and J. Carbon, 2006 Formation of functional centromeric chromatin is specified epigenetically in *Candida albicans*. *Proc. Natl. Acad. Sci. USA* 103: 14877–14882.
- Fabrizio, P., F. Pozza, S. D. Pletcher, C. M. Gendron, and V. D. Longo, 2001 Regulation of longevity and stress resistance by Sch9 in yeast. *Science* 292: 288–290.
- Forche, A., M. Steinbach, and J. Berman, 2009 Efficient and rapid identification of *Candida albicans* allelic status using SNP-RFLP. *FEMS Yeast Res.* 9: 1061–1069.
- Ghosh, S. K., A. Poddar, S. Hajra, K. Sanyal, and P. Sinha, 2001 The IML3/MCM19 gene of *Saccharomyces cerevisiae* is required for a kinetochore-related process during chromosome segregation. *Mol. Genet. Genomics* 265: 249–257.
- Lassak, T., E. Schneider, M. Bussmann, D. Kurtz, J. R. Manak *et al.*, 2011 Target specificity of the *Candida albicans* Efg1 regulator. *Mol. Microbiol.* 82: 602–618.
- McKinley, K. L., and I. M. Cheeseman, 2014 Polo-like kinase 1 licenses CENP-A deposition at centromeres. *Cell* 158: 397–411.

- Measday, V., D. W. Hailey, I. Pot, S. A. Givan, K. M. Hyland *et al.*, 2002 Ctf3p, the Mis6 budding yeast homolog, interacts with Mcm22p and Mcm16p at the yeast outer kinetochore. *Genes Dev.* 16: 101–113.
- Mitra, S., J. Gomez-Raja, G. Larriba, D. D. Dubey, and K. Sanyal, 2014 Rad51-Rad52 mediated maintenance of centromeric chromatin in *Candida albicans*. *PLoS Genet.* 10: e1004344.
- Mukhopadhyay, A., B. Deplancke, A. J. Walhout, and H. A. Tissenbaum, 2008 Chromatin immunoprecipitation (ChIP) coupled to detection by quantitative real-time PCR to study transcription factor binding to DNA in *Caenorhabditis elegans*. *Nat. Protoc.* 3: 698–709.
- Ortiz, J., O. Stemmann, S. Rank, and J. Lechner, 1999 A putative protein complex consisting of Ctf19, Mcm21, and Okp1 represents a missing link in the budding yeast kinetochore. *Genes Dev.* 13: 1140–1155.
- Pascual-Ahuir, A., and M. Proft, 2007 Control of stress-regulated gene expression and longevity by the Sch9 protein kinase. *Cell Cycle* 6: 2445–2447.
- Poddar, A., N. Roy, and P. Sinha, 1999 MCM21 and MCM22, two novel genes of the yeast *Saccharomyces cerevisiae* are required for chromosome transmission. *Mol. Microbiol.* 31: 349–360.
- Roy, B., L. S. Burrack, M. A. Lone, J. Berman, and K. Sanyal, 2011 CaMtw1, a member of the evolutionarily conserved Mis12 kinetochore protein family, is required for efficient inner kinetochore assembly in the pathogenic yeast *Candida albicans*. *Mol. Microbiol.* 80: 14–32.
- Sanyal, K., and J. Carbon, 2002 The CENP-A homolog CaCse4p in the pathogenic yeast *Candida albicans* is a centromere protein essential for chromosome transmission. *Proc. Natl. Acad. Sci. USA* 99: 12969–12974.
- Sanyal, K., S. K. Ghosh, and P. Sinha, 1998 The MCM16 gene of the yeast *Saccharomyces cerevisiae* is required for chromosome segregation. *Mol. Gen. Genet.* 260: 242–250.
- Sanyal, K., M. Baum, and J. Carbon, 2004 Centromeric DNA sequences in the pathogenic yeast *Candida albicans* are all different and unique. *Proc. Natl. Acad. Sci. USA* 101: 11374–11379.
- Schaekel, A., P. R. Desai, and J. F. Ernst, 2013 Morphogenesis-regulated localization of protein kinase A to genomic sites in *Candida albicans*. *BMC Genomics* 14: 842.
- Shang, C., T. R. Hazbun, I. M. Cheeseman, J. Aranda, S. Fields *et al.*, 2003 Kinetochore protein interactions and their regulation by the Aurora kinase Ipl1p. *Mol. Biol. Cell* 14: 3342–3355.
- Stichernoth, C., A. Fraund, E. Setiadi, L. Giasson, A. Vecchiarelli *et al.*, 2011 Sch9 kinase integrates hypoxia and CO₂ sensing to suppress hyphal morphogenesis in *Candida albicans*. *Eukaryot. Cell* 10: 502–511.
- Thakur, J., and K. Sanyal, 2012 A coordinated interdependent protein circuitry stabilizes the kinetochore ensemble to protect CENP-A in the human pathogenic yeast *Candida albicans*. *PLoS Genet.* 8: e1002661.
- Thakur, J., and K. Sanyal, 2013 Efficient neocentromere formation is suppressed by gene conversion to maintain centromere function at native physical chromosomal loci in *Candida albicans*. *Genome Res.* 23: 638–652.

Communicating editor: A. P. Mitchell

GENETICS

Supporting Information

<http://www.genetics.org/lookup/suppl/doi:10.1534/genetics.114.173542/-/DC1>

A Surprising Role for the Sch9 Protein Kinase in Chromosome Segregation in *Candida albicans*

Neha Varshney, Alida Schaekel, Rima Singha, Tanmoy Chakraborty, Lasse van Wijlick,
Joachim F. Ernst, and Kaustuv Sanyal

File S1

Strain construction

C. albicans strain AF1006 producing C-terminally HA-tagged Sch9 was constructed by transformation of heterozygous strain CAS2 by a tagging cassette generated by oligonucleotides Sch9-HA for/rev, as described (SCHAEKEL *et al.* 2013). Correct chromosomal integration was verified by colony PCR using primers Sch9ver and 3' test HA-tag. Both alleles of *SCH9* were deleted in *C. albicans* strain RM1000AH (SANYAL *et al.* 2004) and 8675 (JOGLEKAR *et al.* 2008) using the URA blaster method. The construction of the URA blaster deletion cassette for *SCH9* was described previously (STICHTERNOOTH *et al.* 2011). After the deletion of the first copy, the heterozygous strains were grown on 5-FOA plate to make the cells auxotroph for *URA3* to obtain RMKS1A, RMKS1B and 8675t. Then the same cassette was again used to disrupt the second allele of the gene, to get strains RMKS2A, RMKS2B and 8675T, respectively. To obtain the re-integrant of Sch9 in heterozygous and homozygous mutant background, the entire ORF along with its promoter and terminator was cloned in *KpnI* and *SalI* sites in Clp10 integration vector (MURAD *et al.* 2000). Sch9 orf was re-integrated at *RPS10* locus in the *Candida* genome using *StuI* to obtain RMKS1AR, RMKS1BR, RMKS2AR and RMKS2BR. The correct chromosomal integration of Clp10 was verified by PCR using primers UP-RPS10 and NV207. To check the binding pattern of CENP-A across the centromere in *sch9* mutant by ChIP, one copy of CENP-A was tagged with Prot A using plasmid construct pCaCse4TAPNAT (THAKUR and SANYAL 2013). pCaCse4-TAP-NAT was partially digested with *XhoI* and transformed into RMKS2A to get Prot A tagged CENP-A strain.

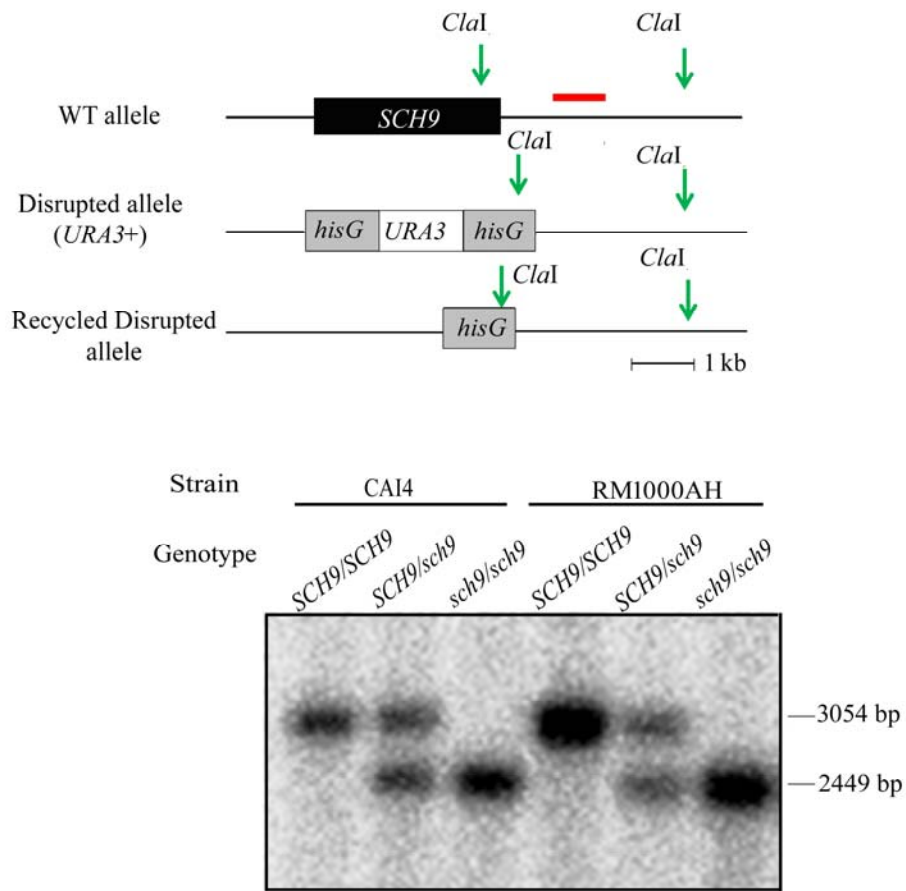


Figure S1 Southern blot analysis. Line diagrams showing wild-type and disrupted alleles of *SCH9*. *Cla*I digested DNA from wild-type strains (CAI4, RM1000AH) and corresponding heterozygous and null mutant strains lacking one or both copies of *SCH9* gene was separated on an agarose gel, blotted and probed with a region marked by the red line. Green arrows indicate *Cla*I sites. Bar, 1 kb.





	Percentage of cells with indicated morphology				Total no. of cells counted
					
CAI4	61.1	24.7	0.4	13.8	247
CAS1	69.1	24.7	0.7	6	133
CCS3	79.2	10.9	1.2	3.6	164

Figure S2 *C. albicans* wild-type (*SCH9/SCH9*), heterozygous (*SCH9/sch9*) and homozygous null mutant (*sch9/sch9*) strains were grown till $OD_{600} \sim 1$ at 30° in normoxic condition in YPDU and were stained with DAPI. A table showing percentages of cells with indicated morphologies of DAPI-stained nuclei.

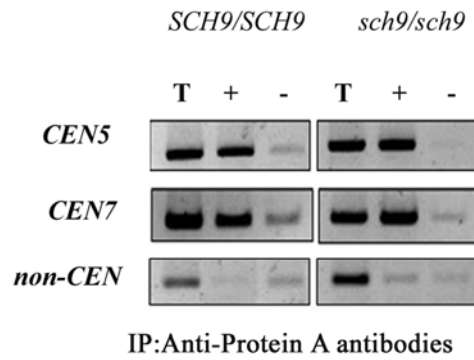


Figure S3 Cse4 localisation at the centromere is not affected by absence of Sch9. Standard ChIP assays were performed on strains CAKS102 (*CSE4-TAP/CSE4;SCH9/SCH9*) and J200T (*CSE4-TAP/Cse4; sch9/sch9*) (grown at 30°) using anti-Protein A (Cse4) antibodies. Enrichment at *CEN7*, *CEN5* and non-centromeric region was analysed using semi- quantitative PCR. PCR using total DNA (T) or ChIP DNA fractions with (+) or without (-) antibodies was performed.

Table S1 Strains used in this study

Name	Parent	Genotype	Reference
CAI4	SC5314	<i>ura3::imm434/ura3::imm434</i>	Fonzi <i>et al</i> 1993
CAS1	CAI4	as CAI4 but <i>SCH9/sch9::hisG-URA3-hisG</i>	Stichernoth <i>et al</i> , 2011
CAS2	CAS1	as CAI4 but <i>SCH9/sch9::hisG</i>	Stichernoth <i>et al</i> , 2011
CCS3	CAS2	as CAI4 but <i>sch9::hisG/sch9::hisG URA3/ura3::imm434</i>	Stichernoth <i>et al</i> , 2011
AF1006	CAS2	as CAS2 but <i>SCH9::(3xHA-URA3)/sch9::hisG</i>	This study
RM1000AH	RM1000	<i>Δura3::imm434/Δura3::imm434Δhis1::hisG/ Δhis1::hisG arg4::HIS1/ARG4</i>	Sanyal <i>et al</i> , 2004
RMKS1A	RM1000AH	<i>Δura3::imm434/ Δura3::imm434 Δhis1::hisG/ Δhis1::hisG arg4::HIS1/ARG4 sch9::hisG/SCH9</i>	This study
RMKS1B	RM1000AH	<i>Δura3::imm434/ Δura3::imm434 Δhis1::hisG/ Δhis1::hisG arg4::HIS1/ARG4 sch9::hisG/SCH9</i>	This study
RMKS2A	RMKS1A	<i>Δura3::imm434/ Δura3::imm434 Δhis1::hisG/ Δhis1::hisG arg4::HIS1/ARG4 sch9::hisG/sch9::hisG- URA3-hisG</i>	This study
RMKS2B	RMKS1B	<i>Δura3::imm434/ Δura3::imm434 Δhis1::hisG/ Δhis1::hisG arg4::HIS1/ARG4 sch9::hisG/sch9::hisG- URA3-hisG</i>	This study
RMKS1AR	RMKS1A	<i>Δura3::imm434/ Δura3::imm434 Δhis1::hisG/ Δhis1::hisG arg4::HIS1/ARG4 sch9::hisG/SCH9/Cip10-SCH9</i>	This study
RMKS1BR	RMKS1B	<i>Δura3::imm434/ Δura3::imm434 Δhis1::hisG/ Δhis1::hisG arg4::HIS1/ARG4 sch9::hisG/SCH9/ Cip10-SCH9</i>	This study
RMKS2AR	RMKS2A	<i>Δura3::imm434/ Δura3::imm434 Δhis1::hisG/ Δhis1::hisG arg4::HIS1/ARG4 sch9::hisG/sch9::hisG- URA3-hisG/ Cip10-SCH9</i>	This study
RMKS2BR	RMKS2B	<i>Δura3::imm434/ Δura3::imm434 Δhis1::hisG/ Δhis1::hisG arg4::HIS1/ARG4 sch9::hisG/sch9::hisG- URA3-hisG/ Cip10-SCH9</i>	This study
8675	BWP17	<i>Δ ura3::λimm434/ Δ ura3::imm434 Δhis1::hisG/Δhis1::hisGΔarg4::hisG/arg4::hisG CSE4/CSE4::GFP::CSE4</i>	Joglekaret <i>et al</i> , 2008

8675t	8675	<i>Δ ura3::λimm434/Δura3::imm434</i> <i>Δhis1::hisG/Δhis1::hisGΔarg4::hisG/Δarg4:: hisG</i> <i>CSE4/CSE4:GFP:CSE4 sch9::hisG/SCH9</i>	This study
8675T	8675t	<i>Δ ura3::λimm434/Δura3::imm434</i> <i>Δhis1::hisG/Δhis1::hisGΔarg4::hisG/Δarg4:: hisG</i> <i>CSE4/CSE4:GFP:CSE4 sch9::hisG/sch9::hisG-URA3-</i> <i>hisG</i>	This study
CAKS102	SN148	<i>Δura3::imm434/Δura3::imm434,</i> <i>Δhis1::hisG/Δhis1::hisG, Δarg4::hisG/Δarg4::hisG,</i> <i>Δleu2::hisG/Δleu2::hisG CSE4/CSE4-TAP(URA3)</i>	Mitra <i>et al</i> , 2014
J200	RM1000AH	<i>Δura3::imm434/ Δura3::imm434 Δhis1::hisG/</i> <i>Δhis1::hisG arg4::HIS1/ARG4 CSE4/CSE4TAP-NAT</i>	Thakur <i>et al</i> , 2013
J200T	J200	<i>ura3::imm434/ ura3::imm434 his1::hisG/his1::hisG</i> <i>arg4::HIS1/ARG4 sch9::hisG/sch9::hisG-URA3-hisG</i> <i>CSE4::CSE4-TAP-NAT</i>	This study

Table S2 Primers used in this study

Primer name	Sequence	Description
2498-21	CTG GTG CAA GAC CCT CAT AGA AGC	Semi-quantitative ChIP PCR primers for CEN7
2498-22	CCT GAC ACT GTC GTT TCC CAT AGC	Semi-quantitative ChIP PCR primers for CEN7
CEN5e	TGTTCTGACATACTGGGTAGACTTT	Semi-quantitative ChIP PCR primers for CEN5
CEN5f	CGAAGCATTTTGTATAACAGCCC	Semi-quantitative ChIP PCR primers for CEN5
CACH5R1	TTCATGGAAGAGGGGTTTCA	qPCR primers for CEN5
CACH5F1	CCCGCAAATAAGCAAACACT	qPCR primers for CEN5
NCEN7-3	GCATACCTGACACTGTCGTT	qPCR primers for CEN7
NCEN7-4	AACGGTGCTACGTTTTTTTA	qPCR primers for CEN7
Ctrl 7 a	ACTCGCCTTCCCCTCCTTAAATAG	qPCR and semi-quantitative ChIP PCR primers for non centromeric region
Ctrl 7 b	CCACTACTACGACTGTGGATCACT	qPCR and semi-quantitative ChIP PCR primers for non centromeric region
Sch9-HA for	GAAGAAGAAGATGAAATGGAAGTTGATGAAGAT CAACATATGGATGATGAATTTGTCAATGGAAGAT TTGATCTTGGTGGTGGTCCGGATCCCCGGGTTAAT TAA	HA tagging
Sch9-HA rev	GCACAAAATGGAGAAGGAGAAAAAGTAGGAAC GGAATTCTATTGAATGGAACAGTTTAGTTCTAGA AGGACCACCTTTGATTG	HA tagging
Sch9ver	GTTGATTCTGGTCATTAGG	Tagging verification primers
3' test HA-tag	CATCGTATGGGTAAAAGATG	Tagging verification primers
NV195	AGTGGTACCGGTGCGATGTATAACTTCATTTTCAT	Clp10 cloning forward
NV196	ACGCGTCGAGCAC AGA CAT TGG GCA AGA AA	Clp10 cloning reverse
UP-RPS10	TTCTGGTGTCTCTCACTGTTAAGC	Clp10 integration confirmation forward
NV207	GAGTTATTAGCCCTGCGATCTTTG	Clp10 integration confirmation reverse

Literature Cited

- JOGLEKAR, A. P., D. BOUCK, K. FINLEY, X. LIU, Y. WAN *et al.*, 2008 Molecular architecture of the kinetochore-microtubule attachment site is conserved between point and regional centromeres. *J Cell Biol* **181**: 587-594.
- MURAD, A. M., P. R. LEE, I. D. BROADBENT, C. J. BARELLE and A. J. BROWN, 2000 Clp10, an efficient and convenient integrating vector for *Candida albicans*. *Yeast* **16**: 325-327.
- SANYAL, K., M. BAUM and J. CARBON, 2004 Centromeric DNA sequences in the pathogenic yeast *Candida albicans* are all different and unique. *Proc Natl Acad Sci U S A* **101**: 11374-11379.
- SCHAEKEL, A., P. R. DESAI and J. F. ERNST, 2013 Morphogenesis-regulated localization of protein kinase A to genomic sites in *Candida albicans*. *BMC Genomics* **14**: 842.
- STICHTERNOOTH, C., A. FRAUND, E. SETIADI, L. GIASSON, A. VECCHIARELLI *et al.*, 2011 Sch9 kinase integrates hypoxia and CO₂ sensing to suppress hyphal morphogenesis in *Candida albicans*. *Eukaryot Cell* **10**: 502-511.
- THAKUR, J., and K. SANYAL, 2013 Efficient neocentromere formation is suppressed by gene conversion to maintain centromere function at native physical chromosomal loci in *Candida albicans*. *Genome Res* **23**: 638-652.



British Mycological
Society promoting fungal science

journal homepage: www.elsevier.com/locate/fbr



Review

Epigenetic determinants of phenotypic plasticity in *Candida albicans*

Laxmi Shanker RAI, Rima SINGHA, Priya BRAHMA, Kaustuv SANYAL*

Molecular Mycology Laboratory, Molecular Biology and Genetics Unit, Jawaharlal Nehru Centre for Advanced Scientific Research, Jakkur, Bangalore 560 064, India

ARTICLE INFO

Article history:

Received 29 April 2017
Received in revised form
20 July 2017
Accepted 24 July 2017

Keywords:

Biofilm
Chromatin
Filamentation
Histones
Opaque
Post-translational modifications

Abbreviations:

PTMs
post-translational modifications
KATs
histone acetyl transferases
KDACs
histone deacetylases
SAPs
secreted aspartyl proteases

ABSTRACT

Epigenetics literally means heritable changes in gene expression without any modification in the DNA sequence. The field of epigenetics is revolutionising our understanding of basic fundamental principles behind the normal development and the diseased state of an individual. However, chromatin modifications during infection, wherein the pathogen interacts with its host, received comparatively little attention. Nevertheless, the role of epigenetics in the establishment of infectious diseases by breaching the host defense system is an emerging area of research. Epigenetic regulation impacts differentiation and expression of virulence attributes of a pathogen. For example, antigenic variations in parasites such as *Giardia lamblia* and *Plasmodium falciparum* are epigenetically determined. Similarly, chromatin modifying elements have been implicated in fungal morphogenesis and virulence. In particular, chromatin modifying enzymes including histone methyl transferases (KMTs), histone acetyl transferases (KATs), and histone deacetylases (KDACs) have been shown to epigenetically modulate pathogenicity of the human opportunistic pathogen *Candida albicans*. The significance of chromatin modifications has the potential for explaining the mechanistic basis for distinct lifestyles of the fungus. In this review, we summarize the existing body of evidence that emphasizes the importance of various chromatin modulations involved in providing phenotypic plasticity of the medically important fungal pathogen *C. albicans*.

© 2017 British Mycological Society. Published by Elsevier Ltd. All rights reserved.

* Corresponding author. Fax: +91 80 2208 2766.

E-mail address: sanyal@jncasr.ac.in (K. Sanyal).
<http://dx.doi.org/10.1016/j.fbr.2017.07.002>

1749-4613/© 2017 British Mycological Society. Published by Elsevier Ltd. All rights reserved.

1. Biology of the human pathogenic fungus, *Candida albicans*

C. albicans is an obligate parasite with no known environmental reservoir (Russell and Lay 1973). It survives as a commensal in the oral cavity, gastrointestinal tract, and genital regions of approximately 70% healthy individuals (Drell et al. 2013; Findley et al. 2013; Hoffmann et al. 2013; Soll 2002). However, commensal colonization could transit into the pathogenic form if hosts develop immunodeficiency, epithelial damage or microbial dysbiosis (Perlroth et al. 2007). The conversion can also occur due to the use of broad spectrum antibiotics, intravenous catheters, and implanted medical devices (Edmond et al. 1999; Fidel 2006; Hobson 2003; Klein et al. 1984; Odds 1994; Weig et al. 1998). Therefore, it is important to understand the mechanism that determines the lifestyle choice of *C. albicans* that exists either as a commensal or a pathogen. *C. albicans*, like many other fungal species, shows phenotypic plasticity in response to specific environmental cues (Lo et al. 1997; Soll 2002). Depending on the host niche, it exhibits various morphological forms and each form is associated with a unique pattern of gene expression (Kumamoto 2008). The important morphological states in this fungus are yeast, pseudohyphae, hyphae, opaque, chlamydospores, gastrointestinally induced transition (GUT) and gray phenotype (Berman and Sudbery 2002; Miller and Johnson 2002; Pande et al. 2013; Slutsky et al. 1987; Sudbery et al. 2004; Tao et al. 2014).

One of the important phenotypic transitions is the switch between the budding yeast and filamentous form (pseudohyphae or hyphae). The yeast-hyphae switch has been extensively studied due to its close association with pathogenicity (Jacobsen et al. 2012). While the yeast cells are primarily viewed as commensals (Noble et al. 2016), the hyphal development is well orchestrated with the expression of adhesins (Hwp1, Als3 and Als10 etc.), tissue degrading enzymes (secreted aspartyl proteases or SAPs) and antioxidant defence proteins (superoxide dismutase) involved in virulence properties (Carlisle et al. 2009; Nantel et al. 2002). However, cells that are trapped either as yeast or filamentous form are defective in the blood stream infection model. This suggests that transition between these two morphological states is required for virulence (Braun and Johnson 1997; Lo et al. 1997). Moreover, yeast cells are essentially suited for dissemination in the tissues (Saville et al. 2003) whereas hyphal cells are required for tissue invasion and penetration (Filler and Sheppard 2006; Thompson et al. 2011). White-opaque switching is another well characterized morphological transition in *C. albicans* (Slutsky et al. 1987). White cells are round and form smooth hemispherical colonies whereas opaque cells are elongated and form flat and gray colonies (Anderson and Soll 1987). White and opaque phenotypes are heritable and show differential gene expression profiles, mating behaviours, preference of niches in the host and interactions with the host immune system (Anderson and Soll 1987; Donlan and Costerton 2002; Miller and Johnson 2002). The 'master switch gene' controlling this transition is *WOR1* (Huang et al. 2006; Srikantha et al. 2006; Zordan et al. 2006), the deletion of which blocks the transition from white to opaque (Zordan et al. 2006).

Establishment of a successful infection in diverse host niches requires a wide range of virulence factors and fitness attributes. One of the most challenging virulence aspects is the development of a three-dimensional community from yeast cells to biofilms on implanted medical devices. Other factors include, expression of adhesins and invasins, thigmotaxis, and, secretion of hydrolytic enzymes (Gow et al. 2002; Hube 1996; Lo et al. 1997; Mayer et al. 2013; Nicholls et al. 2011; Odds 1994). The fungus also possesses other fitness attributes such as rapid adaptation to fluctuations in environmental pH, metabolic flexibility, nutrient acquisition system, and robust stress response machinery, in order to adapt better inside the host niche (Mayer et al. 2013; Nicholls et al. 2011).

The basic structure of chromatin primarily consists of DNA and histones. Histones are positively charged low molecular weight evolutionary conserved proteins. Core histone proteins namely, H2A, H2B, H3 and H4, package and organize DNA into nucleosomes, the fundamental units of chromatin (Richmond and Davey 2003; van Holde 1988). The chromatin structure inside the nucleus is dynamically regulated by various chromatin modifiers in order to carry out important cellular functions (Gelato and Fischle 2008; Probst et al. 2009; Tost 2009; Wu et al. 2009). Hence, any modification at the chromatin level modulates transcription at a global scale.

The relationship between the state of chromatin and the expression of virulence related genes have been established in eukaryotic pathogens like protozoan parasites and fungal pathogens (Bougourd et al. 2009; Croken et al. 2012; Dixon et al. 2010; Hakimi and Deitsch 2007; Rai et al. 2012). Chromatin modifiers including histone modifying enzymes, such as Rtt109, are also shown to be involved in virulence and have been recognized as antifungal targets in *C. albicans* (Wurtele et al. 2010). Thus, chromatin modifiers could be viewed as potential key players in fungal pathogenicity. While KATs and KDACs have been extensively studied and several reviews have highlighted their importance with respect to pathogenicity of *C. albicans* (Garnaud et al. 2016; Kuchler et al. 2016), other chromatin modifiers remain largely unexplored. Here, we summarize the repertoire of known chromatin modifying elements and their role in phenotypic plasticity of *C. albicans* (Table 1).

2. Role of epigenetic elements in phenotypic plasticity of *C. albicans*

Epigenetic regulation in gene expression can be mediated by a variety of factors including DNA methylation, post-translational modifications (PTMs) of histones, incorporation of histone variants, chromatin-remodellers, and non-coding RNAs (ncRNAs) (Bonisch et al. 2008). An excellent example of epigenetic regulation is the development of a multicellular organism, from a single-celled zygote that differentiates into various tissue types via specific gene expression profiling. These epigenetic marks are essential for defining and maintaining the cellular memory (Egger et al. 2004; Turner 2002).

Phenotypic plasticity is a hallmark feature of many fungal species including *C. albicans*, promoting adaptation inside the host. Therefore, rapid and profound alterations in genome-wide expression profiles occur when *C. albicans* transits from

Table 1 – Chromatin modifying elements characterized in *C. albicans* and their functions.

Effectors	Gene	Function	Mutant phenotype	References
KATs	RTT109	Responsible for H3K56ac, DNA repair and genome integrity	Reduced white to opaque switching and compromised virulence	Wurtele et al., 2010; Stevenson and Liu, 2011
	GCN5	Role in invasive and filamentous growth	Attenuated virulence	Pukkila-Worley et al., 2009; Sellam et al., 2009
	ESA1	Responsible for H4K5ac and H4K12ac, hyphal growth	Sensitive to thermal, genotoxic and oxidative stress	Wang et al., 2013
	SAS2	Responsible for H4K16ac, H4K5ac and H4K12ac at higher temperature	Hyper-filamentation at low temperature	Wang et al., 2013
	HAT1/HAT2	Role in filamentation and white-opaque transitions	Constitutive pseudohyphae and susceptibility to caspofungin. Lack of HAT1 or HAT2 increases the frequency of white-opaque	Tscherner et al. 2012
KDAGs	SIR2	NAD-dependent histone deacetylase	Variable colony morphology and high frequency of phenotypic switching	Perez-Martin et al. 1999
	HDA1	Role in histone deacetylation specific to H3K14	Defective in hyphal growth and show enhanced frequency of white-opaque	Srikantha et al. 2001; Hnisz et al., 2010
	RDP3	Role in white-opaque transition	Increase in white-opaque switching in both directions	Srikantha et al., 2001
	HOS2	Role in white-opaque transition	Reduced frequency of white-opaque	Hnisz et al., 2010
	SET3	The Set3/Hos2 complex regulates filamentous growth and dispersion during biofilm development	Reduced white-opaque transition	Hnisz et al., 2010
KMTs	HST3	Histone H3K56 deacetylase	Inviable	Wurtele et al., 2010
	SET1	Responsible for H3K4me	Hyper-filamentation in embedded conditions, and defective in adherence to epithelial cells	Raman et al., 2006
Chromatin remodellers	SWI1/SNF2	Role in virulence	Compromised hyphal growth and virulence	Mao et al., 2006
Histone chaperones	CAF1/HIR	Chromatin assembly factors	CAC2 (a subunit of Caf1) mutants show increase in switching frequencies of white-opaque in both directions	Stevenson and Liu, 2011, 2013
Histone variants	HTA3 (H2A.Z)	Differentially enriched at the WOR1 promoters in white and opaque cells	Mutant not available	Guan and Liu, 2015

a commensal to a pathogen in response to the host environment. The extent and significance of epigenetic modulations in *C. albicans* and its interaction with host is yet to be fully explored. In the following sections, we provide a comprehensive view of chromatin modifying elements identified till date, essential for regulating phenotypic plasticity in *C. albicans*.

3. Yeast-hyphal filament transition

C. albicans lives a distinct parasitic lifestyle that enables this fungus to switch between a harmless commensal and a life-threatening pathogen in the same host environment. Among the reported phenotypic transitions in *C. albicans*, the ability to switch between yeast, hyphae and pseudohyphae has been extensively investigated. These transitions are dependent on a variety of environmental cues including host factors.

The hyphal growth is characterized by the differential expression of several hundred genes encoding cell wall proteins, adhesins and SAPs (Brown 2002). The growing body of evidences indicates the involvement of both genetic and chromatin modifying elements in mediating the yeast-hyphae transition. Multiple signalling pathways are known to regulate hyphal development, including transcription factors that act

as either activators or repressors of hyphal specific genes. Two well characterized signalling pathways are the Cph1 mediated mitogen activated protein kinase (MAPK) cascade (Kohler and Fink 1996) and the transcription factor Efg1-mediated (Cao et al. 2006) cyclic-AMP (cAMP) dependent protein kinase A (PKA) signalling. Other significant pathways include the two component histidine kinase, cyclin-dependent kinase as well as states specific pathways such as pH (Rim 101 mediated) (Davis et al. 2000) and the pathway mediated through transcription factors Cph2, Tec1 and Czf1 (Liu 2001). Additionally, hyphal-specific gene expression is negatively regulated by a complex consisting of the general transcriptional corepressor Tup1, in association with the transcriptional repressor Nrg1 (Braun and Johnson 1997; Kadosh and Johnson 2005; Murad et al. 2001). Mutants of these two repressors constitutively grow as pseudohyphae, and expression of hyphae specific genes is de-repressed. Although several transcription factors and the genes associated with yeast-hyphae transition are known but the molecular mechanism of gene regulation at the chromatin level remains unclear. Recent studies indicate involvement of chromatin modulating elements including DNA methylation, histone modifications, and chromatin remodellers during yeast-hyphal transition.

Among various chromatin modifying elements, PTMs of histones are the most extensively studied in *C. albicans*. The known histone modifications in this fungus are histone acetylation and deacetylation which are brought about by KATs and KDACs respectively. The fungus-specific histone acetyl transferase, Rtt109, involved in acetylation of H3K56 is required for *C. albicans* virulence and, *rtt109* mutants show constitutive filamentation (Lopes da Rosa et al. 2010; Wurtele et al. 2010). Gcn5, another known histone modulating enzyme, has been reported as a component of the transcription activator complex such as Spt-Ada-Gcn5 acetyl transferase (SAGA/ADA) (Brownell et al. 1996). Ada2 is a subunit of this complex, *ada2* mutants exhibits a reduction in H3K9ac, show increased sensitivity to oxidative stress, and were defective in response to filamentation stimulus (Pukkila-Worley et al.

2009; Sellam et al. 2009). Further validation was obtained from the assays performed on murine models of systemic infections, wherein the *gcn5* mutants were found to be avirulent (Chang et al. 2015). In addition, the pathogen harbours the MOZ-Ybf2-Sas2-Tip60 (MYST) family of KATs, where Esa1 and Sas2 are the most characterized proteins. Esa1 primarily acetylates H4K5 and H4K12 while Sas2 acetylates H4K16 and also H4K5 and H4K12, although at a higher temperature (Wang et al. 2013). Esa1 is required for filamentous growth. In contrast, *sas2* mutants are hyper-filamentous at low temperatures (Wang et al. 2013). These results illustrate how acetylation marks bring about differential regulation in the yeast-filamentation transition in *C. albicans*.

KDACs are a class of modifying enzymes involved in the removal of acetylation marks on histones. In *C. albicans*, one

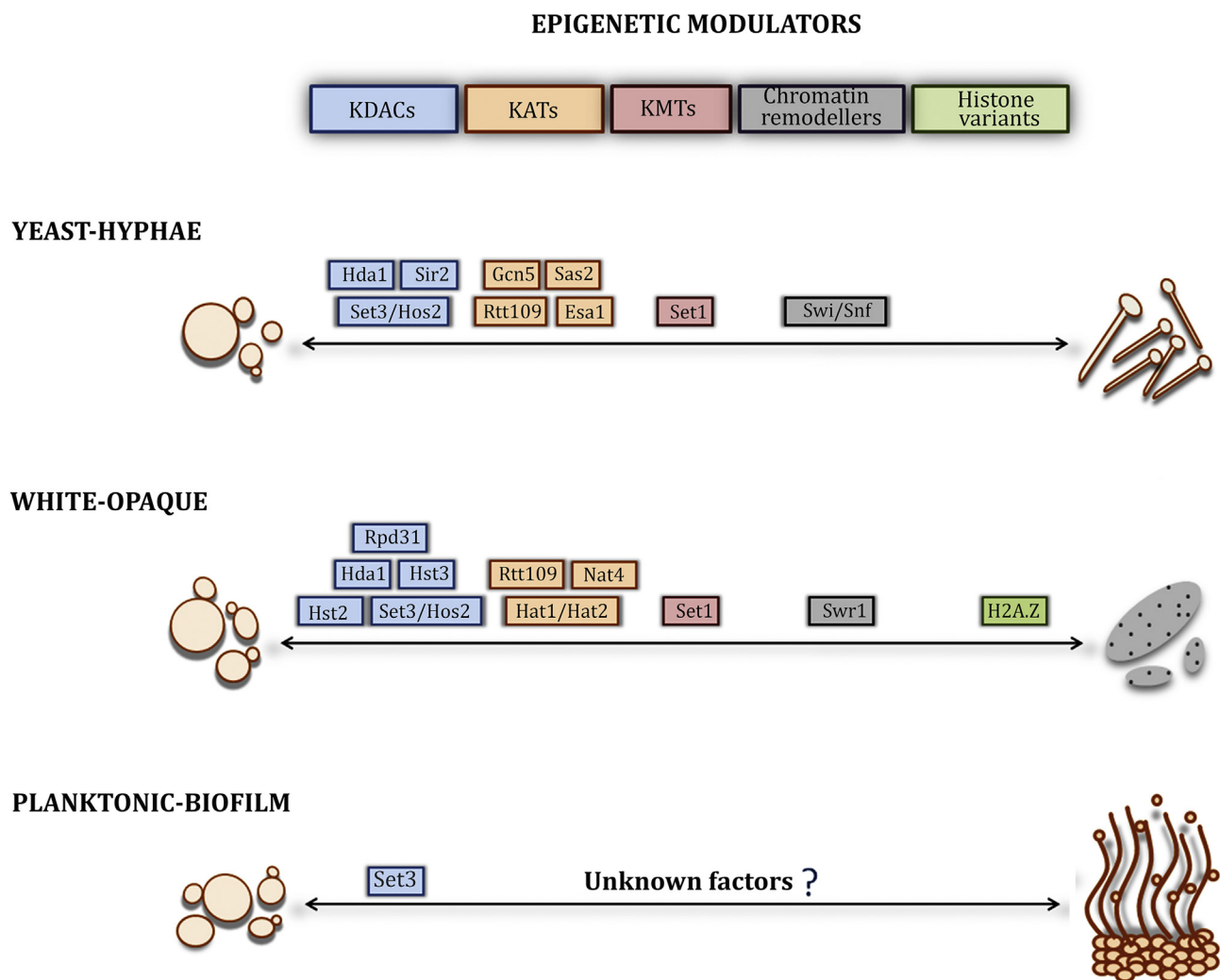


Fig. 1 – Schematic of chromatin modifying elements affecting phenotypic transitions in *C. albicans*. Transcriptional regulation of phenotypic plasticity has been well explored in *C. albicans*. However, the effect of chromatin modifications in regulating gene expression pattern remains less understood. Changes in the epigenetic elements like, DNA methylation, PTMs of histones, and histone variant incorporation modify the chromatin landscape via a genome-wide change in gene expression. Moreover, the epigenetic variations also regulate the commensal and pathogenic attributes which contribute to the fitness of *C. albicans* in a specific host niche. These alterations in the phenotype and fitness attributes directly influence the host–pathogen interaction. The phenotypic effect of epigenetic modulators such as KATs, KDACs, KMTs, chromatin remodellers, and histone variants are shown during various growth transitions.

of the well characterized KDACs is Sir2 (silent information regulator). Mutants of *sir2* display abnormal colony morphologies with a high frequency of phenotypic switching along with spontaneous filamentous growth (Perez-Martin et al. 1999). In addition, Hda1, a class II histone deacetylase is a known repressor of white-opaque switching (Srikantha et al. 2001). Hda1 deacetylates Yng2, which is a subunit of NuA4 histone acetyl transferase, resulting in reduction in occupancy of Yng2 and NuA4 at the promoters of hyphal-related genes. Cells lacking Hda1 are unable to maintain hyphal growth (Lu et al. 2011). Moreover, the Set3/Hos2, KDAC complex inhibits the yeast-hyphal transition and modulates transient expression changes of key transcription factors that influence morphogenesis (Hnisz et al. 2010, 2012). Among the histone methyl transferases (KMTs) in *C. albicans*, Set1 is the only characterized enzyme required for H3K4 methylation. *set1* null mutants show a complete loss of H3K4 methylation and display a hyperfilamentous phenotype in embedded conditions (Guillemette et al. 2011).

Apart from the histone modifications, the yeast-hyphal transition is additionally regulated by chromatin remodellers. Chromatin remodellers are the specialized ATP-dependent nucleosome remodelling complexes that enable access to the DNA by altering the structure and positioning of nucleosomes. These chromatin modifiers contain an ATPase domain responsible for their activity. Depending on the type of ATPase and the factors associated with the enzyme, these complexes catalyse either partial or complete disassembly of nucleosomes (histone eviction) or repositioning of nucleosomes along the DNA (nucleosome sliding) (Becker and Horz 2002; Saha et al. 2006). Swi1 and Snf2 are subunits of Swi/Snf complex which is a well known chromatin remodeller in yeast including *C. albicans*. Deletion of *SWI1* or *SNF2* in *C. albicans* demolishes hyphal development and results in a constitutive pseudohyphal morphology under different growth conditions (Mao et al. 2006). The expression of hyphal-specific genes, such as *ECE1*, *HWP1*, *HYR1*, and *SAP6* are down-regulated in *swi1* mutants; these mutants are avirulent in the mouse model of systemic infection (Mao et al. 2006). Therefore, these subunits of the Swi/Snf complex are important for regulating the expression of genes related to hyphal growth and virulence in *C. albicans* (Fig. 1).

4. White-opaque transition

The second most high-frequency switching and one of the well characterized morphological transitions observed in *C. albicans* is the white-opaque transition (Slutsky et al. 1987). This particular phenotypic transition was first observed in *MTL* homozygous strains (*a/a* or *α/α* cells) as opposed to predominantly occurring *MTL* heterozygous strains (*a/ α*) (Slutsky et al. 1987) of *C. albicans*. *MTL* homozygous (*a/a* or *α/α*) cells in the presence of certain environmental cues such as temperature (25 °C), media containing N-acetylglucosamine (Huang et al. 2010), high CO₂ concentration ($\geq 5\%$ CO₂) (Huang et al. 2009), low doses of UV irradiation (Morrow et al. 1989) and genotoxic and oxidative stress (Alby and Bennett 2009) give rise to opaque cells. Generally, opaque cells are morphologically elongated with pimples on the surface. This

event is rare and stochastic, and the changes are heritable over generations (Zordan et al. 2006). This particular switching event is epigenetically regulated since no obvious changes were observed on the underlined DNA sequence (Zordan et al. 2006).

The white-opaque transition gained prominence when its role was identified in mating (Hull et al. 2000; Magee and Magee 2000; Miller and Johnson 2002). Apart from morphological differences and mating preferences, white and opaque cells also differ in their ability to colonize, survive in specific host niches, and susceptibility to host defense mechanisms (neutrophils and macrophages) (Sasse et al. 2013). Thus, it could be assumed that the white-opaque transition might have evolved as a mechanism to evade immune response. Moreover, white and opaque cells also differ in their filamentation and adhesion behaviour (Lan et al. 2002). Approximately 1000 genes are altered during this transition, suggesting a genome-wide alteration in transcript levels (Lan et al. 2002). Transcriptional regulators involved in this transition have been well studied. *Wor1* and *Efg1* being the central hub with interconnected positive and negative loops (Huang et al. 2006; Srikantha et al. 2006). Other transcriptional regulators include *a1- α 2*, *Wor2*, *Wor3*, *Wor4*, *Czf1* and many more (Lassak et al. 2011; Lohse et al. 2013; Zordan et al. 2006, 2007).

Recent development in this field suggests yet another level of regulation occurring at the chromatin level, modulating the transcriptional circuit. The acetylation level of H3K56 is critical in maintaining the opaque form. Cells lacking *Rtt109* (KAT for H3K56ac) show a reduced switching frequency and are less susceptible to the environmental cues in maintaining the opaque state, whereas a reduction in the copy number of *Hst3*, the corresponding KDAC, enhances the switching frequency to the opaque form (Stevenson and Liu 2011). In budding yeast, H3K56ac has been reported to play a role during histone exchange as well as *rtt109* null mutants show reduced levels of histone turnover (Kaplan et al. 2008) suggesting occurrence of nucleosome-free regions. This may provide transient access to transcription factors at the promoters of opaque specific genes allowing them to maintain the same state. In addition, opaque cells have less chromatin bound histone H3 than the white cells across the promoter of several genes (Stevenson and Liu 2011). *C. albicans* also possesses the *Hat1/Hat2* complex associated with histone H4 acetylation and subsequent mutations show an increased frequency of white-opaque transition (Tscherner et al. 2012). The slow growth of *hat1* mutants might accumulate opaque-specific factors that trigger the switch to the opaque form. A similar trend was observed in the *hat2* mutant as well (Tscherner et al. 2012).

Among other KATs and KDACs, absence of Hda1 shows an increased frequency of white-opaque switching whereas absence of *Set3/Hos2*, *Hst2* or *Nat4* shows a reduction in switching frequency to the opaque form (Hnisz et al. 2009). *Rpd31*, a KDAC, is a repressor of switching in either directions (Klar et al. 2001; Srikantha et al. 2001). The only KMT whose role has been identified in white-opaque transition is *Set1*, a H3K4 methyl transferase. Cells lacking *SET1* show an enhanced white-opaque switching (Hnisz et al. 2009). In addition, nucleosome dynamics is also maintained by histone H2A variant known as H2A.Z. The variant histone helps in creating a

nucleosome-free region at the WOR1 promoter in white cells. This allows the repressors to bind and maintain the repressive state of chromatin (Guan and Liu 2015). Chromatin remodelers, such as Swr1, are also known to regulate the cell fate. It helps in depositing H2A.Z in exchange of H2A. In absence of SWR1, H2A.Z is not incorporated into chromatin, resulting in an increase in the white-opaque switching frequency (Guan and Liu 2015). Studies in *Saccharomyces cerevisiae* suggested that a high level of H3K56ac reduces nucleosome incorporation of histone H2A.Z (Watanabe et al. 2013). The deposition of histone H2A.Z is dramatically reduced on H3K56ac-containing nucleosomes, and also increases the eviction of H2A.Z from nucleosomes. Therefore, it is possible that, interplay between H3K56ac levels and H2A.Z deposition may be a key regulator in maintaining this morphological transition in *C. albicans* (Fig. 1).

5. Planktonic-biofilm transition

C. albicans, like many other microbes, has the ability to form biofilm on human tissues such as oral and vaginal mucosa and implanted medical devices (Dongari-Bagtzoglou et al. 2009; Douglas 2003; Fanning and Mitchell 2012). During biofilm growth, cells attach to abiotic or biotic surfaces and grow as a microcolony that develops into a complex three-dimensional structure, held together by an extracellular matrix (Baillie and Douglas 1999; Hawser et al. 1998). Cells in biofilms are more resistant to conventional antifungal drugs and host immune factors as compared to the free-floating planktonic cells (Donlan and Costerton 2002; Fanning and Mitchell 2012; Nobile and Johnson 2015). Resistance towards drugs is not only due to the complex architecture but also because of altered metabolic status and up-regulation of drug efflux pumps (Fanning and Mitchell 2012; Fox and Nobile 2012).

Biofilm formation in *C. albicans* is a multi-step process involving (1) adherence of cells to the substrates and colonization of yeast cells, (2) proliferation of yeast cells forming the basal layer of anchoring cells, (3) growth of hyphae and pseudohyphae and formation of an extracellular matrix that develops into a complex three-dimensional architecture, and (4) dispersal of cells from biofilm to colonize at the new sites (Baillie and Douglas 1999; Chandra et al. 2001; Fox and Nobile 2012; Nobile and Mitchell 2005). Genome-wide transcriptional profiling and proteomics studies revealed that many hundreds of mRNAs and proteins are differentially expressed between these two distinct modes of growth (Martinez-Gomariz et al. 2009; Thomas et al. 2006; Zarnowski et al. 2014). Moreover, the genetic circuit of biofilm development has been well explored and the network of six master regulators (Bcr1, Brg1, Efg1, Ndt80, Tec1, and Rob1) has been elucidated (Nobile et al. 2012). Each of these transcription factors are essential for biofilm growth in both *in vitro* and *in vivo* rat catheter and rat denture models (Nobile et al. 2012). In addition to the six master regulators, an array of 44 additional transcriptional regulators have been identified; biofilm formation is found to be defective in these mutants under at least one condition (Nobile and Johnson 2015). The role of chromatin modifying elements has not been much explored during planktonic to biofilm transition.

A study on the deletion of a histone deacetylase, Set3 core subunits (Hos2, Sif2, Snt1 and Set3) showed a previously unknown “rubbery” phenotype (Nobile et al. 2014). Set3 core subunit mutants show enhanced cohesiveness, increased resistance to physical perturbation, decreased dispersion and increased drug resistance (Nobile et al. 2014). The Set3 complex also binds directly to the coding regions of five of the six master regulators namely, BRG1, EFG1, NDT80, TEC1 and ROB1, and regulate the transcription kinetics of BRG1, TEC1 and EFG1 biofilm regulators (Hnisz et al. 2012; Nobile et al. 2012). The Set3 complex is also known to control the transcription kinetics of Nrg1, a negative regulator of biofilm dispersal (Hnisz et al. 2012). Therefore, these studies indicate that the Set3 complex modulates the expression of biofilm transcription regulators at the chromatin level (Fig. 1). A recent study suggests the existence of a novel variant histone H3 that seemed to have evolved exclusively in the CTG clade species of ascomycetes including *C. albicans*. Deletion of this variant histone H3 exhibits hyper-filamentation and an enhanced biofilm formation (Rai and Sanyal, unpublished data). Future studies on other chromatin modifying elements should provide mechanistic insights into understanding biofilm growth in *C. albicans* and several other biofilm forming fungi.

6. Future perspective

In this review, we discussed how phenotypic variations are directly or indirectly regulated by various chromatin modifications and the modifying elements including histone PTMs, KMTs, KATs and KDACs. Phenotypic plasticity is the ability of *C. albicans* to survive under different environmental and developmental conditions. This property of the fungus is typically based on variable patterns of gene expression influenced by growth conditions. Modifications to DNA and histones have been implicated as likely candidates for generating and regulating phenotypic plasticity in many pathogens (Gomez-Diaz et al. 2012). However, the mechanism by which gene expression is influenced when *C. albicans* transits from a commensal cell type to a pathogenic form is poorly understood. Therefore, future research should be directed towards chromatin remodeling and histone modifications to gain further knowledge of global gene regulation and thus may be utilized for pharmaceutical intervention. Furthermore, chromatin modifying factors are not only involved in host–pathogen interactions but also in several other cellular processes such as genome defense. We believe that exciting developments in this field are evident by correlating the role of chromatin modifying elements with transcription kinetics that mark distinct lifestyles of *C. albicans*. Therefore, a comprehensive survey of epigenetic determinants of pathogenesis will help in understanding the phenotypic plasticity of *C. albicans* and other fungi. It has been demonstrated that altering the levels of fungal specific KAT, H3K56ac mark influences the virulence properties (Wurtele et al. 2010). This can be further extrapolated to other PTMs which might serve as potential targets for treating *C. albicans* infections.

In metazoans, programmed cell differentiation begins at the earliest stages of development in the pluripotent embryonic stem cells (ESCs) (Schrode et al. 2013) which continues

throughout development till adulthood (Rojas-Rios and Gonzalez-Reyes 2014). The process of stem cell self renewal and differentiation is tightly controlled at the level of chromatin (Hemberger et al. 2009). Cellular changes require increased plasticity during the periods of transition, and reduced plasticity to stabilize these changes. In general, canonical histones are replaced with specific variants during the cellular transition in metazoans. Histone variants such as TH2A (mice), TH2B (mice), H2A.Z (mice) and H3.3 (*Xenopus*) facilitate cellular plasticity during the early development while H2A.X (mice) and macroH2A (in zebrafish and mice) inhibit developmental plasticity after cellular differentiation of embryonic stem cells (Santoro and Dulac 2015). Thus, involvement of histone variants in regulating cellular differentiation suggests that their functional properties are well suited for this purpose (Santoro and Dulac 2015). The role of histone variants have not been explored much with respect to phenotypic transitions in *C. albicans*. Understanding their functions will require detailed analysis of the cell types and conditions under which they are expressed. Therefore, studies on histone variants and their respective chaperones have enormous capacity to unravel the phenotypic plasticity evolved within this organism.

Epigenetic elements, such as small RNA pathways, are also known to globally regulate gene expression and the chromatin state, mediating phenotypic plasticity in many organisms including *Caenorhabditis elegans* (Hall et al. 2013; van Wolfswinkel and Ketting 2010). Although the gene encoding RNA-directed RNA polymerase (RdRP) is absent in the *C. albicans* genome, it harbours a typical argonaute homologue and a non-canonical dicer (lacking both a helicase and a PAZ domain) (Drinnenberg et al. 2009) of the RNAi machinery. Additionally, RdRP homologue is absent in the *S. castellii* genome, and yet the organism is capable of performing silencing of a transgene. Therefore, it could be speculated that argonaute and dicer are sufficient for RNAi activity in *S. castellii*. It has been reported that, *C. albicans* Dcr1 (CaDcr1) is capable of generating small interfering RNA (siRNA) *in vitro* as well as *in vivo* (Bernstein et al. 2012). Moreover, CaDcr1 has the ability to complement *S. castellii* dicer function and restore RNAi-mediated gene repression. Henceforth, future investigation on the role of RNAi in silencing of genes involved in maintaining various morphological forms, seems to be a potential area of research. More efforts are required to understand the impact of each of these factors on the differential morphology-specific gene expression which can make significant contributions to the field of human health and diseases pertaining to *Candida* infections.

Conflict of interest

We have no competing interests.

Acknowledgements

We acknowledge Pallavi Kakade for her comments on the manuscript. KS acknowledges financial support from various Indian government funding agencies and as well as Jawaharlal

Nehru Centre for Advanced Scientific Research (JNCASR). LSR and PB are research fellows supported by the Council for Scientific and Industrial Research (CSIR), Govt. of India. RS is a senior research fellow of University Grants Commission (UGC), Govt of India.

REFERENCES

- Alby, K., Bennett, R.J., 2009. Stress-induced phenotypic switching in *Candida albicans*. *Mol. Biol. Cell* 20, 3178–3191.
- Anderson, J.M., Soll, D.R., 1987. Unique phenotype of opaque cells in the white-opaque transition of *Candida albicans*. *J. Bacteriol.* 169, 5579–5588.
- Baillie, G.S., Douglas, L.J., 1999. Role of dimorphism in the development of *Candida albicans* biofilms. *J. Med. Microbiol.* 48, 671–679.
- Becker, P.B., Horz, W., 2002. ATP-dependent nucleosome remodeling. *Annu. Rev. Biochem.* 71, 247–273.
- Berman, J., Sudbery, P.E., 2002. *Candida albicans*: a molecular revolution built on lessons from budding yeast. *Nat. Rev. Genet.* 3, 918–930.
- Bernstein, D.A., Vyas, V.K., Weinberg, D.E., Drinnenberg, I.A., Bartel, D.P., et al., 2012. *Candida albicans* Dicer (CaDcr1) is required for efficient ribosomal and spliceosomal RNA maturation. *Proc. Natl. Acad. Sci. U. S. A.* 109, 523–528.
- Bonisch, C., Nieratschker, S.M., Orfanos, N.K., Hake, S.B., 2008. Chromatin proteomics and epigenetic regulatory circuits. *Expert Rev. Proteomics* 5, 105–119.
- Bougdour, A., Maubon, D., Baldacci, P., Ortet, P., Bastien, O., et al., 2009. Drug inhibition of HDAC3 and epigenetic control of differentiation in Apicomplexa parasites. *J. Exp. Med.* 206, 953–966.
- Braun, B.R., Johnson, A.D., 1997. Control of filament formation in *Candida albicans* by the transcriptional repressor TUP1. *Science* 277, 105–109.
- Brown, A.J.P., 2002. Expression of Growth Form-specific Factors During Morphogenesis in *Candida albicans*. ASM Press, pp. 87–94.
- Brownell, J.E., Zhou, J., Ranalli, T., Kobayashi, R., Edmondson, D.G., et al., 1996. *Tetrahymena* histone acetyltransferase A: a homolog to yeast Gcn5p linking histone acetylation to gene activation. *Cell* 84, 843–851.
- Cao, F., Lane, S., Raniga, P.P., Lu, Y., Zhou, Z., et al., 2006. The Flo8 transcription factor is essential for hyphal development and virulence in *Candida albicans*. *Mol. Biol. Cell* 17, 295–307.
- Carlisle, P.L., Banerjee, M., Lazzell, A., Monteagudo, C., Lopez-Ribot, J.L., et al., 2009. Expression levels of a filament-specific transcriptional regulator are sufficient to determine *Candida albicans* morphology and virulence. *Proc. Natl. Acad. Sci. U. S. A.* 106, 599–604.
- Chandra, J., Kuhn, D.M., Mukherjee, P.K., Hoyer, L.L., McCormick, T., et al., 2001. Biofilm formation by the fungal pathogen *Candida albicans*: development, architecture, and drug resistance. *J. Bacteriol.* 183, 5385–5394.
- Chang, P., Fan, X., Chen, J., 2015. Function and subcellular localization of Gcn5, a histone acetyltransferase in *Candida albicans*. *Fungal Genet. Biol.* 81, 132–141.
- Croken, M.M., Nardelli, S.C., Kim, K., 2012. Chromatin modifications, epigenetics, and how protozoan parasites regulate their lives. *Trends Parasitol.* 28, 202–213.
- Davis, D., Wilson, R.B., Mitchell, A.P., 2000. RIM101-dependent and-independent pathways govern pH responses in *Candida albicans*. *Mol. Cell Biol.* 20, 971–978.
- Dixon, S.E., Stilger, K.L., Elias, E.V., Naguleswaran, A., Sullivan Jr., W.J., 2010. A decade of epigenetic research in *Toxoplasma gondii*. *Mol. Biochem. Parasitol.* 173, 1–9.

- Dongari-Bagtzoglou, A., Kashleva, H., Dwivedi, P., Diaz, P., Vasilakos, J., 2009. Characterization of mucosal *Candida albicans* biofilms. *PLoS One* 4e7967.
- Donlan, R.M., Costerton, J.W., 2002. Biofilms: survival mechanisms of clinically relevant microorganisms. *Clin. Microbiol. Rev.* 15, 167–193.
- Douglas, L.J., 2003. *Candida* biofilms and their role in infection. *Trends Microbiol.* 11, 30–36.
- Drell, T., Lillsaar, T., Tummeleht, L., Simm, J., Aaspollu, A., et al., 2013. Characterization of the vaginal micro- and mycobiome in asymptomatic reproductive-age Estonian women. *PLoS One* 8e54379.
- Drinnenberg, I.A., Weinberg, D.E., Xie, K.T., Mower, J.P., Wolfe, K.H., et al., 2009. RNAi in budding yeast. *Science* 326, 544–550.
- Edmond, M.B., Wallace, S.E., McClish, D.K., Pfaller, M.A., Jones, R.N., et al., 1999. Nosocomial bloodstream infections in United States hospitals: a three-year analysis. *Clin. Infect. Dis.* 29, 239–244.
- Egger, G., Liang, G., Aparicio, A., Jones, P.A., 2004. Epigenetics in human disease and prospects for epigenetic therapy. *Nature* 429, 457–463.
- Fanning, S., Mitchell, A.P., 2012. Fungal biofilms. *PLoS Pathog.* 8e1002585.
- Fidel Jr., P.L., 2006. *Candida*-host interactions in HIV disease: relationships in oropharyngeal candidiasis. *Adv. Dent. Res.* 19, 80–84.
- Filler, S.G., Sheppard, D.C., 2006. Fungal invasion of normally non-phagocytic host cells. *PLoS Pathog.* 2e129.
- Findley, K., Oh, J., Yang, J., Conlan, S., Deming, C., et al., 2013. Topographic diversity of fungal and bacterial communities in human skin. *Nature* 498, 367–370.
- Fox, E.P., Nobile, C.J., 2012. A sticky situation: untangling the transcriptional network controlling biofilm development in *Candida albicans*. *Transcription* 3, 315–322.
- Garnaud, C., Champlébourg, M., Maubon, D., Cornet, M., Govin, J., 2016. Histone deacetylases and their inhibition in *Candida* species. *Front. Microbiol.* 7, 1238.
- Gelato, K.A., Fischle, W., 2008. Role of histone modifications in defining chromatin structure and function. *Biol. Chem.* 389, 353–363.
- Gomez-Diaz, E., Jorda, M., Peinado, M.A., Rivero, A., 2012. Epigenetics of host-pathogen interactions: the road ahead and the road behind. *PLoS Pathog.* 8e1003007.
- Gow, N.A., Brown, A.J., Odds, F.C., 2002. Fungal morphogenesis and host invasion. *Curr. Opin. Microbiol.* 5, 366–371.
- Guan, Z., Liu, H., 2015. Overlapping functions between SWR1 deletion and H3K56 acetylation in *Candida albicans*. *Eukaryot. Cell* 14, 578–587.
- Guillemette, B., Drogaris, P., Lin, H.H., Armstrong, H., Hiragami-Hamada, K., et al., 2011. H3 lysine 4 is acetylated at active gene promoters and is regulated by H3 lysine 4 methylation. *PLoS Genet.* 7e1001354.
- Hakimi, M.A., Deitsch, K.W., 2007. Epigenetics in Apicomplexa: control of gene expression during cell cycle progression, differentiation and antigenic variation. *Curr. Opin. Microbiol.* 10, 357–362.
- Hall, S.E., Chirm, G.W., Lau, N.C., Sengupta, P., 2013. RNAi pathways contribute to developmental history-dependent phenotypic plasticity in *C. elegans*. *RNA* 19, 306–319.
- Hawser, S.P., Baillie, G.S., Douglas, L.J., 1998. Production of extracellular matrix by *Candida albicans* biofilms. *J. Med. Microbiol.* 47, 253–256.
- Hemberger, M., Dean, W., Reik, W., 2009. Epigenetic dynamics of stem cells and cell lineage commitment: digging Waddington's canal. *Nat. Rev. Mol. Cell Biol.* 10, 526–537.
- Hnisz, D., Bardet, A.F., Nobile, C.J., Petryshyn, A., Glaser, W., et al., 2012. A histone deacetylase adjusts transcription kinetics at coding sequences during *Candida albicans* morphogenesis. *PLoS Genet.* 8e1003118.
- Hnisz, D., Majer, O., Frohner, I.E., Komnenovic, V., Kuchler, K., 2010. The Set3/Hos2 histone deacetylase complex attenuates cAMP/PKA signaling to regulate morphogenesis and virulence of *Candida albicans*. *PLoS Pathog.* 6e1000889.
- Hnisz, D., Schwarzmueller, T., Kuchler, K., 2009. Transcriptional loops meet chromatin: a dual-layer network controls white-opaque switching in *Candida albicans*. *Mol. Microbiol.* 74, 1–15.
- Hobson, R.P., 2003. The global epidemiology of invasive *Candida* infections—is the tide turning? *J. Hosp. Infect.* 55, 159–168 quiz 233.
- Hoffmann, C., Dollive, S., Grunberg, S., Chen, J., Li, H., et al., 2013. Archaea and fungi of the human gut microbiome: correlations with diet and bacterial residents. *PLoS One* 8e66019.
- Huang, G., Srikantha, T., Sahni, N., Yi, S., Soll, D.R., 2009. CO(2) regulates white-to-opaque switching in *Candida albicans*. *Curr. Biol.* 19, 330–334.
- Huang, G., Wang, H., Chou, S., Nie, X., Chen, J., et al., 2006. Bistable expression of WOR1, a master regulator of white-opaque switching in *Candida albicans*. *Proc. Natl. Acad. Sci. U. S. A.* 103, 12813–12818.
- Huang, G., Yi, S., Sahni, N., Daniels, K.J., Srikantha, T., et al., 2010. N-acetylglucosamine induces white to opaque switching, a mating prerequisite in *Candida albicans*. *PLoS Pathog.* 6e1000806.
- Hube, B., 1996. *Candida albicans* secreted aspartyl proteinases. *Curr. Top. Med. Mycol.* 7, 55–69.
- Hull, C.M., Raisner, R.M., Johnson, A.D., 2000. Evidence for mating of the “asexual” yeast *Candida albicans* in a mammalian host. *Science* 289, 307–310.
- Jacobsen, I.D., Wilson, D., Wachtler, B., Brunke, S., Naglik, J.R., et al., 2012. *Candida albicans* dimorphism as a therapeutic target. *Expert Rev. Anti Infect. Ther.* 10, 85–93.
- Kadosh, D., Johnson, A.D., 2005. Induction of the *Candida albicans* filamentous growth program by relief of transcriptional repression: a genome-wide analysis. *Mol. Biol. Cell* 16, 2903–2912.
- Kaplan, T., Liu, C.L., Erkmann, J.A., Holik, J., Grunstein, M., et al., 2008. Cell cycle- and chaperone-mediated regulation of H3K56ac incorporation in yeast. *PLoS Genet.* 4e1000270.
- Klar, A.J., Srikantha, T., Soll, D.R., 2001. A histone deacetylation inhibitor and mutant promote colony-type switching of the human pathogen *Candida albicans*. *Genetics* 158, 919–924.
- Klein, R.S., Harris, C.A., Small, C.B., Moll, B., Lesser, M., et al., 1984. Oral candidiasis in high-risk patients as the initial manifestation of the acquired immunodeficiency syndrome. *N. Engl. J. Med.* 311, 354–358.
- Kohler, J.R., Fink, G.R., 1996. *Candida albicans* strains heterozygous and homozygous for mutations in mitogen-activated protein kinase signaling components have defects in hyphal development. *Proc. Natl. Acad. Sci. U. S. A.* 93, 13223–13228.
- Kuchler, K., Jenull, S., Shivarathri, R., Chauhan, N., 2016. Fungal KATs/KDACs: a new highway to better antifungal drugs? *PLoS Pathog.* 12e1005938.
- Kumamoto, C.A., 2008. Niche-specific gene expression during *C. albicans* infection. *Curr. Opin. Microbiol.* 11, 325–330.
- Lan, C.Y., Newport, G., Murillo, L.A., Jones, T., Scherer, S., et al., 2002. Metabolic specialization associated with phenotypic switching in *Candida albicans*. *Proc. Natl. Acad. Sci. U. S. A.* 99, 14907–14912.
- Lassak, T., Schneider, E., Busmann, M., Kurtz, D., Manak, J.R., et al., 2011. Target specificity of the *Candida albicans* Efg1 regulator. *Mol. Microbiol.* 82, 602–618.
- Liu, H., 2001. Transcriptional control of dimorphism in *Candida albicans*. *Curr. Opin. Microbiol.* 4, 728–735.
- Lo, H.J., Kohler, J.R., DiDomenico, B., Loebenberg, D., Cacciapuoti, A., et al., 1997. Nonfilamentous *C. albicans* mutants are avirulent. *Cell* 90, 939–949.

- Lohse, M.B., Hernday, A.D., Fordyce, P.M., Noiman, L., Sorrells, T.R., et al., 2013. Identification and characterization of a previously undescribed family of sequence-specific DNA-binding domains. *Proc. Natl. Acad. Sci. U. S. A.* 110, 7660–7665.
- Lopes da Rosa, J., Boyartchuk, V.L., Zhu, L.J., Kaufman, P.D., 2010. Histone acetyltransferase Rtt109 is required for *Candida albicans* pathogenesis. *Proc. Natl. Acad. Sci. U. S. A.* 107, 1594–1599.
- Lu, Y., Su, C., Wang, A., Liu, H., 2011. Hyphal development in *Candida albicans* requires two temporally linked changes in promoter chromatin for initiation and maintenance. *PLoS Biol.* 9, e1001105.
- Magee, B.B., Magee, P.T., 2000. Induction of mating in *Candida albicans* by construction of MTL α and MTL strains. *Science* 289, 310–313.
- Mao, X., Cao, F., Nie, X., Liu, H., Chen, J., 2006. The Swi/Snf chromatin remodeling complex is essential for hyphal development in *Candida albicans*. *FEBS Lett.* 580, 2615–2622.
- Martinez-Gomariz, M., Perumal, P., Mekala, S., Nombela, C., Chaffin, W.L., et al., 2009. Proteomic analysis of cytoplasmic and surface proteins from yeast cells, hyphae, and biofilms of *Candida albicans*. *Proteomics* 9, 2230–2252.
- Mayer, F.L., Wilson, D., Hube, B., 2013. *Candida albicans* pathogenicity mechanisms. *Virulence* 4, 119–128.
- Miller, M.G., Johnson, A.D., 2002. White-opaque switching in *Candida albicans* is controlled by mating-type locus homeodomain proteins and allows efficient mating. *Cell* 110, 293–302.
- Morrow, B., Anderson, J., Wilson, J., Soll, D.R., 1989. Bidirectional stimulation of the white-opaque transition of *Candida albicans* by ultraviolet irradiation. *J. Gen. Microbiol.* 135, 1201–1208.
- Murad, A.M., Leng, P., Straffon, M., Wishart, J., Macaskill, S., et al., 2001. NRG1 represses yeast-hypha morphogenesis and hypha-specific gene expression in *Candida albicans*. *EMBO J.* 20, 4742–4752.
- Nantel, A., Dignard, D., Bachewich, C., Harcus, D., Marcil, A., et al., 2002. Transcription profiling of *Candida albicans* cells undergoing the yeast-to-hyphal transition. *Mol. Biol. Cell* 13, 3452–3465.
- Nicholls, S., MacCallum, D.M., Kaffarnik, F.A., Selway, L., Peck, S.C., et al., 2011. Activation of the heat shock transcription factor Hsf1 is essential for the full virulence of the fungal pathogen *Candida albicans*. *Fungal Genet. Biol.* 48, 297–305.
- Nobile, C.J., Fox, E.P., Hartooni, N., Mitchell, K.F., Hnisz, D., et al., 2014. A histone deacetylase complex mediates biofilm dispersal and drug resistance in *Candida albicans*. *MBio* 5, e01201–01214.
- Nobile, C.J., Fox, E.P., Nett, J.E., Sorrells, T.R., Mitrovich, Q.M., et al., 2012. A recently evolved transcriptional network controls biofilm development in *Candida albicans*. *Cell* 148, 126–138.
- Nobile, C.J., Johnson, A.D., 2015. *Candida albicans* biofilms and human disease. *Annu. Rev. Microbiol.* 69, 71–92.
- Nobile, C.J., Mitchell, A.P., 2005. Regulation of cell-surface genes and biofilm formation by the *C. albicans* transcription factor Bcr1p. *Curr. Biol.* 15, 1150–1155.
- Noble, S.M., Gianetti, B.A., Witchley, J.N., 2016. *Candida albicans* cell-type switching and functional plasticity in the mammalian host. *Nat. Rev. Microbiol.* 15, 96–108.
- Odds, F.C., 1994. Pathogenesis of *Candida* infections. *J. Am. Acad. Dermatol.* 31, S2–S5.
- Pande, K., Chen, C., Noble, S.M., 2013. Passage through the mammalian gut triggers a phenotypic switch that promotes *Candida albicans* commensalism. *Nat. Genet.* 45, 1088–1091.
- Perez-Martin, J., Uria, J.A., Johnson, A.D., 1999. Phenotypic switching in *Candida albicans* is controlled by a SIR2 gene. *EMBO J.* 18, 2580–2592.
- Perloth, J., Choi, B., Spellberg, B., 2007. Nosocomial fungal infections: epidemiology, diagnosis, and treatment. *Med. Mycol.* 45, 321–346.
- Probst, A.V., Dunleavy, E., Almouzni, G., 2009. Epigenetic inheritance during the cell cycle. *Nat. Rev. Mol. Cell Biol.* 10, 192–206.
- Pukkila-Worley, R., Peleg, A.Y., Tampakakis, E., Mylonakis, E., 2009. *Candida albicans* hyphal formation and virulence assessed using a *Caenorhabditis elegans* infection model. *Eukaryot. Cell* 8, 1750–1758.
- Rai, M.N., Balusu, S., Gorityala, N., Dandu, L., Kaur, R., 2012. Functional genomic analysis of *Candida glabrata*-macrophage interaction: role of chromatin remodeling in virulence. *PLoS Pathog.* 8, e1002863.
- Raman, S.B., Nguyen, M.H., Zhang, Z., Cheng, S., Jia, H.Y., et al., 2006. *Candida albicans* SET1 encodes a histone 3 lysine 4 methyltransferase that contributes to the pathogenesis of invasive candidiasis. *Mol. Microbiol.* 60, 697–709.
- Richmond, T.J., Davey, C.A., 2003. The structure of DNA in the nucleosome core. *Nature* 423, 145–150.
- Rojas-Rios, P., Gonzalez-Reyes, A., 2014. Concise review: the plasticity of stem cell niches: a general property behind tissue homeostasis and repair. *Stem Cells* 32, 852–859.
- Russell, C., Lay, K.M., 1973. Natural history of *Candida* species and yeasts in the oral cavities of infants. *Arch. Oral Biol.* 18, 957–962.
- Saha, A., Wittmeyer, J., Cairns, B.R., 2006. Chromatin remodelling: the industrial revolution of DNA around histones. *Nat. Rev. Mol. Cell Biol.* 7, 437–447.
- Santoro, S.W., Dulac, C., 2015. Histone variants and cellular plasticity. *Trends Genet.* 31, 516–527.
- Sasse, C., Hasenberg, M., Weyler, M., Gunzer, M., Morschhauser, J., 2013. White-opaque switching of *Candida albicans* allows immune evasion in an environment-dependent fashion. *Eukaryot. Cell* 12, 50–58.
- Saville, S.P., Lazzell, A.L., Monteagudo, C., Lopez-Ribot, J.L., 2003. Engineered control of cell morphology in vivo reveals distinct roles for yeast and filamentous forms of *Candida albicans* during infection. *Eukaryot. Cell* 2, 1053–1060.
- Schrode, N., Xenopoulos, P., Piliszek, A., Frankenberg, S., Plusa, B., et al., 2013. Anatomy of a blastocyst: cell behaviors driving cell fate choice and morphogenesis in the early mouse embryo. *Genesis* 51, 219–233.
- Sellam, A., Askew, C., Epp, E., Lavoie, H., Whiteway, M., et al., 2009. Genome-wide mapping of the coactivator Ada2p yields insight into the functional roles of SAGA/ADA complex in *Candida albicans*. *Mol. Biol. Cell* 20, 2389–2400.
- Slutsky, B., Staebell, M., Anderson, J., Risen, L., Pfaller, M., et al., 1987. “White-opaque transition”: a second high-frequency switching system in *Candida albicans*. *J. Bacteriol.* 169, 189–197.
- Soll, D.R., 2002. *Candida* commensalism and virulence: the evolution of phenotypic plasticity. *Acta Trop.* 81, 101–110.
- Srikantha, T., Borneman, A.R., Daniels, K.J., Pujol, C., Wu, W., et al., 2006. TOS9 regulates white-opaque switching in *Candida albicans*. *Eukaryot. Cell* 5, 1674–1687.
- Srikantha, T., Tsai, L., Daniels, K., Klar, A.J., Soll, D.R., 2001. The histone deacetylase genes HDA1 and RPD3 play distinct roles in regulation of high-frequency phenotypic switching in *Candida albicans*. *J. Bacteriol.* 183, 4614–4625.
- Stevenson, J.S., Liu, H., 2011. Regulation of white and opaque cell-type formation in *Candida albicans* by Rtt109 and Hst3. *Mol. Microbiol.* 81, 1078–1091.
- Stevenson, J.S., Liu, H., 2013. Nucleosome assembly factors CAF-1 and HIR modulate epigenetic switching frequencies in an H3K56 acetylation-associated manner in *Candida albicans*. *Eukaryot Cell* 12, 591–603.
- Sudbery, P., Gow, N., Berman, J., 2004. The distinct morphogenic states of *Candida albicans*. *Trends Microbiol.* 12, 317–324.
- Tao, L., Du, H., Guan, G., Dai, Y., Nobile, C.J., et al., 2014. Discovery of a “white-gray-opaque” tristable phenotypic switching

- system in *Candida albicans*: roles of non-genetic diversity in host adaptation. *PLoS Biol.* 12e1001830.
- Thomas, D.P., Bachmann, S.P., Lopez-Ribot, J.L., 2006. Proteomics for the analysis of the *Candida albicans* biofilm lifestyle. *Proteomics* 6, 5795–5804.
- Thompson, D.S., Carlisle, P.L., Kadosh, D., 2011. Coevolution of morphology and virulence in *Candida* species. *Eukaryot. Cell* 10, 1173–1182.
- Tost, J., 2009. DNA methylation: an introduction to the biology and the disease-associated changes of a promising biomarker. *Methods Mol. Biol.* 507, 3–20.
- Tscherner, M., Stappler, E., Hnisch, D., Kuchler, K., 2012. The histone acetyltransferase Hat1 facilitates DNA damage repair and morphogenesis in *Candida albicans*. *Mol. Microbiol.* 86, 1197–1214.
- Turner, B.M., 2002. Cellular memory and the histone code. *Cell* 111, 285–291.
- van Holde, K.E., 1988. Chromatin.
- van Wolfswinkel, J.C., Ketting, R.F., 2010. The role of small non-coding RNAs in genome stability and chromatin organization. *J. Cell Sci.* 123, 1825–1839.
- Wang, X., Chang, P., Ding, J., Chen, J., 2013. Distinct and redundant roles of the two MYST histone acetyltransferases Esa1 and Sas2 in cell growth and morphogenesis of *Candida albicans*. *Eukaryot. Cell* 12, 438–449.
- Watanabe, S., Radman-Livaja, M., Rando, O.J., Peterson, C.L., 2013. A histone acetylation switch regulates H2A.Z deposition by the SWR-C remodeling enzyme. *Science* 340, 195–199.
- Weig, M., Gross, U., Muhlschlegel, F., 1998. Clinical aspects and pathogenesis of *Candida* infection. *Trends Microbiol.* 6, 468–470.
- Wu, J.I., Lessard, J., Crabtree, G.R., 2009. Understanding the words of chromatin regulation. *Cell* 136, 200–206.
- Wurtele, H., Tsao, S., Lepine, G., Mullick, A., Tremblay, J., et al., 2010. Modulation of histone H3 lysine 56 acetylation as an antifungal therapeutic strategy. *Nat. Med.* 16, 774–780.
- Zarnowski, R., Westler, W.M., Lacmbouh, G.A., Marita, J.M., Bothe, J.R., et al., 2014. Novel entries in a fungal biofilm matrix encyclopedia. *mBio* 5 e01333–14.
- Zordan, R.E., Galgoczy, D.J., Johnson, A.D., 2006. Epigenetic properties of white-opaque switching in *Candida albicans* are based on a self-sustaining transcriptional feedback loop. *Proc. Natl. Acad. Sci. U. S. A.* 103, 12807–12812.
- Zordan, R.E., Miller, M.G., Galgoczy, D.J., Tuch, B.B., Johnson, A.D., 2007. Interlocking transcriptional feedback loops control white-opaque switching in *Candida albicans*. *PLoS Biol.* 5e256.

RESEARCH ARTICLE

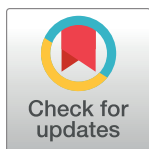
The *Candida albicans* biofilm gene circuit modulated at the chromatin level by a recent molecular histone innovation

Laxmi Shanker Rai^{1,2}, Rima Singha¹, Hiram Sanchez³, Tanmoy Chakraborty^{1*}, Bipin Chand⁴, Sophie Bachellier-Bassi^{1,2}, Shantanu Chowdhury^{5,6}, Christophe d'Enfert^{1,2}, David R. Andes³, Kaustuv Sanyal^{1*}

1 Molecular Mycology Laboratory, Molecular Biology and Genetics Unit, Jawaharlal Nehru Centre for Advanced Scientific Research, Bangalore, India, **2** Unité Biologie et Pathogénicité Fongiques, Institut Pasteur, USC2019 INRA, Paris, France, **3** Department of Medicine, University of Wisconsin, Madison, Wisconsin, United States of America, **4** Genotypic Technology Private Limited, Bangalore, India, **5** GNR Center for Genome Informatics, CSIR-Institute of Genomics and Integrative Biology, New Delhi, India, **6** Proteomics and Structural Biology Unit, CSIR-Institute of Genomics and Integrative Biology, New Delhi, India

* Current Address: Current address: Department of Microbiology, University of Szeged, Közép fasor, Szeged, Hungary

* sanyal@jncasr.ac.in



OPEN ACCESS

Citation: Rai LS, Singha R, Sanchez H, Chakraborty T, Chand B, Bachellier-Bassi S, et al. (2019) The *Candida albicans* biofilm gene circuit modulated at the chromatin level by a recent molecular histone innovation. PLoS Biol 17(8): e3000422. <https://doi.org/10.1371/journal.pbio.3000422>

Academic Editor: Harmit S. Malik, Fred Hutchinson Cancer Research Center, UNITED STATES

Received: April 19, 2019

Accepted: July 17, 2019

Published: August 9, 2019

Copyright: This is an open access article, free of all copyright, and may be freely reproduced, distributed, transmitted, modified, built upon, or otherwise used by anyone for any lawful purpose. The work is made available under the [Creative Commons CC0](https://creativecommons.org/licenses/by/4.0/) public domain dedication.

Data Availability Statement: Gene expression data have been deposited into the NCBI Gene Expression Omnibus (GEO) portal under the accession number GSE72824.

Funding: This project was supported by a Science and Engineering Research Board (SERB), grant no. SR/SO/BB-0107/2012 (URL: <http://www.serb.gov.in/home.php>) to KS. This work was partially supported by the Tata Innovation Fellowship (URL: <http://www.dbtindia.nic.in/tata-innovation-fellowship>) (grant no. BT/HRD/35/01/03/2017) to

Abstract

Histone H3 and its variants regulate gene expression but the latter are absent in most ascomycetous fungi. Here, we report the identification of a variant histone H3, which we have designated H3V^{CTG} because of its exclusive presence in the CTG clade of ascomycetes, including *Candida albicans*, a human pathogen. *C. albicans* grows both as single yeast cells and hyphal filaments in the planktonic mode of growth. It also forms a three-dimensional biofilm structure in the host as well as on human catheter materials under suitable conditions. H3V^{CTG} null (*hht1/hht1*) cells of *C. albicans* are viable but produce more robust biofilms than wild-type cells in both in vitro and in vivo conditions. Indeed, a comparative transcriptome analysis of planktonic and biofilm cells reveals that the biofilm circuitry is significantly altered in H3V^{CTG} null cells. H3V^{CTG} binds more efficiently to the promoters of many biofilm-related genes in the planktonic cells than during biofilm growth, whereas the binding of the core canonical histone H3 on the corresponding promoters largely remains unchanged. Furthermore, biofilm defects associated with master regulators, namely, biofilm and cell wall regulator 1 (Bcr1), transposon enhancement control 1 (Tec1), and non-dityrosine 80 (Ndt80), are significantly rescued in cells lacking H3V^{CTG}. The occupancy of the transcription factor Bcr1 at its cognate promoter binding sites was found to be enhanced in the absence of H3V^{CTG} in the planktonic form of growth resulting in enhanced transcription of biofilm-specific genes. Further, we demonstrate that co-occurrence of valine and serine at the 31st and 32nd positions in H3V^{CTG}, respectively, is essential for its function. Taken together, we show that even in a unicellular organism, differential gene expression patterns are modulated by the relative occupancy of the specific histone H3 type at the chromatin level.

KS, intramural financial support from Jawaharlal Nehru Centre for Advanced Scientific Research (JNCASR) (URL: <http://www.jncasr.ac.in>), and grant no. BT/INF/22/SP27679/2018 of Department of Biotechnology in Life Science Research, Education and Training (DBT-BUILDER) (URL: http://www.dbtindia.nic.in/wp-content/uploads/Guidelines_BiotechFacility12112015.pdf) to JNCASR. This project is also supported by Fondation pour la Recherche Médicale (FRM DBF20160635719) <https://www.frm.org/> L.S.R. Wellcome Trust DBT India Alliance (500127/Z/09/Z). <https://www.indiaalliance.org/> S.C. National Institute of Health (R01AI073289). <https://www.nih.gov/> D.R.A Fondation pour la Recherche Médicale (FRM DBF20160635719) <https://www.frm.org/> C.D. French Government's Investissements d'Avenir program (Laboratoire d'Excellence Integrative Biology of Emerging Infectious Diseases, ANR-10-LABX-62-IBID) <https://anr.fr/Projets/ANR-10-LABX-0062> C.D. The funders had no role in study design, data collection and analysis, decision to publish, or preparation of the manuscript.

Competing interests: The authors have declared that no competing interests exist.

Abbreviations: Als, agglutinin-Like Sequence; Bcr1, biofilm and cell wall regulator 1; BLAST, basic local alignment search tool; Brg1, biofilm regulator 1; ChIP, chromatin immunoprecipitation; Chr, chromosome; CLSM, confocal laser scanning microscopy; CM, complete media; CM+NAG, complete media supplemented with N-acetyl glucosamine; CRISPR-Cas9, clustered regularly interspaced short palindromic repeats-CRISPR associated protein 9; Eap1, enhanced adherence to polystyrene 1; Efg1, enhanced filamentous growth protein 1; FBS, fetal bovine serum; Flo8, flocculation 8; Gal4, galactose metabolism 4; GEO, gene expression omnibus; GPI, glycosylphosphatidylinositol; hH4v, histone H4 variant; Hwp1, hyphal wall protein 1; IP, immunoprecipitated; MNase, micrococcal nuclease; Ndt80, non-dityrosine 80; OD, optical density; PBS, phosphate buffered saline; PTM, post-translational modification; qPCR, quantitative PCR; Rbt1, repressed by *TUP1*; Rfx2, regulatory factor X; Rob1, regulator of biofilm 1; RT-PCR, reverse transcription PCR; SEM, scanning electron microscopy; Tec1, transposon enhancement control 1; YPD, yeast peptone dextrose; YPDU, yeast peptone dextrose supplemented with uridine; Δ Ct, difference in Ct values of a gene of interest and normalization control (in this case, actin); $\Delta\Delta$ Ct, difference in Ct (threshold cycle) values of a gene

Introduction

Histones are highly conserved proteins across eukaryotes. Variant histones, which are nonallelic isoforms of the canonical histones, may exist and differ from their canonical counterparts in the primary amino acid sequence and expression timing during cell cycle [1–3]. These histone variants show sequence divergence that ranges from a stretch of a few amino acids to a large domain [3–5]. Genes encoding canonical histones are usually organized in tandem multicopy clusters [6], whereas noncanonical histone variants are encoded by genes that are scattered throughout the genome [7]. Incorporation of histone variants at specific genomic loci is associated with cellular processes, including DNA replication, transcription, recombination and repair [8–10]. Several lines of evidence suggest that histone variants and their covalent post-translational modifications (PTMs) play a key role in developmental processes such as the initiation and maintenance of pericentric heterochromatin, X chromosome inactivation, and germ cell differentiation [4, 11]. Therefore, histone variants are involved in indexing the eukaryotic genome into many epigenomes. Multiple histone H3 variants are known to exist in animals, plants, and protists [4, 12]. Noncanonical histone H3 variants are also known to be present in the fungal phyla of Basidiomycota and Zoopagomycota [13]. However, it was long thought that only the canonical histone H3 is present in Ascomycota [14], a fungal phylum that includes budding yeast *Saccharomyces cerevisiae* and fission yeast *Schizosaccharomyces pombe* [3, 15]. Moreover, instead of histone H3 variant, a histone H4 variant (hH4v) is present in *Neurospora crassa* with unknown function [16].

Although unicellular, many yeast species are polymorphic in nature. A group of ascomycetes including *Candida albicans* in which CUG often codes for serine instead of leucine belong to the CTG clade. *C. albicans* is primarily a commensal in the oral cavity, digestive tract, and genital regions of a healthy individual [17] and yet is responsible for superficial or disseminated, often deadly infections. *C. albicans* undergoes high-frequency phenotypic transitions [18], among which a reversible switch from a single-celled oval yeast form to a filamentous hyphal form is thought to be required for its pathogenic lifestyle and is shown to be tightly linked with its virulence [19]. These morphological switching events are associated with global changes in transcriptional profiles that usually occur over a short time span in response to cues from the host niche.

C. albicans, like many other microbes, has the ability to form surface-associated, matrix-embedded communities called biofilms [20]. Biofilms can form both in vitro on abiotic surfaces and in vivo on biotic surfaces such as the oral and vaginal mucosa [21, 22]. Because biofilms are associated with a protective extracellular matrix, the cells in biofilms are more resistant to conventional antifungal drugs and host immune factors in comparison with the free-floating planktonic cells. Further, cross contamination through medical devices via biofilm is a major source of infection in hospitals [21, 23, 24]. Under most conditions, both yeast and filamentous hyphal cells of *C. albicans* are essential for proper biofilm formation. The hyphal cells provide a support scaffold required for the architectural stability of the biofilm structure formed by specific arrangements of yeast and hyphal cells. Thus, the ability of a cell to form hyphae is critical for proper biofilm growth and maintenance.

During biofilm development, cells attach to a surface and grow as a microcolony that develops into a complex three-dimensional structure held together by an extracellular matrix [25]. During biofilm growth, many adhesins, which carry a C-terminal sequence for covalent attachment of a glycosylphosphatidylinositol (GPI) anchor, are up-regulated compared with their expression in planktonic cells [26, 27]. Some of these adhesins are Enhanced Adherence to Polystyrene 1 (Eap1) [28], Hyphal Wall Protein 1 (Hwp1) [29], Repressed By *TUP1* (Rbt1),

of interest in a mutant strain compared to the wild type.

and members of the Agglutinin-Like Sequence (Als) family [30, 31, 32]. In addition, a transcriptional network of 6 master regulators (Efg1, Tec1, Bcr1, Ndt80, Rob1, and Brg1) and approximately 1,000 target genes of these transcription factors regulate biofilm development in *C. albicans* both in vitro and in vivo [33]. This biofilm network is further extended by the involvement of the Flo8 Gal4, and Rfx2 transcriptional regulators [34].

In this work, we analyzed a large number of fungal genomes, and we discovered the existence of a novel variant histone H3 that is unique to the CTG clade including *C. albicans*. We present the molecular basis of morphological switching events at the chromatin level modulated by the canonical and variant histone H3 proteins in *C. albicans*. Our results reveal that this hitherto unknown CTG-clade-specific variant histone H3 is a major regulator of the biofilm gene circuitry in *C. albicans*.

Results

A unique histone H3 variant protein is encoded only by the CTG-clade species

Using the *S. cerevisiae* histone H3 (YNL031C) amino acid sequence as the query in a basic local alignment search tool (BLAST) search, a variant of the core histone H3 protein, exclusively present in a group of ascomycetes belonging to the CTG clade (Fig 1A) was identified. The sequence of the newly identified CTG-clade-specific histone H3 variant is different from the core canonical histone H3, as well as the variant histone H3 present in Basidiomycota and Zoopagomycota fungal phyla. In *C. albicans*, *HHT2* (ORF 19.1853) and *HHT21* (ORF 19.1061) code for an identical polypeptide, the canonical histone H3, whereas *HHT1* (ORF 19.6791) encodes a variant protein differing at positions 31, 32, and 80 in the amino acid sequence when compared with *HHT2/HHT21* (Fig 1B and S1A Fig). These changes are found to be conserved in the variant histone H3 of most CTG-clade species (S1B Fig). Moreover, variations in the nucleotide sequences of *HHT1*, *HHT2*, and *HHT21* were inspected using genome sequence data available for 182 *C. albicans* isolates [35]. Only 2 synonymous SNPs were identified in *HHT1*, indicating that the amino acid sequence of Hht1 protein is invariant across the 182 tested *C. albicans* strains. Four synonymous and 1 nonsynonymous SNPs were found in *HHT2*, whereas 8 synonymous and 2 nonsynonymous SNPs were identified in *HHT21* (S1 Table). Notably, these variations do not occur at the 3 positions where Hht1 differs from Hht2 or Hht21 in the primary amino acid sequence. The presence of serine (S) and threonine (T) at position 31 and 80, respectively, in the canonical histone H3 (*HHT2* and *HHT21*) is similar to that of the mammalian histone H3.3. In addition, these 2 amino acid positions (31st and 80th) of the histone H3 polypeptide are known to tolerate variations as evident in other organisms [36]. Therefore, we propose that *HHT1* is indeed encoding a variant histone H3, possibly independently evolved in the CTG clade, and we named it as H3V^{CTG}.

Variant histone H3 is less abundant than the canonical histone H3 in major morphological forms of *C. albicans*

The canonical histone H3 genes *HHT2* and *HHT21* in *C. albicans* are divergently transcribed from the histone H4 genes, *HHF22* (ORF 19.1059) and *HHF1* (ORF 19.1854), respectively, whereas the variant histone H3 gene, *HHT1*, is located outside the canonical histone gene clusters (Fig 1C). Based on genomic locations and sequence features, we considered the polypeptide coded by *HHT21* or *HHT2* as the canonical histone H3 and the one coded by *HHT1* as the variant histone H3 (H3V^{CTG}) found exclusively in the CTG-clade species.

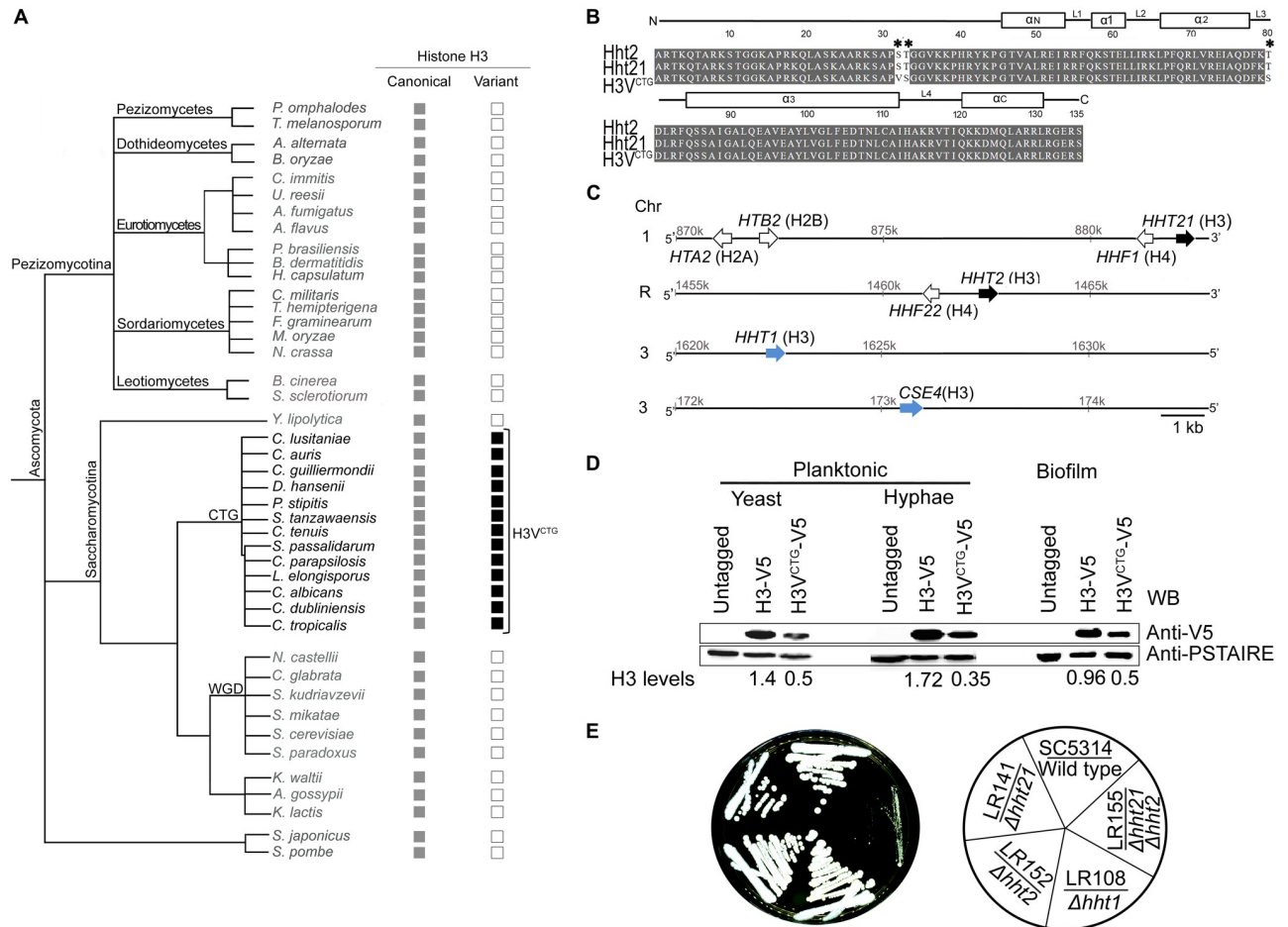


Fig 1. H3V^{CTG} is a CTG-clade specific histone H3 variant. (A) Phylogeny of fungi in the phylum Ascomycota analyzed in this study. The canonical histone H3 genes (gray box) along with the presence (black box) or absence (empty box) of the variant histone H3 of the corresponding species are shown. This tree is illustrative as the branches are not drawn to scale. The species included in this phylogeny are *Aspergillus fumigatus*, *A. flavus*, *Ashbya gossypii*, *Alternaria alternata*, *Botrytis cinerea*, *Blastomyces dermatitidis*, *Bipolaris oryzae*, *Candida lusitaniae*, *C. guilliermondii*, *C. tenuis*, *C. parapsilosis*, *C. albicans*, *C. dubliniensis*, *C. tropicalis*, *C. auris*, *C. glabrata*, *Coccidioides immitis*, *Cordyceps militaris*, *Debaryomyces hansenii*, *Debaromyces Hansenii*, *Fusarium graminearum*, *Histoplasma capsulatum*, *Kluyveromyces waltii*, *K. lactis*, *Lodderomyces elongisporus*, *Magnaporthe oryzae*, *Neurospora crassa*, *Naumovozyma castellii*, *Paracoccidioides brasiliensis*, *Pichia stipitis*, *Pyronema omphalodes*, *Spathaspora passalidarum*, *Suhomyces tanzawaensis*, *Saccharomyces kudriavzevii*, *S. mikatae*, *S. cerevisiae*, *S. paradoxus*, *Schizosaccharomyces pombe*, *S. japonicus*, *Sclerotinia sclerotiorum*, *Torrubiella hemipterigena*, *Tuber melanosporum*, *Uncinocarpus reesii*, and *Yarrowia lipolytica*. (B) Amino acid sequence alignment of histone H3 proteins coded by HHT2, HHT21, and HHT1 in *C. albicans*. Changes in the amino acid sequence among these histone H3 variants are marked by an asterisk. Identical amino acids are shaded, and numbers above the sequence denote amino acid locations on the primary protein sequence. Secondary structures such as α helices and loops of the corresponding sequence are indicated above the alignment. (C) Sketch showing locations of histone H3 genes and histone gene clusters on various chromosomes of *C. albicans*. (D) Expression levels of *C. albicans* histone H3 proteins encoded by HHT21-V5 (H3-V5) and HHT1-V5 (H3V^{CTG}-V5) were monitored by western blot analysis in the planktonic (yeast and hyphae) and biofilm growth conditions. Histone H3 molecular weight is approximately 17 kDa. The parental strain SN148 was used as the untagged control, whereas PSTAIRE (approximately 34 kDa) was used as the loading control. (E) Wild-type SC5314 (HHT1/HHT1), variant histone H3 null mutant LR108 (*hht1/hht1*), canonical histone H3 mutants LR142 (*hht21/hht21*) and LR152 (*hht2/hht2*), and canonical histone H3 null strain LR155 (*hht21/hht21 hht2/hht2*) were streaked on YPD plates and grown at 30 °C for 3 days. Chr, chromosome; YPD, yeast peptone dextrose.

<https://doi.org/10.1371/journal.pbio.3000422.g001>

Reverse transcription PCR (RT-PCR) confirmed that both the canonical histone H3 and the variant histone H3 genes are transcribed (S2A and S2B Fig). Further, epitope tagging of these genes confirmed that the corresponding proteins are translated in planktonic (yeast and hypha) as well as biofilm grown cells of *C. albicans* (Fig 1D). Although no significant difference in relative abundance of the 2 canonical histone H3 proteins was observed in *C. albicans* (S2C Fig), variant histone H3V^{CTG} was expressed in lower abundance than the canonical histone

H3 proteins in both planktonic and biofilm mode of growth in *C. albicans* (Fig 1D). Finally, indirect immunolocalization assays confirmed nuclear localization of both forms of histone H3 proteins, canonical H3 (LR143), or H3V^{CTG} (LR144) (S2D Fig). Although the canonical histone H3 localization was found to be uniform across the entire nucleus, a distinct scattered pattern of nuclear localization of variant histone H3 was observed.

Variant histone H3 assembles into nucleosomes and can support *C. albicans* growth in the absence of canonical histone H3

To test the essentiality of H3V^{CTG} for viability of *C. albicans*, both alleles of *HHT1* were replaced with a recyclable knock-out *SAT1*-flipper cassette [37] in the wild-type *C. albicans* strain SC5314 (S3A and S3B Fig). H3V^{CTG} was found to be dispensable for survival of *C. albicans* in rich media because the homozygous null mutants lacking H3V^{CTG} (LR107 and LR108) and the parent wild-type strain grew at a similar rate (Fig 1E and S3C Fig). Similarly, each of the canonical histone H3 genes, *HHT2* or *HHT21*, was deleted individually by the *SAT1*-flipper cassette. Null mutants of either *HHT2* (LR152) or *HHT21* (LR141) did not show any significant growth defects (Fig 1E). We also examined the expression levels of variant histone H3 (Hht1-V5) in the absence of *HHT21* but did not observe any significant differences in the expression levels of Hht1 (S3D Fig).

To determine whether *C. albicans* could survive in the absence of canonical histone H3, all 4 alleles encoding the canonical histone H3 were knocked out by clustered regularly interspaced short palindromic repeats–CRISPR associated protein 9 (CRISPR-Cas9) [38, 39]. Null mutant cells (*hht2/hht2 hht21/hht21*) lacking the canonical histone H3 genes *HHT2* and *HHT21* (LR155) were viable but grew significantly slower compared with any of the single mutants of histone genes or wild type (Fig 1E). We also examined the cell morphology of canonical histone H3 null mutant. These cells showed an elongated cell morphology compared with the wild type, suggesting they are stressed [40, 41] (S3E Fig). These results suggest that variant histone H3 (*HHT1*) can partially fulfill the functions of canonical histone H3 and is thus probably assembled into nucleosomes to support growth of *C. albicans* in the absence of canonical histone H3 genes.

Variant histone H3 acts as a determinant of major growth transitions in *C. albicans*

To understand the biological relevance of H3V^{CTG} that is present only among the CTG-clade species of Ascomycota, a genome-wide transcriptome analysis of the H3V^{CTG} null mutant (*hht1/hht1*) was carried out. The gene expression profiles of 2 biological replicates of the H3V^{CTG} mutant strain (*hht1/hht1*), LR107 and LR108, as well as 2 different colonies of parental strain SC5314 (*HHT1/HHT1*) grown in planktonic conditions (yeast peptone dextrose supplemented with uridine [YPDU] broth at 30 °C) were analyzed. Approximately one-fifth of all *C. albicans* genes (1,048 genes) were found to have an altered expression (fold change > 1.5, $p < 0.05$) when H3V^{CTG} was absent (S1A Data). Out of these altered genes, 638 genes were up-regulated, whereas the remaining 410 genes were down-regulated in null mutants of H3V^{CTG} compared with the wild type (S1B and S1C Data). Functional categorization of up- and down-regulated genes suggested that the biofilm gene circuit was the most significantly altered pathway due to H3V^{CTG} deletion (Fig 2A and S4A Fig). Transcription and cell cycle were the other 2 significantly altered pathways in null mutants of H3V^{CTG} ($p < 0.05$; S1D Data). Transcription levels of a majority of biofilm-induced genes were found to be up-regulated, whereas biofilm-repressed genes were down-regulated when cells lacked H3V^{CTG}. Adhesins and GPI-anchored cell wall proteins, known to play a crucial role during the biofilm

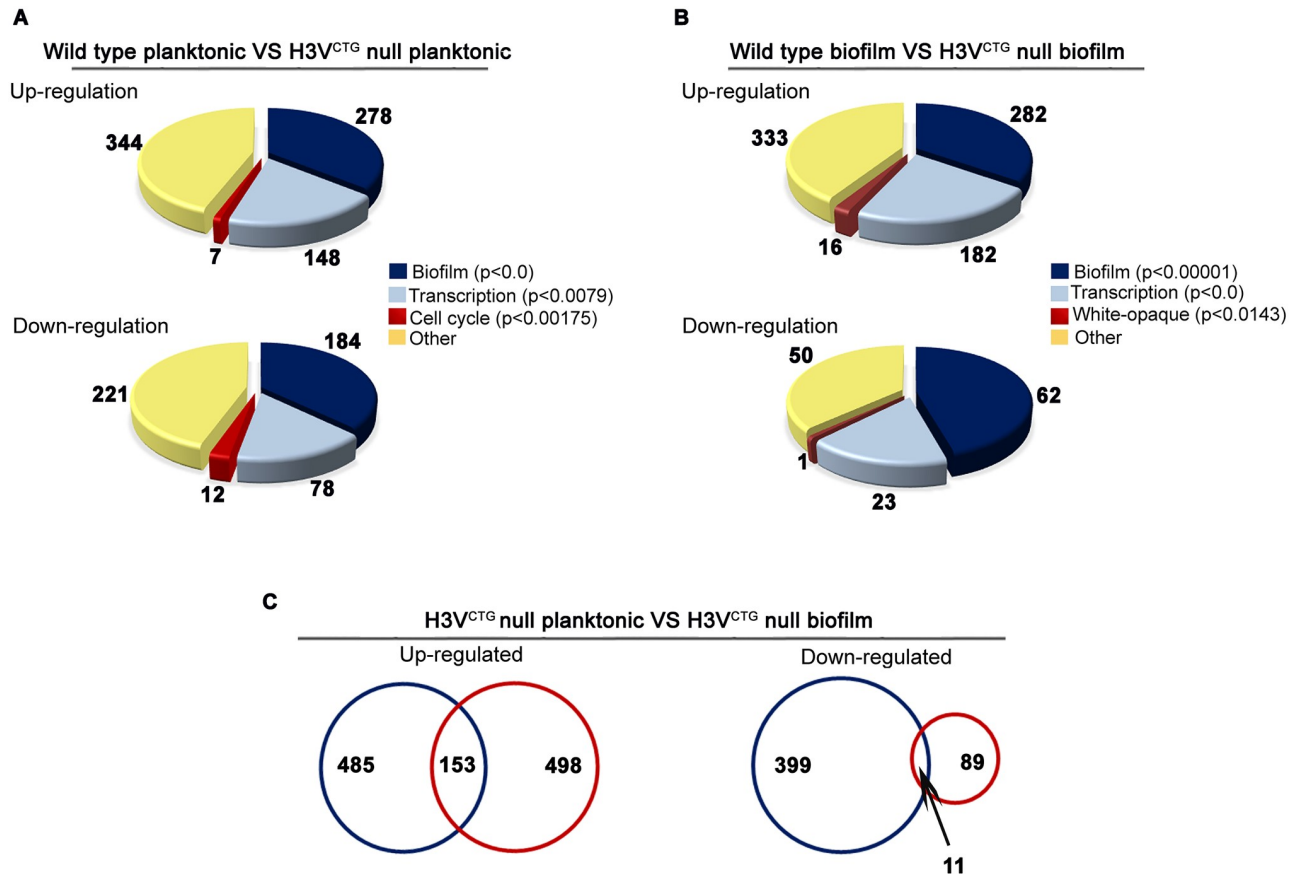


Fig 2. Loss of variant histone H3 activates the gene circuitry for biofilm development in planktonic cells. (A) Global gene expression array analysis was performed in the wild-type and null mutants for H3V^{CTG} grown in YPDU (planktonic mode). Functional classification of genome-wide expression data indicates that the most significantly altered pathways in the H3V^{CTG} null mutants are biofilm, transcription, and cell cycle. (B) A similar pattern of gene expression was observed when the indicated strains were grown in Spider medium under conditions that favor biofilm growth. (C) Genome-wide expression data were compared for common genes that are altered both in planktonic and biofilm growth conditions (blue and red circles, respectively) in the H3V^{CTG} null mutants and represented as Venn diagrams. A total of 153 up-regulated and 11 down-regulated genes are common between these 2 data sets. YPDU, yeast peptone dextrose supplemented with uridine.

<https://doi.org/10.1371/journal.pbio.3000422.g002>

development, were also up-regulated in H3V^{CTG} null mutants. In addition, *SAP5* and *SAP6* genes, which are shown to be involved in biofilm formation [42], were up-regulated in the H3V^{CTG} mutant. Based on the transcription profiling analysis, we posit that H3V^{CTG} favors planktonic growth over biofilm growth in *C. albicans*.

In the laboratory, *C. albicans* cells form biofilms under a variety of conditions on several substrates and media, including Spider medium [24, 27]. Altered expression of biofilm genes in the null mutant of H3V^{CTG} in the planktonic mode prompted us to perform a similar genome-wide transcriptome analysis after growing 2 independent colonies of wild-type (SC5314) and 2 biological replicates of H3V^{CTG} null mutant (LR107 and LR108) in Spider medium-induced biofilm conditions. In the biofilm-inducing conditions, 751 genes were found to be differentially expressed (fold change > 1.5, $p < 0.05$) between the wild-type and H3V^{CTG} null mutants (S1E Data). Among them, 651 genes were up-regulated, whereas the remaining 100 genes were down-regulated in the H3V^{CTG} null mutants (S1F and S1G Data) compared with the wild type (Fig 2B and S4B Fig). Again, the biofilm was the most significantly altered pathway ($p < 0.05$) between the null mutants of H3V^{CTG} and the wild type when the cells were grown in conditions that favor biofilm growth (Fig 2B and S1H Data).

As observed in the planktonic expression profile, several adhesins, GPI-linked cell wall proteins, and biofilm-induced genes were further up-regulated, whereas biofilm-repressed genes were further down-regulated in H3V^{CTG} null mutants compared with the wild type in the biofilm-induced condition. Among those with an altered expression, 164 genes were common to both planktonic and Spider biofilm transcriptome data sets (Fig 2C). Subsequently, we compared the altered gene-sets in the H3V^{CTG} mutants grown either in the planktonic (S4C and S4E Fig) or biofilm (S4D and S4F Fig) condition with genes known to be expressed differentially in planktonic and biofilm modes of growth [33] and represented in the form of a heat map and Venn diagram. These analyses revealed a significant overlap in the altered gene expression profile in the H3V^{CTG} mutants with the biofilm-specific genes.

Loss of variant histone H3 induces biofilm gene circuitry during planktonic growth in vitro

Analysis of the transcriptome data revealed that gene expression profiles previously linked to biofilm formation were enhanced in the H3V^{CTG} mutants compared with the wild type both in planktonic and biofilm conditions. Altered expression of a subset of critical biofilm-related genes (Fig 3A) was verified by quantitative PCR (qPCR) analysis (Fig 3B). Interestingly, *YWPI*, a biofilm-repressed gene, was down-regulated in H3V^{CTG} null mutants. Thus, the microarray data together with qPCR analysis established that H3V^{CTG} contributes to the maintenance of the planktonic growth by repressing the biofilm growth promoting gene circuitry when cells are grown in planktonic conditions. This finding led us to investigate the biofilm-forming ability of the null mutant of H3V^{CTG} compared with the wild type. To test this, wild-type SC5314 (*HHT1/HHT1*), H3V^{CTG} mutants LR107 and LR108 (*hht1/hht1*), and the H3V^{CTG} complemented strain LR109 (*hht1/hht1::HHT1*) were allowed to form biofilm in 6-well polystyrene plates in the Spider medium at 37 °C (Fig 3C, upper panel). A significant enhancement in biofilm growth of H3V^{CTG} mutants compared with the wild-type and H3V^{CTG} complemented strains was observed (Fig 3D). Together the results obtained thus far suggest that the gene circuit for biofilm development is activated in the H3V^{CTG} mutants even when these cells are grown in planktonic conditions. To verify this possibility, we performed the biofilm assay at 30 °C in YPDU medium on silicone squares; biofilm formation was found to be enhanced in H3V^{CTG} null mutants compared with the wild-type or the H3V^{CTG} complemented strain (Fig 3C lower panel and 3E), confirming that deletion of H3V^{CTG} promotes biofilm formation in YPDU medium at 30 °C.

In order to determine the thickness of biofilms formed by the *hht1* null mutant strain compared with wild type, confocal laser scanning microscopy (CLSM) was performed in vitro on silicone squares grown biofilms (see Materials and methods). Our CLSM results suggested that the *hht1* null mutant strain formed a thicker biofilm compared with either the wild-type or the complemented strain (Fig 3F). Finally, to examine the ultrastructure of biofilms formed by the wild-type and H3V^{CTG} null mutant, in vitro biofilms were allowed to grow on human urinary catheters for 48 hours (see Materials and methods). The catheter luminal surfaces were visualized by scanning electron microscopy (SEM). No significant differences were observed in the H3V^{CTG} null mutant compared with the wild type (S5 Fig).

Absence of variant histone H3 enhances in vivo biofilm growth as well

Because of the presence of many uncharacterized host factors, in vivo biofilms may substantially differ from those formed in vitro. To examine whether absence of H3V^{CTG} enhanced biofilm formation in vivo, a well-established rat venous catheter model [43] was used. We inoculated catheters intraluminally with wild type (SC5314), H3V^{CTG} null mutants LR107 and

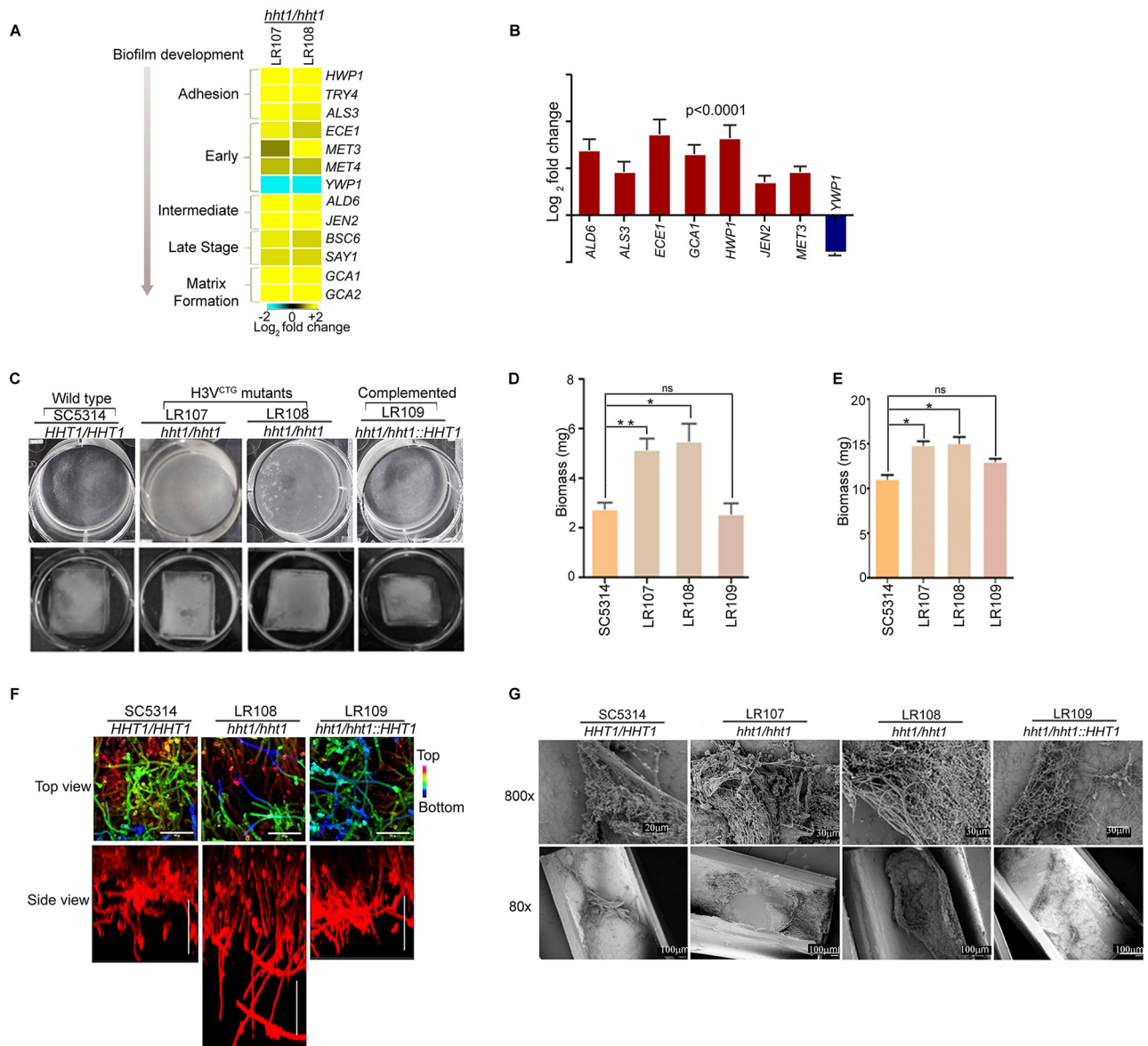


Fig 3. Variant histone H3 null mutants form more robust biofilm than wild type. (A) A heat map was generated for biofilm-related genes with altered levels of expression in the H3V^{CTG} null mutants compared with wild type. Yellow color represents up-regulation, whereas blue color represents down-regulation. Affected genes are arranged according to the step of biofilm development they are involved in. The arrowhead indicates the direction of maturation of biofilm. (B) qPCR analysis was performed for biofilm-related genes with wild-type and H3V^{CTG} null cells grown in YPDU under planktonic conditions. Δ Ct values were derived after normalization of expression of biofilm genes with that of actin, whereas $\Delta\Delta$ Ct values were calculated for relative expression of biofilm-related genes in the H3V^{CTG} null mutants compared with the wild type. The data underlying this figure can be found in [S2 Data](#). (C) Biofilms were grown using the wild type (SC5314), 2 independent transformants of H3V^{CTG} null mutant (LR107 and LR108), and the complemented strain (LR109) in 6-well polystyrene plates in Spider medium at 37 °C. Biofilms were allowed to form for 24 hours at 37 °C (upper panel) or on silicone squares in YPDU medium for 24 hours at 30 °C (lower panel). The wells were washed to remove the nonadherent cells and photographed. (D) Biomass dry weights of the wild-type, H3V^{CTG} null mutants, and H3V^{CTG} complemented strains grown in Spider media at 37 °C are shown. The data underlying this figure can be found in [S2 Data](#). (E) Biomass dry weights of the wild-type, H3V^{CTG} null mutant, and H3V^{CTG} complemented strains after growth in YPDU for 24 hours at 30 °C are shown. The data underlying this figure can be found in [S2 Data](#). (F) Wild-type, H3V^{CTG} null mutant, and the H3V^{CTG} complemented strain were adhered to silicone squares in a 12-well polystyrene plate in YPD medium at 37 °C. Biofilms were allowed to form for 48 hours. Biofilms were stained with concanavalin A-Alexa 594 and imaged by CLSM. Images are projections of the top and side views. False color depth views were constructed, in which the blue color represents cells the closest to the silicone (bottom of the biofilm) and the red color represents cells the farthest from the silicone (top of the biofilm). Representative images of at least 3 replicates are shown. Scale bars: 50 μ m. (G) The biofilm assay was performed in vivo using the rat catheter model. Strains were inoculated in the rat intravenous catheter and were allowed to form biofilms. After 24 hours of incubation, biofilms were visualized using SEM. The images are 80 \times and 800 \times magnification views of the catheter lumens. CLSM, confocal laser scanning microscopy; ns, not significant; qPCR, quantitative PCR; SEM, scanning electron microscopy; YPD, yeast peptone dextrose; YPDU, yeast peptone dextrose supplemented with uridine; Δ Ct, difference in Ct values of a gene of interest and normalization control (in this case, actin); $\Delta\Delta$ Ct, difference in Ct (threshold cycle) values of a gene of interest in a mutant strain compared to the wild type.

<https://doi.org/10.1371/journal.pbio.3000422.g003>

LR108 (*hht1/hht1*), or H3V^{CTG} complemented strain LR109 (*hht1/hht1::HHT1*) of *C. albicans*. After 24 hours of biofilm growth, the catheters were removed, and catheter luminal surfaces were imaged by SEM (Fig 3G). Similar to in vitro results, significantly thicker biofilms were formed by the H3V^{CTG} null mutants (*hht1/hht1*) compared with the wild-type strain SC5314 or the H3V^{CTG} complemented strain LR109. Therefore, these in vivo as well as in vitro observations together support the conclusion that deletion of H3V^{CTG} results in the formation of more robust biofilms than those formed by wild-type *C. albicans*.

Variant histone H3 acts as a molecular switch that favors planktonic growth over biofilm growth

Enhancement of both in vitro and in vivo biofilm formation in the H3V^{CTG} mutant compared with the wild type motivated us to investigate the mechanism by which H3V^{CTG} negatively regulates biofilm growth in *C. albicans*. To understand this mechanism at the molecular level, the V5 epitope was used to tag either the variant histone H3 (H3V^{CTG}) or the canonical histone H3 (encoded by *HHT21* as described above). Based on the complementation assay, the V5-tagged H3V^{CTG} (LR145 and LR146) was proved to be functional when expressed as the only copy in the cell (S6A Fig). Chromatin immunoprecipitation–quantitative PCR (ChIP-qPCR) analysis was performed either in the planktonic or biofilm growth conditions to determine the binding of both canonical and variant histone H3 to the promoters of a set of biofilm-induced and biofilm-repressed genes. The promoter of *ORF19.874*, which was unaltered in the genome-wide study above as well as in the previous report [33] during the planktonic to biofilm growth transition, was used to normalize the binding efficiency of histone H3 molecules in all ChIP-qPCR studies. The untagged parent strain (SN148) was used as a control to calculate the background enrichment. The promoters of biofilm-induced genes (*BMT7*, *CAN1*, *ECE1*, *HWPI1*, *HGT2*, *JEN2*, and *SAP5*), biofilm-repressed genes (*NRG1* and *YWPI1*), and also of an uncharacterized gene (*ORF19.7380*), to which 5 of the 6 biofilm master regulators bind, were examined to study the occupancy of either canonical (Hht21-V5) or variant histone H3 (H3V^{CTG}-V5). The occupancy of H3V^{CTG} was significantly higher at the promoters of biofilm-related genes compared with that of the canonical histone H3 when the cells were grown in the planktonic mode of growth (Fig 4A and S11 Data). Therefore, we posit that a higher occupancy of the variant histone H3 at the promoters of biofilm genes may prevent access of gene expression modulators (transcription activators or repressors) required for induction of the biofilm gene circuitry under planktonic growth conditions. Further, the occupancy of the H3V^{CTG} was compared in both planktonic and biofilm growth conditions. A significant drop in the binding of H3V^{CTG} to the promoters of biofilm genes was observed during the transition from planktonic to biofilm growth, except at *SAP5* and *NRG1* promoters (Fig 4B). We also examined the occupancy of variant histone H3 to the gene body of biofilm-related genes in cells grown in planktonic and biofilm conditions. Similar to the promoter regions, we also observed a drop in the level of variant histone H3 in biofilm condition compared with the planktonic condition (S6B Fig). Further, we did not observe a similar trend of changes in the occupancy of canonical H3 to the promoters of biofilm genes between planktonic and biofilm conditions (Fig 4C). These analyses reveal that the binding of H3V^{CTG} to the promoter of each of the biofilm genes was more efficient in the planktonic than in the biofilm condition. Micrococcal nuclease (MNase) digestion was performed to determine the occupancy of these 2 histone H3 on the *BMT7* gene. Both total DNA MNase digestion and ChIP results show that both histone H3 can occupy the same regions (S6C Fig). This also suggests the possibility of formation of heterotypic nucleosomes, which will be addressed in future studies. Moreover, we examined the total pool of histone H3 molecules bound to the

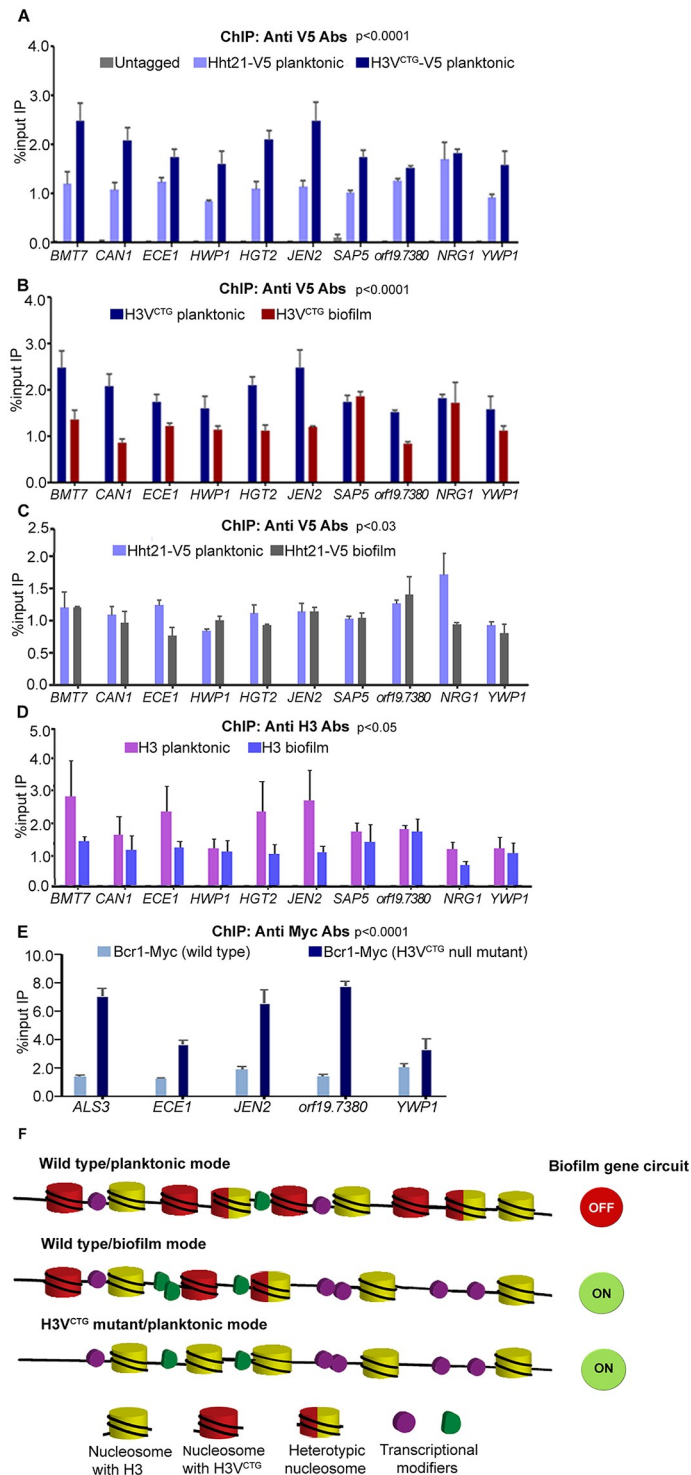


Fig 4. Variant histone H3 limits access of transcription modulators to promoters of biofilm-related genes. (A) ChIP assays with anti-V5 antibodies were performed in cells of LR143 (*HHT21/HHT21-V5*) and LR144 (*HHT1/HHT1-V5*) expressing a V5-tagged canonical histone H3 or variant histone H3 grown in planktonic conditions. IP DNA fractions were analyzed by qPCR with gene-specific promoter primer pairs (see S3 Table) for binding of either canonical histone H3 or H3V^{CTG}. Quantitative PCR (qPCR) was also performed with untagged strain to detect the background DNA elution in the ChIP assay. The enrichment of canonical histone H3 or H3V^{CTG} to the promoters of biofilm-related genes is represented as a normalized percent input IP with SEM. The values from 3 independent ChIP experiments were plotted. A two-way ANOVA test was performed to determine statistical significance. The data

underlying this figure can be found in [S2 Data](#). (B) Similarly, ChIP assays with anti-V5 antibodies were performed in LR144 cells grown as a biofilm. The enrichment of H3V^{CTG} to the promoters of biofilm genes was compared in both planktonic and biofilm conditions. The data underlying this figure can be found in [S2 Data](#). (C) ChIP assays with anti-V5 antibodies were performed in LR143 cells grown in biofilm conditions. The enrichment of H3-V5 to the promoters of biofilm genes was compared in both planktonic and biofilm conditions. The data underlying this figure can be found in [S2 Data](#). (D) ChIP assays with anti-H3 antibodies were performed in SN148 cells grown in planktonic and biofilm conditions. The enrichment of H3 to the promoters of biofilm-related genes was compared in both planktonic and biofilm conditions. The data underlying this figure can be found in [S2 Data](#). (E) The extent of binding of a biofilm master regulator, namely, Bcr1-myc, was examined either in presence or in absence of H3V^{CTG} in the planktonic mode of growth. Bcr1-myc ChIP assays were performed with anti-myc antibodies in both the parental strain (CJN1785) and the H3V^{CTG} mutant (LR133) expressing Bcr1-myc. IP DNA fractions were analyzed by qPCR with promoter specific primer pairs for the binding of Bcr1-myc. The enrichment of Bcr1-myc was calculated and normalized with *ORF19.874*. A two-way ANOVA test was performed to determine statistical significance. The data underlying this figure can be found in [S2 Data](#). (F) A proposed model to depict the role of the H3V^{CTG} in creating repressive chromatin for the biofilm genes. In this model, during planktonic growth, H3V^{CTG} is more efficiently bound to the promoters of biofilm genes compared with the canonical H3 (Hht21-V5), although they can form heterotypic nucleosomes. Possibly H3V^{CTG} restricts binding of biofilm regulators to the promoters of target genes in the planktonic state, resulting in a tight regulation of their expression when cells grow in planktonic conditions. However, in the biofilm state, when nucleosomes containing the variant histone H3 are reduced, or in the absence of H3V^{CTG}, an open chromatin structure is established that allows a more efficient access of biofilm regulators to the promoters of these genes. This causes either up-regulation of biofilm-induced genes (by transcription inducers) or down-regulation (by transcription repressors) of biofilm-repressed genes. Bcr1, biofilm and cell wall regulator 1; ChIP, chromatin immunoprecipitation; IP, immunoprecipitated; qPCR, quantitative PCR; RT-qPCR, real time quantitative PCR; SEM, standard error of the mean.

<https://doi.org/10.1371/journal.pbio.3000422.g004>

promoters of biofilm genes in both planktonic and biofilm growth by ChIP assays using anti-histone H3 antibodies. Our results show a drop in the binding of total histone H3 to the promoters of *BMT7*, *CAN1*, *ECE1*, *HGT12*, *JEN1*, *SAP5*, and *NRG1* in biofilm conditions ([Fig 4D](#)). To assess the occupancy of one of the biofilm master regulators, namely, Bcr1, to the promoters of biofilm-related genes, we performed ChIP-qPCR analysis in the wild-type or the H3V^{CTG} null mutant expressing Bcr1-myc. Binding of Bcr1-myc was analyzed on promoters of a set of genes that showed an altered (up-regulation or down-regulation) expression in the H3V^{CTG} mutant by ChIP-qPCR ([Fig 4E](#)). The results of this analysis indeed confirmed that absence of H3V^{CTG} enhances the binding of the biofilm master regulator Bcr1 to the promoters of these genes in the planktonic conditions. These results were in accordance with the gene expression profile further strengthening the fact that H3V^{CTG} indeed plays a major role in repressing the biofilm promoting gene network during planktonic growth in *C. albicans*. Taken together with all the results presented so far, we propose a general model ([Fig 4F](#)) that suggests H3V^{CTG} is involved in modulating chromatin in a way that limits access of biofilm gene-specific transcription factors to the promoters of biofilm-related genes.

Loss of variant histone H3 rescues biofilm-forming defects of mutants lacking master biofilm regulators

Previously, it has been shown that the overexpression of *ALS3* in the *bcr1/bcr1* mutant rescues the defects in biofilm formation [[44](#)]. On the other hand, overexpression of Bcr1 target genes, such as *ALS1*, *ECE1* or *HWPI*, partially restores biofilm formation of the *bcr1/bcr1* mutant. Because several biofilm-related target genes, including *ALS3*, *ECE1* and *HWPI*, were up-regulated in the H3V^{CTG} null mutants and H3V^{CTG} binds to the promoters of many biofilm-related genes possibly to inhibit biofilm growth and to promote planktonic growth, we next examined the extent of biofilm formation in the absence of both a biofilm master regulator and the possible biofilm repressor H3V^{CTG}. Deletion of each of the 6 master regulators, namely, *BCR1*, *BRG1*, *EFG1*, *NDT80*, *ROB1*, and *TEC1*, has been shown to severely hamper biofilm formation [[33](#)]. To test whether the deletion of H3V^{CTG} can rescue biofilm defects

associated with the absence of biofilm master regulators, we deleted both copies of *HHT1* ($H3V^{CTG}$) in each of the following mutant strains—*bcr1/bcr1*, *brg1/brg1*, *efg1/efg1*, *ndt80/ndt80*, *rob1/rob1*, and *tec1/tec1*—and examined the biofilm-forming ability of these double mutants by growing biofilms in YPD medium. Strikingly, biofilm growth was found to be significantly enhanced in the *bcr1/bcr1 hht1/hht1* and *tec1/tec1 hht1/hht1* double-mutant strains and also partially in *ndt80/ndt80 hht1/hht1* compared with *bcr1/bcr1*, *tec1/tec1*, or *ndt80/ndt80*, respectively (Fig 5A). The remaining 3 double mutants (*brg1/brg1 hht1/hht1*, *efg1/efg1 hht1/hht1*, and *rob1/rob1 hht1/hht1*) did not show any significant change in biofilm formation compared with the mutants lacking only the master regulator (Fig 5A). Next, the enhancement of biofilm formation observed in these double-mutant strains was quantified by standard optical density measurement as well as dry biomass of biofilm formed (Fig 5B and 5C). These results strongly suggest that variant histone H3 is a major regulator of biofilm formation in *C. albicans*. We measured by CLSM the thickness of the biofilm formed by the *tec1 hht1* double-mutant on silicone squares compared to the *tec1* mutant alone (Fig 5D). Finally, we examined in vivo biofilm formation of *tec1/tec1* as well as *tec1/tec1 hht1/hht1* mutant using the rat catheter model (Fig 5E). The double-mutant strain *tec1/tec1 hht1/hht1* formed enhanced biofilms compared with those formed by the *tec1/tec1* single mutant in both in vitro and in vivo conditions. Our results thus confirm that in the absence of $H3V^{CTG}$, biofilm defects in the *tec1/tec1* mutant can be rescued both in vitro and in vivo. We speculate that the genes that are regulated by Bcr1, Ndt80, and Tec1 are derepressed at the chromatin level in the absence of $H3V^{CTG}$. These results together confirm that $H3V^{CTG}$ negatively regulates biofilm growth in *C. albicans*.

Co-occurrence of amino acid residues at position 31 and 32 is essential for the function of variant histone H3

We were also interested to know the contribution of each of the 3 amino acid residues that are different between variant and canonical histone H3. To understand this, we generated single-point mutant strains of Hht1 at each of the positions 31, 32, and 80 similar to that of the canonical histone H3 sequence (Fig 6A). In addition, we were curious to know whether the enhancement in biofilm formation was specifically associated with the loss of the variant histone H3 or if it could be due to the loss of overall histone H3 levels in the cell. We examined the extent of biofilm formation in the null mutant of *HHT21* as well and did not observe any increase in biofilm formation. (Fig 6B and 6C). This confirms that the enhancement of biofilm growth is specifically associated with the loss of $H3V^{CTG}$. In addition, we did not observe any significant differences in biofilm formation between wild-type and point-mutant strains (Fig 6B and 6D). We also generated a double mutant at positions 31 and 32 of Hht1 to change the amino acid residues similar to those of the canonical histone H3 at the corresponding positions. The double mutant yielded a phenotype similar to that of the null mutants of variant histone H3 (Fig 6B and 6D). This suggests that co-occurrence of amino acid residues at positions 31 and 32 is essential for variant histone H3 function as a biofilm repressor during planktonic growth. This further confirms that the phenotype observed in null mutants of variant histone H3 is specifically associated with variant histone H3 and not due to the global levels of histone H3.

Variant histone H3 null mutant is hyperfilamentous

To test whether variant histone H3 has an effect on filamentation, we performed filamentation assays with wild-type SC5314 (*HHT1/HHT1*), $H3V^{CTG}$ (*hht1/hht1*) mutants LR107 and LR108, and the $H3V^{CTG}$ complemented strain LR109 (*hht1/hht1::HHT1*) on solid media. Colony wrinkling was enhanced in the mutant strains (*hht1/hht1*) compared with the wild-type

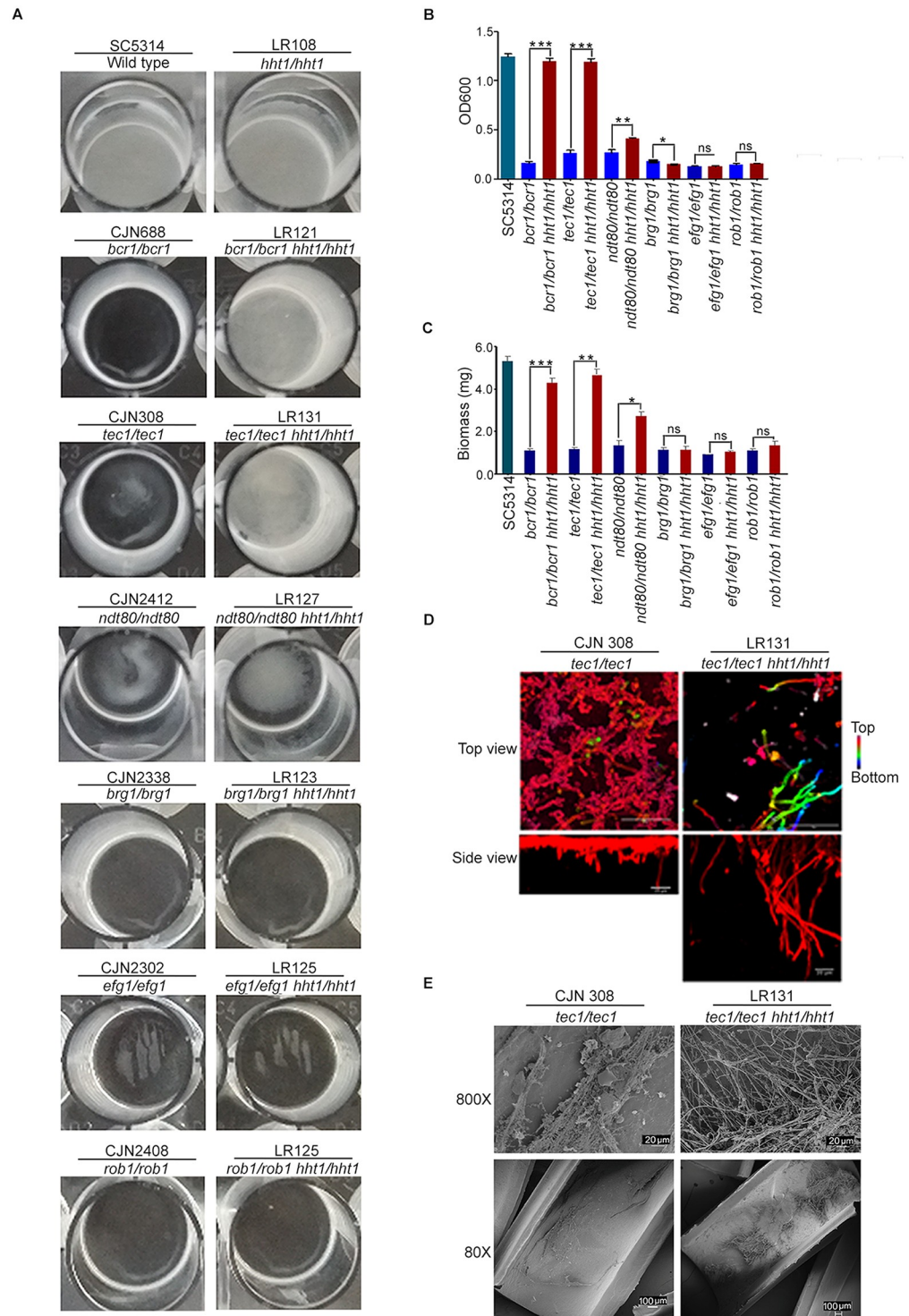


Fig 5. Deletion of the variant histone H3 rescues defects in biofilm formation associated with mutants of 3 biofilm master regulators. (A) In vitro biofilm formation assay was performed using single mutants of each of the 6 master regulators of biofilm formation, (Bcr1, Tec1, Ndt80, Brg1, Efg1, and Rob1) and the corresponding double-mutant strains in which H3V^{CTG} was deleted in each mutant background. Biofilms were grown in YPD medium in 24-well polystyrene plates for 24 hours at 37 °C. Biofilm formation defects were significantly rescued in *bcr1*, *tec1*, and *ndt80* null mutants in the absence of H3V^{CTG}. (B) Biofilm formation was quantified using the Standard Optical Density Assay by measuring OD₆₀₀ of the cells adhered to the bottom of the plates. In vitro biofilm assay was

performed in YPD using indicated single- and corresponding double-mutant strains. Biofilms were grown in 24-well plates for 24 hours at 37 °C. Data are the mean of 3 independent wells per condition. Error bars represent the standard deviation. The data underlying this figure can be found in [S2 Data](#). (C) Biomass of the wild type and each single- and double-mutant strains grown in YPD in 24-well plates for 24 hours at 37 °C. The data underlying this figure can be found in [S2 Data](#). (D) *tec1* single mutant and *tec1 hht1* double mutant were adhered to silicone squares in a 12-well polystyrene plate in YPD at 37 °C, and biofilms were allowed to form for 48 hours at 37 °C. Biofilms were stained with concanavalin A-Alexa Fluor 594 and imaged by CLSM. Images represent projections of the top and side views. Representative images of at least 3 replicates are shown. Scale bars: 50 μm. (E) Biofilm assay was performed in vivo by using a rat catheter model. CJN308 (*tec1/tec1*) or LR131 (*tec1/tec1 hht1/hht1*) were inoculated in the rat intravenous catheter and were allowed to form a biofilm. After 24 hours of incubation, biofilms were visualized using SEM. The images are 80× and 800× magnification views of the catheter lumens. Bcr1, biofilm and cell wall regulator 1; Brg1, biofilm regulator 1; CLSM, confocal laser scanning microscopy; Efg1, enhanced filamentous growth protein 1; Ndt80, non-dityrosine 80; OD, optical density; Rob1, regulator of biofilm 1; SEM, scanning electron microscopy; Tec1, transposon enhancement control 1; YPD, yeast peptone dextrose.

<https://doi.org/10.1371/journal.pbio.3000422.g005>

(*HHT1/HHT1*) and the H3V^{CTG} complemented strain LR109 (*hht1/hht1::HHT1*) at both 30 °C and 37 °C ([S7A Fig](#)). This hyperfilamentation phenotype was specific to H3V^{CTG} mutants because null mutants of neither canonical histone H3 genes produced this phenotype ([Fig 6E](#) and [S7B Fig](#)). We also examined the extent of filamentation in the point-mutant strains. Our results confirm that the double mutant at positions 31 and 32 yields a phenotype similar to that of the null mutant of variant histone H3 ([Fig 6E](#)). The extent of filamentation was also found to be enhanced at the level of colonies derived from a single cell ([Fig 6F](#) and [S7C Fig](#)). Further, to test whether the increase in filamentation observed during growth on solid media can be found in liquid culture, hyphal growth was triggered in YPD containing fetal bovine serum at 37 °C. We did not observe any significant differences in the filamentation patterns between the wild type, the *hht1/hht1* mutant strains, the H3V^{CTG} complemented strain LR109 (*hht1/hht1::HHT1*), and the *hht21/hht21* null mutant or point-mutant strains ([Fig 6G](#)).

Finally, we performed a comparative transcriptome analysis of filamentation-specific genes between the wild type in filamentation inducing conditions [45] and H3V^{CTG} null mutant in planktonic and biofilm conditions. Our analysis does not show a significant overlap of genes with altered expression between *hht1* null mutants and existing filamentation-specific expression profile ([S7D Fig](#)). Taken together, our results suggest that the enhancement in filamentation leading to a more robust biofilm formation in the H3V^{CTG} null mutants is only associated with the solid surface media.

Discussion

C. albicans is an opportunistic fungal pathogen capable of forming biofilms both in vitro and in vivo. Although the transcriptional regulation during the formation of biofilms has been studied, the molecular mechanisms at the chromatin level during this process are less understood. In this study, we identified a variant histone H3 that is exclusively present in the CTG-clade species, including *C. albicans*, but absent in all other ascomycetous fungi analyzed. The histone H3 variant, H3V^{CTG}, is not essential for survival of *C. albicans*, but the null H3V^{CTG} mutant exhibits a more robust biofilm growth as well as enhanced filamentation on solid surfaces compared with the wild type. Supported by a series of evidence, we believe that the CTG-clade specific H3V^{CTG} might have evolved to make chromatin less accessible for biofilm transcription modulators to favor the yeast and planktonic growth of *C. albicans* ([Fig 7](#)). First, ChIP-qPCR analysis revealed that the occupancy of H3V^{CTG} is higher at the promoters of biofilm-related genes compared with that of the canonical histone H3 in planktonic cells. Second, the occupancy of H3V^{CTG} is reduced at the promoters of biofilm-specific genes during the transition of *C. albicans* cells from planktonic to biofilm growth mode. Third, the absence of H3V^{CTG} enhances the binding of Bcr1, a master regulator of biofilm formation, to the

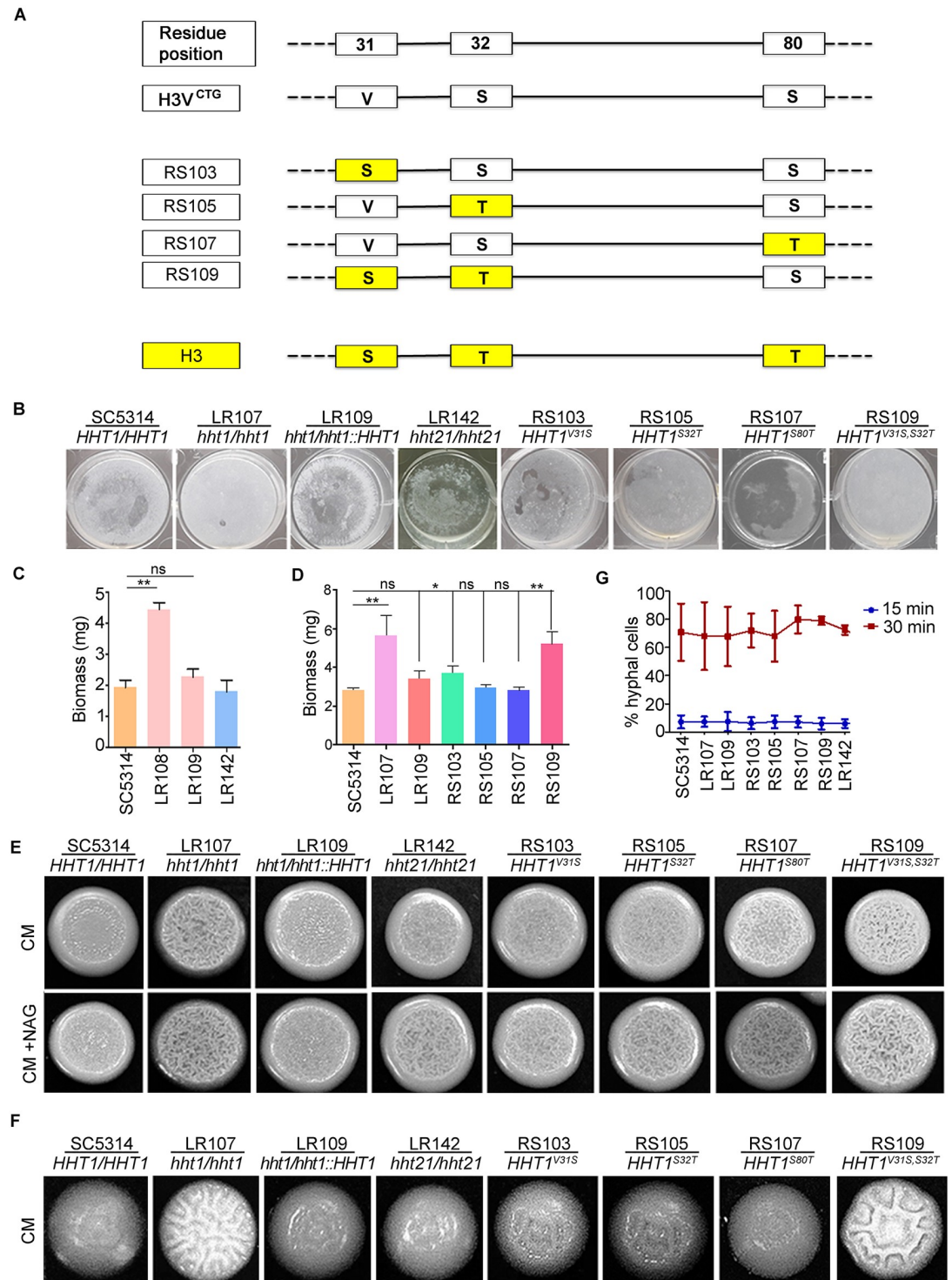


Fig 6. Amino acid residues 31 and 32 are essential for the function of H3V^{CTG}. (A) Schematics represent various point-mutant strains constructed by changing amino acid residues at positions 31, 32, and/or 80 of variant histone H3 to that of the canonical histone H3. (B) SC5314, H3V^{CTG} null mutant LR108, H3V^{CTG} complemented strain LR109, canonical histone H3 mutant LR142 (*hht21/hht21*), point-mutant strains at position 31 (RS103), 32 (RS105), 80 (RS107), and point-mutant strain at positions 31 and 32 (RS109) were allowed to form biofilms in YPDU for 48 hours at 37 °C; wells were washed to remove the nonadherent cells and photographed. (C) Biomass dry weights of the wild-type, H3V^{CTG} null mutant, H3V^{CTG} complemented, and *hht21/hht21* strains grown in YPDU at 37 °C. The data underlying this figure can be found in [S2 Data](#). (D) Biomass dry weights of the wild-type, H3V^{CTG} null mutant, H3V^{CTG} complemented, and point-mutant strains grown in YPDU at 37 °C. The data underlying this figure can be found in [S2 Data](#). (E) SC5314, H3V^{CTG} null mutant LR108, H3V^{CTG} complemented

strain LR109, canonical histone H3 mutant LR142 (*hht21/hht21*), point-mutant strain at position 31 (RS103), 32 (RS105), 80 (RS107), and point-mutant strain at position 31 and 32 (RS109) were spotted on synthetic dextrose medium complemented with essential amino acids (CM) agar plates, and CM+NAG (synthetic dextrose with 1 mM N-acetyl glucosamine) agar plates, and incubated for 3 days at 37 °C. (F) The extent of filamentation was monitored for the indicated strains by growing colonies from single cells on CM medium at 37 °C. (G) SC5314, H3V^{CTG} H3 null mutant LR107, H3V^{CTG} complemented strain LR109, point-mutant strains at position 31 (RS103), 32 (RS105), 80 (RS107), point-mutant strain at positions 31 and 32 (RS109), and canonical histone H3 mutant LR142 (*hht21/hht21*) were allowed to form filaments in liquid YPD with 10% FBS at 37 °C. The proportion of hyphal cells formed by these strains are plotted. The data underlying this figure can be found in [S2 Data](#). CM, complete media; CM+NAG, complete media supplemented with N-acetyl glucosamine; FBS, fetal bovine serum; ns, not significant; YPDU, yeast peptone dextrose supplemented with uridine.

<https://doi.org/10.1371/journal.pbio.3000422.g006>

promoters of the biofilm-related genes. Finally, deletion of H3V^{CTG} rescues biofilm defects associated with 3 biofilm transcription factors, proposed as master regulators, of the biofilm gene circuitry. This repressive behavior of biofilm growth is associated specifically with H3V^{CTG}, because alterations of the amino acid residues of Hht1 simultaneously at positions 31

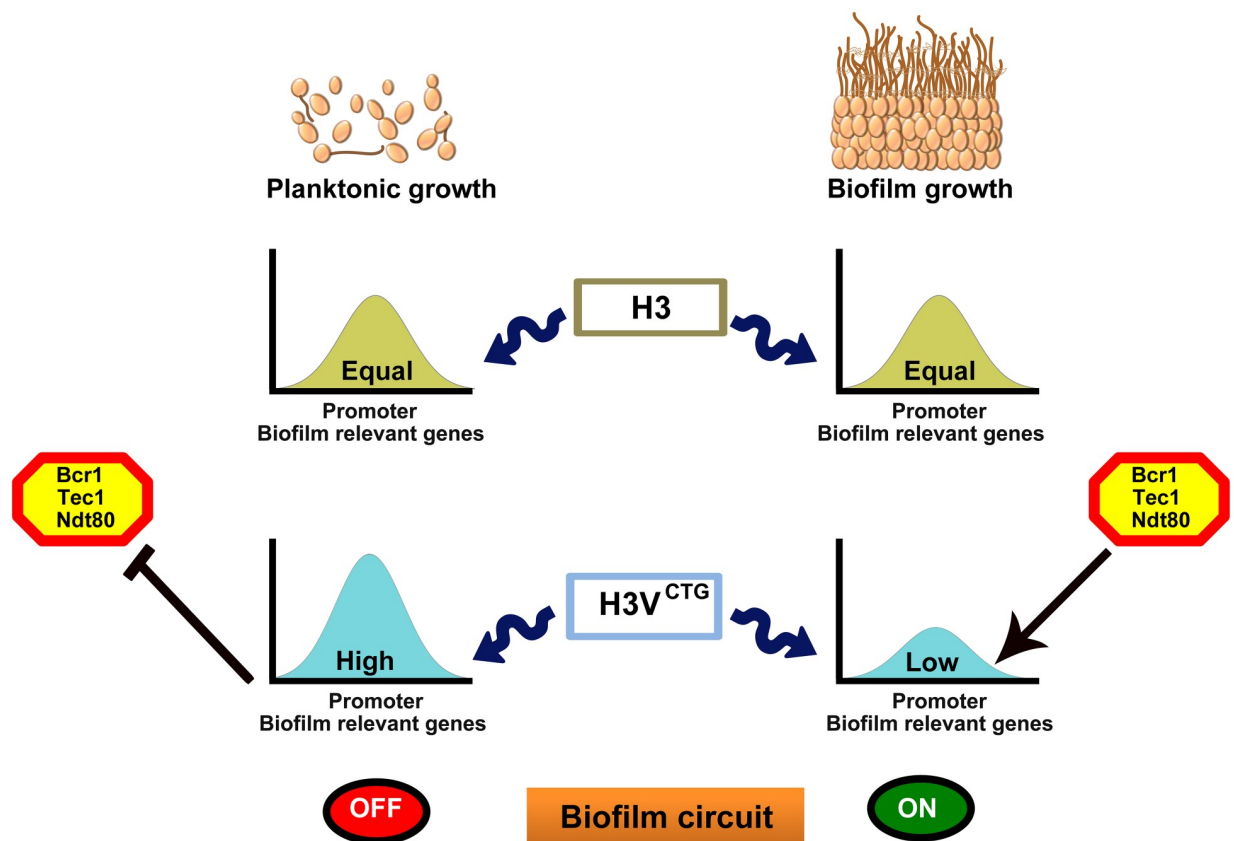


Fig 7. The CTG-clade-specific histone H3 evolved as the molecular switch of morphological growth transitions in *C. albicans*. The variant histone H3 (H3V^{CTG}) is less abundant than its canonical form in *C. albicans*. *C. albicans* can either grow as free-floating individual cells in the planktonic mode in a flask or as a three-dimensional community on a biotic or abiotic surface to form biofilms. Relative occupancy of the canonical histone H3 remains unaltered on the promoters of several biofilm-related genes tested in planktonic and biofilm cells. On the other hand, occupancy of the variant histone H3, H3V^{CTG}, is significantly higher on the promoters of the same set of biofilm genes in the planktonic cells compared with those grown in the biofilm conditions. Based on experimental evidence, we posit that the variant histone H3 nucleosomes make biofilm gene promoters less permissive for binding of transcription modulators (transcription activators or repressors) of biofilm-related genes. When H3V^{CTG} levels drop, biofilm transcription modulators bind to the promoters to modulate the genetic circuitry to favor the biofilm mode of growth. Thus, we unravel a new mechanism modulated at the chromatin level by a CTG-clade-specific histone H3 variant to balance a medically relevant growth transition of a major human pathogen. Bcr1, biofilm and cell wall regulator 1; Ndt80, non-dityrosine 80; Tec1, transposon enhancement control 1.

<https://doi.org/10.1371/journal.pbio.3000422.g007>

and 32 to those of the canonical histone H3 yield phenotypes similar to those associated with the *hht1* null mutant.

Morphogenesis has been extensively studied as a potential pathogenic trait [46]. Most human fungal pathogens, including *C. albicans*, *Histoplasma capsulatum*, *Penicillium marneffei*, *Cryptococcus neoformans*, and *Coccidioides immitis* are dimorphic or polymorphic in nature. *C. albicans* cells that are locked either in yeast (*efg1 cph1* double mutant) or in the filamentous form (*tup1* mutant) show compromised virulence [47, 48]. *C. albicans* cells tend to form hyphal filaments at 37 °C. The hyperfilamentation nature of the H3V^{CTG} mutant on solid surfaces even at 30 °C indicates that H3V^{CTG} suppresses surface-associated filamentation genes at low temperatures.

The genome-wide transcriptome analysis suggests that the pathway most significantly affected in the absence of H3V^{CTG} is the biofilm regulatory network. *C. albicans* is one of the very few fungal species that can form an efficient biofilm in a healthy mammalian host. The biofilm circuit in *C. albicans* probably evolved following divergence from closely related, non-pathogenic fungi [33]. One important step in the biofilm development is the yeast-to-hyphal transition with hyphal filaments being essential components of a mature biofilm. For example, the *bcr1* mutant is defective in biofilm formation, and it also fails to form hyphae under specific conditions, underscoring the importance of hyphal filaments in biofilm formation [49]. Bcr1 is required for expression of cell surface adherence genes (*ALS1*, *ALS3*, and *HWPI*) that are also induced during hyphal growth, suggesting that several common genes play a role during both biofilm and hyphal growth [27]. Genes, namely, *CAN2*, *HWPI*, and *TPO4*, are down-regulated in mutants of all 6 biofilm master regulators, whereas they are all up-regulated in the H3V^{CTG} null mutant during planktonic growth. This inverse correlation suggests that H3V^{CTG} plays an antagonistic role in the biofilm regulatory circuitry compared with that of previously identified biofilm master regulators [33]. Furthermore, we show that this circuit is not only derepressed in the planktonic condition but also in biofilm-induced conditions in the absence of H3V^{CTG}. Taken together with these results, it is expected that the absence of H3V^{CTG} should enhance biofilm formation in *C. albicans*.

The most compelling evidence that H3V^{CTG} acts as a negative regulator of biofilm development in *C. albicans* came from an enhanced biofilm formation by H3V^{CTG} mutant cells both in vitro and in vivo conditions compared to the wild-type or the H3V^{CTG} complemented strain. Further, the H3V^{CTG} null mutant formed an enhanced biofilm in a condition that generally favors planktonic growth. This is probably due to the formation of filaments on solid surfaces by H3V^{CTG} mutant cells at low temperatures and the fact that biofilm and filamentation genes are derepressed at this restrictive temperature.

In metazoans, histone H3 variants play a key role in the differentiation of embryonic stem cells [50]. During cellular differentiation, stem cells undergo dramatic morphological and molecular changes through selective silencing and activation of lineage-specific genes. Therefore, it may be possible that similar to metazoans, H3V^{CTG} evolved to govern the morphogenetic switch in unicellular organisms such as yeast of the CTG clade. Along with various pathogenic traits, up-regulation of several adhesion factors in the absence of H3V^{CTG} indicates that the variant histone H3 appeared in the CTG-clade species to maintain the balance between commensal and pathogenic states. *C. albicans* is a parasite because it primarily exists in a host. Thus, we propose that H3V^{CTG} provides a balance on the pathogenic attributes of *C. albicans*, perhaps to enhance its success as a commensal. Studies are in progress to understand how chromatin changes modulated by this novel histone H3 variant bring genetic innovations to regulate one of the most dramatic morphological growth transitions in a medically relevant human fungal pathogen.

Materials and methods

Ethics statement

All animal procedures were approved by the Institutional Animal Care and Use Committee at the University of Wisconsin according to the guidelines of the Animal Welfare Act, the Institute of Laboratory Animal Resources Guide for the Care and Use of Laboratory Animals, and Public Health Service Policy under protocol MV1947. Ketamine and xylazine were used for anesthesia. CO₂ asphyxiation was used for euthanasia at the end of study.

Media and growth conditions

C. albicans strains were grown in YPDU (1% yeast extract, 2% peptone, 2% dextrose, and 100 µg/ml uridine) at 30 °C unless stated otherwise. For biofilm formation, YPDU, Spider media (1% peptone, 1% yeast extract, 1% manitol, 0.5% NaCl, and 0.2% K₂HPO₄) at 37 °C [51] were used. The filamentation assays were performed with complete medium, Spider medium, and complete media containing 1 mM N-acetylglucosamine [52, 53]. Each strain was diluted to an OD₆₀₀ of 0.080, spotted on a plate, and incubated for 2 or 3 days at 30 °C and photographed [52]. Serum (10%) was used for induction of hyphae in YPDU media at 37 °C. *C. albicans* cells were transformed by the standard lithium acetate method as described previously by Sanyal and colleagues [54]. Nourseothricin was used at a concentration of 100 µg/ml.

Strain construction

All *C. albicans* strains and primer sequences used for the construction of strains in this study are listed in S2 and S3 Tables, respectively. Detailed information about the strain construction is available in the S1 Text.

RNA extraction and cDNA synthesis

RNA was isolated from *C. albicans* strains with the mirVana RNA isolation kit (Ambion, AM1560). Cells were grown in YPDU to an OD₆₀₀ = 0.5 or in biofilm condition from 48 hours grown biofilms. Approximately 4 × 10⁷ cells were taken for spheroplasting. Cells were pelleted down at 4,000 rpm, were washed with 1 ml of Y1 buffer (2.5 M sorbitol, 0.5 M EDTA [pH 8]) and finally were resuspended in 2 ml of Y1 buffer. Approximately 20 µl of lyticase and 2 µl of β-Mercaptoethanol were added and spheroplasting was done at 30 °C at 70 rpm. After 90% spheroplasting was achieved, spheroplasts were isolated by centrifugation at 1,800 rpm for 5 minutes, and RNA was isolated with the mirVana RNA kit. A total of 500 ng of purified RNA was used to make cDNA. The reaction mixture contained 4 µl of RNA, 4 µl of 5× RT buffer, 2 µl of 10 mM dNTPs, 2 µl of 0.1 M DTT, 2 µl of 10 pMol gene-specific reverse primer (H3-4), 1 µl of Superscript Reverse Transcriptase (Invitrogen, 18064–022) added in a final volume of 20 µl. Reactions were carried out at 37 °C for 60 minutes followed by heat inactivation at 85 °C for 5 minutes.

qPCR

The *C. albicans* wild-type SC5314 and H3V^{CTG} null mutant strains were grown in YPD medium till OD = 0.5. RNA was isolated as described before treated with DNase I (NEB, M03032), and the quality of RNA was examined on agarose gel. To ensure the absence of genomic DNA, a control PCR reaction was performed before the reverse transcription step. cDNA was synthesized by reverse transcription using M-MuLV reverse transcriptase (Fermentas, EP0732) and Oligo(dT) primers (Sigma, O-4387). Primers designed for RT-PCR reactions were between 100 and 110 bp long (listed on S3 Table). Analysis of melting curves was also

performed to ensure specific amplification without any secondary nonspecific amplicons (melting curve temperatures, used are 78 °C (*ACT1*), 76 °C (*ALD6*), 79 °C (*ECE1*), 80.5 °C (*HWPI*), 78 °C (*GCA1*), and 79.5 °C (*YWPI*)). PCR was carried out in a final volume of 20 μ l using iQSYBR Green supermix (BIO-RAD, 170-8880AP). The RT-PCR analysis was carried out in i-Cycler (BIO-RAD) using the following reaction conditions: 95 °C for 2 minutes, then 40 cycles of 95 °C for 30 seconds, 55 °C for 30 seconds, 72 °C for 30 seconds. Fold difference in expression of mRNA was calculated by the $\Delta\Delta$ Ct method (RT-PCR applications guide BIO-RAD) [55]. Actin was used as normalization control.

Cell lysate and western blot analysis

Western blot analysis was performed as described before by Chatterjee and colleagues [56]. *C. albicans* strains were grown in YPDU till $OD_{600} = 1$. For hyphal induction, cells were grown in the presence of 10% serum, and to obtain biofilms, *C. albicans* was grown in 6-well polystyrene plates in YPDU. Cells were harvested, washed with lysis buffer (0.2 M Tris, 1 mM EDTA, 0.39 M $(NH_4)_2SO_4$, 4.9 mM $MgSO_4$, 20% glycerol, 0.95% acetic acid [pH 7.8]), resuspended in 0.5 ml of the same buffer, and disrupted using acid-washed glass beads (Sigma, G8772) by vortexing 5 minutes (1 minute vortexing followed by 1 minute cooling on ice) at 4 °C. *C. albicans* cell lysates were electrophoresed on a 12% SDS-PAGE gel and blotted onto a nitrocellulose membrane in a semidry apparatus (BIO-RAD). The blotted membranes were blocked with 5% skim milk containing 1 \times phosphate buffered saline (PBS; pH 7.4) for 1 hour at room temperature and then incubated with the following dilutions of primary antibodies: anti-V5 antibodies at a dilution of 1:5,000 (Invitrogen, R96025), anti-PSTAIRES antibodies (Abcam, ab10345) at a dilution 1:3,000. Anti-PSTAIRES antibodies recognize Cdc28 and are widely used as a protein loading control in *C. albicans*. Next, membranes were washed 3 times with PBST (0.1% Tween-20 in 1 \times PBS) solution. Anti-rabbit HRP conjugated antibodies (Bangalore Genei, 105499) and anti-mouse IgG-HRP antibodies (Bangalore Genei, 105502) were added at a dilution of 1:1,000 and incubated for 1 hour at room temperature followed by 3 to 4 washes with PBST solution. Signals were detected using the chemiluminescence method (Super Signal West Pico Chemiluminescent substrate, Thermo scientific, 34080).

Indirect immunofluorescence

Indirect immunofluorescence was performed as described before by Sanyal and Carbon and Chatterjee and colleagues [54, 56]. Asynchronously grown *C. albicans* cells were fixed with a one-tenth volume of formaldehyde (37%) for 15 minutes at room temperature. Antibodies used were diluted as follows: 1:100 for mouse anti-V5 antibodies (Invitrogen, R96025). The dilutions for secondary antibodies used were Alexa Fluor 488 goat anti-mouse IgG (Invitrogen, A-11001) diluted 1:1,000. DAPI (4, 6-Diamino-2-phenylindole) (Sigma, D9542) was used to stain the nuclei of the cells. Cells were examined under 100 \times magnifications using a GE Delta vision microscope. The digital images were processed with Adobe Photoshop.

Gene expression design and data analysis

The concentration of the extracted RNA was evaluated using Bioanalyzer (Agilent), whereas purity of the extracted RNA was determined by the standard procedure for the same by measuring A_{260} and A_{280} using a Nanodrop Spectrophotometer (Thermo Scientific). The samples were labeled using Agilent Quick Amp labeling kit (Part number 5190-0442). A total of 500 ng RNA was reverse transcribed using Oligo(dT) primer tagged to the T7 promoter sequence. The cDNA obtained was converted to double stranded cDNA in the same reaction. Further, cDNA was converted to cRNA in the in vitro transcription step using T7 RNA polymerase,

and Cy3 dye was added into the reaction mix. During cRNA synthesis, Cy3 dye was incorporated to the newly synthesized strands. cRNA obtained was cleaned up using Qiagen RNeasy columns (Qiagen, 74106). Concentration and the amount of dye incorporated in each sample were determined using a Nanodrop. Samples that passed the QC for the specific activity (minimum RNA concentration 500 ng/ μ l and absorbance 260/280 = 2) were taken for hybridization. A total of 600 ng of labeled cRNA was hybridized on the array (AMADID 29460) using the Gene Expression Hybridization kit (part number 5190–0404; Agilent) in Sure hybridization Chambers (Agilent) at 65 °C for 16 hours. Hybridized slides were washed using Agilent Gene Expression wash buffers (part no. 5188–5327). The hybridized, washed microarray slides were then scanned on a G 2600 D scanner (Agilent). Data extraction from images was done using Feature Extraction software version 10.7 of Agilent. Microarray data was preprocessed using Limma package (Smyth and colleagues, 2005) of statistical R language. Briefly, preprocessing includes (a) background correction (b) within array normalization and (c) fitting data to linear model. Finally, an empirical Bayes moderated statistics was applied to find significant changes in the expression levels. We used a cut-off of $p < 0.05$ and $|\text{fold change}| > 1.5$ for the differential expression of mutant over wild type to define differentially expressed genes. Differentially regulated genes were clustered using hierarchical clustering to identify significant gene expression patterns. All genes represented on the array are annotated using CGD database. The differentially regulated genes (up or down) were categorized under biofilm, cell cycle, transcription, and others based on the gene ontology annotations. Chi-square test was applied to know the significance of the categorized functions. Gene expression data have been deposited into the NCBI Gene Expression Omnibus (GEO) portal under the accession number GSE72824.

In vitro biofilm growth and biomass determination

Biofilm growth in Spider media at 37 °C and dry biomass estimation. To perform the genome-wide expression analysis in the biofilm-induced condition, biofilms were grown in vitro in Spider medium by growing the biofilms directly on the bottom of 6-well polystyrene plates (CELLSTAR, 657160). Biofilms were developed as described by Nobile and Mitchell [49]. Strains were grown in YPD overnight at 30 °C, diluted to an optical density at 600 nm (OD_{600}) of 0.5 in 3 ml of Spider medium. The 6-well plates had been pretreated overnight with fetal bovine serum (FBS) and washed with 2 ml PBS. The inoculated plate was incubated at 37 °C for 90 minutes at 110 rpm agitation for initial adhesion of cells. Plates were then washed with 2 ml PBS, and 3 ml of fresh Spider medium was added, and plates were at 37 °C for 48 hours. Biofilm growth assays of the wild type, the H3V^{CTG} null mutants, and the *HHT1* complemented strain were performed by diluting ON culture to an OD_{600} of 0.2 in 3 ml Spider medium. To estimate the dry biomass of biofilms, biofilms were scrapped, and the content of each well was transferred to preweighed nitrocellulose filters. Biofilm-containing filters were dried overnight at 60 °C and weighed. The average total biomass for each strain was calculated from 3 independent samples after subtracting the mass of the empty filter.

In vitro biofilm growth in YPD medium at 30 °C and biomass determination

To examine the biofilm formation ability of H3V^{CTG} mutant strains in YPDU medium at 30 °C, in vitro biofilm growth assays were carried out by growing biofilms on either the silicone squares substrate as previously described by Nobile and Mitchell [49]. Biofilms were developed as described before, except in this case, YPDU was the medium of choice and the temperature was 30 °C. Finally, medium was removed, and the silicone squares gently washed with 1 \times PBS

prior to being photographed. For dry biomass measurements, the medium was removed and 2 ml of 1× PBS was added to each well to remove unadhered cells. Biofilms were then scrapped, and the content of each well was transferred to preweighed nitrocellulose filter paper, dried, and weighed as described before.

CLSM for biofilm imaging

Biofilms were imaged as described before by Nobile and Mitchell [49]. Biofilms were grown on silicone squares for 48 hours, gently washed with 1× PBS, and stained with 50 $\mu\text{g ml}^{-1}$ of concanavalin A-Alexa Fluor 594 (Invitrogen, C-11253) for 1 hour at 110 rpm. CLSM was performed at PPMS facility of Institut Pasteur using an upright LSM700 microscope equipped with a Zeiss 40X/ 1.0 W plan-Apochromat immersion objective. Silicone squares were placed in a petri dish, and the biofilms were covered with 1× PBS. Images were acquired and assembled into maximum intensity Z-stack projection using ZEN software (Zeiss).

In vivo rat catheter biofilm model

To form biofilm in vivo, the rat central-venous catheter infection model [43] was used, as described previously Nobile and colleagues, Andes and colleagues, Nobile and colleagues, and Dalal and colleagues [33, 43, 44, 57]. For this specific pathogen free Sprague-Dawley rats weighing 400 g each were used. A heparinized (100 U/ml) polyethylene catheter with 0.76 mm inner and 1.52 mm outer diameters was inserted into the external jugular vein. The catheter was secured to the vein with the proximal end tunneled subcutaneously to the midscapular space and externalized through the skin. The catheters were inserted 24 hours prior to infection to permit a conditioning period for a deposition of host protein on the catheter surface. Infection was achieved by intraluminal instillation of 500 μl *C. albicans* cells (10^6 cells/ml). After a 4 hour dwelling period, the catheter volume was withdrawn, and the catheter was flushed with heparinized 0.15 M NaCl. Catheters were removed after 24 hours of *C. albicans* infection to assay biofilm development on the intraluminal surface by SEM. Catheter segments were washed with 0.1 M phosphate buffer (pH 7.2) fixed in 1% glutaraldehyde/4% formaldehyde, washed again with phosphate buffer for 5 minutes, and placed in 1% osmium tetroxide for 30 minutes. The samples were dehydrated in a series of 10 min ethanol washes (30%, 50%, 85%, 95%, and 100%) followed by critical point drying. Specimens were mounted on aluminum stubs, sputter coated with gold, and imaged using a Hitachi S-5700 or JEOL JSM-6100 SEM in the high-vacuum mode at 10kV. Images were processed using Adobe Photoshop software.

ChIP

The ChIP assays were performed as described previously by Chatterjee and colleagues and Mitra and colleagues [56, 58]. Briefly, each strain was grown until exponential phase (approximately 2×10^7 cells/ml) or grown in biofilm condition for 24 hours, and cells were cross-linked with 1% final concentration of formaldehyde for 13 minutes. Chromatin was isolated and sonicated to yield an average fragment size of 300 to 500 bp. The DNA was immunoprecipitated with anti-V5 antibodies (final concentration 20 $\mu\text{g/ml}$) or anti H3 antibodies (Abcam, ab1791) or anti myc antibodies (Cal Biochem, OP10) and purified. The total, immunoprecipitated (IP) DNA, and beads only material were used to determine the binding of H3V^{CTG} to the promoters of biofilm genes by qPCR, as described before. The template used was as follows: 1 μl of 1:100 dilution for input and 1 μl of 1:2 dilution for IP for H3-V5 ChIP and undiluted for H3 and myc ChIP. The conditions used in qPCR were as follows: 94 °C for 2 minutes; the 40 cycles of 94 °C for 30 seconds, 58 °C for 30 seconds, 72 °C for 45 seconds. The results were analyzed

using CFX Manager Software. The graph was plotted according to the percentage input method [59], and the formula for calculation is $100 \times 2^{(\text{adjusted } C_t \text{ input} - \text{adjusted } C_t \text{ of IP})}$. Here, the adjusted value is the dilution factor (log2 of dilution factor) subtracted from the C_t value of diluted input/IP.

Supporting information

S1 Fig. Multiple sequence alignment of histone H3 variants in the CTG-clade species. (A) Comparative analysis of nucleotide sequences of *HHT2*, *HHT21*, and *HHT1*, the 3 *C. albicans* histone H3 encoding genes. (B) Comparative analysis of the amino acid sequences of histone H3 variants of the CTG-clade species. Amino acid sequences were aligned using the Bioedit software. Identical amino acids are indicated as dots and amino acids differing from *C. albicans* Hht1 are given as single letter symbol: *C. albicans* (Ca), *C. dubliniensis* (Cd), *C. tropicalis* (Ct), *C. parapsilosis* (Cp), *C. orthopsilosis* (Co), *Lodderomyces elongisporus* (Le), *Debaryomyces hansenii* (Dh), *Pichia stipitis* (Ps), *C. tenuis* (Cte), *Spathaspora passalidarum* (Sp), *C. guilliermondii* (Cg), *C. lusitaniae* (Cl). Hht1 is labeled as 1 (e.g., Ca1), whereas Hht2/Hht21 is labeled as 2 (e.g., Ca2) for each species. (TIF)

S2 Fig. Both canonical and variant histone H3 are expressed and localized in *C. albicans* nucleus. (A) Structure of the plasmids carrying *HHT21* or *HHT1* genomic DNA sequences as well as upstream and downstream sequences. *HHT21* locus was amplified with the primer pair 1061USFP and 1061DSRP (coordinates 881615 to 883328 of Chromosome 1), whereas the *HHT1* locus was amplified with the primer pair H3.6791USFP and H3.6791DSRP (coordinates 57523 to 59160 of Chromosome 3). PCR fragments were cloned into TZ57R/T (Thermo Scientific). Given PCR conditions were optimized to selectively amplify either *HHT21* or *HHT1*. (B) RT-PCR was performed with primers selectively amplifying either *HHT21* or *HHT1*. –RT acts as negative control, whereas actin serves as positive control. The 217 bp on +RT lanes represents the canonical/variant histone H3 (*HHT21* or *HHT1*) and the lower band of 110 bp on the same lanes corresponds to actin. (C) Expression levels of V5-tagged *C. albicans* canonical histone H3 proteins (approximately 17 kDa), namely, Hht2 and Hht21, were monitored by western blot analysis in the yeast form. The parental strain SN148 was used as the untagged control, whereas PSTAIRE (approximately 34 kDa) was used as the loading control. (D) Subcellular localization of the canonical histone H3 (Hht21-V5) or the variant form (Hht1-V5) was performed in the yeast form of *C. albicans* with anti-V5 antibodies. Nuclei were stained with DAPI. Co-localization of histone H3 with DNA was shown by merging the images. Both interphase (unbudded) and mitotic cells (large budded) are shown. Scale bars: 5 μm . RT-PCR, reverse transcription PCR. (TIF)

S3 Fig. Variant histone H3 can partially fulfill the function of canonical histone H3. (A) Structural schematic of the *HHT1* locus in the diploid *C. albicans* strains, namely, the wild-type SC5314 (*HHT1/HHT1*), heterozygous mutants (*HHT1/hht1*) LR103 and LR104, and homozygous null mutants LR105 and LR107 (*hht1/hht1*). Genomic *NcoI* sites are marked by down arrows. Location of the variant histone H3 gene, *HHT1*, is shown as a gray box, whereas the *SAT1* cassette is shown as a black box. (B) Isolated genomic DNA from each indicated strain was digested with *NcoI* and Southern hybridized with an upstream probe (shown by the black bar in panel A). Expected results for the correct transformants were obtained. (C) Growth assays were performed by growing SC5314, LR107, LR108, and the H3V^{CTG} complemented strain LR109 in YPDU liquid medium until the stationary phase was reached. Optical

density was measured by using Varioskan Flash (Thermo Scientific). The data underlying this figure can be found in [S2 Data](#). (D) Expression levels of histone H3 were monitored by western blot analysis of tagged strains LR144 (H3V^{CTG}-V5) and LR149 (H3V^{CTG}-V5 *hht21/hht21*) grown as yeast; the expected size of Hht1 is approximately 17 kDa. The parental strain SN148 was used as the untagged control, whereas PSTAIRE (approximately 34 kDa) was used as the loading control. Levels of histone H3 are normalized with the corresponding PSTAIRE levels, and values are indicated below each lane. (E) Wild-type (SC5314) and canonical histone H3 null mutant (LR155) strains were grown in YPD medium, and DIC images were taken at 60 \times . Scale bars: 2 μ m. YPD, yeast peptone dextrose; YPDU, yeast peptone dextrose supplemented with uridine.

S4 Fig. Expression data (≥ 1.5 fold difference with $p \leq 0.05$) of genes from wild-type and H3V^{CTG} mutants are illustrated as heat-map. (A) Comparison of gene expression profiles of wild-type SC5314 and variant histone H3 null mutants (*hht1/hht1*) grown in planktonic condition. (B) Comparison of gene expression profiles of wild-type SC5314 and variant histone H3 null mutants (*hht1/hht1*) grown as biofilm. (C) Comparison of common gene expression profiles between *hht1/hht1* null mutant cells grown in planktonic condition and differentially expressed genes in biofilm mode from Nobile and colleagues [33]. (D) Similarly, common genes between *hht1/hht1* null mutant cells grown in biofilm condition and wild-type differentially expressed genes grown in biofilm conditions [33]. (E) Comparative analysis of altered biofilm-related genes between the H3V^{CTG} null mutants grown in planktonic conditions (blue circles) with differentially expressed genes in biofilm conditions (red circles; [33]) in the wild type. A total of 198 up-regulated and 70 down-regulated genes are common between these 2 data sets. (F) Similarly, differentially expressed genes in the H3V^{CTG} null mutants grown in biofilm-inducing conditions (blue circles) was compared with the previously published biofilm-induced microarray data of the wild type (red circles; [33]). A total of 93 up-regulated and 7 down-regulated genes are found to be common between these 2 data sets.

S5 Fig. Ultrastructure of in vitro grown biofilms. (A) Wild-type SC5314 (*HHT1/HHT1*), H3V^{CTG} null mutant, LR108 (*hht1/hht1*), and the H3V^{CTG} complemented strain LR109 were allowed to form biofilms on human urinary catheters for 48 hours at 37 °C. The catheter luminal surfaces were visualized by SEM. SEM, scanning electron microscopy.

S6 Fig. Binding of variant histone H3 to gene bodies in planktonic and biofilm conditions. (A) To examine the functionality of V5 epitope-tagged strains, wild-type, *hht1* null mutant and H3V^{CTG}-V5/*hht1* strains were spotted on Spider medium. (B) ChIP assays with anti-V5 antibodies were performed in the strain LR144 expressing H3V^{CTG}-V5 and grown in planktonic or biofilm conditions. The enrichment of H3V^{CTG}-V5 to the gene bodies of biofilm genes was compared in both planktonic and biofilm conditions. The data underlying this figure can be found in [S2 Data](#). (C) MNase digestion of the genomic DNA isolated from cells of the wild-type and *hht1/hht1* null mutant (LR107) grown in planktonic conditions was performed. The MNase digested DNA was precipitated and quantified by qPCR. The normalized Ct values represent the occupancy of nucleosomes at 2 previously known locations (NBR1, NBR2) at the promoter of the *BMT7* gene. These 2 regions have been predicted to be nucleosome bound. Similarly, MNase ChIP was performed in LR143 (Hht21-V5) and LR144 (H3V^{CTG}-V5) strains. A greater enrichment of H3V^{CTG}-V5 compared to Hht21-V5 was observed at those 2 regions (NBR1, NBR2). The data underlying this figure can be found in

[S2 Data](#). ChIP, chromatin immunoprecipitation; MNase, micrococcal nuclease; qPCR, quantitative PCR.

(TIF)

S7 Fig. The variant histone H3 mutant strain is hyperfilamentous on solid surfaces at both 30° C and 37° C. (A) SC5314, null mutants of H3V^{CTG} (LR107, LR108), and the H3V^{CTG} complemented strain LR109 (*hht1/hht1::HHT1*) were grown in liquid YPD medium and then spotted on CM and CM-containing N-acetyl glucosamine agar plates and incubated for 2 to 3 days at 30° C. (B) SC5314, LR108, H3V^{CTG} complemented strain LR109 (*hht1/hht1::HHT1*), and canonical histone H3 mutant LR153 (*hht2/hht2*) were grown in liquid YPD and then spotted on plates containing the indicated media and incubated for 2 to 3 days at 37° C. (C) Similarly, the extent of filamentation was monitored for the indicated strains by growing colonies from single cells on CM medium at 37° C. (D) Comparative analysis of filamentation-specific genes after excluding genes common between biofilm and filamentation pathways. The Venn diagrams show the comparison of differentially expressed genes between wild-type SC5314 strain grown in filamentation-induced conditions with H3V^{CTG} null mutant grown either in planktonic or biofilm-inducing conditions. An arrow shows the overlapping genes. CM, complete media; YPD, yeast peptone dextrose.

(TIF)

S1 Text. Construction of *C. albicans* strains, plasmids, and description of supplemental methods used in this study.

(DOCX)

S1 Table. Polymorphisms in the histone H3 gene among 182 *C. albicans* isolates.

(DOCX)

S2 Table. Strains and plasmids used in this study.

(DOCX)

S3 Table. Primers used in this study.

(DOCX)

S1 Data. Transcriptome profile of wild-type and *hht1* null mutants grown in planktonic and biofilm conditions. [S1A Table](#) contains a list of all transcriptionally altered genes in the null mutants of *hht1* as compared to the wild type during planktonic growth. [S1B and S1C Table](#) contain lists of up- and down-regulated genes in *hht1* null cells during planktonic growth, respectively. [S1D Table](#) contains p values of pathways altered in *hht1* null mutants when grown in the planktonic condition. [S1E Table](#) contains a list of all transcriptionally altered genes in the null mutants of *hht1* as compared to the wild type during biofilm growth. [S1F and S1G Table](#) contain lists of up- and down-regulated genes in *hht1* null cells in biofilm, respectively. [S1H Table](#) contains p values of pathways altered in *hht1* null mutants grown in the biofilm condition. [S1I Table](#) contains normalized percent immunoprecipitated values.

(XLSX)

S2 Data. Data files related to Figs 3B, 3D, 4A, 4B, 4C, 4D, 4E, 5B, 5C, 6C and 6D, as well as S3C, S6B and S6C Figs.

(XLSX)

Acknowledgments

We thank A. Johnson, A. Mitchell, and C. Nobile for sharing the strains and providing useful suggestions; J. Heitman for useful suggestions and also for critical reading of the manuscript;

M. Ayaiz, B. Thimmappa, and P. Narang for microarray analysis; Jean-Yves Tinevez and the staff at the Image Analysis Hub of Institut Pasteur for reconstruction of biofilms confocal images; BS Suma for microscopy, V. Yadav and K. Guin for help in imaging; and P. Rai for technical assistance. The authors also acknowledge the comments, criticisms, and suggestions by members of the Molecular Mycology Laboratory during the course of this study. LSR was a senior research fellow (SRF) of Council for Scientific and Industrial Research (CSIR); Govt. of India. RS is a SRF of University Grants Commission (UGC).

Author Contributions

Conceptualization: Laxmi Shanker Rai, Rima Singha, Kaustuv Sanyal.

Data curation: Bipin Chand.

Formal analysis: Laxmi Shanker Rai, Rima Singha, Hiram Sanchez, Shantanu Chowdhury, Christophe d'Enfert, David R. Andes, Kaustuv Sanyal.

Funding acquisition: Christophe d'Enfert, David R. Andes, Kaustuv Sanyal.

Investigation: Laxmi Shanker Rai, Rima Singha, Kaustuv Sanyal.

Methodology: Laxmi Shanker Rai, Rima Singha, Hiram Sanchez, Tanmoy Chakraborty, Sophie Bachellier-Bassi, David R. Andes.

Resources: Shantanu Chowdhury, Christophe d'Enfert, David R. Andes, Kaustuv Sanyal.

Supervision: Kaustuv Sanyal.

Validation: Laxmi Shanker Rai, Rima Singha.

Visualization: Laxmi Shanker Rai, Rima Singha, Hiram Sanchez, David R. Andes, Kaustuv Sanyal.

Writing – original draft: Laxmi Shanker Rai, Kaustuv Sanyal.

Writing – review & editing: Laxmi Shanker Rai, Rima Singha, Sophie Bachellier-Bassi, Christophe d'Enfert, David R. Andes, Kaustuv Sanyal.

References

1. Marzluff WF, Gongidi P, Woods KR, Jin J, Maltais LJ. The human and mouse replication-dependent histone genes. *Genomics*. 2002; 80(5):487–98. Epub 2002/11/01. PMID: [12408966](https://pubmed.ncbi.nlm.nih.gov/12408966/).
2. Pusarla RH, Bhargava P. Histones in functional diversification. Core histone variants. *FEBS J*. 2005; 272(20):5149–68. Epub 2005/10/13. <https://doi.org/10.1111/j.1742-4658.2005.04930.x> PMID: [16218948](https://pubmed.ncbi.nlm.nih.gov/16218948/).
3. Szenker E, Ray-Gallet D, Almouzni G. The double face of the histone variant H3.3. *Cell Res*. 2011; 21(3):421–34. Epub 2011/01/26. <https://doi.org/10.1038/cr.2011.14> PMID: [21263457](https://pubmed.ncbi.nlm.nih.gov/21263457/).
4. Hake SB, Allis CD. Histone H3 variants and their potential role in indexing mammalian genomes: the "H3 barcode hypothesis". *Proc Natl Acad Sci U S A*. 2006; 103(17):6428–35. Epub 2006/03/31. <https://doi.org/10.1073/pnas.0600803103> PMID: [16571659](https://pubmed.ncbi.nlm.nih.gov/16571659/).
5. Rogakou EP, Sekeri-Pataryas KE. Histone variants of H2A and H3 families are regulated during in vitro aging in the same manner as during differentiation. *Exp Gerontol*. 1999; 34(6):741–54. Epub 1999/12/01. PMID: [10579635](https://pubmed.ncbi.nlm.nih.gov/10579635/).
6. Jaeger S, Barends S, Giege R, Eriani G, Martin F. Expression of metazoan replication-dependent histone genes. *Biochimie*. 2005; 87(9–10):827–34. Epub 2005/09/17. <https://doi.org/10.1016/j.biochi.2005.03.012> PMID: [16164992](https://pubmed.ncbi.nlm.nih.gov/16164992/).
7. Orsi GA, Couble P, Loppin B. Epigenetic and replacement roles of histone variant H3.3 in reproduction and development. *Int J Dev Biol*. 2009; 53(2–3):231–43. Epub 2009/05/05. <https://doi.org/10.1387/ijdb.082653go> PMID: [19412883](https://pubmed.ncbi.nlm.nih.gov/19412883/).

8. Skene PJ, Henikoff S. Histone variants in pluripotency and disease. *Development*. 2013; 140(12):2513–24. Epub 2013/05/30. <https://doi.org/10.1242/dev.091439> PMID: 23715545.
9. Maze I, Noh KM, Soshnev AA, Allis CD. Every amino acid matters: essential contributions of histone variants to mammalian development and disease. *Nat Rev Genet*. 2014; 15(4):259–71. Epub 2014/03/13. <https://doi.org/10.1038/nrg3673> PMID: 24614311.
10. Filipescu D, Szenker E, Almouzni G. Developmental roles of histone H3 variants and their chaperones. *Trends Genet*. 2013; 29(11):630–40. Epub 2013/07/09. <https://doi.org/10.1016/j.tig.2013.06.002> PMID: 23830582.
11. Banaszynski LA, Allis CD, Lewis PW. Histone variants in metazoan development. *Dev Cell*. 2010; 19(5):662–74. Epub 2010/11/16. <https://doi.org/10.1016/j.devcel.2010.10.014> PMID: 21074717.
12. Cui B, Liu Y, Gorovsky MA. Deposition and function of histone H3 variants in *Tetrahymena thermophila*. *Mol Cell Biol*. 2006; 26(20):7719–30. Epub 2006/08/16. <https://doi.org/10.1128/MCB.01139-06> PMID: 16908532.
13. Talbert PB, Ahmad K, Almouzni G, Ausió J, Berger F, Bhalla PL, et al. A unified phylogeny-based nomenclature for histone variants. *Epigenetics & Chromatin*. 2012; 5:7-. <https://doi.org/10.1186/1756-8935-5-7> PMID: 22650316
14. Ahmad K, Henikoff S. The histone variant H3.3 marks active chromatin by replication-independent nucleosome assembly. *Mol Cell*. 2002; 9(6):1191–200. Epub 2002/06/28. PMID: 12086617.
15. Elsaesser SJ, Goldberg AD, Allis CD. New functions for an old variant: no substitute for histone H3.3. *Curr Opin Genet Dev*. 2010; 20(2):110–7. Epub 2010/02/16. <https://doi.org/10.1016/j.gde.2010.01.003> PMID: 20153629.
16. Hays SM, Swanson J, Selker EU. Identification and characterization of the genes encoding the core histones and histone variants of *Neurospora crassa*. *Genetics*. 2002; 160(3):961–73. PMID: 11901114.
17. Kim J, Sudbery P. *Candida albicans*, a major human fungal pathogen. *J Microbiol*. 2011; 49(2):171–7. Epub 2011/05/04. <https://doi.org/10.1007/s12275-011-1064-7> PMID: 21538235.
18. Slutsky B, Buffo J, Soll DR. High-frequency switching of colony morphology in *Candida albicans*. *Science*. 1985; 230(4726):666–9. Epub 1985/11/08. <https://doi.org/10.1126/science.3901258> PMID: 3901258.
19. Jacobsen ID, Wilson D, Wachtler B, Brunke S, Naglik JR, Hube B. *Candida albicans* dimorphism as a therapeutic target. *Expert Rev Anti Infect Ther*. 2012; 10(1):85–93. Epub 2011/12/14. <https://doi.org/10.1586/eri.11.152> PMID: 22149617.
20. Baillie GS, Douglas LJ. Role of dimorphism in the development of *Candida albicans* biofilms. *J Med Microbiol*. 1999; 48(7):671–9. Epub 1999/07/14. <https://doi.org/10.1099/00222615-48-7-671> PMID: 10403418.
21. Fanning S, Mitchell AP. Fungal biofilms. *PLoS Pathog*. 2012; 8(4):e1002585. Epub 2012/04/13. <https://doi.org/10.1371/journal.ppat.1002585> PMID: 22496639.
22. Dongari-Bagtzoglou A, Kashleva H, Dwivedi P, Diaz P, Vasilakos J. Characterization of mucosal *Candida albicans* biofilms. *PLoS ONE*. 2009; 4(11):e7967. Epub 2009/12/04. <https://doi.org/10.1371/journal.pone.0007967> PMID: 19956771.
23. Donlan RM, Costerton JW. Biofilms: survival mechanisms of clinically relevant microorganisms. *Clin Microbiol Rev*. 2002; 15(2):167–93. Epub 2002/04/05. <https://doi.org/10.1128/CMR.15.2.167-193.2002> PMID: 11932229.
24. Nobile CJ, Johnson AD. *Candida albicans* Biofilms and Human Disease. *Annu Rev Microbiol*. 2015; 69:71–92. Epub 2015/10/22. <https://doi.org/10.1146/annurev-micro-091014-104330> PMID: 26488273.
25. Hawser SP, Baillie GS, Douglas LJ. Production of extracellular matrix by *Candida albicans* biofilms. *J Med Microbiol*. 1998; 47(3):253–6. Epub 1998/03/25. <https://doi.org/10.1099/00222615-47-3-253> PMID: 9511830.
26. Chaffin WL. *Candida albicans* cell wall proteins. *Microbiol Mol Biol Rev*. 2008; 72(3):495–544. Epub 2008/09/06. <https://doi.org/10.1128/MMBR.00032-07> PMID: 18772287.
27. Desai JV, Mitchell AP. *Candida albicans* Biofilm Development and Its Genetic Control. *Microbiol Spectr*. 2015; 3(3). Epub 2015/07/18. <https://doi.org/10.1128/microbiolspec.MB-0005-2014> PMID: 26185083.
28. Li F, Palecek SP. EAP1, a *Candida albicans* gene involved in binding human epithelial cells. *Eukaryot Cell*. 2003; 2(6):1266–73. Epub 2003/12/11. <https://doi.org/10.1128/EC.2.6.1266-1273.2003> PMID: 14665461.
29. Staab JF, Bradway SD, Fidel PL, Sundstrom P. Adhesive and mammalian transglutaminase substrate properties of *Candida albicans* Hwp1. *Science*. 1999; 283(5407):1535–8. Epub 1999/03/05. <https://doi.org/10.1126/science.283.5407.1535> PMID: 10066176.

30. Hoyer LL, Green CB, Oh SH, Zhao X. Discovering the secrets of the *Candida albicans* agglutinin-like sequence (ALS) gene family—a sticky pursuit. *Med Mycol.* 2008; 46(1):1–15. Epub 2007/09/14. <https://doi.org/10.1080/13693780701435317> PMID: 17852717.
31. Monniot C, Boisrame A, Da Costa G, Chauvel M, Sautour M, Bougnoux ME, et al. Rbt1 protein domains analysis in *Candida albicans* brings insights into hyphal surface modifications and Rbt1 potential role during adhesion and biofilm formation. *PLoS ONE.* 2013; 8(12):e82395. Epub 2013/12/19. <https://doi.org/10.1371/journal.pone.0082395> PMID: 24349274.
32. Mayer FL, Wilson D, Hube B. *Candida albicans* pathogenicity mechanisms. *Virulence.* 2013; 4(2):119–28. Epub 2013/01/11. <https://doi.org/10.4161/viru.22913> PMID: 23302789.
33. Nobile CJ, Fox EP, Nett JE, Sorrells TR, Mitrovich QM, Hernday AD, et al. A recently evolved transcriptional network controls biofilm development in *Candida albicans*. *Cell.* 2012; 148(1–2):126–38. Epub 2012/01/24. <https://doi.org/10.1016/j.cell.2011.10.048> PMID: 22265407.
34. Fox EP, Bui CK, Nett JE, Hartooni N, Mui MC, Andes DR, et al. An expanded regulatory network temporally controls *Candida albicans* biofilm formation. *Mol Microbiol.* 2015; 96(6):1226–39. Epub 2015/03/19. <https://doi.org/10.1111/mmi.13002> PMID: 25784162.
35. Ropars J, Maufrais C, Diogo De, Marcet-Houben M, Perin AI, Sertour N, et al. Gene flow contributes to diversification of the major fungal pathogen *Candida albicans*. *Nature Communications.* 2018; 9(1):2253. <https://doi.org/10.1038/s41467-018-04787-4> Ropars2018. PMID: 29884848
36. Kurumizaka H, Horikoshi N, Tachiwana H, Kagawa W. Current progress on structural studies of nucleosomes containing histone H3 variants. *Current opinion in structural biology.* 2013; 23(1):109–15. <https://doi.org/10.1016/j.sbi.2012.10.009> PMID: 23265997.
37. Reuss O, Vik A, Kolter R, Morschhauser J. The *SAT1* flipper, an optimized tool for gene disruption in *Candida albicans*. *Gene.* 2004; 341:119–27. Epub 2004/10/12. <https://doi.org/10.1016/j.gene.2004.06.021> PMID: 15474295.
38. Min K, Ichikawa Y, Woolford CA, Mitchell AP. *Candida albicans* Gene Deletion with a Transient CRISPR-Cas9 System. *mSphere.* 2016; 1(3). Epub 2016/06/25. PMID: 27340698.
39. Vyas VK, Barrasa MI, Fink GR. A *Candida albicans* CRISPR system permits genetic engineering of essential genes and gene families. *Sci Adv.* 2015; 1(3):e1500248. Epub 2015/05/16. <https://doi.org/10.1126/sciadv.1500248> PMID: 25977940.
40. Shi QM, Wang YM, Zheng XD, Lee RT, Wang Y. Critical role of DNA checkpoints in mediating genotoxic-stress-induced filamentous growth in *Candida albicans*. *Molecular biology of the cell.* 2007; 18(3):815–26. <https://doi.org/10.1091/mbc.E06-05-0442> PMID: 17182857.
41. Srinivasa K, Kim J, Yee S, Kim W, Choi W. A MAP kinase pathway is implicated in the pseudohyphal induction by hydrogen peroxide in *Candida albicans*. *Molecules and cells.* 2012; 33(2):183–93. <https://doi.org/10.1007/s10059-012-2244-y> PMID: 22358510.
42. Winter MB, Salcedo EC, Lohse MB, Hartooni N, Gulati M, Sanchez H, et al. Global Identification of Biofilm-Specific Proteolysis in *Candida albicans*. *MBio.* 2016; 7(5). Epub 2016/09/15. <https://doi.org/10.1128/mBio.01514-16> PMID: 27624133.
43. Andes D, Nett J, Oschel P, Albrecht R, Marchillo K, Pitula A. Development and characterization of an in vivo central venous catheter *Candida albicans* biofilm model. *Infect Immun.* 2004; 72(10):6023–31. Epub 2004/09/24. <https://doi.org/10.1128/IAI.72.10.6023-6031.2004> PMID: 15385506.
44. Nobile CJ, Andes DR, Nett JE, Smith FJ, Yue F, Phan QT, et al. Critical role of Bcr1-dependent adhesins in *C. albicans* biofilm formation in vitro and in vivo. *PLoS Pathog.* 2006; 2(7):e63. Epub 2006/07/15. <https://doi.org/10.1371/journal.ppat.0020063> PMID: 16839200.
45. Grumaz C, Lorenz S, Stevens P, Lindemann E, Schock U, Retey J, et al. Species and condition specific adaptation of the transcriptional landscapes in *Candida albicans* and *Candida dubliniensis*. *BMC Genomics.* 2013; 14:212. Epub 2013/04/04. <https://doi.org/10.1186/1471-2164-14-212> PMID: 23547856.
46. Rooney PJ, Klein BS. Linking fungal morphogenesis with virulence. *Cell Microbiol.* 2002; 4(3):127–37. Epub 2002/03/22. PMID: 11906450.
47. Lo HJ, Kohler JR, DiDomenico B, Loebenberg D, Cacciapuoli A, Fink GR. Nonfilamentous *C. albicans* mutants are avirulent. *Cell.* 1997; 90(5):939–49. Epub 1997/09/23. [https://doi.org/10.1016/s0092-8674\(00\)80358-x](https://doi.org/10.1016/s0092-8674(00)80358-x) PMID: 9298905.
48. Braun BR, Johnson AD. Control of filament formation in *Candida albicans* by the transcriptional repressor TUP1. *Science.* 1997; 277(5322):105–9. Epub 1997/07/04. <https://doi.org/10.1126/science.277.5322.105> PMID: 9204892.
49. Nobile CJ, Mitchell AP. Regulation of cell-surface genes and biofilm formation by the *C. albicans* transcription factor Bcr1p. *Current biology: CB.* 2005; 15(12):1150–5. Epub 2005/06/21. <https://doi.org/10.1016/j.cub.2005.05.047> PMID: 15964282.

50. Tanaka TS, Kunath T, Kimber WL, Jaradat SA, Stagg CA, Usuda M, et al. Gene expression profiling of embryo-derived stem cells reveals candidate genes associated with pluripotency and lineage specificity. *Genome Res.* 2002; 12(12):1921–8. Epub 2002/12/06. <https://doi.org/10.1101/gr.670002> PMID: 12466296.
51. Liu H, Kohler J, Fink GR. Suppression of hyphal formation in *Candida albicans* by mutation of a STE12 homolog. *Science.* 1994; 266(5191):1723–6. Epub 1994/12/09. <https://doi.org/10.1126/science.7992058> PMID: 7992058.
52. Homann OR, Dea J, Noble SM, Johnson AD. A phenotypic profile of the *Candida albicans* regulatory network. *PLoS Genet.* 2009; 5(12):e1000783. Epub 2009/12/31. <https://doi.org/10.1371/journal.pgen.1000783> PMID: 20041210.
53. Naseem S, Araya E, Konopka JB. Hyphal growth in *Candida albicans* does not require induction of hyphal-specific gene expression. *Mol Biol Cell.* 2015; 26(6):1174–87. Epub 2015/01/23. <https://doi.org/10.1091/mbc.E14-08-1312> PMID: 25609092.
54. Sanyal K, Carbon J. The CENP-A homolog CaCse4p in the pathogenic yeast *Candida albicans* is a centromere protein essential for chromosome transmission. *Proc Natl Acad Sci U S A.* 2002; 99(20):12969–74. Epub 2002/09/25. <https://doi.org/10.1073/pnas.162488299> PMID: 12271118.
55. Schmittgen TD, Livak KJ. Analyzing real-time PCR data by the comparative C_T method. *Nat Protocols.* 2008; 3(6):1101–8. PMID: 18546601
56. Chatterjee G, Sankaranarayanan SR, Guin K, Thattikota Y, Padmanabhan S, Siddharthan R, et al. Repeat-Associated Fission Yeast-Like Regional Centromeres in the Ascomycetous Budding Yeast *Candida tropicalis*. *PLoS Genet.* 2016; 12(2):e1005839. <https://doi.org/10.1371/journal.pgen.1005839> PMID: 26845548.
57. Dalal CK, Zuleta IA, Mitchell KF, Andes DR, El-Samad H, Johnson AD. Transcriptional rewiring over evolutionary timescales changes quantitative and qualitative properties of gene expression. *eLife.* 2016; 5. <https://doi.org/10.7554/eLife.18981> PMID: 27614020.
58. Mitra S, Rai LS, Chatterjee G, Sanyal K. Chromatin Immunoprecipitation (ChIP) Assay in *Candida albicans*. *Methods Mol Biol.* 2016; 1356:43–57. Epub 2015/11/01. https://doi.org/10.1007/978-1-4939-3052-4_4 PMID: 26519064.
59. Mukhopadhyay A, Deplancke B, Walhout AJ, Tissenbaum HA. Chromatin immunoprecipitation (ChIP) coupled to detection by quantitative real-time PCR to study transcription factor binding to DNA in *Caenorhabditis elegans*. *Nat Protoc.* 2008; 3(4):698–709. Epub 2008/04/05. <https://doi.org/10.1038/nprot.2008.38> PMID: 18388953.

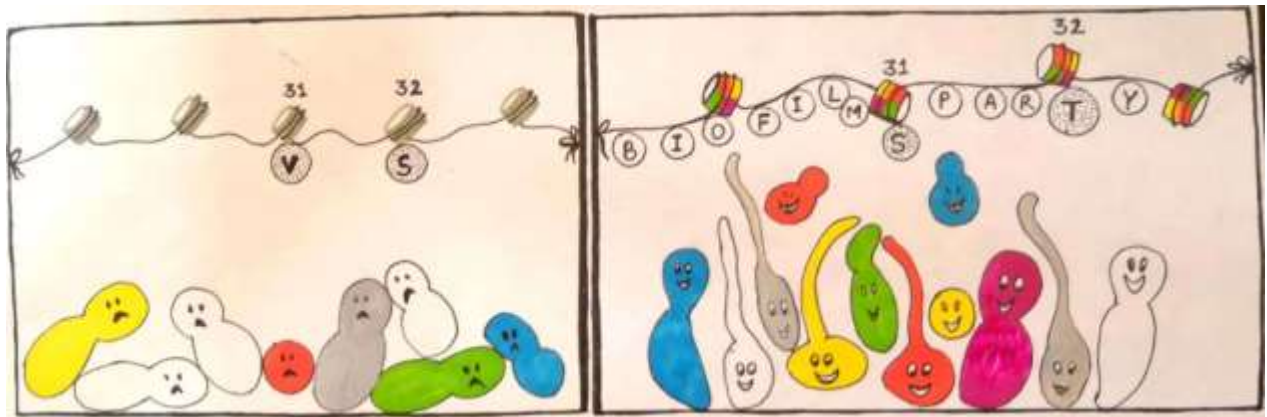


Illustration designed by
Neha Varshney